

THE KINETICS OF THE DISSOLUTION OF CHALCOPYRITE IN CHLORIDE MEDIA

Lilian De Lourdes Velásquez Yévenes

Metallurgical Engineer

This Thesis is presented for the degree of doctor of Philosophy of Murdoch University

Murdoch University, Australia

March 2009

DECLARATION

I declare that this thesis is my own account of my research and contains as its main content work that has not previously been submitted for a degree or examination at any tertiary education institution.

Lilian De Lourdes Velásquez Yévenes

_____ Day of _____ 2009

ABSTRACT

One of the most important outstanding problems with the hydrometallurgy of copper is the low temperature leaching of chalcopyrite. In this thesis, a fundamental study at low temperature was undertaken in order to establish a mechanism, which is consistent with the data obtained in an extensive study of the kinetics of dissolution of several chalcopyrite concentrates.

It will be demonstrated that enhanced rates of dissolution can be achieved at ambient temperatures by the application of controlled potentials in the range 560-650 mV, depending on the concentration of chloride ions. However, control of the potential by the use of electrochemical or chemical oxidation of iron(II) or copper(I) ions is ineffective unless carried out in the presence of dissolved oxygen. The rates of dissolution are approximately constant for up to 80% dissolution for sized fractions of the concentrates with an activation of energy of about 75 kJ mole^{-1} . Chalcopyrite from different sources appears to dissolve at approximately the same rate which is largely independent of the iron and copper ion concentrations, the acidity and chloride ion concentration but depends in some cases on the presence of additives such as fine pyrite or silver ions.

Based on the results of these leaching experiments and detailed mineralogical analyses of the residues, a mechanism involving non-oxidative dissolution of the mineral coupled to oxidation of the product hydrogen sulfide will be proposed. The latter reaction is shown to occur predominantly by a copper ion – catalyzed reaction with dissolved oxygen. The results of an independent study of the kinetics of this reaction will be presented which will demonstrate that the rates are consistent with those obtained for the dissolution of the mineral. The possible involvement of a covellite-like surface layer on the chalcopyrite under some conditions will also be discussed as it relates to the mechanism. It will also be shown that fine pyrite particles can also act as a catalyst surface for the oxidation of hydrogen sulfide. This mechanism is consistent with the mineralogy which confirmed the formation of secondary sulfur which is not associated with chalcopyrite but is associated with fine pyrite if present.

A comparison of this mechanism with that proposed in other more limited studies of the dissolution of chalcopyrite under similar conditions in sulfate solutions has been made.

ACKNOWLEDGEMENTS

There are many people who have contributed significantly to the achievement of this thesis. Most particularly, I would like to express my deepest and sincere thanks to my supervisor Professor Michael J. Nicol for his guidance, tolerance, support, endurance and encouragement during this process. His enthusiasm and motivation inspired me to conduct and complete this research and is immensely appreciated.

I would like to extend my gratitude to the members of the Extractive Metallurgy Department at Murdoch University for assisting me along the road to completion. Specifically, I would like to mention Doctor Hajime Miki whose vast knowledge, talent and indulgence assisted me immeasurably. Thanks also to my fellow postgraduate students Venny Tajandrawan, Alex Senaputra, Dmitry Pugaev and my dear friend Pamela Garrido for their support and advice throughout my PhD.

I acknowledge with thanks the financial support from Murdoch University, BHP Billiton, A.J. Parker Centre and Universidad Católica del Norte Chile, without which the work as described in this thesis would have not been possible. Thanks to Dr Puru Shrestha and his mineralogy team at BHP Billiton for their excellent mineralogical support of this project.

Last but not least, I would like to express my wholehearted thanks to my devoted husband, Raúl Méndez, my precious daughter Camila and my loving son Matías who moved with me, away from their beloved country, and whose support and love made this thesis possible.

Dedicated to my parent Juan and Margarita.

TABLE OF CONTENTS

ABSTRACT	I
ACKNOWLEDGEMENTS	III
LIST OF FIGURES	X
LIST OF TABLES	XXIII
1. INTRODUCTION	1
2. LITERATURE REVIEW	6
2.1. General properties of chalcopyrite	6
2.1.1. The nature of chalcopyrite	6
2.1.2. Physical properties	7
2.1.3. Structure	7
2.1.4. Electronic properties	8
2.1.5. Thermodynamics of the dissolution of chalcopyrite	9
2.1.6. The leaching of chalcopyrite	12
2.1.7. Chloride leaching processes for chalcopyrite	17
2.1.8. Passivation of chalcopyrite	24
2.1.9. Effect of the source of the chalcopyrite	28
2.2. The leaching of chalcopyrite in chloride solutions	29
2.2.1. Chemistry of chloride solutions	29
2.2.2. Thermodynamics of chalcopyrite oxidation in chloride solutions	34
2.2.3. Kinetics of the dissolution of chalcopyrite	41
2.2.4. Temperature	51
2.2.5. Particle size	52
2.2.6. The effect of additives	53
2.2.7. Effect of potential	63
2.3. Mechanism of the dissolution of chalcopyrite in chloride solutions	68
2.3.1. Oxidative dissolution	68
2.3.2. Reductive/Oxidative dissolution	69

2.3.3.	Non-oxidative dissolution	71
2.3.4.	Non-oxidative/oxidative model	73
3.	EXPERIMENTAL METHODS AND MATERIALS	75
3.1.	Materials and Reagents	75
3.1.1.	Sulphuric acid solutions	76
3.1.2.	Hydrochloric acid solutions	76
3.1.3.	Mineral samples	76
3.2.	Experimental Methods	79
3.2.1.	Preparation of concentrates for leaching	79
3.2.2.	Leaching with shake flasks	79
3.2.3.	Agitated leaching in instrumented reactors	80
3.2.4.	E_h Control system	82
3.2.5.	The rate of consumption of dissolved oxygen	87
3.3.	Monitoring system	89
3.3.1.	Measurement of E_h	89
3.3.2.	Measurement of the chalcopyrite electrode potential	92
3.3.3.	Control of solution pH	92
3.3.4.	Measurement of dissolved oxygen	92
3.4.	Analyses	93
3.4.1.	Atomic absorption spectrometer (AAS)	93
3.4.2.	Titrations	94
3.4.3.	Particle size analysis	94
3.4.4.	Miscellaneous analyses	94
4.	PRELIMINARY LEACHING EXPERIMENTS	98
4.1	Introduction	98
4.2	Shake-flask leaching experiments	101
4.2.1	The effect of chloride ion	101
4.2.2	The effect of mixed chloride-sulfate solutions.	106
4.2.3	Variation of potential with addition of chloride ions	108
4.3	Leaching experiments in instrumented reactors	113
4.4	Preliminary leaching experiments with chalcopyrite concentrates from different sources	120

4.4.1	Leaching experiments of chalcopyrite concentrates	120
4.4.2	Leaching of mixed concentrates	125
4.4.3	Mineralogical analyses	127
4.5	Summary and conclusions	139

5. THE EFFECT OF THE SOLUTION POTENTIAL ON THE RATE OF LEACHING OF CHALCOPYRITE **142**

5.1	Introduction	142
5.2	Electrochemical control of the potential	147
5.3	Control of the potential by oxygen addition	150
5.4	Dissolution of chalcopyrite concentrates from different sources	151
5.4.1	Mineral particle size distribution	155
5.4.2	Leaching experiments within the optimal potential window	157
5.5	Effect of low potentials	161
5.6	Recovery	170
5.7	Summary and conclusions	171

6. KINETICS OF THE DISSOLUTION OF CHALCOPYRITE **173**

6.1	Introduction	173
6.2	The effect of temperature	175
6.3	The effect of the concentration of chloride	179
6.4	The effect of cupric ion concentration	183
6.5	The effect of the iron(II) concentration	184
6.6	The effect of particle size	186

6.7	The effect of the type of agitation	187
6.8	The effect of pulp density	188
6.9	The effect of pH	189
6.10	Leaching profiles for the copper sulfide minerals	195
6.10.1	Mineralogical association of sulfur during leaching	201
6.11	Recovery	211
6.12	Summary and conclusions	212
7.	THE EFFECT OF ADDITIVES	215
7.1	Introduction	215
7.2	Effect of addition of pyrite	218
7.2.1	Pyrite in chalcopyrite concentrates	218
7.2.2	Dissolution of pure pyrite	221
7.2.3	The effect of the ratio of chalcopyrite to pyrite	223
7.2.4	The effect of the particle size of pyrite	224
7.2.5	The effect of pyrite on the dissolution of covellite	226
7.2.6	Mineralogy of residues	227
7.3	Effect of addition of silver ions	232
7.5.	Recovery	237
7.6.	Summary and conclusions	239
8.	THE MECHANISM OF THE LEACHING OF CHALCOPYRITE IN CHLORIDE MEDIA	241
8.1.	Introduction	241
8.2.	Reaction Mechanism	243
8.2.1.	High potential region. Oxidative Model	243
8.2.2.	Low potential region. Non Oxidative model	244
8.2.3.	Relevant chemistry of the non-oxidative model	247

8.3.	Consumption of dissolved oxygen with time	251
8.4.	Analysis of experimental data	252
8.4.1.	High ($>0.2 \text{ g L}^{-1}$) copper concentration	255
8.4.2.	Low ($<0.2 \text{ g L}^{-1}$) copper concentration	260
8.4.3.	Results at high copper concentration	261
8.4.4.	The effect of copper (II) concentration	265
8.4.5.	The effect of chloride ion concentration	268
8.4.6.	The effect of acidity	269
8.4.7.	The effect of the addition of fine pyrite	270
8.5.	Summary	272
9.	CONCLUSIONS	275
10.	RECOMMENDATIONS FOR FUTURE STUDY	278
	REFERENCES	280
	APPENDIX	290

LIST OF FIGURES

Figure 2.1	Unit-cell model of chalcopyrite. Copper is shown in red, iron in blue and sulfur in yellow. (Britannica Concise Encyclopedia). 8
Figure 2.2	Partial Eh-pH diagram of Cu-Fe-S-H ₂ O at 25 °C, [Cu ⁺²] = [Fe ²⁺] = [Fe ³⁺] = 0.1 M. 11
Figure 2.3	Mean activity coefficient of HCl in solutions of NaCl or CaCl ₂ (Majima and Awakura, 1981)..... 31
Figure 2.4	Solubility in the CuCl-NaCl-H ₂ O system at various temperatures. Free HCl 8-11 g L ⁻¹ ; 2 g L ⁻¹ Cu(II); ○ 5 ° C; ● 22 ° C; ▲ 75 ° C (Berger and Winand, 1984) 32
Figure 2.5	Solubility of copper(II) in chloride solutions at 50 ° C. ● CuCl ₂ -NaCl-HCl-H ₂ O system; Δ: CuCl ₂ -ZnCl ₂ -NaCl-HCl-H ₂ O system; 1: 0.5 M Zn(II); 2: 1.5 M Zn(II); ○ CuCl ₂ -FeCl ₃ -NaCl-HCl-H ₂ O system; 3: 0.5 M Fe(III); 4: 1 M Fe(III) and 5: 1.5 M Fe(III) (Winand 1991). 33
Figure 2.6	CuCl ₂ solubility in water as function of temperature (Winand 1991). 34
Figure 2.7	Species distribution Cu(I)/Cl ⁻ system at 25°C. [Cu(I)]=1.18x10 ⁻² mol L ⁻¹ 37
Figure 2.8	Species distribution in the Cu(II)/Cl ⁻ system at 25 °C. [Cu ²⁺] = 6.68x10 ⁻² mol L ⁻¹ 37
Figure 2.9	Species distribution in the Fe(III)/Cl ⁻ system at 25 °C. [Fe(III)] = 5.38x10 ⁻³ mol L ⁻¹ 38
Figure 2.10	Variation of formal potential of various couples with the concentration of chloride ions. [Cu(II)] = [Fe(II)] = [Fe(III)] = 0.1 M, [Cu(I)] = 10 ⁻³ M. 40

Figure 3.1	Instrumented Reactor	81
Figure 3.2	Control system	83
Figure 3.3	Schematic of the electrochemical potential control system .	85
Figure 3.4	Schematic of the air potential control system	86
Figure 3.5	Schematic of the N ₂ /O ₂ potential control system	87
Figure 3.6	Schematic of the apparatus for measurement of the consumption of dissolved oxygen.....	88
Figure 3.7	MLA (Mineral Liberation Analyser) system.....	95
Figure 4.1	Effect of addition of chloride on the dissolution of Ok Tedi chalcopyrite after 24 h with 1% pulp density. Data at 0.2 M chloride in absence of Fe(III).....	103
Figure 4.2	Effect of ferric chloride concentration on the dissolution of chalcopyrite from Ok Tedi samples after 24 h at 50 °C.	104
Figure 4.3	Effect of chloride concentration on the rate of dissolution of Ok Tedi chalcopyrite in aerated solutions in the absence of ferric ions.	105
Figure 4.4	Effect of chloride concentration on dissolution of chalcopyrite from Andina concentrate in aerated 0.2 M HCl at 35 °C.....	106
Figure 4.5	Effect of chloride ions on the dissolution of Ok Tedi chalcopyrite in aerated hydrochloric acid (0.2 M) and sulphuric acid (0.2 M) solutions in the absence of iron(III) ions. (a) 25 °C, (b) 35 °C and (c) 50 °C.....	107
Figure 4.6	Effect of chloride concentration on the potentials during the dissolution of Ok Tedi chalcopyrite in aerated 0.2 M HCl and 0.2 M H ₂ SO ₄ solutions at 35 °C. (A) Solution Potential, (B) Mixed Potential.	109

Figure 4.7	Variation of potentials with addition of chloride in dissolution of Ok Tedi chalcopyrite in aerated 0.2 M HCl and 0.2 M H ₂ SO ₄ solutions at 50 °C. (A) Solution Potential, (B) Mixed Potential.....	110
Figure 4.8	Variation of potentials with addition of chloride for the dissolution of Andina concentrate in aerated 0.2 M HCl at 35 °C.....	111
Figure 4.9	Effect of addition of iron(III) on the potential during dissolution of Ok Tedi chalcopyrite 0.2 M HCl at 50 °C. (A) Solution Potential, (B) Mixed potential.	112
Figure 4.10	Dissolution of copper and iron from Andina concentrate in 800 mL of solution containing 0.2 M HCl at 35 °C in air. (a) 15 g unscreened sample and (b) 8 g screened (+25-38 µm) sample.	114
Figure 4.11	Dissolution of copper from screened (+25-38 µm) Andina concentrate in solutions of varying HCl acidity in air at 35 °C.	115
Figure 4.12	Dissolution of copper from screened Andina concentrate with 0.5 g L ⁻¹ Cu(II) in various HCl acid concentration and air at 35 °C.	115
Figure 4.13	Variation of solution potentials and copper dissolution during leaching of Andina concentrate at 35 °C in air. (A) 0.1 M HCl and 0.5 g L ⁻¹ Cu(II), (B) 0.2 M HCl and 0.5 g L ⁻¹ Cu(II) and (C) 0.5 M HCl and 0.5 g L ⁻¹ Cu(II).	117
Figure 4.14	Effect of Fe(II) and Fe ₃ O ₄ on dissolution of copper from unscreened Andina concentrate (a) 0.2 M HCl, 0.5 g L ⁻¹ Cu(II) and 0.5 g/L Fe(II), (b) 0.2 M HCl, 0.5 g L ⁻¹ Cu(II), 0.5 g L ⁻¹ Fe(II) and 5 g of Fe ₃ O ₄ , (c) 0.2 M H ₂ SO ₄ , 0.5 g L ⁻¹ Cu(II) and 0.5 g L ⁻¹ Fe(II) and (d) 0.2 M H ₂ SO ₄ , 0.5 g L ⁻¹ Fe(II), 0.5 g L ⁻¹ Cu(II) and 5 g Fe ₃ O ₄	118
Figure 4.15	Variation of potentials and copper dissolution during leaching of Andina concentrate at 35 °C in air. (a) 0.2 M HCl and 0.5 g L ⁻¹ Fe(II), (b) 0.2 M HCl, 0.5 g L ⁻¹ Fe(II) and 5 g of Fe ₃ O ₄ , (c) 0.2 M H ₂ SO ₄ and 0.5 g L ⁻¹ Fe(II) and (d) 0.2 M H ₂ SO ₄ , 0.5 g L ⁻¹ Fe(II) and 5 g Fe ₃ O ₄	119

Figure 4.16	Size distribution of chalcopyrite concentrates after dry-screened at +25-38 μm	121
Figure 4.17	Dissolution of chalcopyrite from different sources (+25-38 μm) in 0.2 M HCl and 0.5 g L ⁻¹ of Cu(II). (A) Copper dissolution and (B) iron dissolution	122
Figure 4.18	Variation of potential and copper extracted during leaching of several concentrates (A) Andina, (B) Spence, (C) PQS1 and (D) Ok Tedi.....	124
Figure 4.19	Dissolution of mixed chalcopyrite concentrates (+25-38 μm) in 0.2 M HCl and 0.5 g L ⁻¹ Cu(II).(A) Copper dissolution and (B) iron dissolution	126
Figure 4.20	Variation of solution potential during dissolution of mixed concentrates.....	127
Figure 4.21	Association of chalcopyrite with other minerals in the Andina leach residue.....	129
Figure 4.22	Mineral map of Andina concentrate after leaching shows (a) liberated sulfur (dark green) and (b) chalcopyrite (green) with minor amounts of associated sulfur.....	129
Figure 4.23	Optical microphotograph showing department of sulfur in the Andina leach residue.....	130
Figure 4.24	Size distribution for chalcopyrite in dry-screened Andina head sample (+25-38 μm) compared with the leach residue. Also shown is the size distribution of the sulfur in the residue.....	130
Figure 4.25	Association of chalcopyrite with other minerals in the PQS1 residue.....	132
Figure 4.26	Mineral map of the residue from dissolution of the PQS1 concentrate showing sulfur (blue) associated with pyrite (black).	132

Figure 4.27	Optical microphotograph shows sulfur in globular form in the PQS1 leach residue.	133
Figure 4.28	Association of chalcopyrite with other minerals in the Spence leach residue.	134
Figure 4.29	Mineral map of the residue from dissolution of the Spence concentrate showing sulfur (blue) associated with pyrite (black).	135
Figure 4.30	Optical micrograph showing globular sulfur and uncoated chalcopyrite particles in the Spence leach residue.	135
Figure 4.31	Association of chalcopyrite with other minerals in the Ok Tedi leach residue.	137
Figure 4.32	Partial mineral map showing sulfur associated with pyrite in the leach residue of the Ok Tedi concentrate.	137
Figure 4.33	Optical micrograph globular sulfur in the Ok Tedi leach residue.	138
Figure 4.34	Size distribution for dry-screened Ok Tedi head samples (+25-38 μm) compared with the leach residue.	138
Figure 5.1	The effect of solution potential on the extent of copper dissolution from OKTedi after 24 h in the presence of chloride.	143
Figure 5.2	The effect of solution potential on the extent of copper dissolution from OKTedi after 24 h in the absence of chloride	144
Figure 5.3	Copper dissolution from Andina concentrate under electrochemical control. (a) 560 mV, (b) 580 mV, (c) 600 mV and (d) 610 mV.	148
Figure 5.4	Copper dissolution from Andina concentrate under electrochemical control. (a) nitrogen, (b) oxygen, (c) reactor sealed and (d) air.	149

Figure 5.5	Concentration of dissolved oxygen. (b) oxygen, (c) reactor sealed and (d) air.	149
Figure 5.6	Copper dissolution from Andina chalcopyrite concentrate at 35 °C under air control. (a) 540 mV (b) 560 mV, (c) 580 mV, (d) 600 mV and (e) 620 mV.....	151
Figure 5.7	Andina +25-38 µm mineral size distribution.....	156
Figure 5.8	CCHYP -38 µm mineral size distribution	156
Figure 5.9	PQS2 -38 µm mineral size distribution	156
Figure 5.10	Pinto Valley (PV) -38 µm mineral size distribution.....	157
Figure 5.11	Dissolution of copper from chalcopyrite concentrates from different localities.....	158
Figure 5.12	Dissolution of CCHYP concentrate under standard conditions at different nominal potential set-points as controlled by nitrogen addition. (a) 560 mV, (b) 580 mV, (c) 600 mV, (d) 620 mV, (e) 640 mV and (f) 660 mV.	159
Figure 5.13	Dissolution of CCHYP concentrate under standard conditions and a higher chloride ions concentration at 660 mV with the oxygen control system. (a) 50 g L ⁻¹ chloride ions, (b) standard conditions and (c) 50 g L ⁻¹ chloride ions.	160
Figure 5.14	Dissolution of CCHYP concentrate in 0.2 M HCl, 0.5 g L ⁻¹ Cu(II) and 50 g L ⁻¹ chloride ions at various potentials	161
Figure 5.15	Dissolution of copper from Andina concentrate under standard conditions initially at low potential (450 mV) and subsequently at the optimum potential (550 mV). (a) potential increased after 600 h, (b) potential increased after 900 h, and (c) potential at 580 mV throughout.	162
Figure 5.16	Chalcopyrite electrode after immersion in a solution containing 0.2 M HCl and 0.5 g L ⁻¹ Cu(II) at a potential of 450 mV for several days.....	163

Figure 5.17	Same electrode as above immersed in the standard solution at 650 mV for one week.....	163
Figure 5.18	Association of chalcopyrite with other sulfides (the fraction of free surface of the mineral boundary that is in contact with other minerals in a polished section.)	165
Figure 5.19	Optical micrograph showing the replacement of chalcopyrite by covellite and chalcocite after 936 h of dissolution of Andina concentrate under standard conditions at a low potential (450 mV).	166
Figure 5.20	Partial mineral map of the residue after 936 h of dissolution at low potential (450 mV) showing free chalcopyrite particles.	166
Figure 5.21	Optical micrograph of replacement of chalcopyrite by covellite and chalcocite after 2640 h of dissolution of Andina concentrate under standard conditions at 550 mV.....	168
Figure 5.22	Optical micrograph showing covellite associated with partially reacted chalcopyrite and pyrite after 2640 h of dissolution of Andina concentrate under standard conditions at 550 mV.168	
Figure 5.23	Mineral maps after 2640 h of leaching illustrating most of chalcopyrite particle are free and few of them rimmed by sulphur.	169
Figure 5.24	Mineral maps after 2640 h of leaching illustrating elemental sulfur.	169
Figure 6.1	Effect of temperature on the rate of dissolution of copper from Andina chalcopyrite concentrate in 0.2 M HCl and 0.5 g L ⁻¹ Cu(II) under controlled potential of 580 mV.....	175
Figure 6.2	Effect of temperature on the rate of dissolution of copper from CCHYP concentrate in 0.2 M HCl, 0.5 g/L Cu(II) and 50 g L ⁻¹ Cl ions at a controlled potential of 580 mV.....	176
Figure 6.3	Arrhenius plot for the dissolution of chalcopyrite from Andina 25-38 µm concentrate between 25 and 65 °C under standard conditions	178

Figure 6.4	Arrhenius plot for the dissolution of chalcopyrite from CCHYP -38 μm concentrate between 25 and 65 $^{\circ}\text{C}$ under standard conditions	179
Figure 6.5	Effect of NaCl concentration on copper extraction from +25-38 μm Andina concentrate in 0.2 M HCl, 0.5 g L^{-1} Cu^{2+} at 35 $^{\circ}\text{C}$	181
Figure 6.6	Effect of NaCl concentration on copper extraction from -38 μm CCHYP concentrate in 0.2 M HCl, 0.5 g L^{-1} Cu^{2+} at 35 $^{\circ}\text{C}$..	182
Figure 6.7	Variation of pH during dissolution of Andina concentrate in a solution containing 0.2 M HCl, 0.5 g L^{-1} Cu^{2+} at 35 $^{\circ}\text{C}$ with various chloride concentrations.....	182
Figure 6.8	Effect of initial cupric ion concentration on copper dissolution from 25 -38 μm Andina concentrate in 0.2 M HCl at 35 $^{\circ}\text{C}$	184
Figure 6.9	Effect of ferrous ion concentration on the dissolution of copper from 25-38 μm Andina concentrate in 0.2 M HCl at 35 $^{\circ}\text{C}$...	185
Figure 6.10	Leaching curves for the dissolution of two size fractions of Andina chalcopyrite sample in chloride media at 35 $^{\circ}\text{C}$	186
Figure 6.11	Effect of the type of agitation on the rate of dissolution of Andina concentrate . a) Instrumented reactor with Ti impellor, b) Magnetically stirred.	188
Figure 6.12	Effect of increasing pulp density on the rate of dissolution of Andina concentrate.	189
Figure 6.13	The effect of pH on the rate of dissolution of Andina chalcopyrite concentrate.....	191
Figure 6.14	The effect of pH on the solution potential during the initial stage of dissolution of Andina concentrate at low and high pH	191
Figure 6.15	Sensitivity of potential to small change of dissolved oxygen during the leaching of Andina chalcopyrite concentrate at low pH (pH 0.34).	192

Figure 6.16	The effect of pH on the rate of dissolution of CCHYP chalcopyrite concentrate.....	192
Figure 6.17	Comparison of the rates of dissolution of copper and iron from the CCHYP concentrate at pH 2. Conditions as in Fig. 6.16.	193
Figure 6.18	Effect of pH on the modal mineralogy of the residues from the dissolution of Andina concentrate at different pH values.....	194
Figure 6.19	Department of sulfur in the residues from dissolution at various pH values.	195
Figure 6.20	Dissolution of copper and iron from CCHYP concentrate leached under standard conditions at a controlled potential of 580 mV at 35 °C.	198
Figure 6.21	Mineral dissolution from CCHYP concentrate leached under standard conditions.	199
Figure 6.22	Dissolution of copper obtained from MLA and solution analyses.	200
Figure 6.23	Dissolution of iron obtained from MLA and solution analyses	200
Figure 6.24	Sulfur association with other sulfides during leaching of CCHYP concentrate.....	201
Figure 6.25	Chalcopyrite association with other sulfides during leaching of CCHYP concentrate.	202
Figure 6.26	Optical micrograph of CCHYP concentrate sample after 144 h of leaching.	203
Figure 6.27	Partial mineral map of CCHYP concentrate after 144h of leaching under standard conditions chalcopyrite (bright green), pyrite (black), covellite (red), bornite (aqua), enargite (yellow).....	203
Figure 6.28	Optical micrograph of CCHYP concentrate sample after 264 h of leaching.	205

Figure 6.29	Partial mineral map showing liberated, uncoated chalcopyrite particles after 264 h of dissolution. Chalcopyrite (bright green), pyrite (black), covellite (red), bornite(aqua), enargite (yellow).	205
Figure 6.30	Optical micrograph of CCHYP concentrate sample after 432 h of leaching.	206
Figure 6.31	Partial mineral map showing liberated chalcopyrite (bright green) after 432 h of leaching.	207
Figure 6.32	Optical micrograph of CCHYP chalcopyrite concentrate sample after 528 h of leaching.	208
Figure 6.33	Partial mineral map showing largely liberated chalcopyrite particles after 528 h of leaching, chalcopyrite (bright green), pyrite (black), bornite (aqua) and sulfur(green).	208
Figure 6.34	Optical micrograph of CCHYP concentrate sample after 696 h of leaching.	209
Figure 6.35	Partial mineral map showing liberated chalcopyrite after 696 h of leaching.	209
Figure 6.36	Partial mineral map after 696 h of leaching showing (a) liberated pyrite (black) and sulfur particles and (b) chalcopyrite (bright green) and sulfur grains (green).	210
Figure 7.1	Typical EDS spectrum of pyrite particles.	220
Figure 7.2	Particle size distribution of -25 μm pyrite sample.	220
Figure 7.3	Particle size distribution of milled -25 μm pyrite sample.	221
Figure 7.4	Dissolution of 12 μm pyrite. (a) Standard conditions 0.2 M HCl and 0.5 g L ⁻¹ Cu(II) at 35 °C, (b) as in (a) after adjustment of the pH to 2.0	222
Figure 7.5	Optical micrograph showing pyrite particles in the residues after leaching for 800 h under standard conditions.	222

Figure 7.6	The effect of pyrite (25-38 μm) on the rate of copper extraction from Andina concentrate (25-38 μm) at 35 $^{\circ}\text{C}$	223
Figure 7.7	The effect of pyrite (25 μm) on the rate of copper extraction from PQS2 concentrate (-38 μm) at 35 $^{\circ}\text{C}$	224
Figure 7.8	Effect of pyrite on the rate of copper extraction from Andina concentrate at various ratios of chalcopyrite to pyrite at 35 $^{\circ}\text{C}$. Ratios (a) 1:0, (b) 1:1, (c) 1:5 with 12 μm pyrite particles (d) 1:5 with 5 μm pyrite particles.....	225
Figure 7.9	Effect of pyrite on the pH during dissolution of Andina concentrate at various ratios of CuFeS_2 to FeS_2 . Conditions as in Figure 7.8.	225
Figure 7.10	Comparison of the effect of pyrite on the dissolution of covellite and chalcopyrite (a) covellite, (b) covellite: pyrite ratio 1:5, 25-38 μm pyrite, (c) covellite: pyrite 1:5 ratio, 12 μm pyrite and (d) as in (c) but with chalcopyrite.....	226
Figure 7.11	Department of sulfur in residues after dissolution of Andina concentrate in the presence of fine pyrite.....	228
Figure 7.12	Mineral map of Andina concentrate residue after dissolution under standard conditions. Pyrite (black), chalcopyrite (bright green), sulfur (green) and enargite (yellow).....	229
Figure 7.13	Partial mineral map of chalcopyrite and sulfur after dissolution in the presence of fine pyrite (12 μm) in a ratio of 1:5 under standard conditions. Chalcopyrite particles are bright green and sulphur green.	230
Figure 7.14	Partial mineral map showing layers of sulfur around fine pyrite particles. Pyrite particles are black and sulfur green. Conditions as in Figure 7.13.	230
Figure 7.15	Partial mineral maps of residual covellite after dissolution using (a) standard conditions in the absence of pyrite, (b) standard conditions with addition of pyrite (12 μm) at a ratio of 1:5. Covellite particles are shown in red and sulfur blue/green.	233

Figure 7.16	Effect of the addition of 1ppm of silver on the dissolution of several concentrates under standard conditions. The results obtained in the absence of silver ions are shown as the solid lines.	234
Figure 7.17	Effect of silver ions (1 ppm) on the dissolution of CCHYP concentrate (a) Standard conditions at 580mV, (b) 0.2 M HCl, 0.5 g L ⁻¹ Cu(II) and 50 g L ⁻¹ chloride ions at 580 mV and (c) 0.2 M HCl, 0.5 g L ⁻¹ Cu(II) and 50 g L ⁻¹ chloride ions at 650 mV. Results obtained in the absence of silver ions shown as solid lines.	235
Figure 7.18	Effect of pyrite and silver ions on the rate of dissolution of PV concentrate under standard conditions (a) addition of 1 ppm Ag, (b) addition of Ag followed by addition of pyrite (12 μm), (c) addition of pyrite (12 μm) followed by addition of Ag and (d) addition of pyrite and Ag at the beginning.	236
Figure 7.19	Concentration of silver ions during dissolution of PV concentrate under standard conditions. (a) Addition of 1 ppm Ag, (b) addition of pyrite (12 μm) followed by addition of 1 ppm Ag and (c) addition of pyrite and Ag at the beginning.....	237
Figure 8.1	Oxidative leaching of chalcopyrite	244
Figure 8.2	Non-oxidative leaching of chalcopyrite in chloride media	246
Figure 8.3	Catalytic effect of pyrite on chalcopyrite leaching	247
Figure 8.4	Species distribution in a saturated solution of CuS in 0.2 M HCl with increasing concentration of NaCl at 35 °C	248
Figure 8.5	Formal potentials of the various couples in the system Cu(II)/Cu(I)/S/Cl at 25 °C at various chloride concentrations	250
Figure 8.6	Apparatus for dissolved oxygen measurements.....	252
Figure 8.7	The consumption of dissolved oxygen at 35°C in 4 mL of 0.2 M HCl + 0.8 M NaCl solution after addition of 40 μL 0.01 M S ⁻² solution (data taken from Hajime Miki personal communication).	253

Figure 8.8	Experimental curve for the consumption of dissolved oxygen on addition of 40 μL 0.01 M S^{-2} solution to 4 mL of 0.2 M HCl + 0.8 M NaCl + 0.5 g L^{-1} Cu(II) at 35 $^{\circ}\text{C}$ (data taken from Hajime Miki personal communication).	254
Figure 8.9	Experimental curve for the consumption of dissolved oxygen on addition of 40 μL 0.0191 M Cu(I) solution to 4 mL of 0.2 M HCl + 0.8 M NaCl + 0.5 g L^{-1} Cu(II) at 35 $^{\circ}\text{C}$ (data taken from Hajime Miki personal communication)	255
Figure 8.10	1 st and 2 nd order kinetic plots of the data from Figure 8.8....	257
Figure 8.11	Plot of the data in Fig. 6 according to the overall rate equation (8.16) with $k_2 = 1 \times 10^{-5} \text{M}$	259
Figure 8.12	First- and second-order plots for the rate of consumption of dissolved oxygen on addition of 40 μL 0.01 M S^{-2} solution to 4mL of 0.2 M HCl + 0.8 M NaCl + 0.05 g L^{-1} Cu(II) at 35 $^{\circ}\text{C}$	260
Figure 8.13	The effect of initial copper(II) concentration on the rate of consumption of oxygen at 35 $^{\circ}\text{C}$ in 4 mL of 0.2 M HCl + 0.8 M NaCl with addition of either 40 μL or 20 μL 0.01 M S^{-2} solution.	266
Figure 8.14	The effect of initial copper(II) concentration on the rate of consumption of oxygen at 35 $^{\circ}\text{C}$ in 4 mL of 0.2 M HCl with addition of 40 μL 0.01M S^{-2} solution.	266
Figure 8.15	The effect of copper(II) concentration on the first-order rate constant at 35 $^{\circ}\text{C}$ in 4 mL of 0.2 M HCl + 0.8 M NaCl with addition of 40 μL 0.01 M or 0.005 M S^{-2} solution.	267
Figure 8.16	The effect of the concentration of chloride on the rate constant at 35 $^{\circ}\text{C}$ in 4 mL of 0.2 M HCl + 0.5 g L^{-1} Cu(II) + x M NaCl	269
Figure 8.17	The effect of pH on the rate constant at 35 $^{\circ}\text{C}$ in 4 mL of x M HCl + (1-x) M NaCl + 0.5 g L^{-1} Cu(II).....	270
Figure 8.18	Consumption of dissolved oxygen at 35 $^{\circ}\text{C}$ in 4 mL of 0.2 M HCl + 0.04 g pyrite suspension with and without addition of 40 μL 0.1 M S^{-2} solution.	271

LIST OF TABLES

Table 2.1	Thermodynamic data for possible reactions in the dissolution of chalcopyrite at 25 °C (Unit activity of soluble species)	12
Table 2.2	Advantages and disadvantages of chloride processes.....	17
Table 2.3	Chloride Processes.	18
Table 3.1	Chemicals Reagents	75
Table 3.2	Chemical data (% elemental composition)	77
Table 3.3	Trace element composition (ppm)	77
Table 3.4	Mineralogical composition of concentrates (Wt%).....	78
Table 3.5	CSR (copper source ratio) of major copper minerals	79
Table 3.6	Conversion of potential measurements to the SHE scale....	91
Table 4.1	Leaching conditions of shake flask experiments	100
Table 4.2	Leaching conditions of instrumented reactor experiments in air	100
Table 4.3	Rates of dissolution based on initial surface area (9 g of samples)	125
Table 4.4	Andina (dissolution rate shown in Figure 4.17) modal mineralogy (mass,%)	128
Table 4.5	PQS1 modal mineralogy (mass,%) (dissolution rate shown in Figure 4.17).....	131

Table 4.6	Spence modal mineralogy (mass,%).....	134
Table 4.7	Ok Tedi modal mineralogy (mass,%)	136
Table 5.1	Details of leaching conditions	146
Table 5.2	Chemical data (elemental composition, %)	152
Table 5.3	Mineralogical composition of concentrates (Wt, %)... ..	153
Table 5.4	Pyrite content and CSR (copper source ratio) (mass %) of major copper minerals in concentrates.....	154
Table 5.5	Percentage of chalcopyrite in head samples associated with other sulfide minerals	154
Table 5.6	Traces element analyses (ppm)	155
Table 5.7	Chemical analysis of samples (mass %) as obtained by MLA of Andina concentrate (+25-38 μm) and residues after dissolution under the conditions of Test (b) in Figure 5.15	164
Table 5.8	Modal mineralogical analysis (mass %) of Andina concentrate (+25-38 μm) and residues after dissolution under the conditions of Test (b) in Figure 5.15	165
Table 5.9	Copper recovery based on solution and residue analyses ..	170
Table 6.1	Experimental conditions of leaching tests studied	174
Table 6.2	Rate constants as a function of temperature for leaching of 25-38 μm Andina chalcopyrite concentrate	177
Table 6.3	Rate constants as a function of temperature for leaching of -38 μm of CCHYP chalcopyrite concentrate	177
Table 6.4	Initial surface area of chalcopyrite present in each concentrate	187

Table 6.5	Chemical assay data (%) obtained from MLA analyses for Cu, Fe S and Si in CCHYP concentrate samples taken during leaching with 0.2 M HCl-0.5 g L ⁻¹ Cu ²⁺ at 35 °C at a controlled potential of 580 mV.....	197
Table 6.6	Modal mineralogy analyses (weight %) for CCHYP concentrate samples during leaching in 0.2 M HCl-0.5 g L ⁻¹ Cu ²⁺ at 35 °C at a controlled potential of 580 mV.....	197
Table 6.7	Copper recoveries based on solution and residue analyses	211
Table 7.1	Experimental conditions of leaching tests.....	217
Table 7.2	Pyrite content (mass %) and CSR (copper source ratios) in the concentrates.....	218
Table 7.3	Association (mass %) of chalcopyrite with others minerals .	219
Table 7.4	Modal analysis of residues (mass%)	227
Table 7.5	Trace elements in concentrates (ppm)	232
Table 7.6	Copper recoveries based on solution and residue analyses	238
Table 8.1	Experimental conditions and results of oxidation of copper(I) at 35 °C.	261
Table 8.2	Experimental conditions and results of experiments with [H ₂ S] ₀ =0.1 mM.	263
Table 8.3	Experimental conditions and results of experiments with [H ₂ S] ₀ = 0.05 mM	264

1.INTRODUCTION

The extractive metallurgy of copper is based largely on traditional pyrometallurgical processes (mineral processing, smelting, electro refining). In recent years, hydrometallurgical processes (dump and heap leaching, SX-EW) have been widely applied to low grade ores as alternatives to pyrometallurgy. These methods not only reduce environmental pollution, but also offer many other potential advantages. These advantages include the formation of elemental sulphur rather than sulphur dioxide, viability at either small or large scale, lower capital and operating costs and greater ease of control.

On the other hand, it is well known that the leaching of chalcopyrite (CuFeS_2), which is the most important and abundant copper mineral has very slow kinetics. A substantial amount of research work has been undertaken in order to enhance the leaching rate of this mineral, but this has not been fully successful and the mechanism of dissolution is still the subject to considerable controversy.

The generally higher reactivity of sulfide minerals in chloride as opposed to sulfate solutions has resulted in many studies of chloride systems for the hydrometallurgical treatment of sulfide minerals. A comparison of chloride and sulfate based leaching

processes shows that there are various advantages associated with the former. Thus, chloride leaching can be carried out at ambient temperatures whereas sulfate processes generally require elevated temperatures. In addition, in chloride systems, the copper(I) ion is stable and this allows the use of copper(II) ions as an oxidant in addition to iron(III). In the case of chalcopyrite, several aspects still require clarification such as the role of impurities, mineral particle size and origin, the nature of the passivation layer and the deportment of sulfur.

The dissolution of sulfide minerals, and, in particular, the passivation of chalcopyrite are potential-dependent reactions and many studies have been carried out in order to establish the relationship between the solution potential and the leaching rate. It is now well known that the leaching rate in sulfate solutions is dependent on the potential and that the rate is enhanced in a certain potential range (Nicol and Lazaro, 2002). Many studies have been devoted to the elucidation of the potentials at which dissolution is possible and at which apparent passivation occurs. Thus, Nicol and Lázaro (2003) used electrochemical and chemical experiments to establish the relevant leaching potential region as being 0.45 to 0.75 V under appropriate experimental conditions. However, few actual dissolution studies (Hiroyoshi et al., 2000; Rivera-Velasquez et al., 2006; Third et al., 2002) have been conducted under controlled potential conditions, particularly in chloride media.

In order to enhance the rate of leaching of chalcopyrite, several catalysts and/or promoters have been proposed such as pyrite, activated carbon and the ions of Ag(I), Sn(II), Co(II), Hg(II), Bi(III) and Mn(II). The effect of pyrite on the leaching of chalcopyrite has been investigated by some researchers (Abraitis et al., 2004; Al-Harashseh et al., 2006a; Dutrizac, 1982; Harmer et al., 2006; Parker et al., 2003). Most

of these investigations have focused principally on the role of galvanic interactions in the leaching of sulfide minerals. It has been postulated that when chalcopyrite and pyrite are in intimate electrical contact with each other they form a galvanic couple as a result of which chalcopyrite behaves as an anode and dissolves more rapidly, while pyrite behaves as a cathode. However, none of these investigations has directly verified the formation of such galvanic couples by electrochemical experiments.

A number of investigations have been conducted to elucidate the reaction kinetics and delineate the important variables for the leaching of chalcopyrite in both chloride and sulfate systems. Although relevant work has been reported by many researchers, some ambiguities still remain.

The potential dependence of the rate of dissolution of chalcopyrite in sulfate solutions has been reported by Hiroyoshi et al. (2000) and a reaction model proposed according to which the rate of leaching is enhanced as a result of reduction of chalcopyrite by iron(II) to chalcocite in the presence of copper(II) ions. The more reactive chalcocite is, in turn, oxidized by iron(III) more rapidly than chalcopyrite. In this mechanism, the iron(II)/iron(III) couple acts, unusually, as simultaneously both reducing and oxidizing. In this thesis, an alternative reaction model based on a non-oxidative process in which chalcopyrite dissolves or is converted to a covellite-like species by a non-oxidative reaction coupled to oxidation of hydrogen sulfide by one of several oxidants as described by Nicol et al. (2003) is applied to the chloride system. A crucial step in this mechanism is the rate of oxidation of hydrogen sulfide and this thesis addresses this aspect as part of the overall mechanism in chloride solutions containing copper(II) ions as the main oxidant.

The present study involved the following objectives:

- To obtain fundamental data on the kinetics of dissolution of chalcopyrite in acidic chloride and mixed chloride/sulfate solutions.
- To establish the role of the important parameters in the rate of leaching of chalcopyrite from minerals and concentrates.
- To establish the role of silver and pyrite in the rate of leaching of chalcopyrite.
- To establish a mechanism(s) for the dissolution of chalcopyrite in acidic chloride solutions.

This thesis is divided into 9 chapters. The following chapter is devoted to a detailed literature review on fundamental studies of chalcopyrite oxidation and dissolution while a brief overview of the development of copper hydrometallurgy and current commercial and demonstration scale processes is also presented.

The methods and materials used in this study are presented in chapter 3. This includes a full mineralogical and chemical description of each mineral used in the leaching experiments and a specific description of each method to control potential on the leaching experiments.

Chapters 4 to 8 are devoted to the experimental investigations and discussion of the results. Each chapter contains an introduction to the research field, presentation of results and discussion of their implications followed by a summary section. Chapter 4 presents all the preliminary leaching experiments using a simple shake-flask technique and subsequently in instrumented stirred reactors in order to establish the effects of various parameters on the rate of dissolution. Detailed mineralogical analyses have been used to complement the leaching testwork.

Chapter 5 starts by defining the potential range for optimum chalcopyrite leaching using three different potential control systems and by establishing whether or not chalcopyrite concentrates from different localities leach at different rates under the same conditions. A more detailed study of the effects of a number of leach parameters on the rate of dissolution of chalcopyrite from several concentrates is presented in Chapter 6. Chapter 7 summarizes the results of a study of the catalytic effect exerted by pyrite and silver ions on the dissolution of chalcopyrite in chloride media. Chapter 8 summarizes the mechanism proposed to explain the dissolution of chalcopyrite in chloride media while Chapter 9 highlights the experimental findings of this investigation and makes some conclusions about the mechanism of the dissolution of chalcopyrite.

2. LITERATURE REVIEW

2.1. *General properties of chalcopyrite*

2.1.1. The nature of chalcopyrite

Chalcopyrite is a copper iron sulphide mineral with a theoretical composition by mass of 34.6% Cu, 30.5% Fe and 34.9% S. Its name is derived from the Greek word *chalkos* which means copper and *pyros* which means fire. Chalcopyrite is a deep brass yellow mineral that looks like pyrite but it tarnishes to a bronze colour. Chalcopyrite is predominantly found in porphyry copper and hydrothermal vein deposits. In these deposits it is normally associated with pyrite (FeS_2), bornite (Cu_5FeS_4), sphalerite (ZnS), chalcocite (Cu_2S), covellite (CuS), enargite (Cu_3AsS_4) or molybdenite (MoS_2), frequently in a quartz (SiO_2) matrix with other minerals like tourmaline $((\text{Na,Ca})(\text{Mg,Fe,Li})_3\text{Al}_6(\text{BO}_3)_3(\text{Si}_6\text{O}_{18})(\text{OH})_4)$ or chlorite $((\text{Mg,Fe,Al})_6(\text{Al,Si})_4\text{O}_{10}(\text{OH})_8)$. Chalcopyrite is also found together with other secondary enrichment minerals such as azurite, malachite, cuprite, native copper, chrysocolla, and turquoise (Hurlbut Cornelius S., 1998). In terms of value it is

interesting to compare the percentage of copper in the main sulphide minerals being native copper, 100%; chalcocite, 79.8%; covellite, 66.4% and chalcopyrite, 34.6%.

2.1.2. Physical properties

The crystal habit resembles two opposing wedges constituting a tetrahedron. The average density is 4.1 to 4.3 Kg m⁻³. It is moderately hard being 3.5 to 4.0 on the Mohs scale (Habashi, 1978). It often has poor cleavage properties and tends to fracture conchoidally. The resistivity of chalcopyrite ranges between 150-9000 x 10⁻⁶ Ωm (Koch 1975; cited reference in Habashi, 1978). Stable α-chalcopyrite transforms to a cubic β-chalcopyrite form accompanied by a minor loss of sulphur (<1%) at 550 °C (Habashi, 1978). This phase is isostructural with sphalerite. The system is complex with bornite (Cu₅FeS₄), and talnakhite (Cu₉Fe₈S₁₆) appearing at intermediate transition temperatures (Habashi, 1978).

2.1.3. Structure

In a hydrometallurgical process the nature of the minerals present are important in determining the rate of dissolution during leaching. For example, under acidic oxidizing conditions, copper is dissolved very much more rapidly from chalcocite than it is from chalcopyrite. Several investigators have attempted to explain these differences in terms of the nature and interatomic distances in the crystal structure lattices. Chalcopyrite is tetragonal with c = 525 pm and a = 1032 pm and is based on the zinc blende unit cell with four zinc atoms being replaced by two copper and two iron atoms (Figure 2.1). Thus, the chalcopyrite unit cell is twice the volume of the unit cell of sphalerite. Each metal atom is coordinated by a tetrahedron of sulphur atoms and each sulphur atom by a

tetrahedron of metal atoms (2 copper and iron) (Habashi, 1978). Sulphur atoms are displaced slightly from the centre of the metal tetrahedral towards the iron-iron axis with inter-atomic distances $d_{\text{Cu-S}}=2.30 \text{ \AA}$, $d_{\text{Fe-S}}=2.26 \text{ \AA}$ and $d_{\text{Cu-Fe}}=d_{\text{Cu-Cu}}=d_{\text{Fe-Fe}}=3.71 \text{ \AA}$ (Edelbro et al., 2003).

The oxidation state of the cations in chalcopyrite has been subject to considerable controversy. While some researchers claim, on the basis of spectroscopic studies, that copper is present as Cu(I) and iron as Fe(III), others postulate an oxidation state intermediate between $\text{Cu}^+\text{Fe}^{3+}(\text{S}^{2-})_2$ and $\text{Cu}^{2+}\text{Fe}^{2+}(\text{S}^{2-})_2$ (Habashi, 1978).

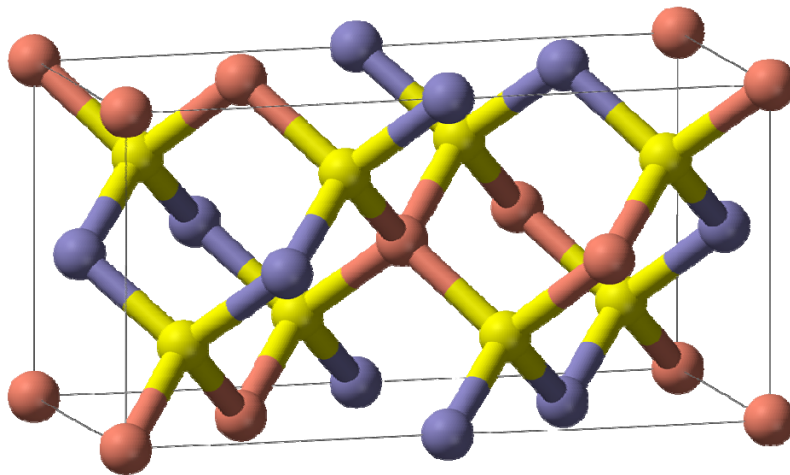


Figure 2.1 Unit-cell model of chalcopyrite. Copper is shown in red, iron in blue and sulfur in yellow. (Britannica Concise Encyclopedia).

2.1.4. Electronic properties

The semiconductor properties of chalcopyrite can be important in minerals processing and in hydrometallurgy as both processes are influenced by the properties of the mineral surface. Chalcopyrite behaves as a typical semiconductor. At room temperature chalcopyrite possesses n-type conduction (electron donation to the conduction band)

with band gap of 0.5 eV, 0.33 eV and 0.6 eV (Parker, 2005). An n-type semiconductor should favour chemisorption of cations and a p-type favour (electron acceptor to the conduction band) sorption of anions. However, it is possible to modify the surface of a mineral from n-type to p-type and vice versa (Parker, 2005). Crundwell (1988) suggested that the electronic structure of the solid must be considered in any fundamental study of the anodic behaviour of semiconducting minerals. Due to the relatively small band gap (less than 0.6 eV) it is likely that both holes and electrons can contribute to the dissolution. A more detail discussion of the electronic properties of chalcopyrite can be found in Crundwell (1988) and Parker (2005).

According to Habashi (1978), chalcopyrite undergoes two phase transformations at 550 and 657 °C (Neel temperature) both with a slight loss of sulphur. The first is $\alpha - CuFeS_2(\text{tetragonal}) \rightarrow \beta - CuFeS_2(\text{cubic})$ and the second is an antiferromagnetic transition. These lead to an irreversible increase in conductivity due to the loss of sulphur.

2.1.5. Thermodynamics of the dissolution of chalcopyrite

In order to establish suitable aqueous conditions for the leaching of a particular mineral, Eh-pH diagrams are invaluable in identifying the predominant species present at equilibrium with respect to the reduction potential and the hydrogen ion concentration. The diagrams also enable one to identify intermediate solid phases that could form during decomposition. However, Eh-pH diagrams represent only the equilibrium and do not indicate which leaching pathway will be the most appropriate nor the kinetics of the reactions involved. In the case of chalcopyrite, the diagram is very complex and does

not reflect the observed behaviour of the mineral during leaching in acidic solutions. This is due to the high thermodynamic stability of the sulfate ion relative to the other sulphur species. In addition, the focus of this project is on the leaching of chalcopyrite in acidic chloride solutions and inclusion of the effect of chloride in the diagram will add to the complexity. In the light of these limitations of the use of Eh-pH diagrams in this case, the thermodynamics will be dealt with in terms of the actual reactions considered likely in this system.

In general, the thermodynamics of the dissolution of chalcopyrite can be summarized in the Cu-Fe-S-H₂O Eh-pH diagram at 25 °C. Figure 2.2 is a partial diagram with a focus on the copper sulphide minerals only in the absence of any complexing ligands for the metal ions. In this diagram, elemental sulphur is metastable but is well known as the product of oxidation of these minerals in acidic solutions.

The diagrams generally shown in the literature for metal sulphides are drawn with sulfate included as a stable species. As it is well known, the introduction of sulfate results in diagrams do not reflect the chemistry of these systems in acidic solutions.

It is apparent from this diagram that chalcopyrite is unstable with respect to both chalcocite (Cu₂S) and covellite (CuS) at low potentials and oxidation of chalcopyrite could be expected to produce at least covellite as an intermediate product, especially at potentials close to 0.6 V under the conditions chosen for the diagram.

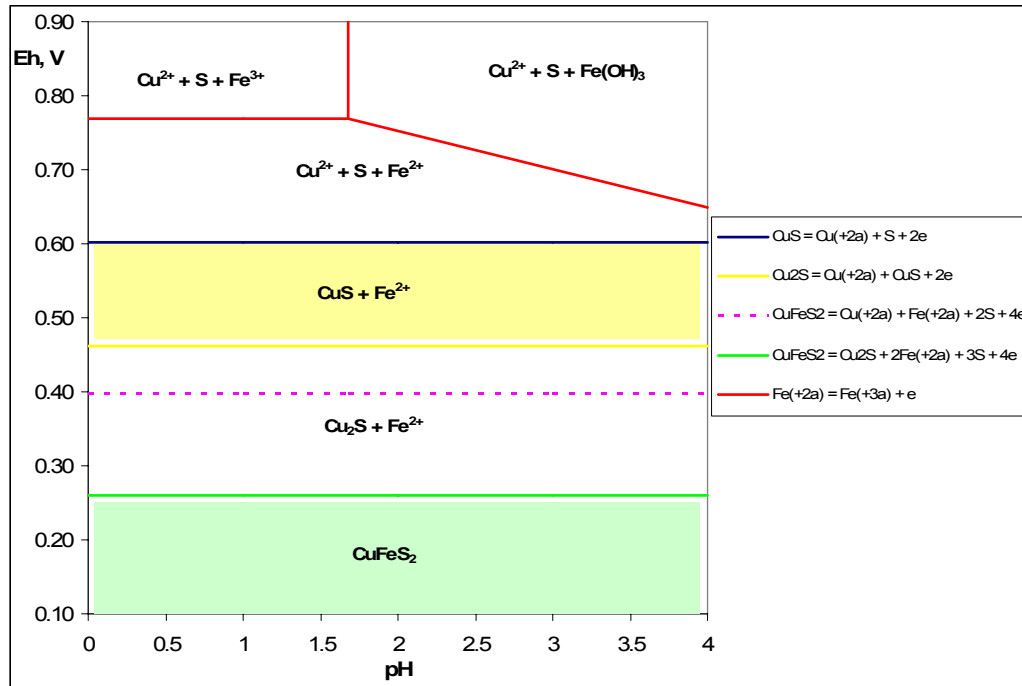


Figure 2.2 Partial Eh-pH diagram of Cu-Fe-S-H₂O at 25 °C, [Cu⁺²] = [Fe²⁺] = [Fe³⁺] = 0.1 M.

Table 2.1 presents thermodynamic information for a number of possible reactions and half-reactions as calculated using Outokumpu-HSC Ver. 6.0 software. The effect of chloride on these equilibria will be dealt with in Section 2.2.2.

Table 2.1 Thermodynamic data for possible reactions in the dissolution of chalcopyrite at 25 °C (Unit activity of soluble species)

Reactions	K	ΔG (KJ mol ⁻¹)	E° (V vs SHE)
Oxidative			
$CuFeS_2 = CuS + Fe^{2+} + S + 2e^-$		42.36	0.220
$2CuFeS_2 = Cu_2S + 2Fe^{2+} + 3S + 4e^-$		111.718	0.290
$CuFeS_2 = Cu^{2+} + Fe^{2+} + 2S + 4e^-$		164.009	0.425
Reductive			
$2CuFeS_2 + 6H^+ + 2e^- = Cu_2S + 2Fe^{2+} + 3H_2S$		28.788	0.149
$5CuFeS_2 + 12H^+ + 4e^- = Cu_5FeS_4 + 4Fe^{2+} + 6H_2S$		27.949	0.072
Non-oxidative			
$CuFeS_2 + 2H^+ = CuS + Fe^{2+} + H_2S$	2.642×10^{-3}	14.714	-
$CuFeS_2 + 4H^+ = Cu^{2+} + Fe^{2+} + 2H_2S$	8.928×10^{-20}	108.72	-
$2CuFeS_2 + 4H^+ = Cu_2S + Fe^{2+} + S + 2H_2S$	1.296×10^{-10}	56.431	-

Adapted from Lázaro- Báez (2001) and augmented

2.1.6. The leaching of chalcopyrite

Chalcopyrite is the most abundant copper sulfide mineral and pyrometallurgy is the main route for the production of copper from this mineral. This is partially due to the fact that the mineral is refractory to leaching for reasons that will be discussed at a later stage. There has been a vast amount of research work published in the area of oxidative leaching of chalcopyrite with the most common lixivants being sulfate, chloride, nitric

acid and ammonia. However, there is still few commercially operating full-scale leach plant for chalcopyrite concentrates or ore.

2.1.6.1. Sulfate Media

Most of the research has focussed on the use of sulphuric acid media in conjunction with various oxidizing agents, especially ferric ions, largely because of lower costs, minimal corrosion problems, and the ability to regenerate sulphuric acid during the electrowinning of copper. However, in these solutions chalcopyrite leaches more slowly than in chloride solutions. The oxidation of chalcopyrite with ferric ion in sulfate media can, depending on the conditions, produce variable proportions of sulphur or sulfate (Jones and Peters, 1976). Although a number of investigations have been conducted to elucidate the reaction kinetics, the actual mechanism remains controversial. Some researchers concluded that the leaching of chalcopyrite in sulfate media follows a parabolic rate (Dutrizac et al., 1969; Hackl et al., 1995; Munoz et al., 1979) while others have postulated linear kinetics over extended leaching periods under different conditions. (Jones and Peters, 1976; Majima et al., 1985).

2.1.6.2. Chloride

The superior leaching characteristics of chloride as a lixiviant ion have interested many researchers for the hydrometallurgical treatment of sulfide minerals. It has been found that the leaching rate of chalcopyrite in acidic chloride solutions is greater than that in sulfate solutions. A review by Flett (2002) included a comparison between chloride and sulfate based leaching processes and showed that there are various advantages in chloride leaching. Thus, chloride leaching can be carried out at ambient temperatures

compared to sulfate processes that require elevated temperatures that are not suitable for heap leaching of chalcopyrite. Pyrite is not attacked by chloride and according to Dutrizac (1992), most of the investigations have reported that more than 95% of the sulphide reports as elemental sulphur in chloride media. In the chloride system the copper(I) oxidation state is stable which allows electrodeposition of copper via a one electron transfer reaction, thus reducing energy consumption.

Recently, as a result of the fact that sulphuric acid and common salt are cheaper than hydrochloric acid, the use of a mixed acidic chloride/sulfate solutions has increased for the leaching of copper ores and concentrates containing chalcopyrite. Lu et al. (2000a) employed a mixed chloride-sulfate oxygenated solution to leach chalcopyrite under atmospheric pressure conditions. These researchers claimed that the addition of ferric ions (believed to be important in the overall leaching process) is not necessary because they are produced as the reaction proceeds and the concentration of ferric ions may be controlled by precipitation as natrojarosite.

According to Carneiro and Leão (2007), chloride enhancement of chalcopyrite leaching is due mainly to three reasons being the formation of chloro-complexes, the greater anodic activity in chloride media and changes to the morphology of surface and reaction products.

2.1.6.3. Nitrate

Due to its powerful oxidising properties, nitric acid also can be used for extraction of copper from chalcopyrite. Normally leaching takes place in the presence of sulphuric acid, which supplies additional protons for completion of the reaction. In the first stage the products are Cu(II) and Fe(III) and some of the sulphur formed will be oxidised to

sulphate. In the second stage nitric oxide gas from the leaching is captured and reconverted to nitric acid by oxidation with air and absorption in aqueous solution. The copper and iron are separated by crystallisation (Prasad and Pandey, 1998).

2.1.6.4. Ammonia

Another possible lixiviant for chalcopyrite is ammonia which has the advantage of being used in basic solution which alleviates the corrosion problems with chloride and the often high acid consumption by gangue minerals. Oxidants that have been used in the ammoniacal leaching of copper sulphides are bromates, chlorates, oxygen, peroxides and persulfates. However, attempts to leach chalcopyrite have failed or produced controversial results. The ammoniacal leaching system is complex and is influenced by a number of factors. The most accepted stoichiometry of the dissolution of chalcopyrite is as following



This process was developed by Anaconda Company and leaching takes place under pressure in presence of oxygen with vigorous agitation (Prasad and Pandey, 1998). Sulphur is converted to sulfate and copper is recovered from the leach liquor by solvent extraction and electrowinning, which requires conversion to an acidic sulphate electrolyte.

2.1.6.5. Bioleaching

The bioleaching of chalcopyrite occurs in an acidic medium that often contains a considerable concentration of Fe(III). It involves electrochemical and chemical

reactions of the mineral with the leach solution and the bacteria (Lopez-Juarez et al., 2006). At the present time more than 40 bacteria have been discovered (Watling, 2006). The most often used bacteria to leach chalcopyrite are mesophilic, acidithiobacillus ferrooxidans, thiobacillus thiooxidans, leptospirillum ferrooxidans and related acidophilic species (Gomez et al., 1997a). Even though bioleaching processes have been practiced for decades, the mechanism is still not resolved. Crundwell (2003) summarized three mechanisms by which microorganisms might interact with a sulphide mineral:

- i) The indirect mechanism, in which bacteria oxidize ferrous ions to ferric ions in the bulk solution and ferric ions leach the mineral.
- ii) The indirect contact mechanism, in which bacteria attached to the mineral surface oxidize ferrous ions to ferric ions within layer of bacteria and exopolymeric material and the ferric ions generated within this layer oxidize the mineral.
- iii) The direct contact mechanism, in which bacteria attached to the mineral surface oxidize the mineral directly by biological means without the need for ferric or ferrous ions.

The main disadvantage of bioleaching for chalcopyrite is the very slow extraction of copper (Watling, 2006). Many attempts have been made to explain the cause of this slow kinetics and to improve the bioleaching of chalcopyrite and several catalysts and/or promoters have been proposed (Gomez et al., 1997a; Hiroyoshi et al., 2002; Lopez-Juarez et al., 2006).

2.1.7. Chloride leaching processes for chalcopyrite

Numerous leaching studies have been advocated for the leaching of copper sulphides ores and concentrates in chloride media. Most of the studies agree that chloride processing of chalcopyrite offers several potential advantages over sulphate processing. Despite the apparent advantages of the chloride processing route for conventional chalcopyrite-rich copper concentrates, the technology is still under development. The main challenge is the requirement to overcome the slow and incomplete leaching of chalcopyrite at lower temperatures and to clarify the nature of the passive film on the chalcopyrite surface under variety of oxidative leaching conditions. In a recent study, Dreisinger (2006) reviewed new developments in commercial hydrometallurgy of primary copper sulphides.

The advantages and disadvantages of chloride processes over sulphate-based processes are summarized in Table 2.2. (Dreisinger, 2006; Peacey J., 2005).

Table 2.2 Advantages and disadvantages of chloride processes

Advantages	Disadvantages
Faster kinetics at low temperature and atmospheric pressure	Excessive corrosion
Very low sulphur to sulphate oxidation	Unconventional and difficult electrolysis step
Recovery of valuable by-products	Large energy requirements for mixing and oxygen dispersion
Use of existing capital. SX/EW	Poor quality copper product that requires electrorefining

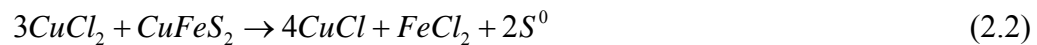
Table 2.3 Chloride Processes.

Processes	Status	Feed	Lixiviant	Temp. °C	Extraction	Purification	Observations	References
Bureau of Mines/Mintek	Obsolete	Concentrates	Ferric chloride	105	95% in 8 h	SX-EW	oxidation-hydrolysis route	(Dutrizac, 1992)
Cominco	Laboratory	Concentrates	Ferric chloride	95	99% in 12 h		Fe ₂ O ₃	(Dutrizac, 1992)
Cymet Clear	Pilot plant	Concentrate	FeCl ₃ -CuCl ₂ -NaCl	98	99%	H ₂ reduction	Atmospheric	(Wang, 2005)
	Commercial (1976-1982)	Concentrate	CuCl ₂ -FeCl ₃ -NaCl-KCl	105/150	High	Autoclave SX-EW	Pressure leach Jarosite/βFeO·OH	(Peacey J., 2005)
Minemet Recherche	Laboratory		CuCl ₂ -NaCl	100	98%	SX-EW	2-stage counter-current	(Dutrizac, 1992)
Cuprex GCM	Pilot Laboratory	Concentrate Concentrate	Ferric chloride FeCl ₃ -NaCl	95-100	>96% 99%	SX-EW Electrolysis-EW	Atmospheric 2 counter-current stages.	(Dalton et al., 1988) (Dutrizac, 1992)
Intec process	Pilot plant	Concentrates	Cu ²⁺ -BrCl ₂ ⁻ -NaCl-NaBr-air	85	98% after 12 h	Via diaphragm cell EW	Atmospheric. Oxygen supplied via air	(Moyes and Houllis, 2002)
Outokumpu	Demonstration plant under construction.	Copper Concentrates	Cu ²⁺ /Cl ₂ /NaCl/air	85-95	98%	EW	Atmospheric. 3-stage counter-current	(Lundstrom et al., 2005)
Antler. Noranda	Laboratory	Concentrates	HCl-CuCl ₂ -CuSO ₄	135-145		SX-EW	2 stages. Pressure	(Peacey J., 2005)
BHAS	Operating plant.	Copper-lead matte	H ₂ SO ₄ -Cl-	low	95%	SX-EW	Atmospheric. 100% Ag in residue at 15% Chloride	(Peacey J., 2005)
CESL	Plant , Operating	Chalcopyrite concentrates	H ₂ SO ₄ -Cl ion	150	95-98%	Autoclave. SX-EW	2-stages pressure. Sulphur recovery	(http://www.cesl.com)
Cuprochlor	Operating	Ore	H ₂ SO ₄ and CaCl ₂ 90g L ⁻¹ Chloride and 0.5 g L ⁻¹ Cu	25	90%	SX-EW	Agglomeration with acid and CaCl ₂ . Atmospheric	(Cuprochlor, 2001)
First Quantum Minerals, Kansanshi	Operating plant	Chalcopyrite concentrate	Acid and ferric ions	high	high	Autoclaves, SX/EW	Two autoclaves and a oxygen plant	(First Quantum Minerals, 2009)

Table 2.3 summarizes the most important proposed chloride processes for the leaching of sulfide minerals and several of the more important processes will be discussed in more detail in the following paragraphs while details of others can be found in the respective references provided.

2.1.7.1. CLEAR Process

The plant was closed in 1982 soon after commissioning due to economic reasons, which included the fact that the copper product did not meet LME specifications. The main leaching reactions were assumed to be:



Due to the high temperature and O₂ pressure of the second stage (150°C) a significant conversion of the mineral sulphide to sulfate occurred which, together with iron was controlled by precipitation of jarosite and β-FeO·OH. The CLEAR process (Dutrizac, 1992) achieved high copper extractions from chalcopyrite concentrate without SO₂ emission and few corrosion problems were found in the leaching. However, in the electrowinning stage besides the generation of Cu and CuCl₂, some Cl₂ gas was evolved and most of the silver leached was codeposited with copper.

2.1.7.2. Cuprochlor Process

The Cuprochlor heap leach process was developed in the Michicha mine in Chile. The originators claim that the process can be used on a variety of copper ores and also

chalcopyrite concentrates but there is no supporting evidence of the latter claim. The process consists of agglomeration of finely crushed ore with water, calcium chloride and sulphuric acid. The calcium chloride is dissolved in water and mixed with the ore where it reacts with sulphuric acid to form gypsum and chloride ions. Gypsum acts as a binding agent for the ore particles, improving the physical properties of the agglomerate. The formation of chloride ions stabilises cuprous ions and accelerates the regeneration of ferric ions. Copper in the leaching solution can be recovered by means of standard methods such as SX, cementation or direct electrowinning. (Cuprochlor, 2001).

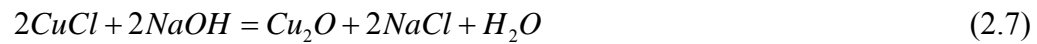
2.1.7.3. Outokumpu HydroCopper™ Process

In this recently developed process, a copper concentrate is leached in a strong sodium chloride solution (250-300 g dm⁻³) containing CuCl₂ in agitated reactors at atmospheric pressure. Air is necessary to precipitate iron. Almost all sulphide minerals are dissolved and elements such as Zn, Pb, Ni and Ag report to the leaching solution. In the last stage the redox potential of the solution increases to values such that gold is dissolved as a chloro-complex. The main reactions in the process are as follows



The pregnant leach solution typically contains Cu⁺, Cu²⁺ and other metals in minor amounts. A significant advantage of the process is that gold can be leached in the same circuit as copper as a chloro-complex and recovered with activated carbon. Copper is

recovered from the purified leach solution by precipitating copper(I) oxide using caustic soda and the product is reduced by hydrogen, melted and cast into a copper product (Reaction (2.7))



The main feature of this process is the use of chlor-alkali electrolysis technology to regenerate chemicals: sodium hydroxide solution to precipitate copper(I) oxide; chlorine for oxidation of the leaching solution; and hydrogen for reduction of copper(I) oxide (Olli Hyvarinen, 2005).

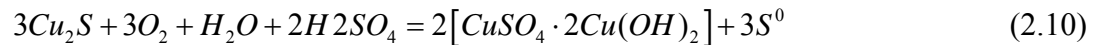
This process has been proven in a demonstration plant producing one ton of copper per day at Pori, Finland in 2003 and 2004 and has been found to be applicable for a number of different concentrates and is apparently tolerant of different impurities (Haavanlammi et al., 2005).

2.1.7.4. Intec Process

In this process which has been under development for a number of years, the main components of the leaching solution are sodium chloride, bromide and $BrCl_2^-$ which is produced at the anode in a unique electrowinning cell. Silver is precipitated with mercury as a chloride for further processing while gold is recovered onto activated carbon. High purity copper is electrowon in a special cell as a dendritic copper product, which is washed and dried under inert atmosphere then melted and cast. The Intec process has been developed and proven at both pilot plant scale and the demonstration plant scale (Wood, 2001).

2.1.7.5. CESL Copper Process

The CESL process is based on oxidation of sulfide concentrates at elevated pressure and temperatures in the presence of low concentrations of chloride ions. The concentrate slurry is fed to the autoclave in which the copper sulphides are oxidized to form basic copper sulphate (Reactions 2.8 to 2.10). A second stage atmospheric leach is incorporated to maximize copper extraction. Copper is recovered from solution by conventional SX/EW. Gold is recovered from the residue by cyanidation following elemental sulphur removal (Barr et al., 2005).

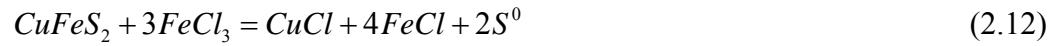
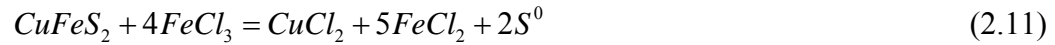


The CESL process has been proven with different concentrates at both pilot and demonstration plant scale. A plant known as “Usina Hidrometalúrgica Carajás” in Brazil operated by Sossego copper mine Vale was constructed during 2006-2007 and its commissioning commenced in early 2008 and it is expected to operate for at least 2 years (<http://www.cesl.com>). (CESL)

2.1.7.6. Cuprex Process

In the Cuprex process (Dalton et al., 1988) a copper concentrate is leached in two stages with excess of ferric chloride at atmospheric pressure after which the pregnant liquor is

sent to the extraction stage of the SX circuit and the resulting solution of copper chloride is then sent to the electrolysis section. The main reactions are:



The Cuprex process has several claimed advantages such as the production of high purity copper powders at high current efficiencies; the silver content of the copper is less than 1 ppm and the SX circuit is relatively straightforward and does not require pH control. On the other hand, the Cuprex process (Dutrillac, 1992) suffers disadvantages such as the ion-selective membrane cells used which will be difficult to maintain in a plant environment. Furthermore, electrowinning is carried out from the cupric state and particulate copper is produced.

Most of the above processes were carried out at low pressures and temperatures with finely milled ore or concentrates and leaching near the solution boiling point where required to obtain high extractions of copper from chalcopyrite. To ensure a high potential during leaching, oxygen is necessary to reoxidise Fe(II) and/or Cu(I). Normally in the presence of high concentrations of chloride some silver and gold remain in the leaching residue. Copper is recovered by SX/EW and silver by cementation. In some processes, gold is not recovered mainly due to presence of elemental sulphur in the residue or its association with pyrite.

There are several key problems in the use of chloride that must be resolved. Some of the most important of which are copper product purity and morphology, adoption of sulfate

SX techniques to solutions containing chloride, recovery of elemental sulphur and precious metals from the leach residues.

2.1.8. Passivation of chalcopyrite

Several studies have shown that chalcopyrite leach rates decrease with leaching time and eventually cease suggesting that dissolution has been inhibited by the formation of a passivating layer (Dutrizac, 1978; Dutrizac, 1990; Dutrizac et al., 1969; Parker et al., 1981; Peters, 1976). Electrochemical studies have confirmed that passivation occurs in the potential region associated with oxidative dissolution and is due to the formation of a surface layer that inhibits dissolution. There is also recent agreement that passivation occurs at a critical potential which is influenced by the chloride concentration, temperature and the presence of some impurities. Although many studies have addressed the nature of the passivating layer and the conditions under which it is formed, it is still probably the most controversial aspect of the leaching of chalcopyrite. As a result there are many proposals for the cause of passivation including the formation of a sulphur layer, a polysulfide or metal deficient layer and even precipitated iron compounds.

2.1.8.1. Sulphur layer

Although it is generally accepted that elemental sulphur is formed during leaching, many authors do not accept that sulphur is the cause of the passivation phenomenon. Dutrizac et al. (1989; 1990; 1969) claimed that in ferric chloride leaching of chalcopyrite, only elemental sulphur is formed and no intermediate phase between the elemental sulphur and chalcopyrite was observed. Klauber et al. (2001) examined

residues of chalcopyrite treated by acid ferric and ferrous sulfate and chloride solutions and claimed that elemental sulphur and disulphide surfaces are produced. Harmer et al. (2006) using X-Ray photoelectron spectroscopy (XPS), secondary ion mass spectrometry (TOF-SIMS) and scanning electron microscopy (SEM) of a chalcopyrite surface leached in perchloric acid suggested that the surface layers formed during chalcopyrite leaching occur in three steps. In the first step the polymerisation of S^{2-} to polysulfide S_n^{2-} occurs followed by the reformation of S^{2-} and other chain polysulfides which with further oxidation recrystallize to form crystalline sulphur. Lu et al. (2000b) postulated that chloride ions modify the morphology of the deposited sulphur which is more crystalline and porous, thus permitting the dissolution reaction to proceed. In addition, Havlik and Kammel (1995) obtained higher extractions in the presence of CCl_4 as a solvent for elemental sulphur produced during leaching of chalcopyrite in ferric chloride solutions.

2.1.8.2. Intermediate sulfide layer

Jones and Peters (1976) identified covellite (CuS) as an intermediate product in anodic dissolution of chalcopyrite. Later Ammou-Chokroum et al. (1981) and McMillan et al. (1982) in their study of the anodic dissolution of chalcopyrite in chloride media suggested the formation of a product layer consisting of covellite and elemental sulphur. They concluded that CuS dissolves and reforms, resides in the pores of the elemental sulphur and thus inhibits further dissolution. Furthermore, Parker et al. (1981) observed that blue covellite was formed on the surface of chalcopyrite which was oxidized at 0.4 V in acidic chloride solutions. They suggested that CuS may be a product of reaction of $CuCl_2^-$ with sulphur or a product of non-oxidative processes involving the formation of

H₂S in the acid HCl solutions. In a study, Lázaro (2001) observed the presence of copper sulphides in anodic stripping curves but admitted that was very difficult to confirm CuS as the product and the only evidence of CuS was the presence of a few blue spots on a chalcopyrite surface as observed microscopically.

2.1.8.3. Polysulfide layer

Parker et al. (1981) rejected the concept that the sulphur film is the cause of slow kinetics in chalcopyrite leaching and proposed a metal-deficient polysulfide with semiconductor properties. Hackl et al. (1995) in a study using Auger electron spectroscopy and X-ray photoelectron spectroscopy found that elemental sulphur is sufficiently porous that the rate is not limited by reactant/product diffusion through the sulphur layer but that the passivating layer is a copper polysulfide CuS_n. In an electrochemical study of the behaviour of chalcopyrite in a mixed chloride-sulfate media, Lu et al. (2000b) (supported in a later study by Arce and Gonzalez (2002) agree with the view that the passivation phenomenon is not due to elemental sulphur formation, but rather that the passivating layer is a metal-deficient surface layer (Cu_{1-x}Fe_{1-y}S_{2-z}). Further support of this view has been obtained by several studies which have shown that washing of the surface of the mineral with CS₂ did not remove the passive film, thereby demonstrating that elemental sulphur is not the cause of slow kinetics. However, according to Parker (2005) there is a form of elemental sulphur (polymeric sulphur, S_μ) which is insoluble even in CS₂ at 20 °C. In addition the same authors claim that bulk copper polysulfides are unstable in acidic solution and thus would be unlikely to form a thick layer on the mineral surface.

2.1.8.4. Precipitation of iron compounds

Recently Stott et al. (2000) postulated that precipitation of jarosite on the mineral surface during leaching of chalcopyrite coincided with a decrease in dissolution rate. They postulated that the iron-hydroxy precipitates hinder chalcopyrite leaching by restricting mass transfer of ions to the surface. This layer can completely cover the chalcopyrite surface and prevent further leaching. A study by Parker et al. (2003) using X-ray photoelectron spectroscopy using residues of chalcopyrite treated by acid ferric and ferrous sulfate confirmed the formation of a precipitate of jarosite which was suggested as causing passivation. Although the precipitation of jarosite may contribute in some way to passivation, the phenomenon still occurs under conditions in which jarosite cannot form, such as in chloride solutions. If jarosite formation is the cause, one could reasonably expect pyrite to show the same behaviour as chalcopyrite but it is well known that pyrite does not undergo passivation. Covellite shows a passivation phenomenon similar to chalcopyrite and in this case, there is no iron present to precipitate as jarosite. Furthermore, the passivation is known to occur even at pH's below that at which jarosite can form.

Even though many studies have been undertaken using the latest surface analysis technology, the results are still unclear. Parker (2005) attributes the variation in results and interpretation to sample preparation and analysis techniques and to inconclusive spectral referencing. However, the majority of the workers agree that the species remains on the surface and forms a barrier to electron transfer.

2.1.9. Effect of the source of the chalcopyrite

An ongoing uncertainty is whether the rate of chalcopyrite dissolution depends on the origin or source of the mineral. The situation is divided in that some researchers have reported similar rates of dissolution for chalcopyrite samples of different origin and others have found differences in the leaching behaviour. Dutrizac and McDonald (1969) found differences in the leaching rate between synthetic and natural chalcopyrite, but later the authors explained that this difference was due to much larger surface area of the former and minor amounts of other copper sulfide impurities in the latter samples. It appears that the only comprehensive study to clarify this issue was completed by Dutrizac (1982) who leached eleven different chalcopyrite concentrates in $\text{FeCl}_3\text{-HCl}$ and $\text{FeSO}_4\text{-H}_2\text{SO}_4$ solutions. According to the results, all samples leached at the same rate. Dutrizac (1982) offered various reasons to explain the variations in chalcopyrite leaching rate reported in the literature which are summarized as follows

- Removal of flotation reagents (minimal effect)
- Crystal orientation and crystal strain (minimal effect)
- Particle size of the mineral sample i.e. a well defined chalcopyrite surface area.
(main reason)
- Impurities (major effect if <90% chalcopyrite). Galvanic effects could be significant.
- The fractional area of the chalcopyrite could be greater than the corresponding chemical fraction in the concentrate.

It seems that variable particle size distribution alone does not account for differences in mineralogical properties relevant to leaching behaviour. According Olubambi et al. (2006), the process of comminution affects mineral and elemental distribution within

particle size ranges and thus mineralogical information of each size distribution should be taken in account. This suggests that mineralogical differences within varying particle sizes could affect their response and behaviour in the leaching process. In addition, to understand the influence of particle size on the dissolution process it is important to take into account possible galvanic interactions at different particle sizes that result from differences in mineralogical composition (Olubambi et al., 2007).

Even though the application of quantitative mineralogical analyses of feed and leach residues has provided valuable information on leach chemistry and reaction mechanism, there has been no published systematic quantitative study of mineralogical effects. As a result of the recent development of advanced mineralogical techniques such as MLA (Mineral Liberation Analyser) or the similar Qemscan analyser, the quantification of the effects of specific sulphides, oxide and gangue minerals on leaching efficiency under controlled conditions is now possible.

2.2. The leaching of chalcopyrite in chloride solutions

2.2.1. Chemistry of chloride solutions

The beneficial effect of chloride on the leaching can be partially explained by changes in the physic-chemical properties of such solutions. For example, in highly concentrated chloride solutions, faster leaching kinetics under atmospheric conditions could be ascribed to the enhanced proton activity and the enhancing effect of chloride ions to the formation of stable metal-chloride complex ions.

2.2.1.1. Ion activity

In concentrated solutions of chloride, ion activities are modified and traditional Debye-Huckel and Davies equations cannot be applied. Activity coefficients can increase due to changes in the activity and structure of water. Therefore, the prediction or calculation of important properties of the system based upon ideal thermodynamic data can differ significantly from those which are readily measurable. Thus, greater leach kinetics in a chloride system can, in some instances, be caused by the enhanced proton activity (Senanayake, 2007b) in that the addition of chloride solvates free water causing an increase in the proton activity (Muir, 2002). In other words, a very small amount of acid can be used to keep the pH low in a concentrated chloride solution and obtain high dissolution of copper if the rate depends on the proton activity.

To the date, numerous attempts have been made to determine the proton activity in concentrated hydrochloric acid using both theoretical and experimental methods. Muir (2002) reviewed some of these methods to estimate activities namely the Debye-Huckel, Meissner, Pitzer, Harned and Majima and Awakura methods.

The Figure 2.3 depicts experimental measurements of the activity of HCl in moderately concentrated solutions of NaCl and CaCl₂ as reported by Majima and Awakura (1981). According to the data, the HCl activity increases significantly with increasing salt concentration with CaCl₂ more effective than NaCl. Therefore, salts of ions with high charges and high hydration numbers ($Mg^{2+} > Ca^{2+} > Na^{+}$) are more effective in increasing the activity of species such as the proton.

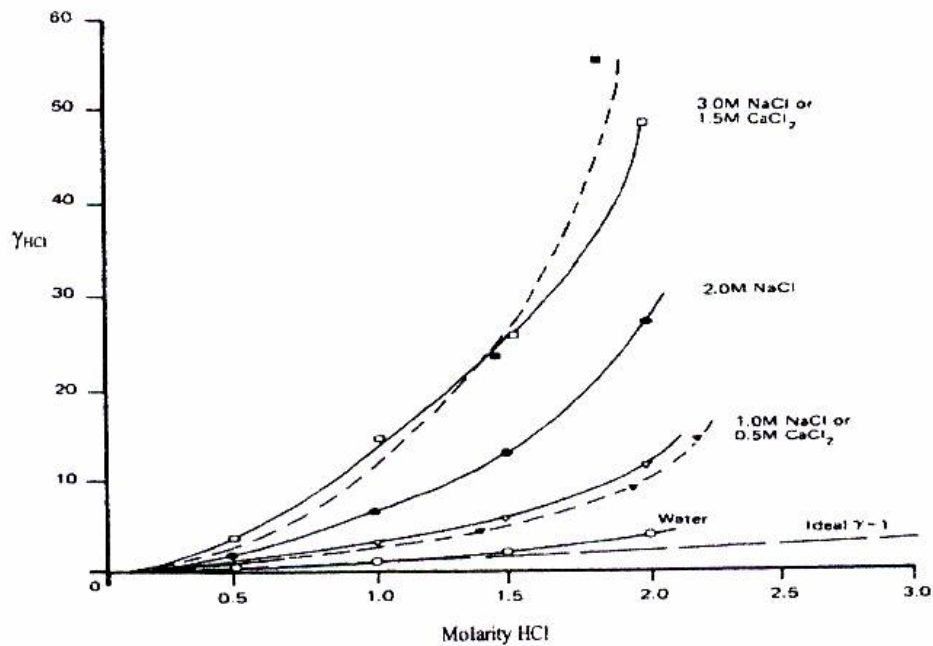


Figure 2.3 Mean activity coefficient of HCl in solutions of NaCl or CaCl₂ (Majima and Awakura, 1981)

2.2.1.2. Solubility

In hydrometallurgy processes is very important that the metal of interest possesses a suitable solubility in the lixiviant to minimize precipitation and possible passivation. The solubilities of metal ions can be significantly increased by the addition of chloride ions due to the formation of metal-chloride complexes.

Cuprous ion solubility

The solubility of cuprous chloride in water is very low, of the order of 2×10^{-7} M at 25 °C. However, the solubility increases significantly with increasing addition of chloride ions as demonstrated by many researchers (Berger and Winand, 1984; Winand, 1991). Figure 2.4 shows the solubility limits in the CuCl-NaCl-H₂O system at various temperatures (Berger and Winand, 1984). In addition the same researchers showed that

in a system $\text{CuCl-FeCl}_2\text{-ZnCl}_2\text{-NaCl-HCl}$ at $30\text{ }^\circ\text{C}$, addition of Zn(II) ions decreases the cuprous solubility whereas the addition of Fe(II) ions increases solubility of cuprous ions. An explanation of this is that the FeCl_2 complex ion acts as a Cl^- ligand donor to the cuprous ion whereas the ZnCl_2 complex ion is a Cl^- ligand acceptor from the cuprous complexes ions. According to data reported by Winand (1991) the following classification of the chloride donor/acceptor properties can be used

(Cl^- donors) $\text{HCl, NaCl, KCl} < \text{FeCl}_2 < \text{FeCl}_3 < \text{CuCl}_2 < \text{ZnCl}_2 < \text{PbCl}_2$
 $< \text{CuCl} < \text{AgCl}$ (Cl^- acceptors)

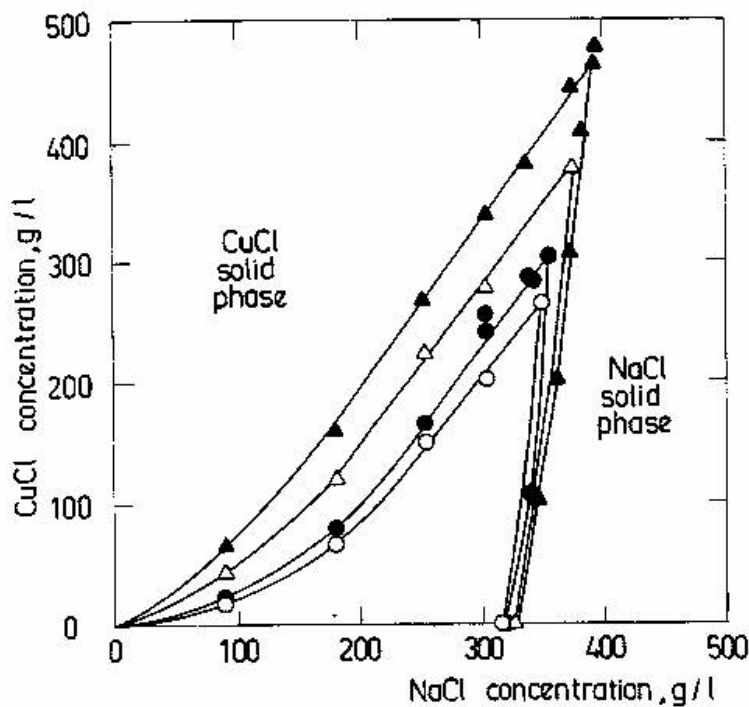


Figure 2.4 Solubility in the $\text{CuCl-NaCl-H}_2\text{O}$ system at various temperatures. Free HCl $8\text{-}11\text{ g L}^{-1}$; 2 g L^{-1} Cu(II) ; \circ $5\text{ }^\circ\text{C}$; \bullet $22\text{ }^\circ\text{C}$; \blacktriangle $75\text{ }^\circ\text{C}$ (Berger and Winand, 1984)

Cupric ion solubility

Cupric chloride is highly soluble in water. Figure 2.5 presents solubility data for Cu(II) in chloride solutions at 50 °C as presented by Winand (1991). Of significant importance is that the solubility decreases slightly with increasing concentration of NaCl. A decrease is also noted when ZnCl₂ or FeCl₃ are added to this system. Thus, the common ion effect is larger than the opposing effect of complex formation as copper(II) forms significantly weaker chloride complexes than copper(I). Increasing temperature greatly increases the solubility of cupric ions as shown in Figure 2.6 (Winand, 1991).

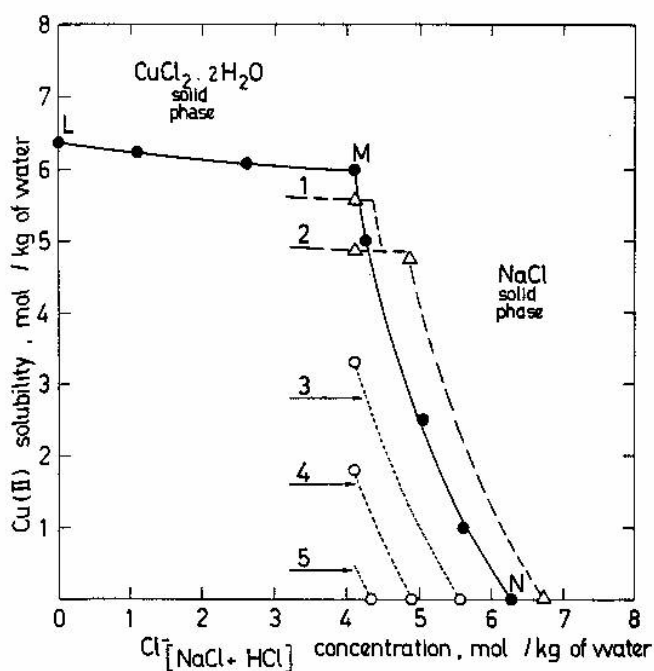


Figure 2.5 Solubility of copper(II) in chloride solutions at 50 °C. ● CuCl₂-NaCl-HCl-H₂O system; ▲ CuCl₂-ZnCl₂-NaCl-HCl-H₂O system; 1: 0.5 M Zn(II); 2: 1.5 M Zn(II); ○ CuCl₂-FeCl₃-NaCl-HCl-H₂O system; 3: 0.5 M Fe(III); 4: 1 M Fe(III) and 5: 1.5 M Fe(III) (Winand 1991).

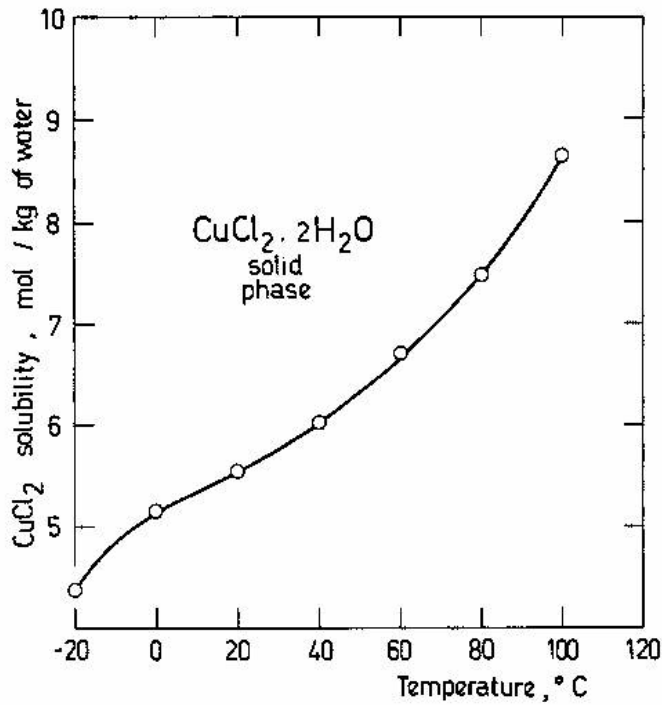


Figure 2.6 CuCl_2 solubility in water as function of temperature (Winand 1991).

In summary, it is desirable that sufficient chloride ions are present to complex copper at a moderate temperature considering the relative chloride ion donor or acceptor character of every constituent salt of the complex chloride solution.

2.2.2. Thermodynamics of chalcopyrite oxidation in chloride solutions

As shown in Figure 2.2, the thermodynamics of the oxidation of chalcopyrite are largely independent of pH (horizontal lines) in the pH range of interest. Of more importance in the case of leaching in chloride solutions is the variation of the equilibrium potentials for the various couples as a function of the chloride concentration or activity. In solutions with high concentrations of chloride the copper (I) state is thermodynamically stable and copper(II) ions can be used as an oxidising agent.

2.2.2.1. Chloride complexes

It is known that, depending on the conditions, cupric or cuprous ions or both can be formed as result of the dissolution of chalcopyrite. Both ions form complexes with chloride ions, the stability of which depend on the solution composition and temperature. Thus, in sulfate media, essentially all of the soluble copper is present as cupric ions while in chloride media both cuprous and cupric ions are stable species.

In general a metal complex ion is formed by successive addition of a complexing ligand (Wilson and Fisher, 1981). In the case of copper in chloride solutions,



The stepwise formation constants are given by

$$K_1 = \frac{(CuCl^{m-1})}{(Cu^{+m})(Cl^{-})} \quad (2.16)$$

$$K_2 = \frac{(CuCl_2^{m-2})}{(CuCl^{m-1})(Cl^{-})} \quad (2.17)$$

$$K_3 = \frac{(CuCl_3^{m-3})}{(CuCl_2^{m-2})(Cl^{-})} \quad (2.18)$$

In a given solution the fraction of each species present is given by

$$\alpha_0 = \frac{1}{1 + \beta_1(Cl^-) + \beta_2(Cl^-)^2 + \beta_3(Cl^-)^3 + \dots} \quad (2.19)$$

$$\alpha_1 = \alpha_0 \beta_1(Cl^-)$$

$$\alpha_2 = \alpha_0 \beta_2(Cl^-)^2 \quad (2.20)$$

$$\alpha_3 = \alpha_0 \beta_3(Cl^-)^3 \quad (2.21)$$

in which α_0 is the fraction of uncomplexed ion, α_1 is the fraction of $CuCl^{m-1}$, α_2 is the fraction of $CuCl_2^{m-2}$, etc, and $\beta_1=K_1$, $\beta_2=K_1K_2$, $\beta_3= K_1K_2K_3$, etc. The same procedure can be used to describe the formation of iron chloro-complexes.

Using published stepwise formation constants for the metal ions, the fraction of each complex can be calculated for a particular solution composition.

Speciation diagrams

Speciation diagrams show the fraction of a metal present as each of its complexes over an appropriate range of ligand concentrations. Speciation diagrams are produced using the appropriate thermodynamic data (in this case from the NIST Database). Examples provided by M.J. Nicol (personal communication, July 8, 2007) are given in Figure 2.7 to Figure 2.9. Figure 2.7 and Figure 2.8 show the fraction of copper as each chloro complexes for copper(I) and copper(II) respectively while Figure 2.9 shows the fraction of iron(III) as each chloro complex.

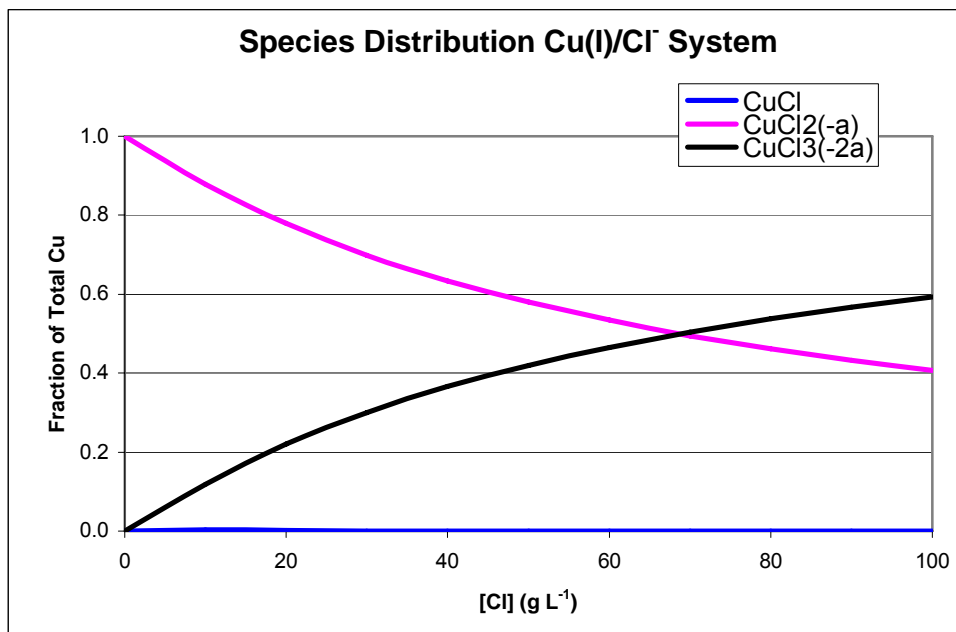


Figure 2.7 Species distribution Cu(I)/Cl⁻ system at 25°C. [Cu(I)]=1.18x10⁻² mol L⁻¹

Figure 2.7 shows that CuCl₂(-a) and CuCl₃(-2a) are the predominant species in this range of chloride concentration while, in the cupric-chloride system, CuCl(+a) is the predominant complex (Figure 2.8). In the ferric-chloride system FeCl(+2a) is the predominant species except at low chloride concentrations (Figure 2.9).

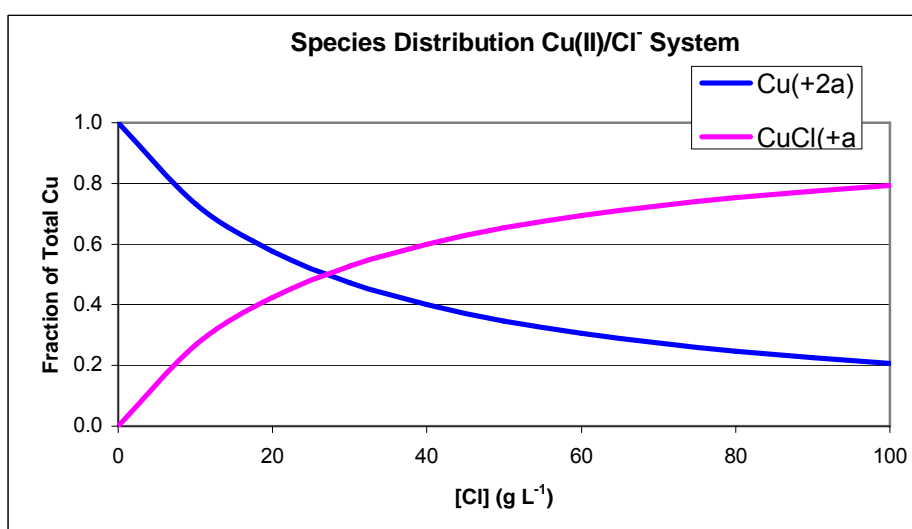


Figure 2.8 Species distribution in the Cu(II)/Cl⁻ system at 25 °C. [Cu²⁺] = 6.68x10⁻² mol L⁻¹

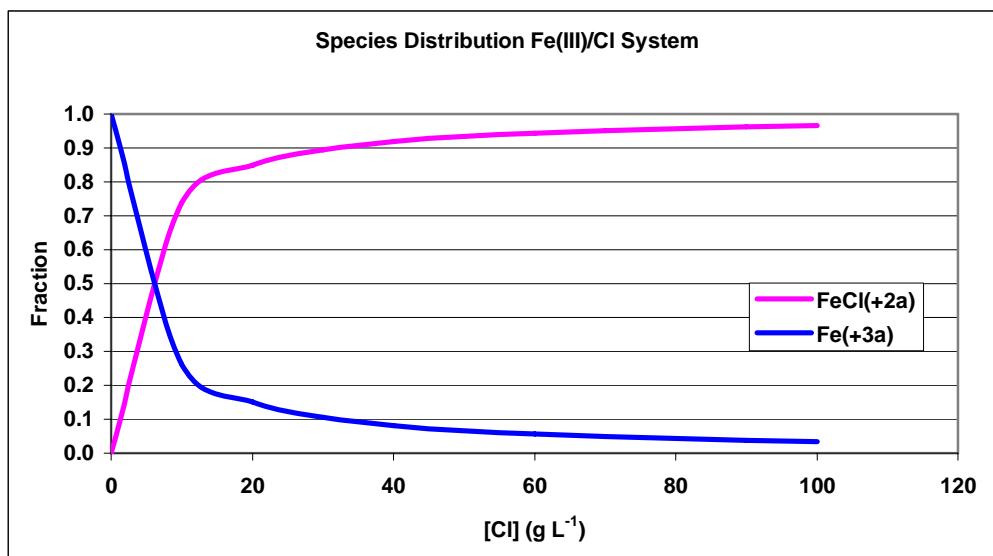


Figure 2.9 Species distribution in the Fe(III)/Cl⁻ system at 25 °C. [Fe(III)] = 5.38×10^{-3} mol L⁻¹

Recently Senanayake (2007a) pointed out the importance of consideration of the effect of temperature on the speciation of chloro-complexes. The author compared the effect of chloride concentration on the speciation of copper chloride complexes at 25 and 102 °C. CuCl⁺ and CuCl₂⁻ are the predominant species at low chloride concentrations of less than 0.5 mol L⁻¹ and 0.8 mol L⁻¹ at 25 °C respectively while CuCl₂⁰ (higher chloride concentration), CuCl⁺ (low chloride concentration) and CuCl₂⁻ (chloride concentrations less than 1 mol L⁻¹) are the predominant species at 102 °C.

2.2.2.2. Effect of complexation on reduction potential

The formation of complexes between a metal ion and a ligand can have a significant effect on the value of the standard reduction potential for couples involving the metal ion. Thus, the reduction potential in chloride media can be calculated from

$$E_{MCl^{z-n}/M^0} = E_{M^{z+}/M^0}^0 - \frac{0.059}{z} \log \frac{\beta_n^0 a_{Cl^-}^n}{a_{MCl^{z-n}}} \quad (2.22)$$

$$\beta_n = \frac{a_{M^{z-n}}}{a_{M^{z+}} a_{Cl^-}^n} \quad (2.23)$$

where β is the overall stability constant for the metal-chloro complex and a is the activity of species. Thus, the reduction potential at which metal species are reduced to their metallic states decreases with increasing β and increasing concentration of chloride.

The effect of complexation can be explained as a reduction in the activity of free ions which make it more difficult for it to be reduced to metal (Muir, 2002). For weakly complexed ions as in the case of cupric complexes, the reduction potential is a few mV different from the standard potential in absence of chloride ions. On the other hand, for the strongly complexed copper(I) ion, the potential can change substantially and reduce the activity of the electro-active species by several orders of magnitude.

Maintaining the copper in the cuprous state has the advantage of allowing deposition of copper via a one electron transfer when direct electrowinning is used with consequent energy savings compared with cupric deposition that require two electrons per atom. In addition, the Cu^+/Cu^0 deposition is faster due to the single electron transfer with an exchange current density of 2400 A m^{-2} in chloride solution (5 M NaCl) compared to that of the Cu^{2+}/Cu^0 deposition in sulfate of between $20\text{-}200 \text{ A m}^{-2}$ (Winand, 1991).

Of significant importance is the effect of the concentration of chloride on the reduction potential of the couples involved in the leaching of chalcopyrite in chloride solutions.

Thus, Figure 2.10 is such a diagram in which the potentials for selected couples at fixed

metal ion concentrations have been plotted as a function of the chloride concentration (M.J. Nicol, personal communication, July 8, 2007). As a result of the fact that copper(I) forms stronger complexes with chloride than copper(II) ions, the ratio of free $\text{Cu}^{2+} / \text{Cu}^+$ increases with increasing chloride concentration. As a result of this the potential of Cu(II)/Cu(I) couple increases with increasing chloride concentration. Also shown are the potentials of the other important couples in the leaching of chalcopyrite. In all these cases, the potential decreases with increasing concentration of chloride.

Conversely, the reduction potential of the Fe(III)/Fe(II) couple decreases slightly with increasing chloride concentration because iron(III) forms stronger complexes with chloride ions than iron(II). Thus, the ratio of free Fe(III)/Fe(II) decrease with increasing chloride concentration causing the potential of the couple to decrease.

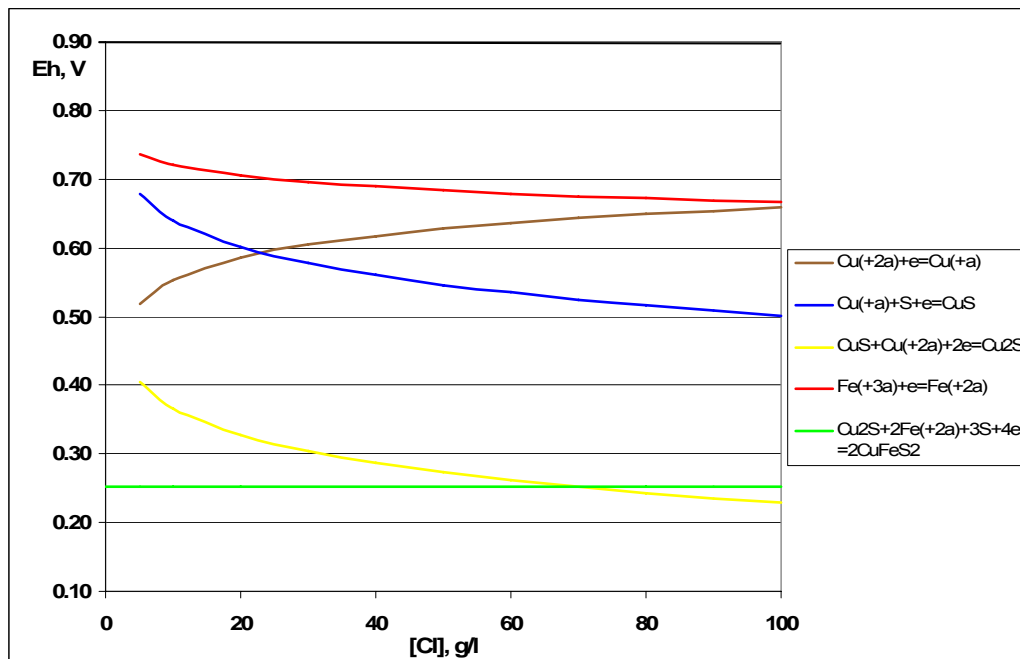


Figure 2.10 Variation of formal potential of various couples with the concentration of chloride ions. $[\text{Cu(II)}] = [\text{Fe(II)}] = [\text{Fe(III)}] = 0.1 \text{ M}$, $[\text{Cu(I)}] = 10^{-3} \text{ M}$.

It is apparent from the data s Figure 2.10 that copper(II) can oxidize chalcopyrite to covellite at all chloride concentrations but that covellite can only be oxidized by copper(II) at chloride concentrations above about 20 g L⁻¹ at a Cu(II)/Cu(I) ratio of 100. On the other hand, iron(III) can oxidize chalcopyrite to copper ions and sulphur at all chloride concentrations.

It should be noted that, because of the rapid equilibrium,



the iron and copper ion couples are essentially always in equilibrium and therefore, at any chloride concentration, the ratios of Cu(II)/Cu(I) and Fe(III)/Fe(II) should be adjusted to give the same reduction potential for each couple.

2.2.3. Kinetics of the dissolution of chalcopyrite

The kinetics of a leaching process are particularly important for process design, optimisation and control. The kinetic information can only be derived from experimentation and observation and is influenced by a number of factors such as mineralogy, surface area, reactant concentrations, product layer formation and temperature. Although many studies have been conducted to establish these factors in the case of the leaching of chalcopyrite, variable results and conclusions have been published due largely to the different conditions employed. This has made direct comparisons somewhat difficult.

Thus, despite the considerable literature on the kinetics of leaching in ferric and more recently cupric solutions, there is no agreement among the various authors about the rate-determining step, activation energy, form of the leaching curves and the dependence on the solution composition.

Table 2.4 summarizes some of the important conclusions relevant to the dissolution of chalcopyrite in chloride solutions as reported in the literature. High activation energy generally indicates that the rate of the reaction is controlled by the rate of a chemical or electrochemical reaction while a low activation energy suggests a diffusion-controlled process. However, no agreement has been reached on the value of activation energy which varies between 20 and 135 kJ mol⁻¹ and even higher values have been reported. Researchers claim that the activation energy is dependent on the range of temperature studied and on the value of the ratio of Cu(II)/Cu(I) present in the system (Bonan et al., 1981) and most of the reported values in Table 2.4 were obtained under different leaching conditions and in different ranges of temperature.

Most of the studies agree that rate of leaching of chalcopyrite in chloride media is linear with time, but some of them suggest parabolic or paralinear kinetics. In this context Dutrizac explained that the paralinear kinetics obtained by Ammou-Chokroum et al. (see Table 2.6) are due to experimental limitations involving an unsintered disk containing very fine and very coarse particles.

In regard to the rate limiting step, the reported data are very controversial in that some authors have concluded that it is mass transport controlled while others have suggested chemical control. Some of the studies reporting mass transport control are questionable given that the activation energies (see Table 2.4) are too high to be indicative of mass transport control; in other studies the rates are slower and independent of rotation speed. For example Havlik and Kammel (1995) suggested chemical control at higher temperatures (45-80 °C) and diffusional control at lower temperatures (35-45 °C) based on values of the activation energy.

Table 2.4 Kinetic parameters for the leaching of chalcopyrite in chloride media

Material	Leaching medium	Temp. °C	Kinetics	Rate-determining Step	Activation Energy, kJ mol ⁻¹	Reference
Pure chalcopyrite	FeCl ₃	90	Linear	Anodic reaction	84.9	(Jones and Peters, 1976)
Synthetic chalcopyrite	FeCl ₃	25-70	Paralinear		38±4	(Ammou-Chokroum et al., 1981)
Synthetic and natural chalcopyrite	FeCl ₃ -HCl	50-100	Linear	Chemical reaction	45.9	(Dutrizac, 1978)
Chalcopyrite concentrate	CuCl ₂	90	Linear	Anodic reaction	134.7	(Wilson and Fisher, 1981)
Chalcopyrite concentrate	CuCl ₂	>85	Parabolic	Solid state diffusion	30.0-58.5	(Bonan et al., 1981)
Chalcopyrite concentrate	CuCl ₂	<85		E _A too high for diffusion control	33.4	(Bonan et al., 1981)
Natural chalcopyrite	FeCl ₃ 40-100°C	90	Linear	Chemical reaction	42	(Dutrizac, 1981)
Natural chalcopyrite	Acidic chloride	>70	Linear	Electrochemical	~50	(Mc Millan 1982)
Chalcopyrite ore	CuCl ₂	80		Diffusion	37	
Natural chalcopyrite	FeCl ₃	>70	Linear	Chemical reaction	69	(Majima et al., 1985)
Chalcopyrite crystals grade	museum FeCl ₃	>70	Linear	One electron transfer.	69 chemical 59.5 anodic	(Hirato et al., 1986)
Chalcopyrite crystals grade	museum CuCl ₂	70	Linear	One electron transfer	82 chemical 60 electrochemical	(Hirato et al., 1987)
99% pure chalcopyrite	FeCl ₃ -HCl-NaCl	95			68.1±13.2	(O'Malley and Liddell, 1987)
Natural chalcopyrite	FeCl ₃ -HCl	3.5-80	Linear	45-80°C chemical reaction 3.5-45°C, diffusion control	68.9 1.1	Havlik and Kammel (1995)
Natural chalcopyrite	FeCl ₃ -HCl-CCl ₄	40-90	Linear	Diffusion	31.2	Havlik and Kammel (1995)
Chalcopyrite concentrate	Sulfate/NaCl	>85		<85 Chemical and>85 diffusion control	20 below 85 °C 48 above 85 °C	(Lu et al., 2000a)
Chalcopyrite concentrate	Mn ore-HCl	30-60			24.7	(Devi et al., 2000)
Chalcopyrite electrodes	Cupric chloride	70-90		Diffusion product layer	35-45 anodic	(Lunstrom 2005)

Another controversial aspect that has appeared in published kinetic studies is the effect of the nature and concentration of the reactants on the rate of dissolution. Tables 2.5 and 2.6 summarize the results in this regard of some recent studies on the leaching of chalcopyrite in FeCl_3 and CuCl_2 media. A summary of previous studies can be found in the review made by Dutrizac (1990).

Ferric Chloride

It is generally accepted that the ferric ion is effective as an oxidant in the leaching of chalcopyrite. However, it has been shown that in the sulfate system an increase in the concentration above a minimum value does not increase the leaching rate of chalcopyrite (Antonijevic and Bogdanovic, 2004; Dutrizac, 1981; Dutrizac et al., 1969). The situation in chloride solutions is less clear. Thus, Jones and Peters (1976) observed that increasing the FeCl_3 concentration from 0.1 to 1 M approximately doubled the rate of dissolution suggesting a 0.3 power dependence on the ferric ion concentration. In 1978, Dutrizac reported a 0.8 power dependence on the rate of leaching of disks of synthetic chalcopyrite and in a later publication, the same author (1981) found that at all temperatures the rate increases fairly sharply with increasing the ferric chloride concentration. At both 95°C and 65 °C the rate varies with the 0.8 power of the ferric chloride concentration.

More recent studies show that the leaching rate of chalcopyrite is half-order with respect to the ferric chloride concentration (Hirato et al., 1986; Majima et al., 1985). Dutrizac (1990) showed that although more extensive sulphur coverage was observed with increasing FeCl_3 concentration, the morphology of the sulphur reaction product appeared to be independent of the initial FeCl_3 and HCl concentrations. On the other hand, Lu et al. (2000a) postulated

that it is not necessary to include ferric ion in the leaching solution in chloride media because it is produced as the reaction proceeds.

Another important aspect is the effect of the ferrous ion concentration on the chalcopyrite leaching rate. However, again controversial findings have been reported. Thus the presence of ferrous ions has been reported to decrease the leaching rate of chalcopyrite in sulphate solutions (Dutrizac, 1981; Dutrizac et al., 1969; Jones and Peters, 1976). However, others (Hiroyoshi et al., 1997; Hiroyoshi et al., 2000) have shown that chalcopyrite is more effectively leached in a ferrous sulfate solution than in a ferric sulfate solution. These authors explained this effect on the basis of a model which involves the intermediate formation of chalcocite. In chloride solutions, the presence of ferrous ions even at high concentrations has negligible effect (Dutrizac, 1978; Hirato et al., 1986; Jones and Peters, 1976; Majima et al., 1985). The latter authors also found that the presence of ferrous chloride does not affect the mixed potential of chalcopyrite suggesting that the anodic reaction of ferrous ions on the chalcopyrite surface is slow.

Table 2.5 Studies on the leaching of chalcopyrite in FeCl₃ media (adapted from Dutrizac (1992) and augmented)

Material	Main conclusion	Reference
Natural chalcopyrite crystal of museum grade	Production of a porous elemental sulphur layer which is not a barrier to further leaching Leaching rate of chalcopyrite in a FeCl ₃ is 10 times greater than in FeSO ₄ Insignificant effect of FeCl ₂ concentration Rate increases with increasing concentration of NaCl	Majima et al. (1985)
Natural chalcopyrite crystal of museum grade	Mixed potential determined by the anodic and cathodic reactions: $CuFeS_2 = Cu^{2+} + Fe^{2+} + 2S + 4e$ $FeCl_2^+ + e = FeCl_2^0$ The CuCl ₂ obtained as a product of leaching plays an important role as oxidant in the later stages of leaching.	Hirato et al. (1986)
Pure chalcopyrite (99% purity)	FeCl ₃ -HCl-NaCl leaching: At higher chloride concentrations 90% of Cu(II) was reduced to Cu(I) with drop in solution potential. Slight inhibitory effect of Fe(II). Leaching possible in initial absence of oxidant.	O'Malley and Liddell (1987)
Chalcopyrite concentrate (98% chalcopyrite)	90% elemental S with less than 5% sulphate formed. FeCl ₃ concentration does not have any effect on the amounts of S or SO ₄ formed. Air or O ₂ do not have effect on the amount of S or SO ₄ formed. Sulphur globules formed on large particles while smaller particles become completely covered in a layer of sulphur after 15 min of leaching. Morphology does not change with concentration of either FeCl ₃ or HCl.	Dutrizac (1990)
Natural chalcopyrite	Additions of CCl ₄ to the FeCl ₃ solution leaching enhance chalcopyrite dissolution with elemental sulphur dissolution. Structure of partially leached chalcopyrite showed a shift of lattice parameters to defect structures. Different types of reaction mechanism up to 45 °C.	Havlik and Kammel (1995)
Chalcopyrite concentrate and ore	5M chloride leach solution at 90°C: Leaching as received concentrate achieved 75% dissolution in 5 h. Mechanically activated concentrates yielded 95% after 3 h.	Maurice and Hawk (1998)
Mechanically activated Sulphide minerals containing Chalcopyrite	Changes in reaction mechanism were observed at higher temperature (50-90 °C) with the rate-determining step changing from mixed to diffusion control	Godociková et al. (2002)

Cupric chloride

Dutrizac (1981) reported that addition of cupric ions slightly decreased the leaching rate of chalcopyrite in sulfate media. However, a different result was obtained by Hiroyoshi et al. (2001) when he studied the effect of cupric ions in presence of ferrous and ferric ions in sulfate media at 30 °C. He showed that in the presence of high concentrations of cupric ions, chalcopyrite dissolution was enhanced by high concentrations of ferrous ions and that copper extraction was mainly controlled by the ferrous to ferric ion concentration ratio. Even under anaerobic conditions chalcopyrite oxidation due to ferric ions is enhanced by ferrous ions in the presence of high concentrations of cupric ions. On the other hand, when the cupric ion concentration was low, ferrous ions suppressed the rate of dissolution. In order to understand the synergistic effect of cupric and ferrous ions, the same authors (2004) carried out electrochemical measurements. They found that the coexistence of cupric and ferrous ions causes activation or de-passivation. In agreement with this, Elsherief (2002) claimed that increasing cupric ion concentrations resulted in a corresponding increase in the leaching rate of chalcopyrite, and further increases are observed when ferrous ions are added together with cupric ions in sulfate media.

In the chloride system, chalcopyrite has been successfully leached in presence of cupric ions (Bonan et al., 1981; Dutrizac, 1978; Guy et al., 1983; Hirato et al., 1986; Hirato et al., 1987; Wilson and Fisher, 1981) (see Table 2.6). According to Wilson (1981) cupric ions do not take part in the rate controlling step of the dissolution of chalcopyrite at 90 °C because an insignificant change in the rate was observed with increasing concentration of cupric

ions. In contrast, Hirato et.al. (1987) reported that the leaching rate increases at 70 °C with increasing of cupric ion concentration.

Jones and Peters (1976) proposed that the fast kinetics for the ferric chloride system were a result of catalysis of the reaction by cupric ions and that ferric chloride leaching is in reality cupric chloride leaching. The authors explain this phenomenon by suggesting that the ferric ion serves to suppress the concentration of cuprous ions, and raise the potential of the Cu(II)/Cu(I) couple which exhibits a high degree of reversibility on the chalcopyrite surface. Hirato et al. (1986) agree but they suggest that ferric chloride is the oxidant for chalcopyrite during the initial stage of leaching and the accumulated cupric ions may take the place of ferric ions during the later stages of leaching.

Moreover, it has been noted that chalcopyrite is leached more rapidly by cupric rather than ferric ions due to the greater reversibility of the Cu(II)/Cu(I) chloride couple on a chalcopyrite surface. Thus, the mixed potential, the corrosion current and hence the rate of oxidation are higher in the presence of cupric than ferric ions (Parker et al., 1981). Furthermore, a combination of ferric and cupric is more effective than a cupric chloride system, because the iron(III) oxidizes the product copper(I) ions and maintains a high activity of copper(II) and a high mixed potential. In addition, Muir (2002) explained this behaviour and suggested that in chloride media, copper(II) is a better oxidant than iron(III) due to higher rates of electron transfer, enhanced crystalline of the sulphur and lack of passivation in chloride media rather than to the redox potential of the solution.

Table 2.6 Studies on the leaching of chalcopyrite in CuCl₂ media

Material	Main conclusion	Reference
Chalcopyrite crystal of museum grade	Production of porous elemental sulphur layer on chalcopyrite surface Rate increase as [CuCl ₂] ^{0.5} Rate decrease as [CuCl] ^{-0.5} Rate increase with increasing concentration of NaCl up to 2 M after that a declining tendency is observed Electrochemical mechanism	Hirato et al. (1986)
Chalcopyrite concentrate	The rate of leaching is enhanced by addition of NaCl into the leaching solution via formation of complexes. Particle size of the chalcopyrite has negligible effect on the leaching rate. Passivation layer was not observed.	Skrobjan et al. (2004)
Natural chalcopyrite	CuCl ₂ concentrations above 9 g L ⁻¹ increase the rate. Reaction rate controlled by the diffusion of cupric ions through the reaction layer. Optimum conditions are high cupric ion concentration, high pH and high temperature.	Lundstrom et al. (2005)
Natural chalcopyrite	With NaCl, 280 g L ⁻¹ and Cu ²⁺ , 1-40 g L ⁻¹ at 90 °C atmospheric pressure and pH 2: Cathodic reactions are the reduction of [CuCl] ⁺ to [CuCl ₃] ²⁻ , the reduction of [CuCl ₃] ²⁻ to Cu ⁰ and hydrogen evolution.	Lundstrom et al. (2007)

According to Burkin (2001), the leaching of chalcopyrite using copper(II) chloride as oxidant differs from the reactions using iron(III) sulfate or chloride. Whereas the Fe(III)-Fe(II) couple provides an adequate thermodynamic driving force as long as the metal ion activities and pH are suitable, in the copper chloride system the thermodynamics of the overall reactions have to be considered in order to achieve suitable conditions for leaching to proceed.

Concentration of chloride ions

Increasing the concentration of chloride ions has been one of the frequently adopted methods to increase the rate of dissolution of chalcopyrite. In an early study, Dutrizac and MacDonald (1971) reported that minor additions of NaCl additions to a ferric sulfate solution promoted the chalcopyrite leaching reaction above 50 °C, but that there was no

apparent effect at lower temperatures. Dutrizac (1978) and Palmer et al. (1981) agreed that the leaching rate of chalcopyrite increases with an increase in chloride concentration at low concentrations and that the increase in rate tends to a maximum with further increases in total chloride concentration.

Totally different results from those reported by the above authors were found by Majima et al. (1985). They reported that the activity of HCl increases significantly upon adding NaCl or CaCl₂ to the solution. Thus, the mean ionic activity coefficient of 1 M HCl is three times higher in 1 M NaCl and 20 times higher in 3 M NaCl than in the absence of salt. In addition, they found that the same molar concentration of CaCl₂ is twice as effective as NaCl, but FeCl₂ is not as effective because of ion pairing of chloride with Fe(II). Therefore, solutions of HCl in strong brine could be effective for non-oxidative leaching of chalcopyrite. These results confirmed that the leaching rate is sensitive to the chloride concentration. In order to resolve these differences, Hirato et al. in 1986 found that the leaching rate doubled in the presence of sodium chloride in 0.1 M FeCl₃ at 70 °C, but its role cannot be explained by an electrochemical mechanism because the change in solution potential was insignificant. However, these authors did not measure the effect of chloride on the mixed potential at the mineral surface.

On the other hand the same authors in a later paper showed the leaching rate increases with an increase in the chloride ions up to 2 M, at 70 °C in 0.1 M CuCl₂ and 0.2 M HCl with a decrease at higher chloride concentrations.(Hirato et al., 1987). Cheng et al. (1991) postulated that the effect of the chloride ions is to promote the formation of large sulphur crystals, allowing the reactants to penetrate the sulphur layer and making the sulphide

surface available for reaction. Lu et al. (2000a) showed clearly that increasing the chloride concentration above 0.5 M in sulphate media does not increase the leaching kinetics and they concluded that the important factor is the presence of even small concentrations of chloride ions.

Skrobian et al.(2004) reported that increasing concentrations of NaCl increases the rate of dissolution of copper from a chalcopyrite concentrate, but that, after extended periods, consumption of chloride by other sulphide minerals such as ZnS in the concentrate decreases the effect. Carneiro and Leão (2007) confirmed the enhanced rate of leaching of chalcopyrite in the presence of chloride and suggested that this was due to a reduction in passivation, increasing surface area and porosity of the product layer.

It is apparent from the results that the effect of chloride ions is still not completely resolved and that further investigations are necessary to elucidate this issue.

2.2.4. Temperature

Even though temperature is one of the most important parameters in the kinetics of the leaching of copper ores and concentrates, it has been difficult to determine its effect accurately for chalcopyrite in chloride media (Dutrizac, 1981). According to this author, the difficulty is due in part to the presence of even small amounts of secondary copper mineralization that can seriously affect the interpretation of leaching data, especially at low temperatures where the total dissolution is small. However, the agreement among the various authors is that an increase in temperature produces a substantial increase in the rate of dissolution.

The effect of temperature can be quantified by calculating the activation energy which depends on the method employed for calculating the rates. According to Lu et al. (2000b) suitable corrections must be made to the measured reaction rates due to the variation of oxygen solubility. If the leaching curves are not linear, different activation energies will be produced depending on the method used to derive a rate parameter and close agreement in reported activation energies should not be expected. As a result of this, published literature shows (Table 2.4) that the value the activation energy varies from 11 to 135 kJ mol⁻¹

2.2.5. Particle size

Although it has been widely believed that fine grinding promotes more rapid dissolution of chalcopyrite, Jones and Peters (1976) reported that the leaching rate of chalcopyrite in 0.1 M ferric sulfate was independent of particle size below 149 μm at 90 °C. Conversely, the rate of leaching in ferric chloride was increased substantially with finer particles. Later studies showed that the reaction rate was directly proportional to sample surface area (Wilson, 1981) as reported by Dutrizac (1981). They showed that the parabolic rate constant for the dissolution of chalcopyrite particles at 90 °C in sulfate solutions varied directly as the area of chalcopyrite. To clarify these differences, Dutrizac leached chalcopyrite at 90 °C in sulfate and chloride solutions. He found that in the sulfate system the rate increases as the mean particle size is decreased below 149 μm. He also observed similar behaviour in chloride system, except that the rates were more rapid. The same behaviour was found by Lu et al. (2000a) when chalcopyrite was leached in 0.8 M H₂SO₄ and 1 M NaCl at 95 °C. However, after 9 h of leaching, the copper extraction in the fine

concentrate and the coarse concentrate was almost identical, suggesting that finer grinding does not further liberate chalcopyrite from the gangue. Skrobjan et al. (2004) showed that the particle sized has a negligible effect on the rate of chalcopyrite leaching in chloride media.

According to Dutrizac (1981), the surface area is one of the principal variables, and any kinetic study must adequately characterize the area. He suggested that the ideal method for producing a sized feed for kinetics studies is wet cyclosizing of small batches, but wet screening is acceptable if carried out thoroughly enough to remove all fines. Even though some researchers such as Jones and Peters (1976) have found that chalcopyrite leaching in sulfate media is independent of particle size most authors agree that the rate of dissolution increases as the mean particle size decreases. Dutrizac (1982) suggested that the use of dry screening was ineffective in the study carried out by Jones and Peters. In chloride media, it has been found that the leaching rate is directly proportional to the surface area (Wilson and Fisher, 1981). Lu et al. (2000a) found the same result however, after 9 h of leaching; the copper extraction from the different size fractions was almost identical.

2.2.6. The effect of additives

It has been well known that the addition of some ions such as Ag(I), Sn(II), Co(II), Hg(II) and Mn(II) and addition of pyrite under certain conditions accelerate copper dissolution from chalcopyrite.

2.2.6.1. Effect of silver ions

Among the ions which enhance the dissolution of chalcopyrite, silver ion has been shown to be the most effective (Ballester et al., 1992; Ballester et al., 1990; Hiroyoshi et al., 2007; Hiroyoshi et al., 2000), but because of the cost of silver and the difficulty in recovery from solution this technique has limited industrial application. However, it is considered still important to establish the mechanism of the catalytic effect of silver ions in order to develop alternative methods to improve the rate of chalcopyrite leaching.

The mechanism of silver catalysis proposed by Miller et al. (1981) and later reported by many researchers (Ballester et al., 1992; Ballester et al., 1990; Sato et al., 2000; Wang et al., 2004; Yuehua et al., 2002) involves a rapid reaction of Ag^+ with chalcopyrite to form a blue-black product on the chalcopyrite surface according with the following reaction:



Since the complex porous layer produced is less tenacious than the protective S^0 layer in the uncatalysed reaction, it does not inhibit electron transport processes on mineral surface.

The authors explained that Ag^+ ion can be regenerated through the oxidation of Ag_2S by ferric ions as shown in eq.(2.26). The silver ions released will again react with chalcopyrite.

However, Parker et al. (2003) in a photoelectron spectroscopy study of the mechanism of

the oxidative dissolution of chalcopyrite contradicted the second step because no elemental sulphur was identified in the XPS spectra. They also suggested without experimental evidence that ferric ion is not essential for copper dissolution in the presence of low levels of silver and that the catalysed pathway does not require a redox step for dissolution.

In the well known catalytic effect of silver ions in the bacterial leaching of chalcopyrite the reaction mechanism proposed by Miller is appropriate (Yuehua et al., 2002). According to Ahonen and Tuovinen (1990) (referred in Sato (2000)) the role of bacteria is to maintain a favourable ratio of $\text{Fe}^{3+}/\text{Fe}^{2+}$ by oxidizing ferrous iron and thereby contribute to the ferric-iron dependent oxidation of silver sulphide.

Many researchers have experimentally verified the above model involving the formation of Ag_2S on the surface of chalcopyrite. However, its role is not yet completely understood and many interpretations of the model have been proposed.

Thus, Wang et al. (2004; 1997) suggested that the covalent radius of silver ions is similar to that of copper and ferrous ions which are leached in the system and that the silver ions can replace the copper and ferrous ions in chalcopyrite (Eq. (2.25)) and form a flat, loose silver sulphide film on the surface of the mineral grains. The rapid diffusion of silver ions into the chalcopyrite particle is a key step in the process.

Parker et al. (1981) suggested that Ag_2S catalyses the leaching of chalcopyrite because, based on the electrode potentials, Ag_2S is more noble than CuFeS_2 . Yuehua (2002) in their

assessment of the publication by Price and Warren in 1986, assumed that the formation of the Ag_2S -Ag film on the surface of the chalcopyrite modified the morphology of the sulphur layer and increased its conductivity thereby increasing the rate of electron transfer to ferric ions. On the other hand, Ahonen and Tuovinen (1990) have pointed out that Ag_2S would behave cathodically with respect to chalcopyrite. Escudero (1993) postulated that in the chalcopyrite-silver sulphide redox couple, the anodic dissolution of Ag_2S and the cathodic reduction of O_2 occurred on the chalcopyrite surface.

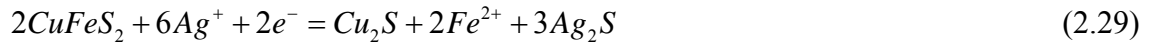
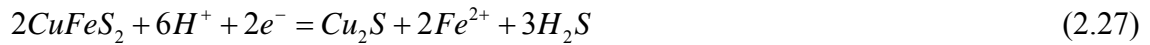
Another important point is that the rate of dissolution increases as the amount of silver added to the system is increased. Results from Gomez et al., (1997b) show that the fastest dissolution is obtained using an addition of silver of less than 0.3 g of silver kg^{-1} concentrate. Higher concentrations result in loss of silver as a jarosite.

Although Dutrizac (1982) indicated that the silver content of the chalcopyrite does not have a major effect on the rate of dissolution, Yuehua et al. (2002) found that copper dissolution from an argentite (Ag_2S) bearing chalcopyrite concentrate was greatly enhanced during bioleaching. This result suggests the possibility of leaching low-grade chalcopyrite concentrates with concentrates containing argentite as the catalyst.

It has been demonstrated that the presence of sphalerite and secondary copper sulphides has a negative effect on the catalytic action of silver on chalcopyrite leaching. Barriga et al. (1987) suggested that secondary sulphides act as sequestering agents for silver preventing its catalytic action on chalcopyrite dissolution. Therefore, in order to study the effect of

silver on chalcopyrite leaching, experiments must be carried out after the removal of these sulphides. Perhaps Dutrizac (1982) in his study did not take into account that the low leaching rates found for the chalcopyrite material with the highest amount of silver as due to presence of sphalerite in the concentrate. On the other hand, Romero et al. (2003) found that it was difficult to obtain a copper extraction higher than 95% in ferric sulphate leaching with silver as catalyst from a chalcopyrite concentrate with secondary copper sulphides. As a result, they added silver ions after 1 or 2 h from the start of leaching resulting in more rapid dissolution than in the test in which silver was added at the beginning of leaching.

Hiroyoshi et al., (2002, 2007) have proposed a different mechanism for the catalytic effect of silver ions in sulphuric acid solutions. This model is based on a previous Hiroyoshi et al. (2000, 2001) reaction model (see section 2.3.2) designed to interpret the redox potential dependence of the rate of chalcopyrite leaching in terms of which the leaching rate is higher at redox potentials below a critical value. In a system containing silver ions, the critical potential of silver, $E_c(\text{Ag})$ is much higher than the critical potential of copper, $E_c(\text{Cu})$, even at low activities of silver ions. They explained that silver ions react with hydrogen sulphide released during chalcopyrite reduction (eq.2.27) to form an intermediate silver sulphide precipitate (eq. 2.28) and decrease the concentration of hydrogen sulphide in the solution thereby increasing the critical potential of Cu_2S formation and broadening the potential range in which rapid dissolution extraction takes place. Equation (2.29) shows the overall reaction.



In addition to Ag_2S formation the authors claim without experimental verification that metallic silver may be also be formed according Eq. (2.30) and Eq. (2.31).



Dutrizac (1992) affirmed that silver catalysis appears to be effective in ferric sulfate solutions. This is not true in chloride media possibly due to the low solubility of silver ions in dilute chloride solutions. Silver recovery and recycling is a continuing concern in both systems. Sato et al. (2000) found that the addition of silver chloride in the bioleaching of chalcopyrite concentrate accelerated the dissolution of copper. During the initial stages of the bioleaching experiments, the dissolution rate of copper was higher with silver chloride than with the addition of silver sulfate solution. Finally, they found that the recovery of copper increased with increasing amount of silver chloride added. Romero et al. (2003) suggested that recovery of silver may be achieved by leaching the residue in an acid-brine medium with 200 g L⁻¹ of NaCl at 70 °C and either HCl or H₂SO₄ acid, provided that elemental sulphur has been previously removed by hot filtration.

2.2.6.2. Effect of Hg(II) and Bi(III)

According to the studies of Gomez et al. (1997a), and Escudero et al. (1993) the addition of Hg(II) and Bi(III) ions increase the bioleaching rate of the chalcopyrite in concentrates, but to a lesser extent than in the case of Ag(I). In other study, Gomez et al.,(1997b) used scanning electron microscopy (SEM) and Auger electron spectroscopy (AES) to study the surface changes occurring on chalcopyrite when the bioleaching medium contained Ag(I), Hg(II) and Bi(III). Both Ag(I) and Hg(II) ions formed a coating of the corresponding sulphide. However in the presence of Bi(III) an oxidised compound is formed which suggests an alternative mechanism of interaction with the chalcopyrite surface. Hiroyoshi et al.(2006) studied the effects of similar added metal ions on the critical potential for chalcopyrite leaching. The results indicate that the critical potential increases with the addition of Ag(I) and Bi(III), but is not affected by Hg(II) and other metal ions.

2.2.6.3. Effect of addition of pyrite

It has been demonstrated by early workers (Mehta, 1983) that the rate of dissolution of chalcopyrite is greatly increased in the presence of pyrite. Berry et al., (1978) in a study of galvanic interaction between chalcopyrite and metallic copper observed the rapid conversion of chalcopyrite to chalcocite. Nicol (1975) also noted the same galvanic effect during a study of reduction of chalcopyrite by copper, iron or lead metals in acid solution. Abraitis et al. (2004) also reported that galvanic interaction promoted chalcopyrite leaching.

They obtained higher dissolution of chalcopyrite when this was in contact with pyrite in 0.1 M HCl at room temperature. However, the galvanic effect was not experimentally confirmed.

When two sulphide minerals of different rest potential are in contact with each other in acid solution, the mineral with the higher rest potential would normally act as the cathode and is protected galvanically. For oxygen as the oxidant, the following reaction will occur on the surface of the more noble sulphide mineral.



Conversely, the mineral with the lower rest potential acts as an anode



in which MS is the metal sulphide. The galvanic reaction at the mixed potential is given by:



The rest potential for chalcopyrite in acid solutions (0.5 V versus SHE) is lower than that for pyrite, (0.6 V versus SHE) (Mehta, 1983). Thus, if they are in electrical contact in acidic solution containing an oxidant, chalcopyrite would act as an anode and undergo dissolution while pyrite is galvanically protected as the cathode. Recently studies carried out by Al-Harahsheh et al., (2006b) have demonstrated this phenomenon. From a SEM analysis, they showed that chalcopyrite is preferentially attacked when it is in contact with pyrite. The rate of electron transfer increased significantly due to this galvanic interaction causing a higher rate of chalcopyrite dissolution. The authors highlight the importance of

the pyrite phase for chalcopyrite oxidation not only when pyrite is present as a bulk phase in electric contact with chalcopyrite but also when pyrite is formed as a result of a surface reconstruction mechanism which was not, however, demonstrated.

Mehta et al. (1983) studied the effect of galvanic interactions generated by addition of different amounts of pyrite with different particle size to constant amounts of chalcopyrite. X-ray analysis of the residue for which maximum copper dissolution was achieved showed that the pyrite particles were unleached and were surrounded by chalcopyrite particles demonstrated that an excellent contact between pyrite and chalcopyrite existed whenever enhanced copper extraction was observed. On the other hand, the results showed that when a finer size fraction of pyrite was added, the rate of copper extraction was found to be greatly reduced. They suggested that the finer pyrite was covered with an iron hydroxide precipitate that reduced the contact with chalcopyrite.

Cruz et al., (2005) concluded that galvanic interactions depend on the mineralogical association between the phases present in the concentrate. They showed that even small quantities of impurities cause a significant modification in the pyrite reactivity (described as the capacity of pyrite to react under a given set of conditions). The authors proposed that a comparison be made in terms of the electrochemical behaviour before and after leaching thereby possibly enabling a prediction to be made of the reactivity of sulfide minerals in different hydrometallurgy systems.

In a recently published paper Dixon et al. (2007) claim that the cathodic half-cell reaction (ferric reduction) is slow on the surface of chalcopyrite and limits the overall rate of leaching. However, it is suggested that the presence of pyrite in electrical contact with chalcopyrite can catalyse the reduction of ferric ions and thereby increase the overall rate of leaching. The so-called GALVANOX process involves the leaching of chalcopyrite in sulphate media at low potentials (440 to 470 mV) at 80 °C in the presence of pulverized pyrite. The addition of pyrite should be two or four times that of chalcopyrite to ensure rapid and complete copper extraction, producing a solid sulfur residue according to the overall reaction:



Due to only a few conflicting studies; the complex nature of the effect of pyrite on chalcopyrite dissolution requires further work to develop a more detailed understanding of this issue.

2.2.6.4. Activated carbon

It has been reported that some types of carbonaceous compounds such as activated carbon, graphite and coal can catalyse the leaching of chalcopyrite. The main characteristics of activated carbon are large surface area and absorption capacity together with a degree of electronic conductivity and refractory nature. Miki et al. (2003) confirmed the catalytic effect of activated carbon on chalcopyrite leaching and showed that the critical potential was higher in the presence of carbon. This enhancement was suggested as being due to galvanic interaction between activated carbon and chalcopyrite above the critical potential and also to reduction of chalcopyrite by activated carbon at the critical potential.

2.2.7. Effect of potential

Recently, the use of the solution redox potential as a parameter that can control the rate of oxidation of the mineral has increased. However, it has been pointed out by Nicol (1975); and Nicol and Lázaro (2002) that most of studies in this respect have assumed that the potential (E_h) measured with a platinum electrode in the bulk of a leaching solution or a pulp is identical to the potential at the surface of a dissolving mineral (mixed potential). They showed from experimental measurements and theoretical considerations that the potential in the solution (E_h) and that on the mineral are not necessarily equal. Lázaro (2003) noted that although some authors have raised the concept of mixed potential very few have actually measured it and/or have incorrectly interpreted the measurements.

2.2.7.1. E_h potential

Monitoring of an oxidation process in solution is commonly carried out by measurement of the redox potential (ORP) using a platinum indicating electrode and a reference electrode (saturated calomel or silver/silver chloride electrode). When the redox potential is converted to a potential on the normal hydrogen electrode scale (SHE), this potential is denoted E_h .

A redox potential is created when electrons in two phases (oxidant-reductant) are in equilibrium. Thus for redox couple



the potential can be expressed by the general form of the Nernst equation

$$E = E^0 + \frac{RT}{nF} \log \frac{[Ox]}{[Red]} \quad (2.35)$$

in which E^0 is the standard reduction potential (the potential under conditions of unit activity for Ox and Red and $[Red]$, and $[Ox]$ are the activity of species generally approximated to the concentrations).

Thus, for the dissolution of chalcopyrite



the equilibrium potential is given by

$$E = 0.427 - \frac{0.0592}{2} \log \frac{1}{[Cu^{2+}][Fe^{2+}]} \quad (2.37)$$

Heterogeneous reactions at an electrode are not only dependent on the concentrations of reacting species but also on the electrochemical potential difference across the solid/solution interface. A diagram of current density (rate of electrode reaction) versus potential can represent the dependence of the rate as a function of the potential on the electrode (mineral surface). Figure 2.11 shows that the rate of the anodic reaction increases with increasing potential and that of the cathodic process increases with decreasing potential. Under open circuit conditions ($i=0$) the rates of the anodic and cathodic reactions are equal at the equilibrium potential E_e . If there are no interfering reactions, E_e will be equal to that given by the Nernst equation, Eq. (2.35).

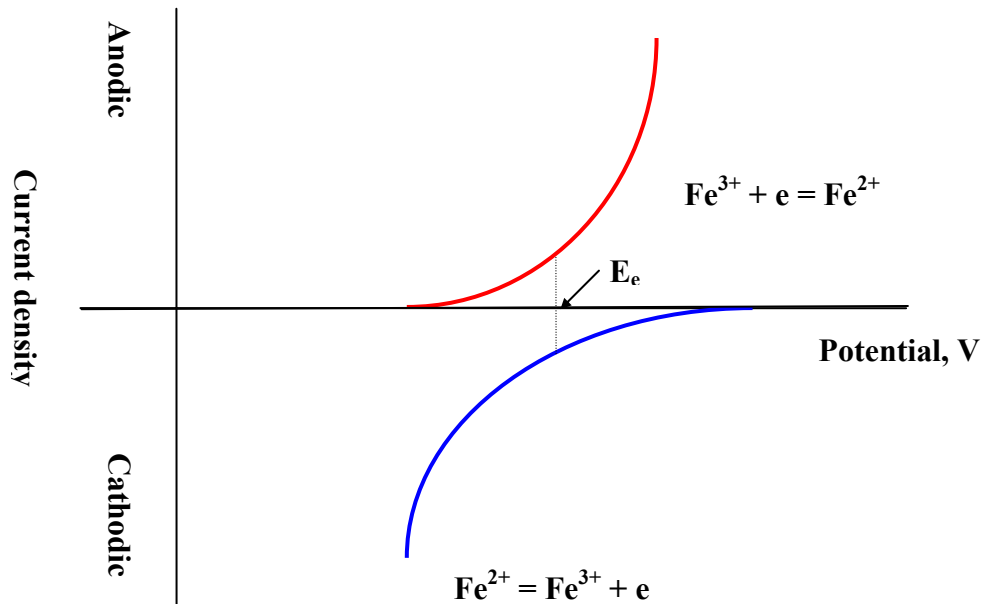


Figure 2.11 Schematic curve showing the dependence of the rate (current) for the Fe(II)/Fe(III) couple on a platinum electrode as a function of the potential in a solution containing both species.

The current versus potential curve can be represented by the Butler-Volmer equation for electrode kinetics,

$$i = i_0 \exp\{\alpha_a F/RT (E - E_e) - \alpha_c F/RT (E_e - E)\} \quad (2.38)$$

in which i is the current density, i_0 is the exchange current density, and α_a and α_c are the anodic and cathodic transfer coefficients (for a single-electron transfer $\alpha_a = \alpha_c = 0.5$)

In the case of most minerals, it is possible to operate with metastable solutions that can be saturated with oxygen but still have measured E_h values that do not reflect the equilibrium potential of the solution (Nicol, personal communication, 2005).

2.2.7.2. *Mixed potential, E_m*

The mixed potential model has been used to explain the kinetics observed in many hydrometallurgy process involving solids which are electronic conductors such as metals, metal sulphides and oxides (Nicol and Lazaro, 2002). A mixed potential is established when two or more reactions occur on the same surface independently of each other.

The rate as a function of the potential at a mineral surface also can be depicted in terms of a diagram of current versus potential the form of which will depend upon the nature and properties of the mineral surface. Figure 2.12 is a schematic of the mixed potential model as applied to a sulphide mineral surface in the presence of ferric ions. Also shown are the curves for the iron(III)/iron(II) couple previously shown in Figure 2.11. Note that the mixed potential is determined by the requirement that the sum of all anodic currents must equal that of all cathodic currents. The difference between the mixed potential (E_m) on the mineral surface and the equilibrium potential of the solution (E_h) can be seen in the diagram.

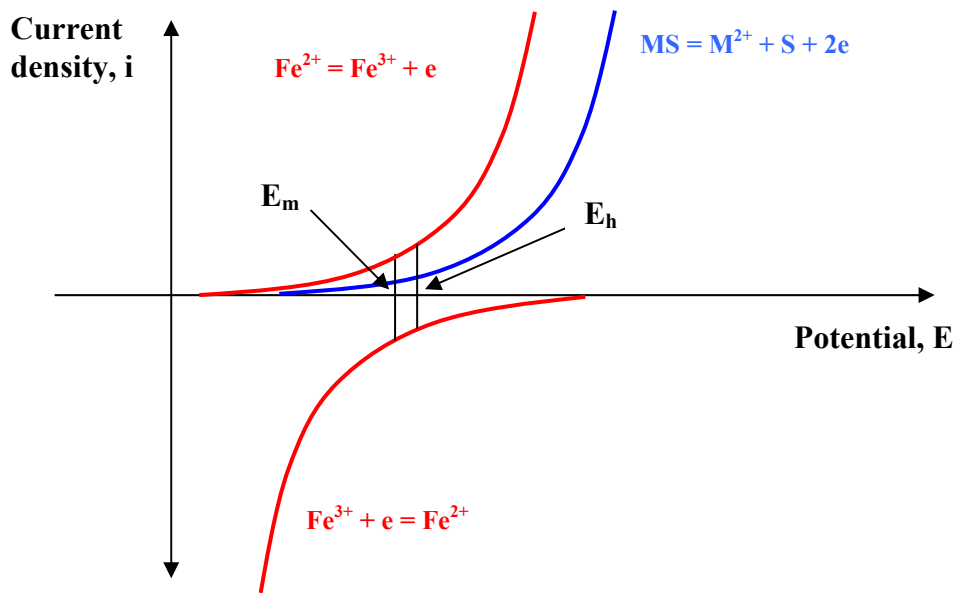


Figure 2.12. Difference between E_h and E_m in a sulfide leaching system

The mixed potential is invariably lower than E_h for two reasons:

- i) The anodic oxidation of the mineral introduces an additional anodic current which must be balanced by an additional cathodic current as shown in Figure 2.12.
- ii) As a result of a reduction of the oxidant at the mineral surface, the concentration of the oxidant is reduced and the reduced form of the couple increases. As a result, E_h and E_m decrease at the surface of the mineral. This decrease in potential will be dependent on the relative rates of mass transfer to the surface and that of the leaching reaction.

In the case of chalcopyrite, the perturbation of E_h and E_m is not significant unless mass transport is impeded as result of, for example, the distribution of the mineral in pores and cracks.

2.3. Mechanism of the dissolution of chalcopyrite in chloride solutions

While it is difficult to compare information from various studies because of the differing conditions, it appears that mechanism for the dissolution of chalcopyrite in chloride media is still very controversial. According to Dutrizac (1978) the leaching behaviour of chalcopyrite in ferric chloride and ferric sulfate media are substantially different. Thus, the author believes that different mechanisms are operative for the two systems and, consequently, the data for one medium should not be used to support a mechanistic interpretation in the other. Many studies have been carried out to explain the role of potential on the dissolution of chalcopyrite. However, according to Nicol and Lázaro (2003) the potential region studied in most of these cases was above the potential region in which the mineral actively dissolves. Several alternative mechanisms have been suggested involving oxidative, reductive/oxidative, non-oxidative and a combination of non-oxidative/oxidative reactions each of which are described in the following sections.

2.3.1. Oxidative dissolution

The oxidative dissolution of chalcopyrite in acidic ferric or cupric chloride solutions can be described by the normal mixed potential electrochemical model based on the following reactions



coupled to



or



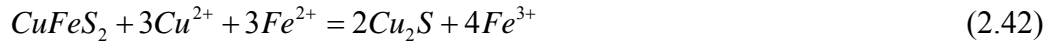
This mechanism is characterized by a rapid initial dissolution rate which decays to a slow rate at longer times. This has been shown to be the case for potentials within the so-called passive region in the anodic curve for the oxidation of chalcopyrite and is typical of the situation with ferric ions as the oxidant under ambient conditions (Hiroyoshi et al., 2004). The rate of the oxidative process is not significantly affected by the potential between 0.55 and 0.75 V and greatly increases in the transpassive region above 0.75 V which is not accessible with common oxidants.

2.3.2. Reductive/Oxidative dissolution

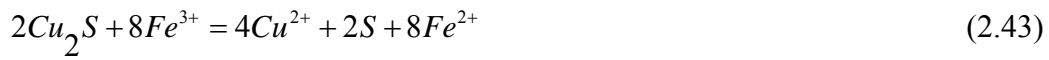
In a study of oxidative leaching of chalcopyrite with dissolved oxygen and/or ferric ions, Hiroyoshi et al. (2001; 2000) found that the rate was promoted by high concentrations of ferrous ions in sulphuric acid solutions containing cupric ions. However, they could not explain their results in terms of the typical oxidative model according to which the rate of copper extraction should be decreased by (or independent of) the addition of cupric and ferrous ions because these ions are the products of the anodic and cathodic reactions.

In order to interpret the enhancement of chalcopyrite leaching by ferrous and cupric ions, these researchers proposed a two-step reaction model.

(1) Chalcopyrite is reduced by ferrous ions to Cu_2S in the presence of cupric ions.



(2) The intermediate Cu_2S is oxidized by ferric ions



The sum of reactions (2.42) and (2.43) gives the generally reported reaction for ferric leaching of chalcopyrite in sulfate media. The model predicts that the formation of intermediate Cu_2S and ferrous promoted chalcopyrite leaching will occur when the redox potential of the solution is below a critical potential that is function of the ferrous and cupric ion concentrations. Cu_2S is more rapidly oxidized than chalcopyrite and this causes the enhanced copper extraction at low potentials in the presence of cupric and ferrous ions. They found that active-passive behaviour is observed in the anodic polarization curves of chalcopyrite electrodes only when cupric and ferrous ions coexist in the solutions. Hiroyoshi et al. (2004) explained that Cu_2S oxidation in eq. (2.43) consists of the following two reactions in agreement with Dutrizac et al. (1978)



On the other hand, according to Nicol and Lázaro (2003) this model fails to explain how step (42) can be achieved at potentials in which this process is likely not to occur from thermodynamic point of view. A mechanism in which Fe(II) acts as a reducing agent and simultaneously Fe(III) is an oxidant is unlikely. Another interesting result is that the dissolution of chalcopyrite in sulfuric acid solution under nitrogen atmosphere was higher in the absence of either cupric and or ferrous ions than in their presence. This result was explained in terms of the effect of residual oxygen by these authors. Similar results were obtained by Ammou-Chokroum et al. (1981), but according to Nicol and Lázaro (2003) this can simply be explained in terms of a non-oxidative process.

Variations on this model have been made that include alternative reactions to explain, for example, catalysis of the reaction by silver ions (Hiroyoshi et al., 2002). These variations assume that during the reduction of chalcopyrite, hydrogen sulphide is released which reacts with silver ions to form silver sulphide thereby decreasing the concentration of hydrogen sulphide in the solution. This in turn should increase the critical potential of Cu_2S formation and broaden the potential range in which rapid copper extraction takes place. The authors recognize that this model does not agree with the conventional model proposed by Miller et al. (1981).

2.3.3. Non-oxidative dissolution

According to data in Table 2.1 dissolution of chalcopyrite in acidic solutions under non-oxidative conditions is not spontaneous under normal conditions. This process was

proposed in separate publications of Parker (1981) and Ammou-Chokroum (1981). However, it was not investigated in any detail until Nicol (1983) and Nicol and Lázaro (2003) published more information. According to these authors, the lack of studies has been mainly due to two reasons (1) low concentrations of the dissolved species in solution make analysis very difficult and (2) authors such as Ammou-Chokroum (1981) and Hiroyoshi et al. (2001) have suggested that this behaviour can be attributed to dissolution caused by residual oxygen. According to Nicol and Lázaro the latter reason is uncertain since the suggested residual oxygen must be less than 1 ppm and the slow reduction kinetics of oxygen on chalcopyrite surface would make this improbable.

Nicol and Lázaro observed that dissolution of chalcopyrite can occur to some extent in the absence of any oxidizing reagent and they proposed a non-oxidative process based on the following considerations

- i) It has been confirmed that under non-oxidative conditions soluble copper ions, hydrogen sulphide are metastable products of reaction, which are converted into an undefined copper sulphide. During non-oxidative dissolution, reaction (2.46) occurs and the copper ions can precipitate as shown in reaction (2.47). In the presence of a suitable oxidant agent such as Fe(III) or Cu(II), reaction (2.48) will remove H₂S and sustain the non-oxidative process. The extent to which a sulphide such as CuS will form will depend on the rate of reaction (2.48).



- ii) It is suggested that the rate of the non-oxidative reaction decreases as the potential of the chalcopyrite surface is increased from 0.5 to 0.7 V
- iii) The rate of reaction (2.46) is governed by two steps:
- Rapid dissolution to assure equilibrium between soluble species at the surface of mineral and the solid.
 - Rate-determining diffusion of the soluble species away from the mineral surface
- iv) The maximum rate, in terms of H₂S production, of the non-oxidative dissolution reaction will be given by

$$\text{Max Rate} = K_m (4K)^{1/4} [H^+]$$

in which k_m is the mass transport coefficient for transport of H₂S from the surface of the mineral, K is the equilibrium constant for reaction (49) and $[H^+]$ is the surface proton concentration. The calculated rate of this non-oxidative process was shown to approximate that observed.

2.3.4. Non-oxidative/oxidative model

Nicol and Lázaro (2003) extended the non-oxidative model to include the oxidative dissolution process. Thus, the reactions (2.46) and (2.48) can be combined to give the overall reaction.



Assuming that the rate of reaction (2.48) is rapid compared to the rate of diffusion of H₂S from the surface, the above authors applied Fick's second law at steady-state with some

assumptions based on a re-analysis of the data of Tekin et al. (1999) (cited in Nicol and Lázaro, 2003) for the rate of reaction (2.48). The following expression was derived for the flux of copper ions from the surface of the chalcopyrite

$$J = (4K)^{1/4} [H^+]_0 \left[(K[Fe(III)]_0 D / [H^+]_0)^{0.5} \coth \left[(K[Fe(III)]_0 D / [H^+]_0)^{0.5} / K_m \right] \right]$$

in which J is the flux, D is the diffusion coefficient for Fe(III), k_m is the mass transfer coefficient and $k = 6 \text{ s}^{-1}$ at $60 \text{ }^\circ\text{C}$.

It is of interest to note that the above model predicts that the rate of dissolution of chalcopyrite should not increase significantly with addition of Fe(III) above about 0.1 M, that increasing concentrations of acid should not increase the rate and that addition of ferrous ions should reduce the rate of dissolution. The results of the simulated rates of dissolution were found to be comparable with some reported studies of the kinetics of dissolution in acid solutions.

It should be apparent from the above review of the mechanisms of the dissolution of chalcopyrite in both sulfate and chloride media that there is very little agreement between the researchers who have tackled this problem over many years. It is therefore one of the objectives of this thesis project to contribute to the understanding of this complex but very important problem.

3. EXPERIMENTAL METHODS AND MATERIALS

3.1. *Materials and Reagents*

Table 3.1 lists the chemical reagents as used in this study without further purification. All solutions were made up with analytical grade reagents and Millipore quality water.

Table 3.1 **Chemicals Reagents**

Reagents	Formula	Purity	Purpose
Oxygen gas	O ₂	Industrial grade	Oxidation/ potential control
Nitrogen gas	N ₂	High purity grade	Removal of oxygen
Copper (II) sulfate	CuSO ₄ ·5H ₂ O	AR	Addition to lixiviant
Sodium chloride	NaCl	AR	Addition to lixiviant
Ferric sulfate	Fe ₂ (SO ₄) ₃ ·xH ₂ O	AR	Oxidation
Ferrous sulfate	FeSO ₄ ·7H ₂ O	AR	Reduction
Silver in HNO ₃	Ag	AAS	Catalysis
Hydrochloric acid	HCl	36.5%	Lixiviant
Sulphuric acid	H ₂ SO ₄	98%	Lixiviant

3.1.1. Sulphuric acid solutions

Various different concentrations of sulphuric acid solutions were prepared using fixed volumes of 98% concentrated acid, assuming a specific gravity for H₂SO₄ of 1.8 g cm⁻³.

3.1.2. Hydrochloric acid solutions

All solutions employed were prepared using fixed volumes of 36.5% concentrated acid calculated assuming a specific gravity for HCl of 1.18 g cm⁻³.

3.1.3. Mineral samples

Chalcopyrite concentrates from Andina and Cerro Colorado (CCHYP) in Chile, Escondida in Chile (PQS), Pinto Valley in Arizona (PV) and Spence in Chile were produced by flotation at the Johannesburg Technology Centre of BHP Billiton. A sample of massive chalcopyrite from Ok Tedi in Papua New Guinea was also used in this study. The majority of the experiments were carried out using samples of a specific size fraction. Preliminary experiments were carried out with samples that were dried screened. The rest of the experiments were carried out with materials sized by wet screening to minimize agglomeration. Most experiments were carried out with -38+25 µm samples (Andina and OK Tedi) and -38 µm samples for the other concentrates due to the limited amounts of these concentrates available for leach testwork. The chemical compositions of the materials used are given in Table 3.2 while the trace element analyses are given in Table 3.3.

Table 3.2 Chemical data (% elemental composition)

Sample	Size μm	Screened	Cu	Fe	S
Ok Tedi	25-38	dry	20.7	30.5	35.4
Andina	25-38	dry	29.9	26.5	31.2
Andina	25-38	wet	32	30.5	32.4
Spence	25-38	dry	15.2	34.2	45.3
PQS2	-38	wet	8.1	30	35.3
PV	-38	wet	13.2	21.8	23.3
CCHYP	-38	wet	14.7	23.8	26.8
Covellite	25-38				

Table 3.3 Trace element composition (ppm)

Sample	Size (μm)	Screen	Ag	Bi	Sb	Cd	Sn	Co	Ni	As
OK Tedi	head	dry	355	52.3	0.3	3.1	45.9	1.0	<1	60
Andina	head	dry	81	46.4	220	25.1	3.2	21	12.0	2650
Spence	25-38	dry	44.0	10.3	300	28.8	13.0	195	230	2400
PQS2	-38	wet	18.0	5.3	32.5	20.3	9.6	190	170	720
PV	-38	wet	24.0	1.4	2.3	10.4	13.4	110	105	40
CCHYP	-38	Wet	20.0	4.5.0	11.6	30.1	6.6	1120	245	80

The mineralogical compositions of the concentrates were obtained by Mineral Liberation Analysis (MLA) at the Newcastle Technology Centre of BHP Billiton and the results shown in Table 3.4. A detailed mineralogical study has been carried out on most of the mineral samples and the results will be described in the next chapter.

The amount (as a percentage) of copper contained in each mineral for each concentrate sample is shown in Table 3.5 as the so-called CSR.

Table 3.4 Mineralogical composition of concentrates (Wt%)

Mineral	Andina 25-38 µm	PQS1 25-38 µm	PQS2 -38 µm	Spence 25-38 µm	Ok Tedi unsized	PV -38 µm	CCHYP -38 µm
Chalcocite	0.00	0.47	0.0	0.00	0.00	0.0	2.49
Chalcopyrite	82.50	44.60	17.6	27.40	77.90	45.8	32.98
Covellite	0.16	14.30	5.0	7.50	0.00	0.0	5.65
Bornite	3.40	2.80	1.7	2.90	0.01	0.1	2.68
Enargite	1.70	1.80	1.2	4.10	0.00	0.0	0.73
Brochantite	0.00	0.19	0.0	0.01	0.00	0.0	0.23
Chrysocolla	0.00	0.00	0.0	0.01	0.00	0.0	0.04
Other Cu Min	0.00	0.10	0.0	0.12	0.00	0.1	0.05
Pyrite	2.70	29.30	62.2	50.80	17.90	20.9	34.33
Quartz	5.00	2.00	3.4	2.90	0.02	9.6	5.33
Galena	0.47	0.41	0.1	1.69	0.41	0.1	0.1
Gangue	4.03	4.02	8.8	2.57	4.02	23.4	15.39
Total	100	100	100	100	100	100	100

Table 3.5 CSR (copper source ratio) of major copper minerals

Sample	Andina 25-38 μ m	PQS2 -38 μ m	Spence 25-38 μ m	OK Tedi unsized	PV -38 μ m	CCHYP -38 μ m
Chalcopyrite	90.2	54.0	51.7	100	99	59.1
Covellite	0.2	31.0	27.4	0	0	19.6
Bornite	6.8	9.0	10.0	0	0.4	8.8
Enargite	2.6	5.0	10.8	0	0	1.8

3.2. Experimental Methods

3.2.1. Preparation of concentrates for leaching

The samples described in Table 3.2 were either dry or wet screened. The selected size fractions were cleaned by repeated washing with tap water in a sieve shaker, washed thoroughly in acetone and finally vacuum dried at room temperature. All concentrates were stored in sealed bags in a cold room to minimize oxidation.

3.2.2. Leaching with shake flasks

Leach tests using shake flasks were carried out to provide rapid preliminary data. In a typical experiment, 0.02 g of Ok Tedi unscreened sample and 20 cm³ of solution were each added to 100 cm³ Erlenmeyer flasks. The flasks were placed on an orbital shaker (200 rpm) and incubated at one of three different temperatures 25, 35 and 50 °C. A few experiments were also carried out with 0.4 g of unscreened Andina concentrate added to 40 cm³ of

solution at 35 °C. These experiments were designed to semi-quantitatively establish the effect of chloride ions, temperature, acid and ferric ions on the rate of chalcopyrite leaching. In experiments in which a nitrogen purge was necessary, the flask was capped with a rubber septum and two injection needles inserted through the septum. Nitrogen, saturated with water vapour, was introduced into the flask at a rate of about 1 dm³ min⁻¹ using the needles as inlet and outlet. After 15 min, the needles were removed. When a nitrogen purge was not desired, a stopper of cotton wool was used.

At various times, samples of the leach solution were obtained by use of a membrane filter (pore size 0.2 µm) on a syringe. Copper and total dissolved iron concentrations were determined by atomic absorption spectroscopy.

Before and after experiments, the redox potential of leaching solution was measured by using a platinum electrode and a saturated calomel reference electrode. The mixed potential of a chalcopyrite electrode was measured by using a chalcopyrite electrode and a saturated calomel electrode. All potentials were converted to values against the standard hydrogen electrode (SHE).

3.2.3. Agitated leaching in instrumented reactors

Agitated leaching experiments were carried out in instrumented reactors constructed in the workshop at Murdoch University. The baffled cylindrical glass reactors have a volume of 1000 cm³ and are sealed with a multi-port PVC lid on which is mounted a stirrer motor with a titanium or plastic-coated impeller. The lid also can be equipped with ORP and

chalcopyrite electrodes and nitrogen or oxygen gas inlets. The reactor is enclosed in a temperature-controlled PVC surround. Figure 3.1 shows a photograph of the instrumented reactor.

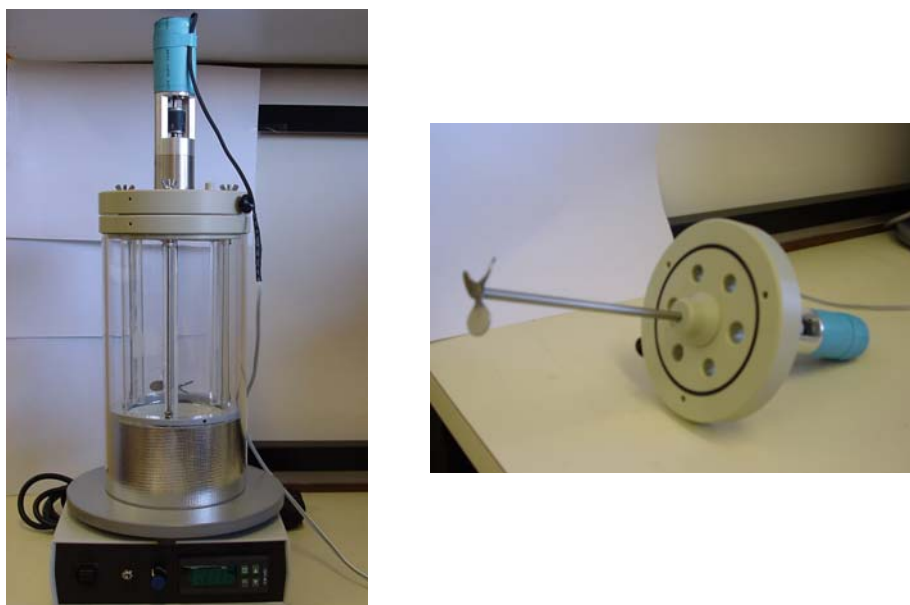


Figure 3.1 Instrumented Reactor

Except where mentioned, agitated leaching experiments were carried out using 9 g of sized chalcopyrite samples in 900 cm³ of solution at 35 °C with a stirring speed of 800 rpm. The stirring speed was measured using a hand held tachometer.

In all leaching tests, liquid samples were withdrawn periodically after compensating for evaporation by the addition of distilled water and settling of suspended solids for approximately 30 min. An equal volume of the lixiviant was added to replace that removed in the sample. The samples were filtered (0.2 µm) prior to analysis for copper, total iron

and in some cases silver using Atomic Absorption Spectrometry (AAS). When solid samples were required, a slurry sample was collected from the reactor and vacuum filtered. The solid was washed and dried in air. The dried solid samples were sent to the Newcastle Technology Centre of BHPBilliton for MLA analysis and optical examination in some cases.

The solution and mixed potentials were monitored online using suitable electrodes (Section 3.3) connected to high impedance analogue input channels on a National Instruments data acquisition board together with LabviewTM software. Daily measurements of pH and the dissolved oxygen concentration were also made manually.

3.2.4. E_h Control system

In all the leach experiments, reaction of the mineral sample with the oxidant results in a decrease in the potential (E_h) of the solution. The E_h can be maintained constant by the introduction of additional oxidant and, in the case of the chloride system, re-oxidation of copper(I) by dissolved oxygen is generally adequate to maintain potentials in the range of 550 to 700 mV (SHE).

The solution potential in the leach reactor was maintained at a constant E_h set point by a computer controlled valve attached to a suitable gas supply. National Instruments data acquisition boards and LabviewTM software was used in the development of the system that controlled the solution potential. The control algorithm was based on digital acquisition of the solution potential and control, of the gas flow into the reactor by way of a solenoid valve. Depending on the reaction under investigation, air, oxygen or nitrogen could be used

to control the potential in this way. In some initial experiments, control of the potential was achieved by in-situ electrochemical oxidation of copper(I) and/or iron(II) using platinum electrodes in the leach slurry. Figure 3.2 shows a photograph of the control equipment.



Figure 3.2 Control system

3.2.4.1. *Electrochemical control system*

Figure 3.3 shows the schematic of the potential control system based on electrochemical oxidation. This system operates on the principle that anodic oxidation of cuprous and/or ferrous ions produced as a product of reduction of ferric ions also as a product of oxidation of mineral can be used to regenerate ferric ions. The system consists of an Eh electrode and two platinum generating electrodes. The anode consisted of a 1 cm² of platinum plate and

the cathode was a platinum wire separated from the leach pulp by a fritted glass tube. The system operates as follows:

- i) The redox potential of solution is measured by a combined Eh electrode and this value is read into the computer via the data acquisition board.
- ii) The measured potential is compared with the set point value by the LabView software. If the measured E_h is lower than the set point, an analogue voltage proportional to the difference between the measured and set potentials is converted into a current.
- iii) The current (0 to 50 mA maximum) is applied to the generating electrode in the slurry to re-oxidise ferrous or cuprous ions.

On the surface of platinum anode the following reaction occurs



and at the isolated platinum cathode



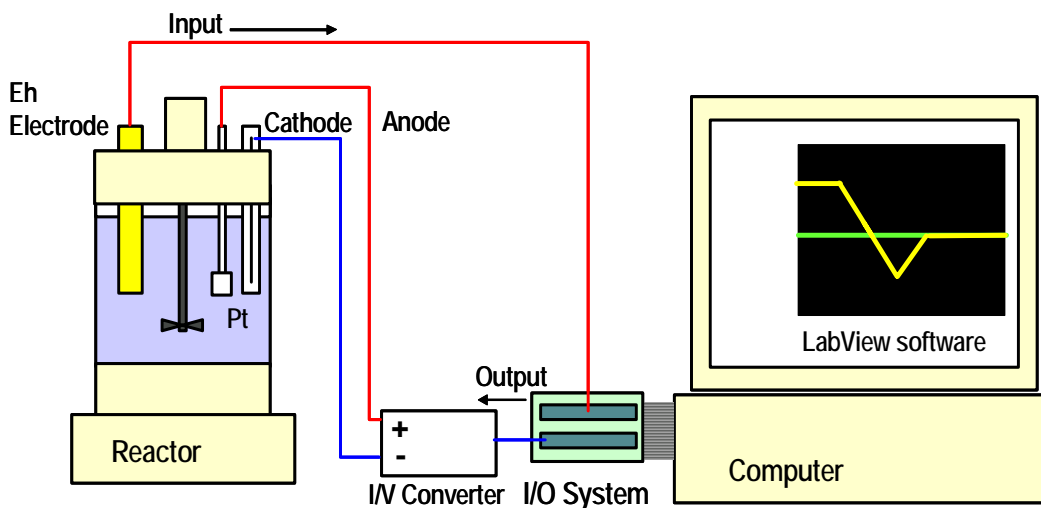


Figure 3.3 Schematic of the electrochemical potential control system

3.2.4.2. *Air potential control system*

This system controls the potential by the use of air to reoxidise cuprous or ferrous ions in the leach slurry.



Figure 3.4 shows the schematic of this system. The reactor is equipped with a combined E_h probe and a gas injection tube.

As above, the E_h electrode is connected to the data acquisition system while an air pump is connected to the air injection tube. The pump can be controlled by a solid-state switch activated by a digital output port on the acquisition board. The control algorithm is similar to that described above.

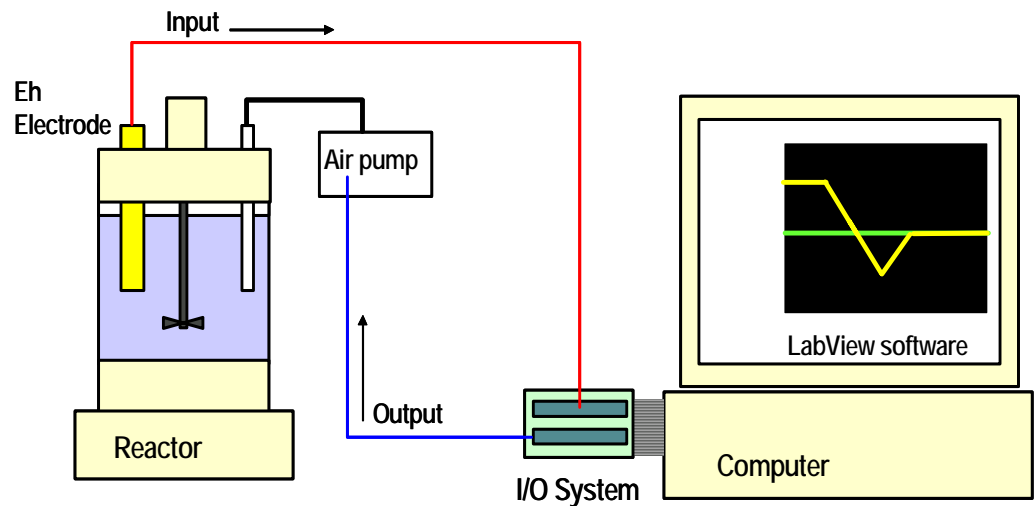


Figure 3.4 Schematic of the air potential control system

3.2.4.3. *N₂/O₂ potential control system*

Figure 3.5 shows a schematic of the potential control system which uses either nitrogen or oxygen as used in most of leaching experiments. The system consists of a combined Eh probe, gas sparger and a gas control valve.

The control algorithm is similar to that above and the only difference is the use of a digitally controlled gas valve to allow oxygen or nitrogen into the leach reactors. In some experiments, air was allowed to diffuse into the reactor through open ports in the lid. Nitrogen was used to reduce the partial pressure of oxygen in the reactor thereby permitting control of the potential.

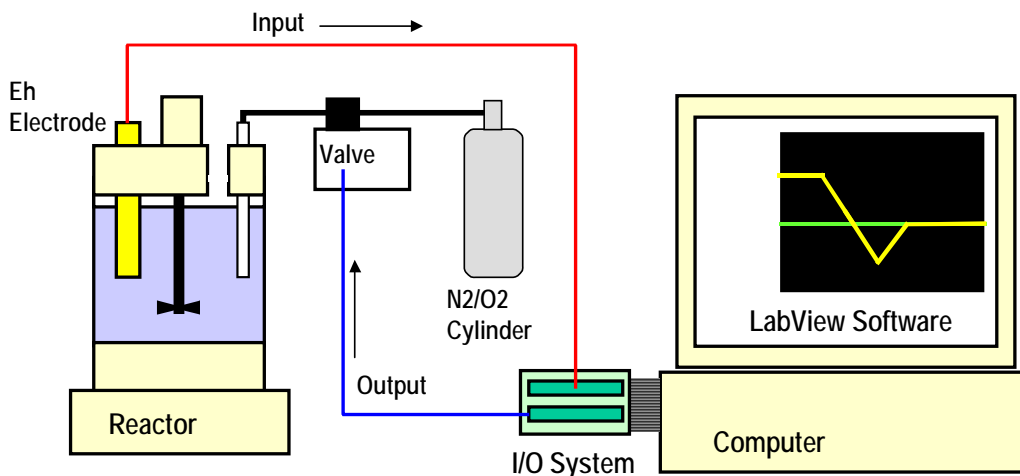


Figure 3.5 Schematic of the N_2/O_2 potential control system

3.2.5. The rate of consumption of dissolved oxygen

The rate of the copper-catalysed oxidation of H_2S by dissolved oxygen was measured using an oxygen probe with the apparatus shown in Figure 3.6. An YSI model 5301 biological oxygen was used to measure dissolved oxygen consumption. Four millilitre of the appropriate solution was placed into the cell which was stirred by a small magnetic bar. The dissolved oxygen probe holder was designed to act like a plunger which fitted the cylindrical glass cell. A small groove machined along the length of the probe allowed air to be expelled as the probe was lowered into the cell. The cell was immersed into a temperature controlled water bath maintained at $35\text{ }^\circ\text{C}$. After temperature equilibration a small amount of Na_2S solution was injected into the cell using a thin Teflon tube and micropipette inserted into the groove. The dissolved oxygen concentration was recorded as a function of time using NI data acquisition and Labview software.

All reagents used were analytical grade. The Na_2S solution was analysed by titration with standard AgNO_3 solution.

In several comparative experiments, a copper(I) solution was injected into the reactor instead of a Na_2S solution. The copper(I) solution was prepared from reagent grade CuCl and HCl and was stored under a nitrogen atmosphere in the presence of a piece of copper wire to minimize oxidation to copper(II).

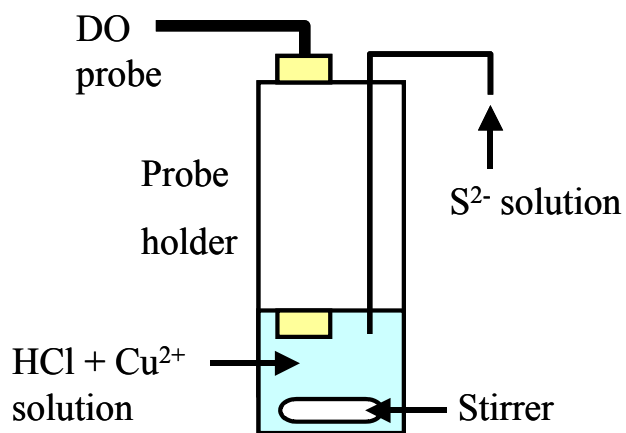


Figure 3.6 Schematic of the apparatus for measurement of the consumption of dissolved oxygen

3.3. Monitoring system

3.3.1. Measurement of E_h

The solution or slurry potential was continuously monitored and recorded with the LabView™ data acquisition system using platinum and chalcopyrite electrodes. In experiments involving the oxidation of the concentrates, a chalcopyrite electrode was used to monitor the potential response of the mineral in solution.

Platinum ring electrodes with a combined Ag/AgCl reference electrode (3 M KCl) (Metrohm Model 6.0451.100) were used. The E_h probe was immersed continuously in the reactor and the cable of the electrode wired to the I/O connector block connected to the data acquisition system. All values of the potential reported in this study have been converted to a potential on the normal hydrogen electrode scale.

When a platinum electrode is placed in a redox system which comprises a redox couple Red/Ox, at equilibrium



The measured potential can be expressed by the general form of the Nernst equation:

$$E = E^0 + 2.303 \frac{RT}{nF} \log \frac{[\text{Ox}]}{[\text{Red}]} \quad (3.5)$$

in which E^0 is the standard reduction potential i.e. the potential under conditions of unit activity for *Ox* and *Red*, $[Red]$ is the activity (generally approximated to the concentration) of species Red and the factor $2.303 RT/nF = 0.0592 V$ for $n = 1$ at 25 °C.

Since Eh is defined as the potential with respect to the standard hydrogen electrode at all temperatures, the potential of the reference electrode relative to a standard hydrogen electrode must be added to the measured potential to obtain the Eh (Eq. 3.6). Table 3.6 summarizes the values used for this conversion of the potential measurements to the SHE scale (Scholz, 2005).

$$E_h = E + E_{Ag} \quad (3.6)$$

where E_{Ag} is the potential of the reference electrode.

Table 3.6 Conversion of potential measurements to the SHE scale.

T/°C	$E_{\text{Ag}}/\text{mV (Ag/AgCl)}$				
	M (KCl)		[KCl]		
	1 mol kg ⁻¹	1 mol L ⁻¹	3 mol L ⁻¹	3.5 mol L ⁻¹	saturated
0	236.6	249.3	224.2	222.1	220.5
5	234.1	246.9	220.9	218.7	216.1
10	231.4	244.4	217.4	215.2	211.5
15	228.6	241.8	214.0	211.5	206.8
20	225.6	239.6	210.5	207.6	201.9
25	22.3	236.3	207.0	203.7	197.0
30	219.0	233.4	203.4	199.6	191.9
35	215.7	230.4	199.8	195.4	186.7
40	212.1	227.3	196.1	191.2	181.4
45	208.4	224.1	192.3	186.8	176.1
50	204.5	220.8	188.4	182.4	170.7
55	200.6	217.4	184.4	178.0	165.3
60	196.5	213.9	180.3	173.5	159.8
65		210.4	176.4	169.0	154.3
70	187.8	206.9	172.1	164.5	148.8
75		203.4	167.7	160.0	143.3
80	178.7	199.9	163.1	155.6	137.8
85		196.3	158.3	151.1	132.3
90	169.5	192.7	153.3	146.8	126.9
95	165.1	189.1	148.1	142.5	121.5

3.3.2. Measurement of the chalcopyrite electrode potential

The electrodes were prepared from samples of the pure mineral provided from the Mineral Science Department collection at Murdoch University. The specimens were cut into cylindrical rods and one face attached to a stainless steel holder using silver epoxy resin (Lázaro 2001). Following this, the electrode was mounted in araldite resin leaving the opposite face exposed to the solution. Before each experiment, the electrode surface was polished on successively finer silicon carbide papers. The potential of the electrodes were measured using the same reference electrode as used in the combined electrode probes.

3.3.3. Control of solution pH

Measurement of pH was taken with a Metrohm refillable combination electrode with a glass body, rugged bulb and ceramic junction. Refilling of the electrode was done with 3 M KCl. BHD colour coded buffers ranging from pH 2 to pH 7 were used for the calibration of pH electrodes before each use. The electrode was connected to Smart CHEM-Lab meter for measurement. The solution pH was manually controlled by addition of hydrochloric acid, sulphuric acid or sodium hydroxide as required.

3.3.4. Measurement of dissolved oxygen

Measurements of the dissolved oxygen (DO) concentration are important as will be demonstrated. Dissolved oxygen in solution was measured with a TPS Model ED1M dissolved oxygen probe connected to a Smart CHEM-Lab meter. The probe was calibrated

with sodium sulphite for zero dissolved oxygen and in air for 100% dissolved oxygen. The saturated value of DO at 35 °C used in this study was 6.5 ppm.

3.4. Analyses

All the chemicals used for the analyses were AR grade in purity. A detailed description of the reagents employed in the analyses can be found in Table 3.1.

3.4.1. Atomic absorption spectrometer (AAS)

This technique was used to measure total copper, iron and silver concentrations in solution after dissolution of chalcopyrite under different conditions. A GBC Avanta AAS Model 933 with an air/acetylene flame was employed.

3.4.1.1. Analysis for copper and iron

Dissolved copper standards were prepared from 1000 mg l⁻¹ Cu dissolved in HCl solution and diluted to 1, 3 and 5 mg L⁻¹ Cu. Dissolved iron standards were prepared from 1000 mg L⁻¹ Fe having 1, 3 and 5 mg L⁻¹ Fe. At the wavelengths for copper and iron of 324.8 nm and 248.3 nm respectively, the detection limits for copper and iron are 0.05 mg L⁻¹. The analysis of Cu and Fe had an uncertainty of less than 3%.

3.4.1.2. *Analysis for silver*

A silver standard solution of 1000 mg L⁻¹ Ag from ALDRICH was employed to prepare 1, 2, 3 and 5 mg L⁻¹ Ag solutions for analysis by AAS. At the recommended wavelength of 328.1 nm, the detection limit of Ag was 2.8-11 µg mL⁻¹.

3.4.2. Titrations

This technique was employed to standardize the sulfide ion solution used in experiments involving oxidation by DO. 2.8 g of sodium sulfide was dissolved in 100 mL volumetric flask to make a 0.1 M sodium sulfide solution. 20 mL of this solution was pipetted into a 100 mL stirred beaker and the redox potential measured with an ORP electrode. A standard 0.1 M silver nitrate solution was added as titrant in a potentiometric titration according to the reaction



3.4.3. Particle size analysis

A MICROTRAC Model SRA150 laser size analyser was used to measure the particle size distribution of the mineral samples after wet-sieving.

3.4.4. Miscellaneous analyses

Ultra Trace Laboratory, WA, carried out Head and residues assays of the chalcopyrite concentrate and residue samples.

3.4.4.1. *Mineralogical analysis (based on material prepared by Y. Gu D. Sutherland & P. Guerney)*

To investigate the effect of mineralogy on the dissolution of chalcopyrite, covellite and pyrite samples, head and residue samples from selected leach tests were mounted in an epoxy block. The block was sectioned, polished and analysed at the BHP Billiton Newcastle Technology Centre using MLA (Mineral Liberation Analyser), a system developed at the JKMRC. A photograph of this system is shown in Figure 3.7.

The MLA system consists of a specially developed software package and a standard modern scanning electron microscope (SEM) fitted with an energy dispersive spectrum (EDS) analyser. The MLA software package controls the SEM, captures sample images, performs necessary image analysis and acquires EDS x-ray spectra of the mineral grains.



Figure 3.7 MLA (Mineral Liberation Analyser) system

Three different MLA modes are used to handle different sample types and to meet different mineralogical information requirements. These are as follows:

- Standard BSE (back-scattered electron) liberation analysis is the most basic liberation analysis method, in which a series of images are collected on-line and then processed off-line to produce liberation data. Mineral discrimination is based on BSE grey level distribution. The BSE method is the basis for all the other methods.
- Extended BSE liberation analysis (XBSE) is a more advanced method, in which each BSE image is collected and segmented to delineate mineral grain boundaries in each particle, then each mineral grain is analysed using EDS. The off-line processing generates particle maps from particle segmentation data and x-ray spectra. This method can be used to handle various complex ore types.
- X-ray Modal Analysis (XMOD) is a typical point counting method, in which the minerals identification is determined by one x-ray analysis at each counting point. This method only uses BSE to discriminate particle matter from background. For each grid point on a particle, one x-ray spectrum is collected and saved for off-line classification. This method only produces modal mineralogy information, i.e. percentages of the mineral components of the sample.

Analysis of the data is easily achieved off-line using MLA data presentation software with which it is possible to create tables and graphs from quantitative results in the database folder and MLA viewer software with which it is possible to study the images in the images folder. The information collected is as follows:

1. Volumetric proportions of the minerals in the sample
2. Surface areas of minerals and particles
3. Interfacial areas between minerals (i.e. mineral associations)
4. Sizes and shapes of minerals and particles
5. Particle compositions of a large number of particles (50000-100000 point/sample which requires about 2-3 h/sample).

3.4.4.2. *Optical analysis*

Optical microscope analysis was also carried out at NTC to assist in some cases with a comprehensive mineralogical study of the samples. The samples were riffled, mixed with graphite, de-agglomerated and each aliquot for measurement was then mounted in a 30 mm epoxy resin block. Polished blocks were analysed by reflected light microscopy and the images recorded photographically.

4. PRELIMINARY LEACHING EXPERIMENTS

4.1 Introduction

The generally higher reactivity of sulfide minerals in chloride as opposed to sulfate solutions has resulted in many studies of chloride systems for the hydrometallurgy treatment of sulfide minerals. A comparison of chloride and sulfate based leaching processes shows that there are various advantages associated with the former. Thus, chloride leaching can be carried out at ambient temperatures whereas sulfate processes generally require elevated temperatures. In addition, in the chloride system, the Cu(I) ion is stable and this allows electrodeposition of copper via a one electron transfer process. In the case of chalcopyrite, several aspects still require clarification such as the role of impurities, mineral particle size and origin, the nature of passivated layer and the deportment of sulfur.

Because of the fact that sulphuric acid and common salt are cheaper than hydrochloric acid, the use of mixed acidic chloride/sulfate solutions in the leaching of ores and concentrates containing chalcopyrite has increased. Lu et al. (2000a) employed a mixed chloride-sulfate

oxygenated solution to leach chalcopyrite under atmospheric pressure conditions. They claimed that there is no need for the addition of ferric ions, which are believed to be important in the overall leaching process, because these ions are products of the reaction.

This chapter presents several investigations of the kinetics of the dissolution of chalcopyrite in hydrochloric and mixed chloride-sulfate acid solutions during which no attempt was made to control the potential of the solution during leaching. Pure chalcopyrite (CuFeS_2) minerals and various chalcopyrite concentrates containing typical copper sulfide minerals such as chalcocite (Cu_2S), covellite (CuS), and bornite as impurities were used. The chapter opens with preliminary leaching experiments carried out using a simple shake-flask technique and subsequently in instrumented stirred reactors. The effects of various parameters such as the concentrations of Fe(III), Cl⁻, acidity and the temperature were examined. Further experiments were conducted with chalcopyrite concentrates from different localities as individual and binary mixtures of the samples in order to establish a possible role of mineralogy on the rate of leaching. A detail mineralogical study of chalcopyrite head and residue samples using the latest mineralogical analysis system, MLA is also presented. Table 4.1 and Table 4.2 summarize the conditions employed in all leaching experiments carried out in the present chapter.

Table 4.1 Leaching conditions of shake flask experiments

Sample			Condition					
Figure	Test	Sample	Mass g	T °C	Acid M	FeCl ₃ M	NaCl M	Gas
4.1	(a)	Ok Tedi	0.02	25	0.2/HCl	0.1	0.1	air
	(b)			35				air/N ₂
	(c)			50				air/N ₂
4.2, 4.9		Ok Tedi	0.02	50	0.2/HCl	0.1-1	0	air/N ₂
4.3	(a)	Ok Tedi	0.02	25	0.2/HCl	0	0.1-2	air
	(b)			35				
	(c)			50				
4.4*		Andina	0.4	35	0.2/HCl	0	0.1-2	air
4.5-4.8	(a)	Ok Tedi	0.02	25	0.2/HCl	0	0.1-2	air
	(b)			25	0.2/H ₂ SO ₄			
	(c)			35	0.2/HCl			
	(d)			35	0.2/H ₂ SO ₄			
	(e)			50	0.2/HCl			
	(f)			50	0.2/H ₂ SO ₄			

*leached in 40 mL of solution all the other test were carried out in 20 mL of solution

Table 4.2 Leaching conditions of instrumented reactor experiments in air

Sample			Condition					
Figure	Test	Sample	Mass g	T °C	Acid M	NaCl g L ⁻¹	Cu g L ⁻¹	Fe(II) g L ⁻¹
4.10*	(a)	Andina	15	35	0.2/HCl	0	0	0
	(b)		8					
4.11	(a)	Andina	9	35	0.2/HCl	0	0	0
	(b)				0.5/HCl			
	(c)				1/HCl			
4.12-4.13	(a)	Andina	9	35	0.1/HCl		0.5	0
	(b)				0.2/HCl			
	(c)				0.5/HCl			
4.14-4.15**	(a)	Andina (unscreened)	9	35	0.2/HCl	0	0.5	0.5
	(b)				0.2/HCl			
	(c)				0.2/H ₂ SO ₄			
	(d)				0.2/H ₂ SO ₄			
4.17-4.18	(a)	Andina	9	35	0.2/HCl	0	0.5	0
	(b)	Spence						
	(c)	PQS1						
	(d)	Ok Tedi						
4.19-4.20	(a)	Andina+PQS1	4.5+4.5	35	0.2/HCl	0	0.5	0
	(b)	Andina+Spence	4.5+4.5					
	(c)	OkTedi+PQS1	4.5+4.5					
	(d)	OkTedi+Spence	4.5+4.5					

*(a) Unscreened and (b) screened +25-38 µm leached in 800 mL of solution all the other test carried out in 900 mL

** (b) and (d) with addition of 5 g of magnetite.

4.2 Shake-flask leaching experiments

4.2.1 The effect of chloride ion

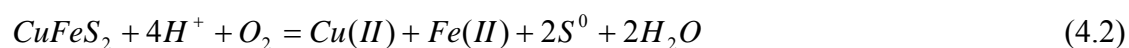
Increasing the concentration of chloride ions has been one of the methods adopted to increase the rate of dissolution of chalcopyrite even in mixed sulfate/chloride media. However, there is no general agreement on the role of chloride. Thus, Dutrizac (1981) reported that minor sodium chloride additions to a ferric sulfate solution promoted the chalcopyrite leaching reaction above 50 °C, but not at lower temperatures where the rates are difficult to determine accurately. Recently, Lu et al. (2000a) and Kinnunen and Puhakka (2004) showed clearly that increasing the chloride concentration above 0.5 M does not increase the leaching kinetics and they concluded that the important factor is the presence of a minimum concentration of chloride ions.

In order to compare with previous experiments on chalcopyrite leaching carried out by a Japanese group (Hiroyoshi et al., 2001; 2000) using iron(III) ions in sulfate solutions, this work started with experiments under similar conditions but in hydrochloric acid solution. The presence of chloride ions on the kinetics at different temperatures was investigated and compared with results obtained in the absence of ferric ions.

4.2.1.1 In the presence of initial Fe(III)

The initial shake flask leaching experiments were carried out in 0.2 M HCl acid containing 0.1 M FeCl₃ with different amounts of chloride ions obtained by adding sodium chloride. Figure 4.1 shows the extent of copper dissolution after 24 hours as a function of added

chloride ion in air and nitrogen. For comparison, experiments were carried out in 0.2 M HCl in absence of Fe(III) and these results are shown as the first points to the left in the graphs. It is apparent that in this concentration region (0.5-2 M chloride), the effect of chloride on the rate is negligible. Since the extent of dissolution of copper in air and nitrogen is almost the same, it appears that oxidation of chalcopyrite is mainly due to Fe(III) (Eq. 4.1) while the rate of chalcopyrite oxidation by dissolved oxygen (Eq. 4.2) can be ignored under these conditions.



Comparison of the extent of dissolution in the presence and absence of iron(III) suggest that the dissolution of copper is higher in aerated solutions in the absence of added iron(III) ions.

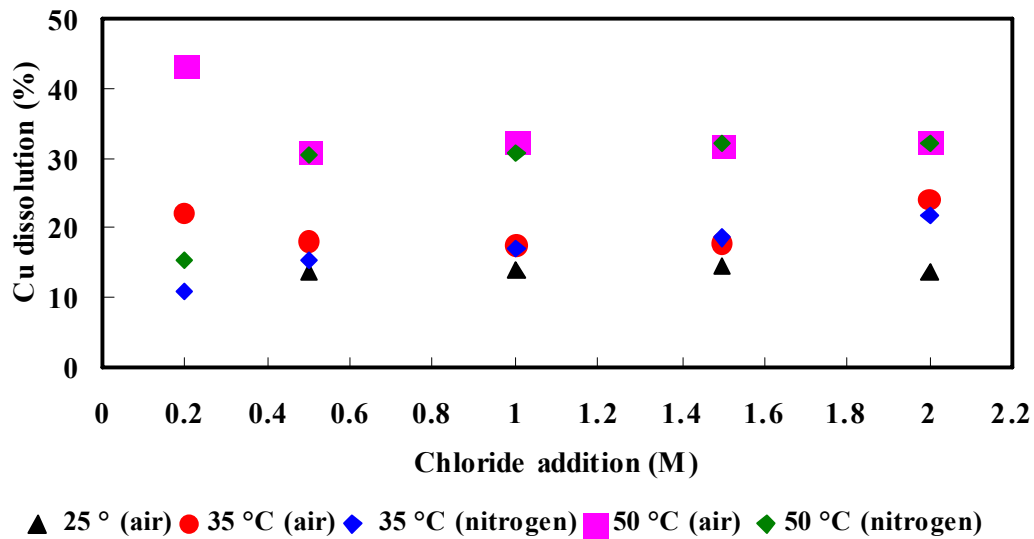


Figure 4.1 Effect of addition of chloride on the dissolution of Ok Tedi chalcopyrite after 24 h with 1% pulp density. Data at 0.2 M chloride in absence of Fe(III).

It is clear from Figure 4.1 that the rate of dissolution increases with increasing temperature but increasing the chloride concentration does not increase the rate at all temperatures. These results are in agreement with those of previous researchers (Hirato et al., 1987; Majima et al., 1985; Munoz et al., 1979). According to Dutrizac (1981) even small quantities of secondary copper minerals associated with chalcopyrite can mask the leaching of chalcopyrite, especially at low temperatures where the total dissolution is small.

It is generally accepted that the rate of dissolution depends on the concentration of ferric ions in sulphuric acid solutions. Even though, Jones et al. (1976), Dutrizac (1978; 1981), Majima et al. (1985) and Hirato et al. (1986) observed that increasing the FeCl_3 concentration increases the rate of dissolution, in a chloride system the dependence on the concentration of the ferric ion is not clear.

In the present study, the leaching behaviour in the presence and absence of ferric ions appears to be different and the effect of ferric concentration was therefore investigated. Figure 4.2 shows the amount of copper extracted as a function of the iron(III) concentration at 50 °C in 0.2 M HCl in air and nitrogen.

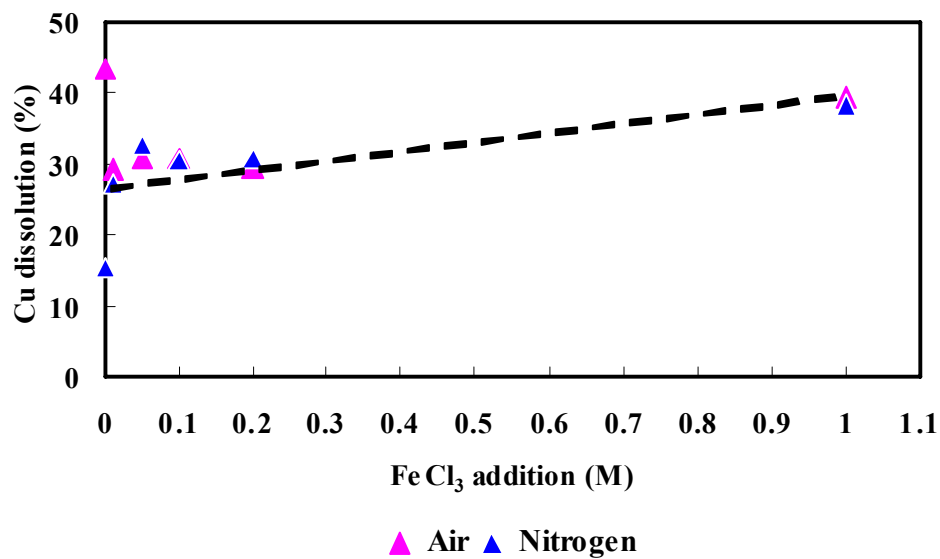


Figure 4.2 Effect of ferric chloride concentration on the dissolution of chalcopyrite from Ok Tedi samples after 24 h at 50 °C.

It is obvious that the rate of dissolution is higher in air in the absence of ferric ions than in its presence. The Figure also shows that the rate does not increase substantially with increasing concentration of ferric ions.

4.2.1.2 In the absence of initial ferric ions

Following the observation that the leaching rate in the absence of ferric ion is higher than in its presence, the effect of chloride and sulfate ion concentrations on the rate were investigated in the absence of ferric ions. Figure 4.3 summarizes the results of experiments on the effect of chloride ion concentration on the rate of dissolution in air at 25, 35 and 50 °C. The leach solution contained 0.2 M HCl and the chloride concentration was varied by addition of known amounts of sodium chloride.

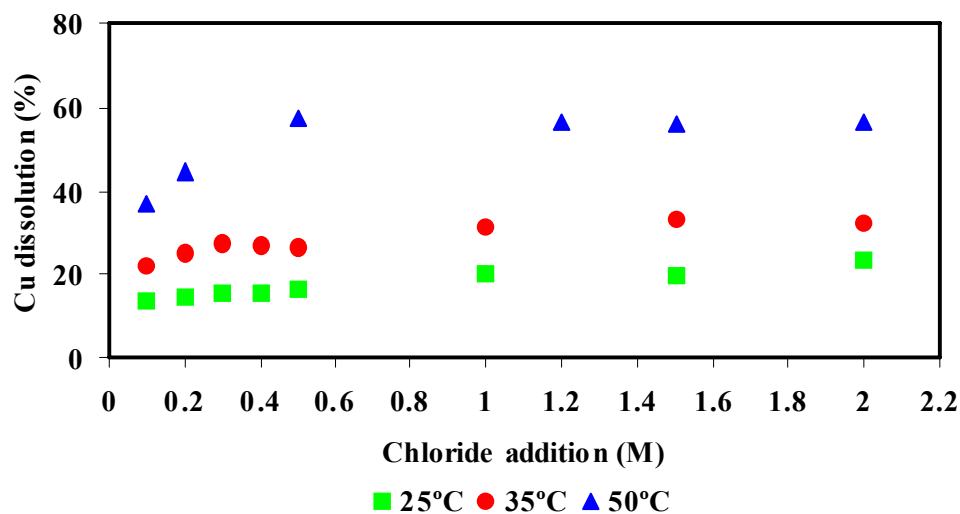


Figure 4.3 Effect of chloride concentration on the rate of dissolution of Ok Tedi chalcopyrite in aerated solutions in the absence of ferric ions.

It is clear from Figure 4.3 that in the absence of ferric ions the rate of dissolution increases with increasing temperature. It is interesting to note that the rate in the absence of ferric ions does not increase with increasing chloride concentration above about 0.5 M and that the effect is more noticeable at the lower temperatures.

The effect of increasing chloride concentration on the rate of leaching of Andina concentrate is shown by the data in Figure 4.4. These results confirm the previous results on the Ok Tedi sample, which suggested that an increase in the concentration of chloride ions above about 0.2 M does not improve the rate of dissolution of chalcopyrite.

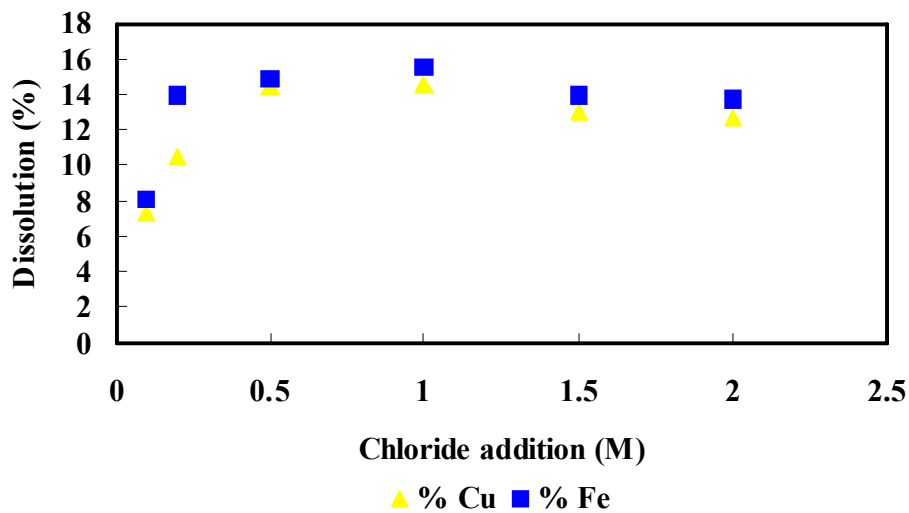


Figure 4.4 Effect of chloride concentration on dissolution of chalcopyrite from Andina concentrate in aerated 0.2 M HCl at 35 °C.

4.2.2 The effect of mixed chloride-sulfate solutions.

The majority of commercial copper heap leach plants employ sulphuric acid as the leachant. A vast amount of work has been published in the area of oxidative leaching of chalcopyrite, which has focused on either sulfate or chloride media but not a combination of the two. However, Lu et al. (2000a) used a mixed chloride-sulfate oxygenated solution to leach chalcopyrite at 95 °C under atmospheric pressure conditions. They found excellent leaching kinetics and established that temperature and oxygen partial pressure had a substantial

effect on the rate under these conditions. The recently developed CESL process for copper concentrates makes use of a sulfate system to which is added small amounts of chloride (Barr et al., 2005).

In the present study, the effect of a mixed chloride-sulfate solution was tested by carrying out experiments with sulphuric acid containing various amounts of sodium chloride. Figure 4.5 summarizes the results of these runs together with those in the presence of hydrochloric acid for comparison. From these results is apparent that the rate of dissolution is essentially the same in both systems. These results suggest that sulphuric acid can be used in combination with a soluble chloride salt such as sodium chloride.

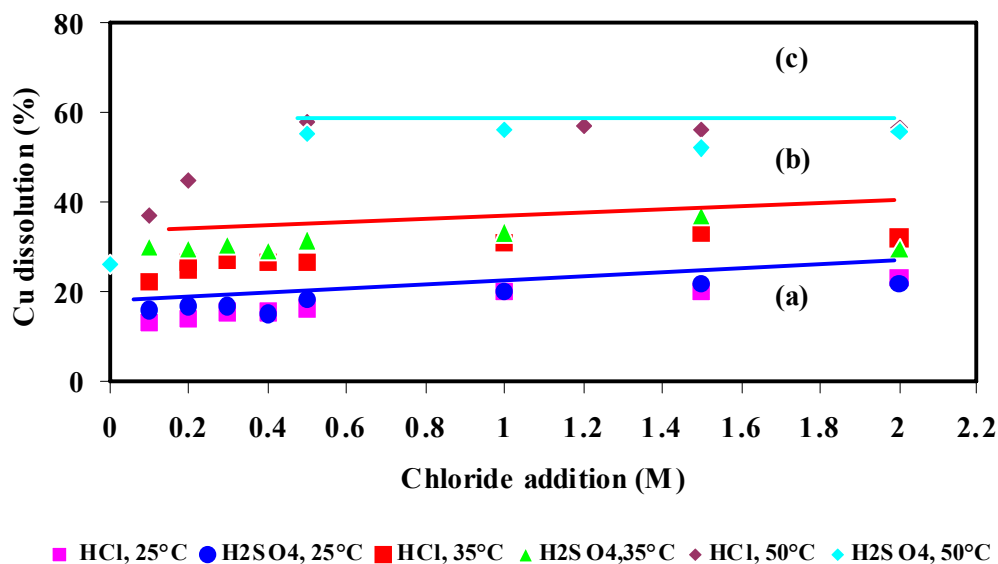


Figure 4.5 Effect of chloride ions on the dissolution of Ok Tedi chalcopyrite in aerated hydrochloric acid (0.2 M) and sulphuric acid (0.2 M) solutions in the absence of iron(III) ions. (a) 25 °C, (b) 35 °C and (c) 50 °C.

4.2.3 Variation of potential with addition of chloride ions

Figures 4.6 and 4.7 summarize the initial and final potentials of the solution (E_h) and of a chalcopyrite electrode (E_m) immersed in the solution during the leach experiments using the Ok Tedi sample as a function of the increasing chloride ion concentration in the absence of added iron(III). It is apparent that an increase in the chloride concentration has a negligible effect on the solution and mixed potentials. As expected, the mixed potentials are lower than the solution potentials by up to 150 mV.

The corresponding potentials are shown for the experiments with the Ok Tedi sample at 50 °C and with the Andina concentrate at 35 °C. It can be generally concluded that chloride ions have negligible effect on the solution and mixed potentials except at low chloride concentrations at 50 °C.

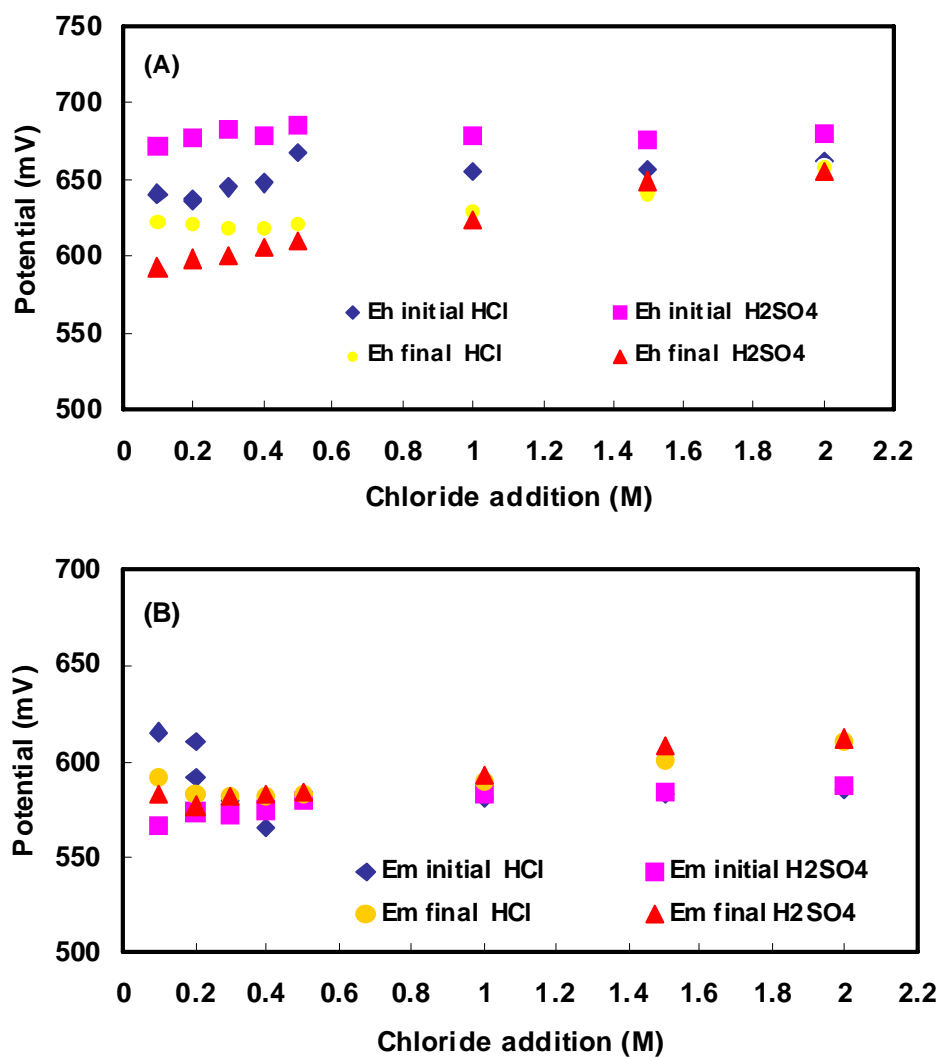


Figure 4.6 Effect of chloride concentration on the potentials during the dissolution of Ok Tedi chalcopyrite in aerated 0.2 M HCl and 0.2 M H₂SO₄ solutions at 35 °C. (A) Solution Potential, (B) Mixed Potential.

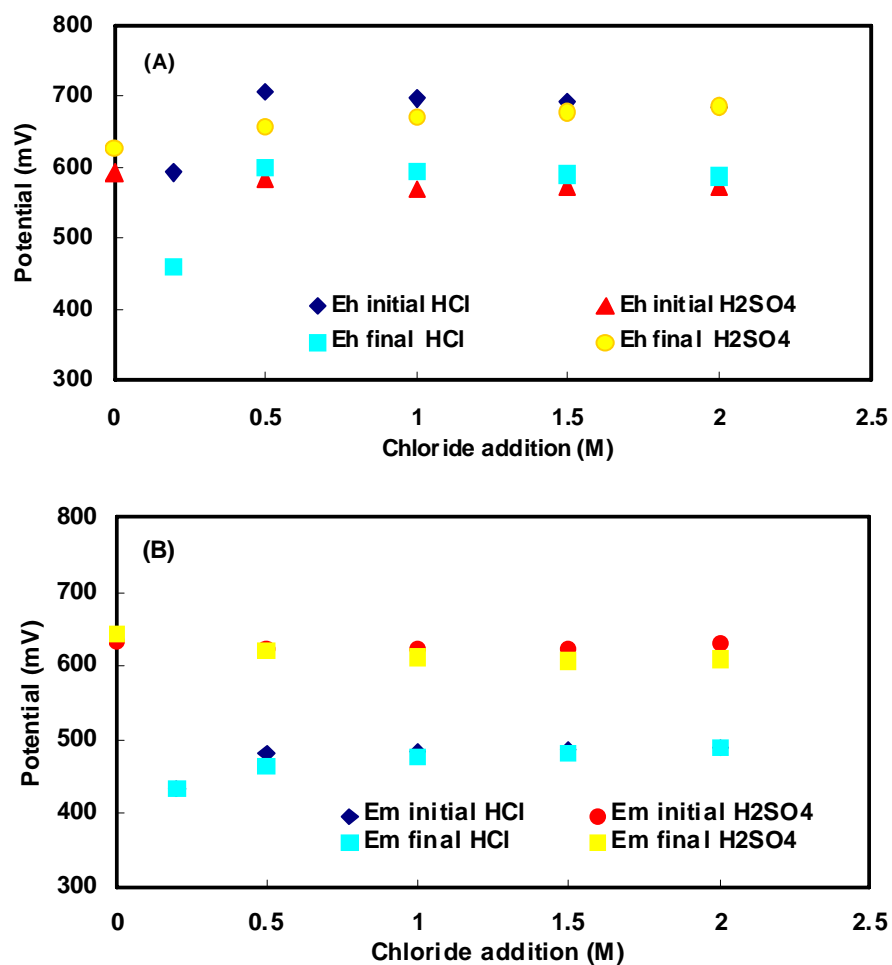


Figure 4.7 Variation of potentials with addition of chloride in dissolution of Ok Tedi chalcopyrite in aerated 0.2 M HCl and 0.2 M H₂SO₄ solutions at 50 °C. (A) Solution Potential, (B) Mixed Potential.

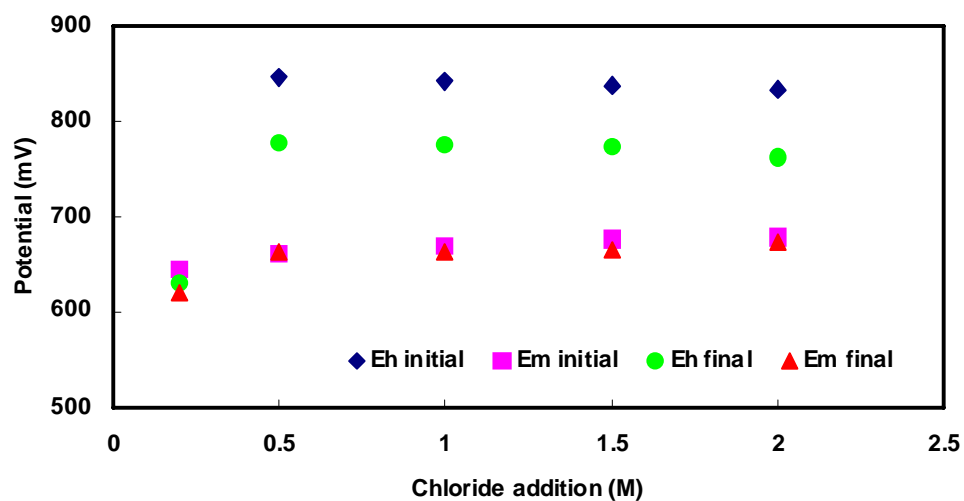


Figure 4.8 Variation of potentials with addition of chloride for the dissolution of Andina concentrate in aerated 0.2 M HCl at 35 °C.

It is apparent from Figure 4.9 that both the mixed potential and the final solution potential increases as could be expected with increasing concentrations of iron(III) ions.

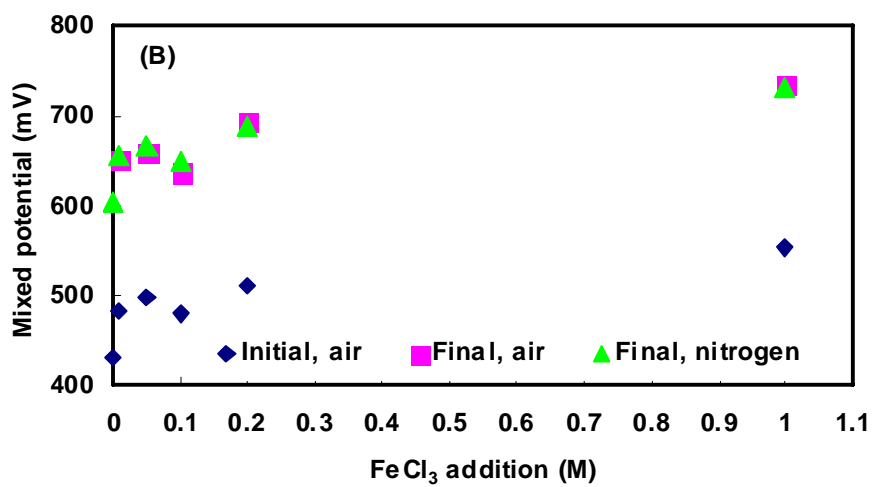
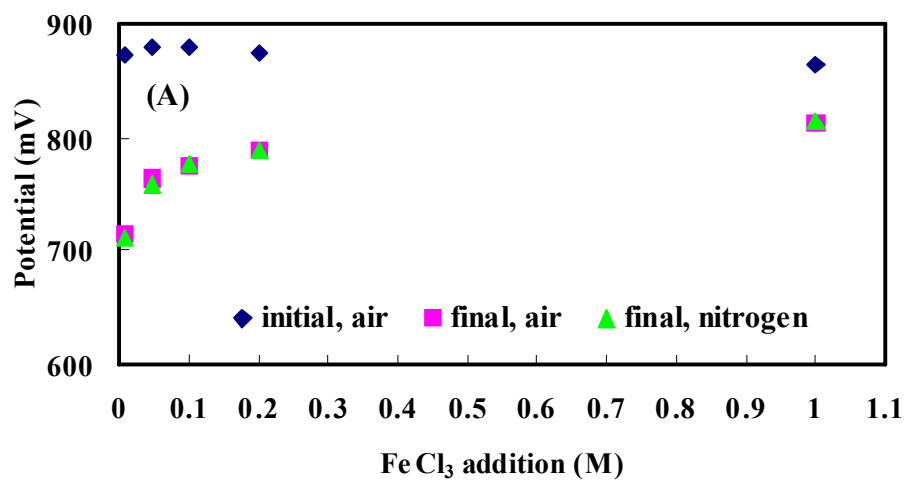


Figure 4.9 Effect of addition of iron(III) on the potential during dissolution of Ok Tedi chalcopryrite 0.2 M HCl at 50 °C. (A) Solution Potential, (B) Mixed potential.

4.3 Leaching experiments in instrumented reactors

To establish the role of the important parameters in the rate of leaching of chalcopyrite, additional experiments were carried out using instrumented reactors. Agitated leaching experiments of chalcopyrite concentrates were initially studied using an unscreened chalcopyrite concentrate sample from Andina in Chile. The conditions were chosen based on the results from the shake flask experiments described above which showed that the rate is not dependent on the chloride concentration above about 0.2 M. The leach conditions initially selected used 15 g of Andina concentrate with 800 mL of a solution containing 0.2 M of HCl in air at 35 °C. The results are presented in Figure 4.10 and suggest that the rate of dissolution of copper and iron slowly decreases with time up to about 50% dissolution. In order to investigate the effect of particle size 8 g of sized (+25-38 μm) Andina concentrate was leached under the same conditions. As shown in Figure 4.10, the extent of dissolution increases linearly with time and as expected, the rate of dissolution is significantly higher than that of the unscreened sample, reaching about 90% in 600 h. The initial rapid dissolution of about 10% of the copper is due to the more rapid leaching of small amounts of bornite in the concentrate.

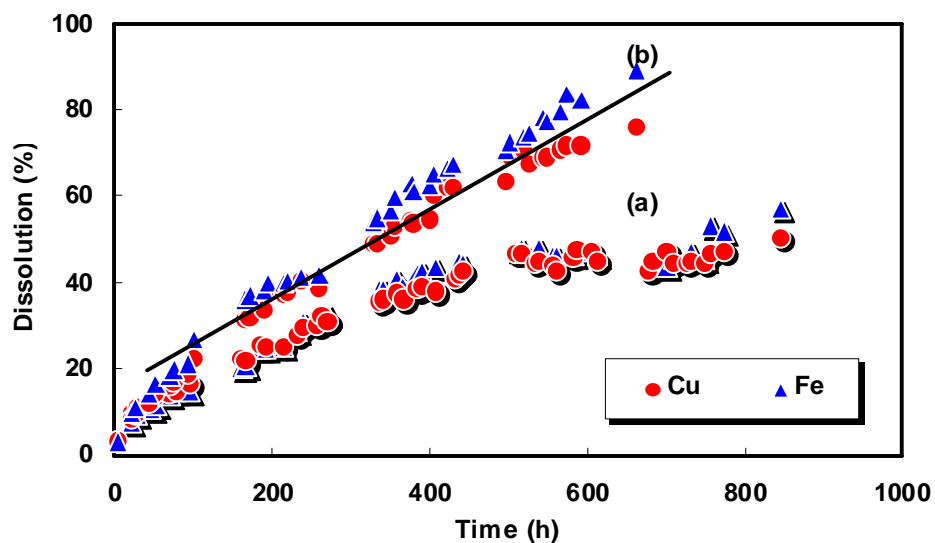


Figure 4.10 Dissolution of copper and iron from Andina concentrate in 800 mL of solution containing 0.2 M HCl at 35 °C in air. (a) 15 g unscreened sample and (b) 8 g screened (+25-38 μm) sample.

Following the observation that the leaching rate is higher when a sized sample is used at lower pulp density, the effect of acidity and chloride concentration on the rate was studied using samples of 9 g of screened (+25-38 μm) Andina concentrate in 900 mL of solution. The results are shown in Figure 4.11 and Figure 4.12. As the extents of dissolution of iron and copper were almost the same in all experiments, only the latter is plotted. From Figure 4.11 it appears that the rate does not increase with increasing acidity in agreement with the shake flask experiments. However, in the presence of added copper ions, the rate was lower at the lower and higher acid concentrations with the most effective leaching obtained in a solution containing 0.2 M HCl and 0.5 g L⁻¹ of Cu (II) with close to 100% dissolution after 700 h. In this particular experiment, the solution was deaerated with nitrogen for the first 150 h during which period very little dissolution occurred. On introduction of air, the rate increased significantly as shown.

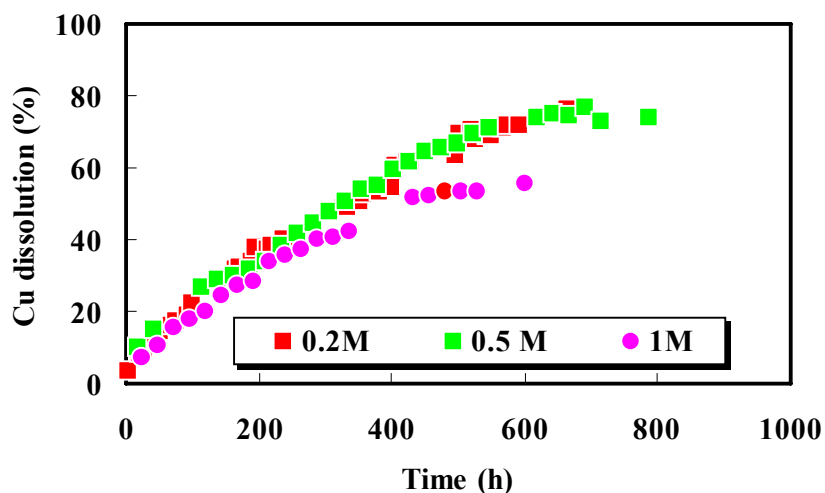


Figure 4.11 Dissolution of copper from screened (+25-38 μm) Andina concentrate in solutions of varying HCl acidity in air at 35 °C.

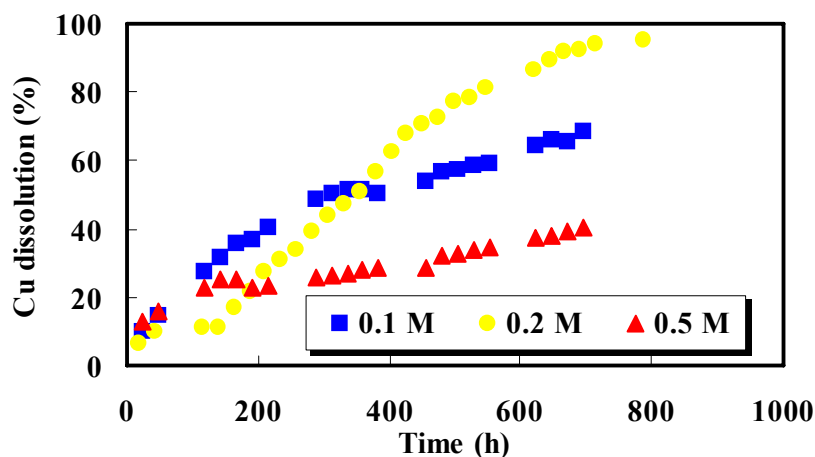


Figure 4.12 Dissolution of copper from screened Andina concentrate with 0.5 g L^{-1} Cu(II) in various HCl acid concentration and air at 35 °C.

The potentials measured during these experiments are given together with the copper dissolution in Figure 4.13. It is apparent that the mixed and solution potentials are quite similar under these conditions. In the solution containing 0.1 M acid, the rate increased until about 300 h after which it appeared to slow substantially while at the same time the

potential decreased from around 560 mV to 525 mV. An increase in the potential to about 550 mV resulted in an increase again in the rate of dissolution after 450 h. At the apparent optimum acidity of 0.2 M, the potential varied between 580 and 600 mV except during the initial period when dissolved oxygen was excluded from the reactor. On the other hand, at the higher acidity, the potential was generally above about 650 mV throughout the run.

It thus appears that the apparent effect of acidity on the rate may be due to the different potentials with an optimum potential in the range 550-600 mV while lower rates are observed at potentials below 550 mV and above about 650 mV.

In order to investigate the effect of addition of iron as Fe(II) ions and magnetite (Fe_3O_4) on the rate of dissolution, experiments were carried out in HCl and H_2SO_4 solutions using unscreened Andina chalcopyrite concentrate at 35 °C. As the results in Figure 4.14 show, the rate of dissolution was lower in the presence of these additives. The low rate of dissolution observed in curve (a) can be compared with that shown in Figure 4.10 curve (A) for which the unscreened material was also used. The addition of magnetite reduced the rate slightly in chloride but had little effect in sulfate solutions. It is possible that the reduced rates observed in all these experiments was due to the presence of additional Fe(II).

Figure 4.15 show the potentials logged during these experiments. In chloride media, the potential appears to be close to the optimum value while it is about 50 mV higher in sulfate solutions. This could account for the relatively poor leaching rate in sulfate.

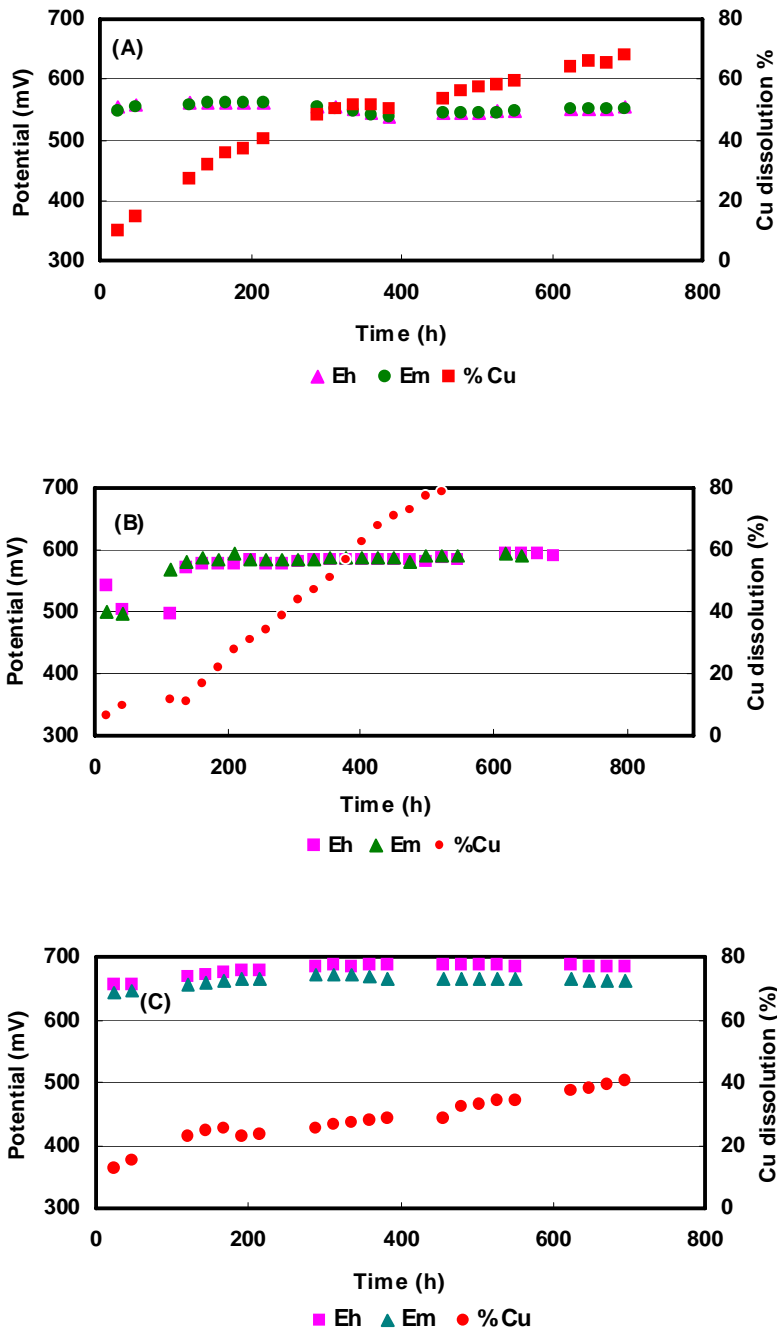


Figure 4.13 Variation of solution potentials and copper dissolution during leaching of Andina concentrate at 35 °C in air. (A) 0.1 M HCl and 0.5 g L⁻¹ Cu(II), (B) 0.2 M HCl and 0.5 g L⁻¹ Cu(II) and (C) 0.5 M HCl and 0.5 g L⁻¹ Cu(II).

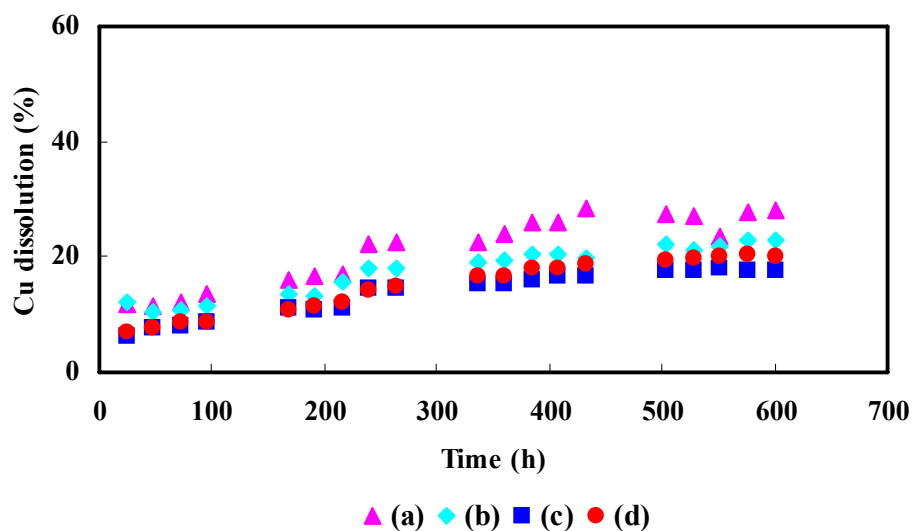
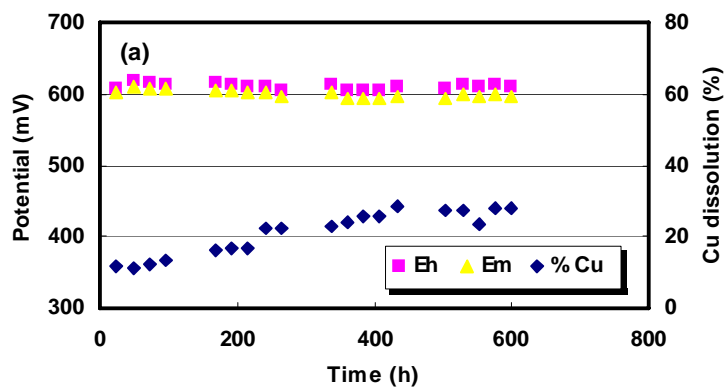


Figure 4.14 Effect of Fe(II) and Fe₃O₄ on dissolution of copper from unscreened Andina concentrate (a) 0.2 M HCl, 0.5 g L⁻¹ Cu(II) and 0.5 g/L Fe(II), (b) 0.2 M HCl, 0.5 g L⁻¹ Cu(II), 0.5 g L⁻¹ Fe(II) and 5 g of Fe₃O₄, (c) 0.2 M H₂SO₄, 0.5 g L⁻¹ Cu(II) and 0.5 g L⁻¹ Fe(II) and (d) 0.2 M H₂SO₄, 0.5 g L⁻¹ Fe(II), 0.5 g L⁻¹ Cu(II) and 5 g Fe₃O₄.



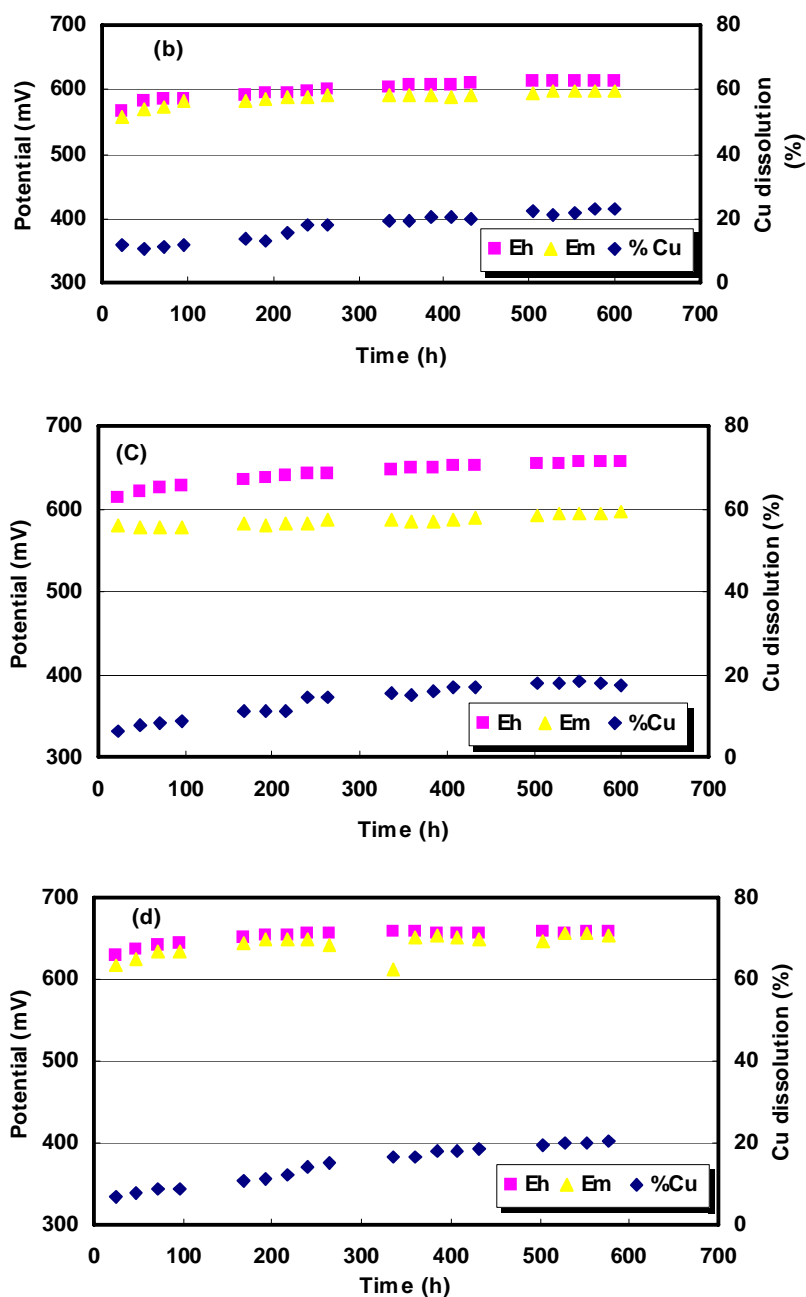


Figure 4.15 Variation of potentials and copper dissolution during leaching of Andina concentrate at 35 °C in air. (a) 0.2 M HCl and 0.5 g L⁻¹ Fe(II), (b) 0.2 M HCl, 0.5 g L⁻¹ Fe(II) and 5 g of Fe₃O₄, (c) 0.2 M H₂SO₄ and 0.5 g L⁻¹ Fe(II) and (d) 0.2 M H₂SO₄, 0.5 g L⁻¹ Fe(II) and 5 g Fe₃O₄.

4.4 Preliminary leaching experiments with chalcopyrite concentrates from different sources

4.4.1 Leaching experiments of chalcopyrite concentrates

Several experiments were conducted to investigate whether the source of the chalcopyrite has an influence on its rate of dissolution under identical conditions. Samples of Andina, Spence and PQS1 concentrates from Chile and Ok Tedi chalcopyrite from Papua New Guinea were chosen for this study. With the exception of the OK Tedi material, the samples were dry screened to produce a 25-38 μm fraction and 9 g of the each sample was leached in 900 mL of solutions containing 0.2 M HCl and 0.5 g L⁻¹ Cu(II) in oxygen at 35 °C in four instrumented stirred reactors. The results of the MLA analysis of these dry-screened samples showed (Figure 4.16) that the samples contained significant quantities of fine agglomerated material with only the PQS1 sample having the expected size distribution. The OK Tedi material was significantly finer than the other samples.

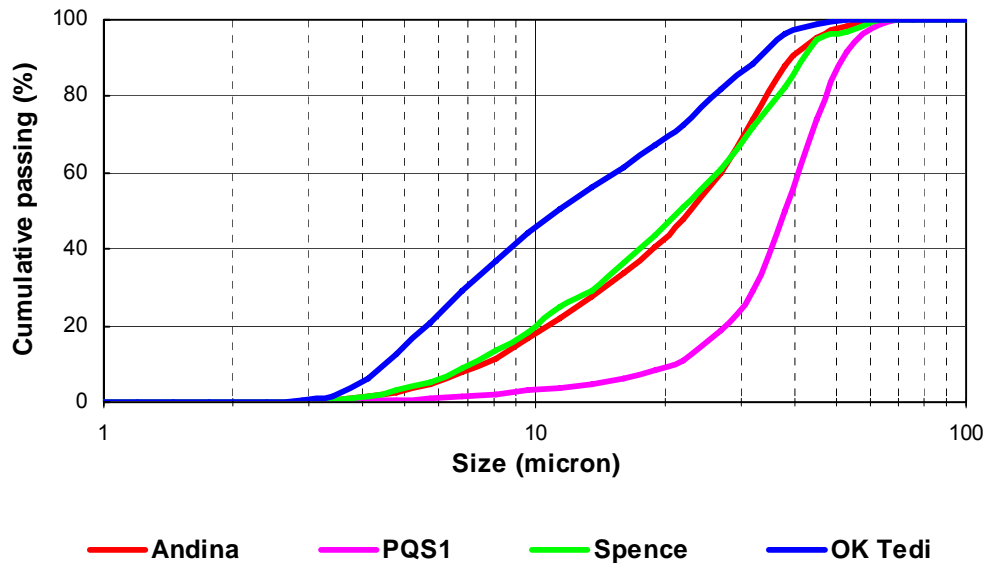


Figure 4.16 Size distribution of chalcopyrite concentrates after dry-screened at +25-38 μm

As can be seen from Figure 4.17, the highest dissolution of copper of about 90% is attained after 280 h of leaching by the OK Tedi sample followed by Andina with 70%, PQS1 with 55% and Spence with 30%. The dissolution of total iron is lower than that of copper in the PQS1 and Spence samples that contain significant amounts of secondary copper minerals that are low in iron. Almost linear rates are observed for the Andina and Spence samples while the other concentrates exhibit the parabolic kinetics typical of dissolution in sulfate systems.

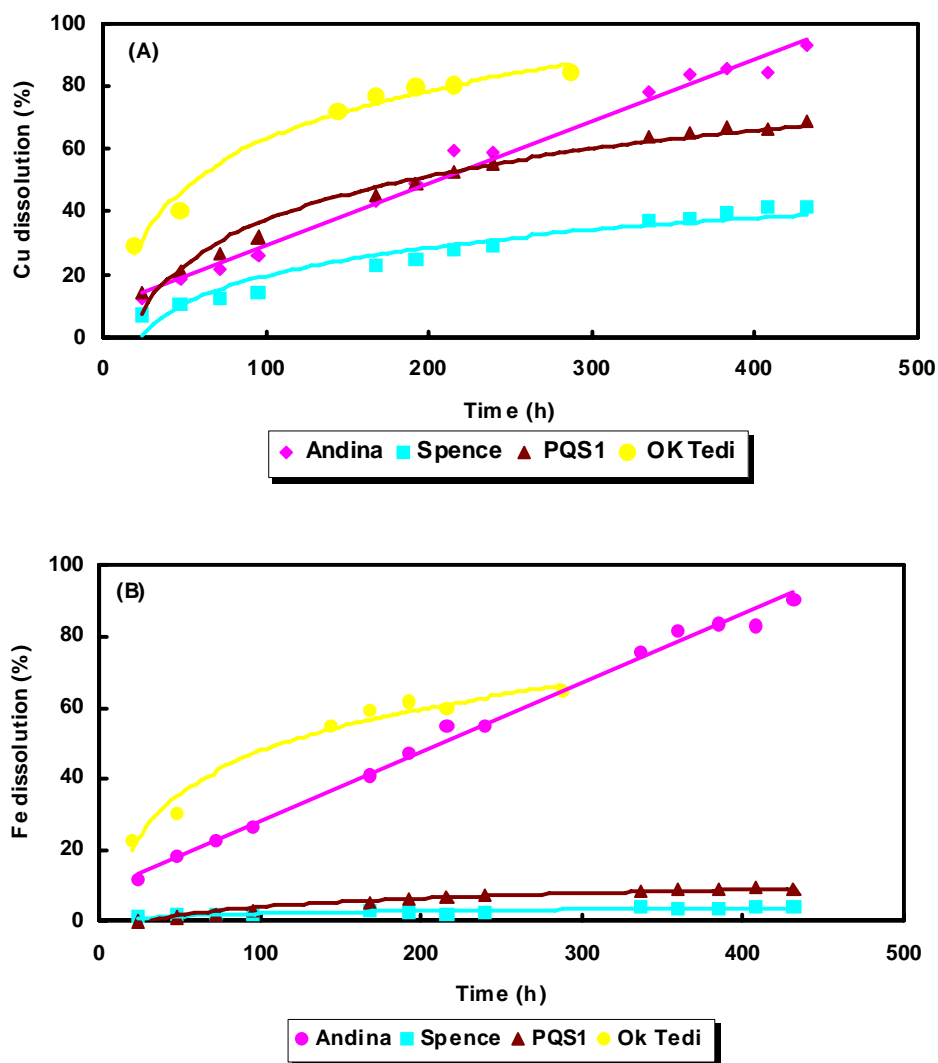
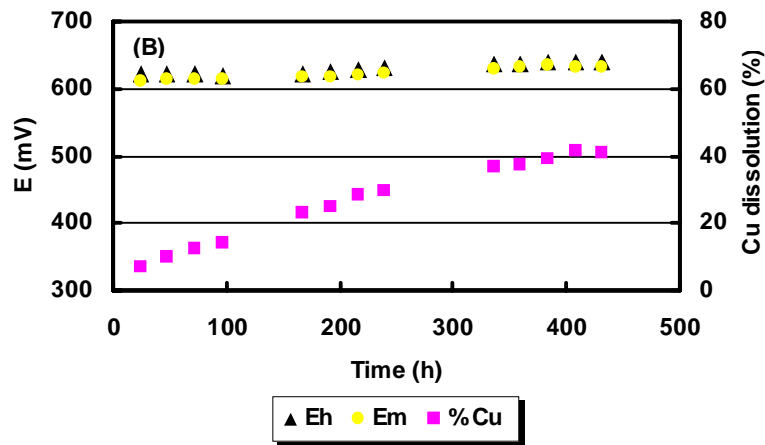
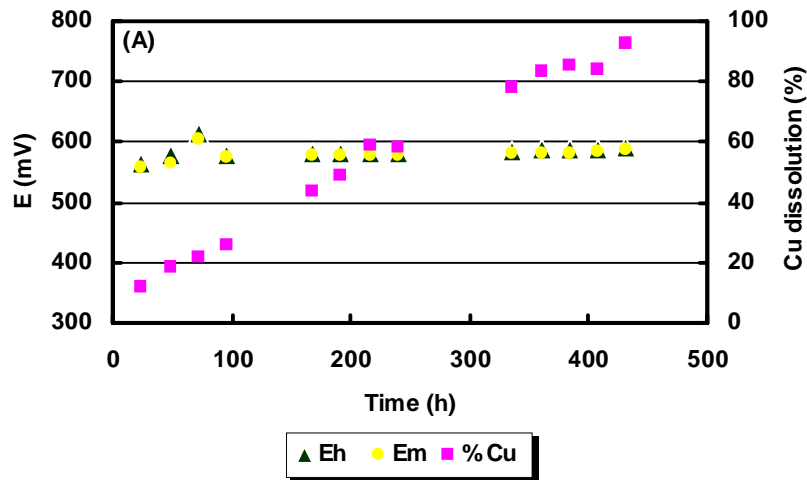


Figure 4.17 Dissolution of chalcopyrite from different sources (+25-38 μm) in 0.2 M HCl and 0.5 g L⁻¹ of Cu(II). (A) Copper dissolution and (B) iron dissolution

The results for the dissolution of copper from each sample are compared with the potentials measured during the leach experiments in Figure 4.18. It was found that, the solution potential, E_h , is similar to the mixed potential, E_m , in all cases. While the potential during dissolution of the Andina concentrate was fairly stable under 600 mV, in the case of the

other concentrates, the potential increased to above 600 mV during the leaching period and this increase appears to be associated with a reduction in the rate of dissolution.



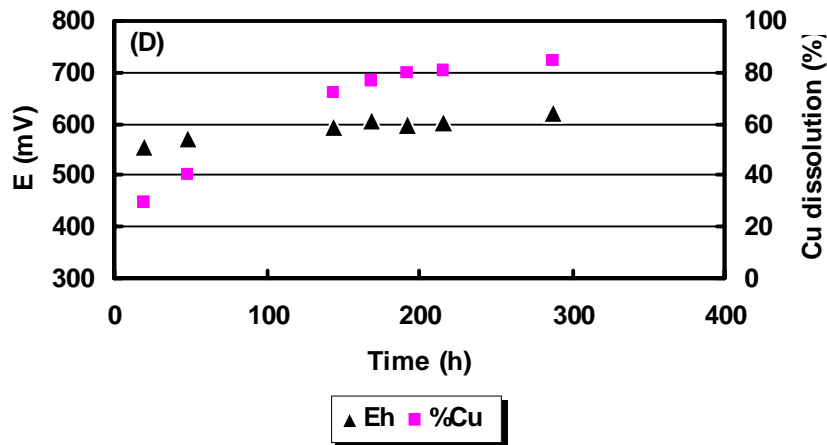
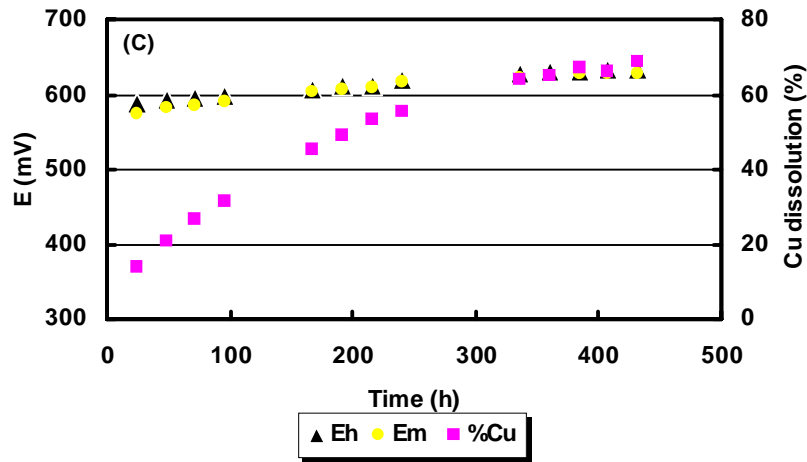


Figure 4.18 Variation of potential and copper extracted during leaching of several concentrates (A) Andina, (B) Spence, (C) PQS1 and (D) Ok Tedi

In order to compare these results, an attempt has been made to estimate the rates of dissolution of chalcopyrite per unit area of chalcopyrite surface. Thus, the information obtained from the MLA analysis of the feed materials is shown in Table 4.3 as the chalcopyrite surface area for a 9 g of sample. Also shown the total mass of chalcopyrite lost as estimated from the MLA analysis of the residue after the specified time of leach. It is apparent from the average rates of dissolution that there is a difference of a factor of about

four between the highest and lowest rates. The lower rates for the Spence and PQS1 samples are possibly due to the higher potentials during these runs and the fact that the chalcopyrite content of the residues may be overestimated because a large proportion of the very fine elemental sulfur product is not accounted for in the MLA analysis.

Table 4.3 Rates of dissolution based on initial surface area (9 g of samples)

	Surface Area cm ²	Time h	ΔCp g	Rate g cm ⁻² s ⁻¹	Rate mol cm ⁻² .s ⁻¹	Main Eh mV
Andina	7480	384	5.95	5.8E-10	3.1E-12	585
Ok Tedi	12020	192	6.90	8.3E-10	4.5E-12	593
Spence	2580	408	0.75	2.0E-10	1.1E-12	631
PQS1	2117	432	0.92	2.8E-10	1.5E-12	614

4.4.2 Leaching of mixed concentrates

In order to establish a possible role of mineralogy on the rate of leaching of chalcopyrite, experiments were carried out with binary mixtures of the samples (4.5 g of each sample) in oxygenated solutions containing 0.2 M HCl and 0.5 g L⁻¹ Cu(II) at 35 °C. It is interesting to note that as shown in Figure 4.19(A) and 4.19(B) the PQS1/Ok Tedi mixture exhibited a greater leaching rate than that observed with the other mixtures and this appears to correlate with a lower potential during the dissolution (Figure 4.20) of the former mixture. In the case of the other mixtures, the potential was generally above the optimum value of about 600 mV. An alternative explanation could be along lines suggested by Dutrizac (1981) that

the presence of secondary copper mineralization and other non-copper minerals can possibly alter the leaching rate of chalcopyrite.

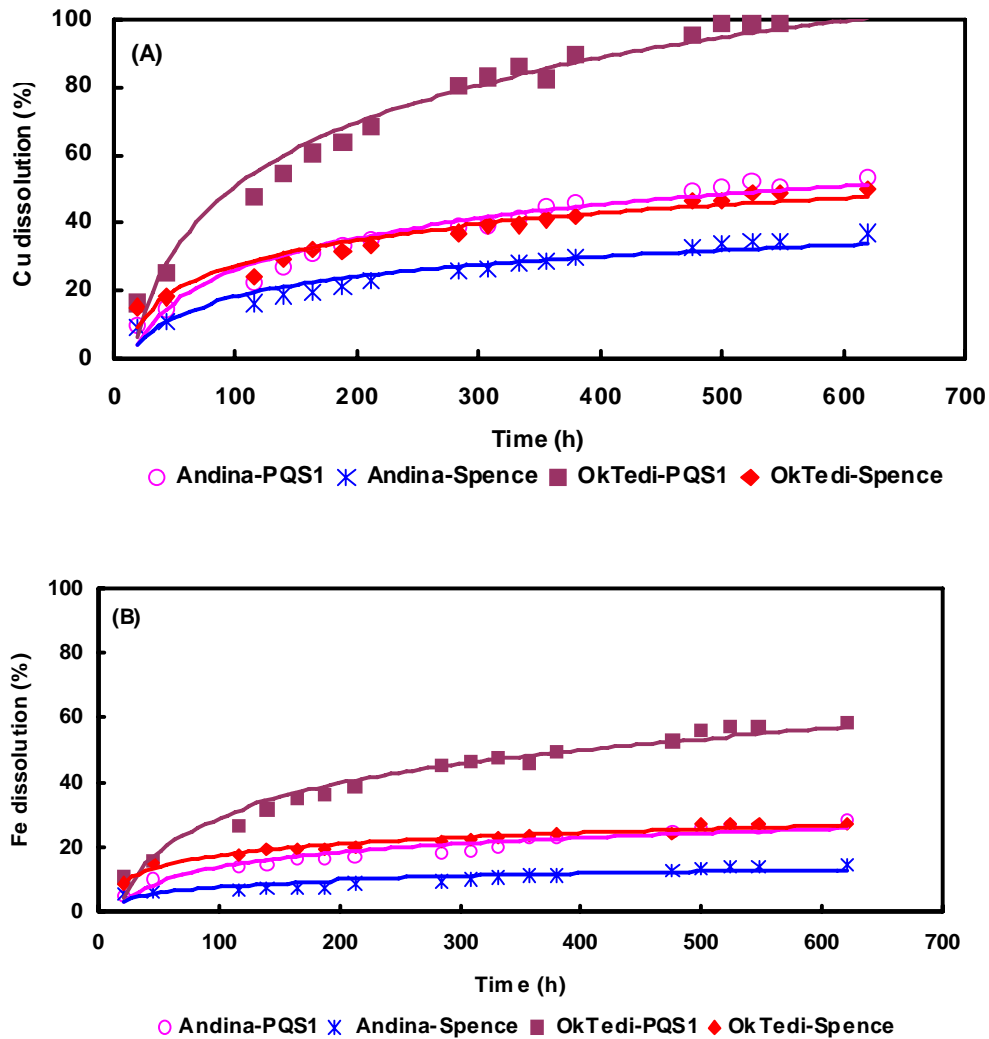


Figure 4.19 Dissolution of mixed chalcopyrite concentrates (+25-38 μm) in 0.2 M HCl and 0.5 g L⁻¹ Cu(II). (A) Copper dissolution and (B) iron dissolution

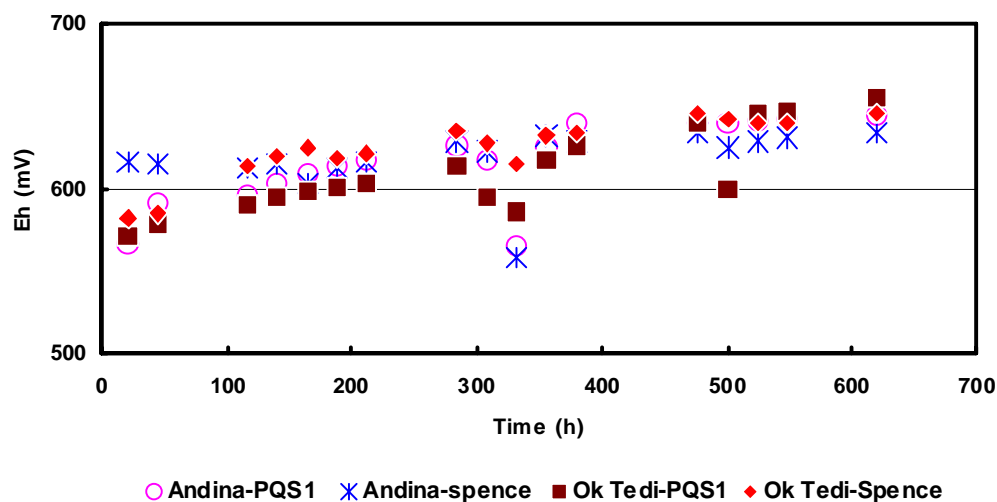


Figure 4.20 Variation of solution potential during dissolution of mixed concentrates.

4.4.3 Mineralogical analyses

A detailed mineralogical study of the head and leach residue of each of the chalcopyrite samples, i.e. Andina, PQS1, Spence and Ok Tedi leached in 0.2 M HCl and 0.5 g L⁻¹ of Cu(II) (section 4.4.1) was undertaken by BHP Billiton Newcastle Technology Centre mainly using the MLA system. It should be noted that the difficulty of preventing loss of elemental sulfur from the sections during polishing was found to affect the quantitative analysis for sulfur and this should be borne in mind.

4.4.3.1 *Andina concentrate*

According Table 4.4 the Andina head is predominantly chalcopyrite with small amounts of bornite and pyrite. It is apparent from these results that most of chalcopyrite and all covellite and chalcocite were dissolved and that 20% of the residue mass is elemental sulfur. Figure 4.21 shows that most of the chalcopyrite in the residue (dissolution shown in Figure

4.17) is liberated and that only about 12% is associated with sulfur. A portion of the mineral map shown in Figure 4.22 confirms that most of chalcopyrite and sulfur remaining in the residue are liberated. Sulfur appears mainly as small porous globules as shown in Figure 4.23 in agreement with observations of Dutrizac (1990). It seems from Figure 4.24 that these porous globules of sulfur (with $p_{80} = 25 \mu\text{m}$) are smaller than the chalcopyrite in the residue which also shows a reduced particle size distribution compared with chalcopyrite in the head sample.

Table 4.4 Andina (dissolution rate shown in Figure 4.17) modal mineralogy (mass,%)

Mineral	Head	Residue	Leach (%) MLA
Chalcocite	0.00	0.00	-
Chalcopyrite	82.50	41.10	74.66
Covellite	0.16	0.00	100.00
Bornite	3.40	0.03	99.55
Native Copper	0.00	0.00	-
Enargite	1.70	8.30	-
Brochantite	0.00	0.00	-
Chrysocolla	0.00	0.00	-
Other copper minerals	0.00	0.05	-
Pyrite	2.70	11.50	-
Quartz	5.00	5.10	-
Galena	0.47	0.00	100.00
Sulfur	0.00	20.50	-
Other Gangue	4.03	11.00	-
Total	100	98	

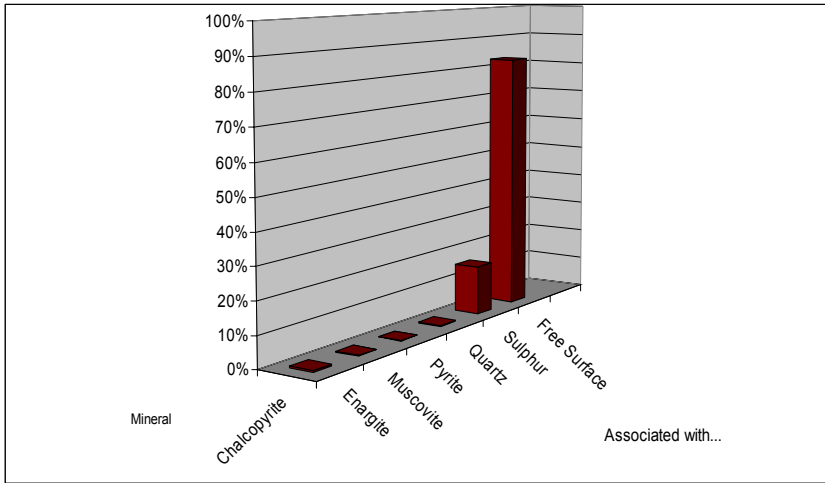


Figure 4.21 Association of chalcopyrite with other minerals in the Andina leach residue.

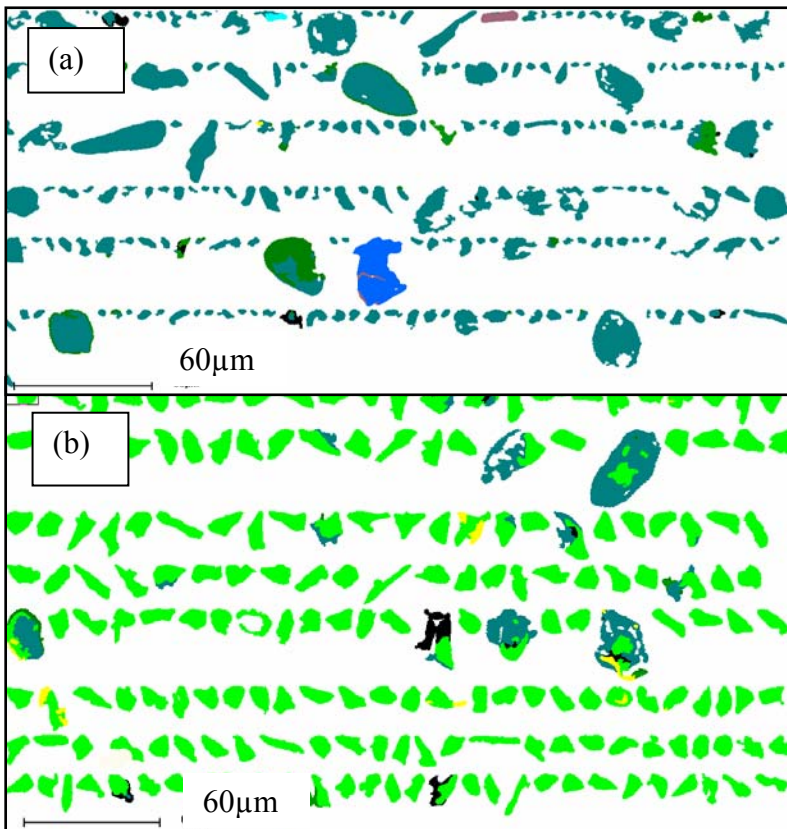


Figure 4.22 Mineral map of Andina concentrate after leaching shows (a) liberated sulfur (dark green) and (b) chalcopyrite (green) with minor amounts of associated sulfur.

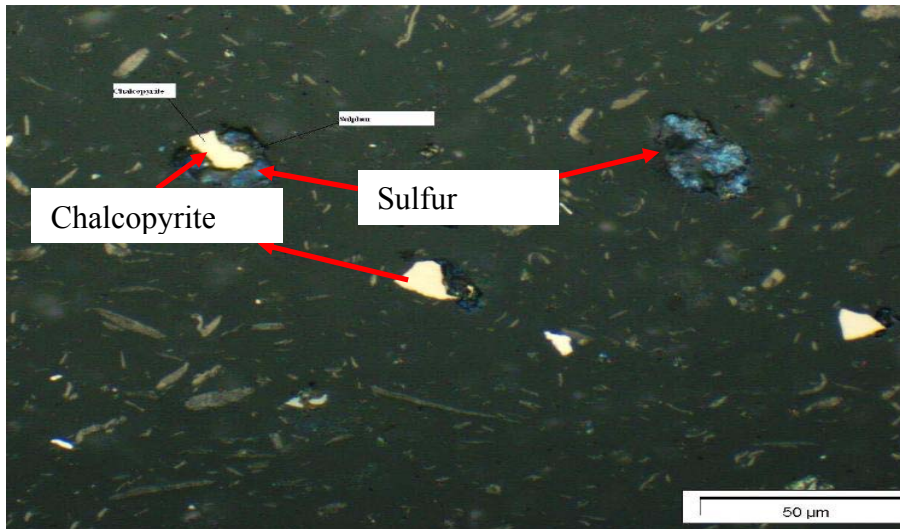


Figure 4.23 Optical microphotograph showing deposition of sulfur in the Andina leach residue.

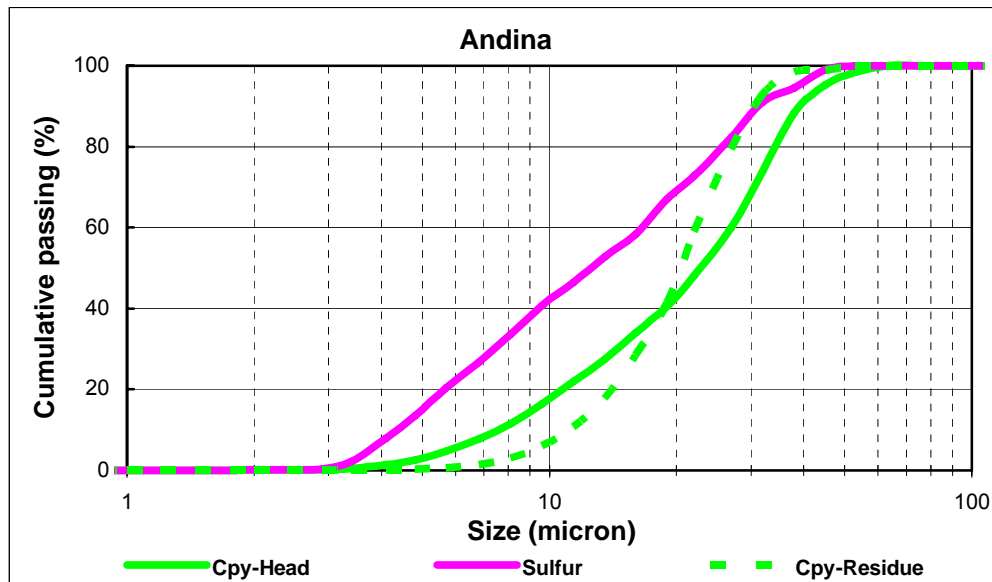


Figure 4.24 Size distribution for chalcopyrite in dry-screened Andina head sample (+25-38 μm) compared with the leach residue. Also shown is the size distribution of the sulfur in the residue.

4.4.3.2 PQS1 concentrate

Table 4.3 shows that the PQS1 head sample is predominately composed of chalcopyrite and pyrite, about 14% covellite and very little chalcocite and bornite. As shown in Table 4.5 and Figure 4.25, most of the chalcopyrite in the residue (dissolution rate is shown in Figure 4.17) is liberated and less than 10% of it is associated with sulfur. It is interesting to note in Figure 4.26 that some elemental sulfur is associated with pyrite despite the fact that pyrite is not oxidised under the conditions of the leach experiments. However, this could be due to association of copper sulfides with pyrite in the head sample. It is also likely that secondary sulfur is formed on fine pyrite particles as a result of oxidation of H₂S catalysed by the pyrite surface (see Chapter 8). As in the Andina leach residue, sulfur occurs as globular grains as shown in Fig. 4.27.

Table 4.5 PQS1 modal mineralogy (mass,%) (dissolution rate shown in Figure 4.17)

Mineral	Head	Residue	Leach (%) MLA
Chalcocite	0.47	0.00	100.00
Chalcopyrite	44.60	46.80	14.05
Covellite	14.30	1.90	89.12
Bornite	2.80	0.56	83.62
Native Copper	0.00	0.00	-
Enargite	1.80	0.51	76.79
Brochantite	0.19	0.01	95.69
Chrysocolla	0.00	0.00	-
Other copper minerals	0.10	0.10	19.14
Pyrite	29.30	36.40	-
Quartz	2.00	1.30	-
Galena	0.41	0.00	100.00
Sulfur	0.00	6.90	-
Other Gangue	4.02	4.39	-
Total	100	99	-

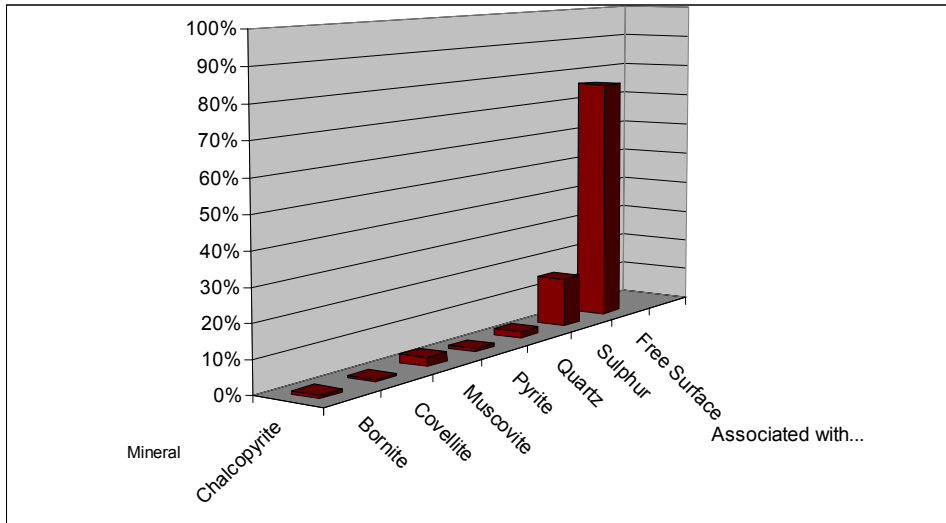


Figure 4.25 Association of chalcopyrite with other minerals in the PQS1 residue.

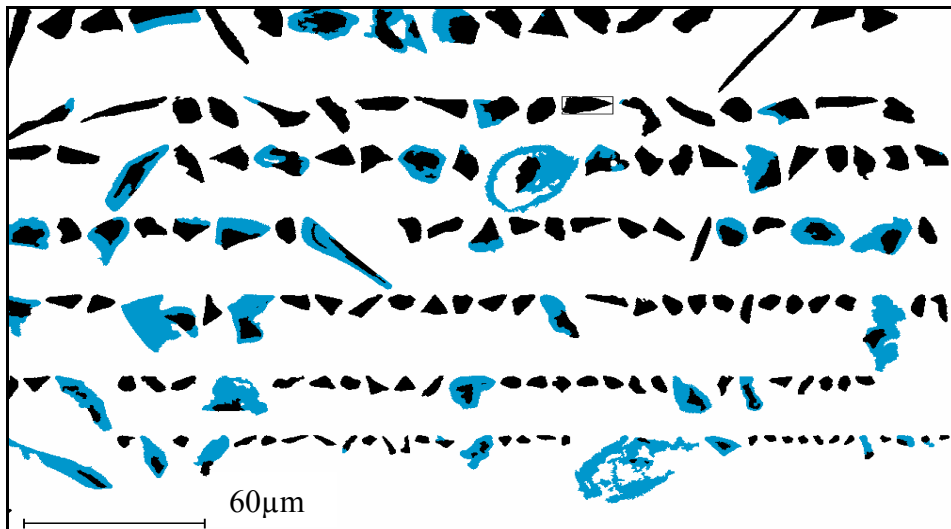


Figure 4.26 Mineral map of the residue from dissolution of the PQS1 concentrate showing sulfur (blue) associated with pyrite (black).

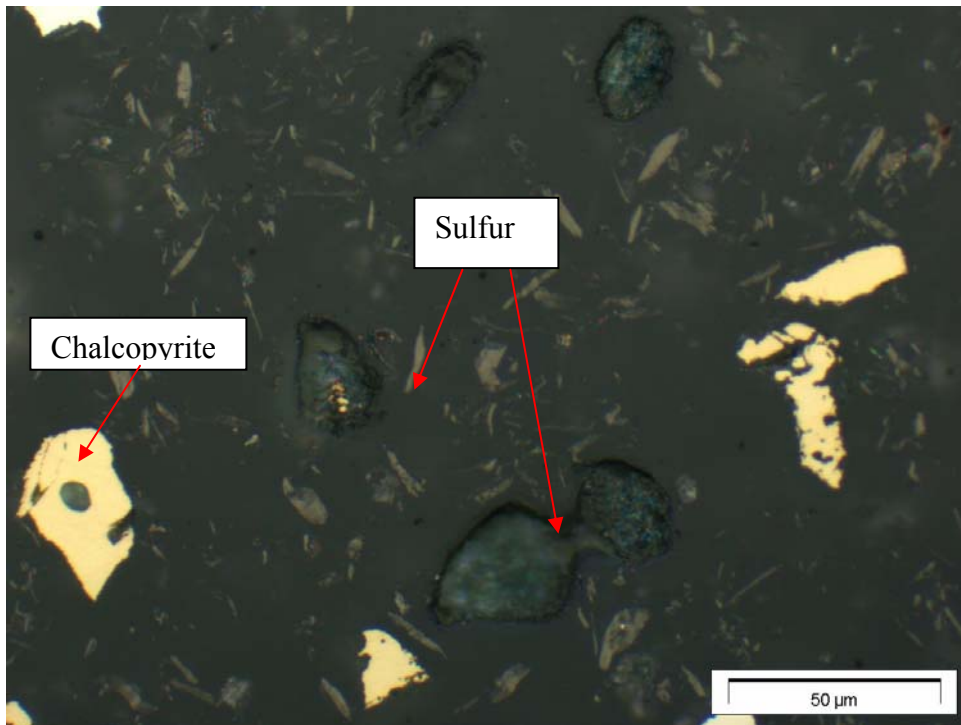


Figure 4.27 Optical microphotograph shows sulfur in globular form in the PQS1 leach residue.

4.4.3.3 Spence concentrate

More than half of the Spence head sample (Table 4.6) is composed of pyrite with the predominant copper mineral being chalcopyrite and minor amounts of covellite, enargite and bornite all of which decrease after leaching. In Figure 4.28, it can be observed that chalcopyrite association with other minerals follows the same trend as observed with the Andina and PQS1 leach residues. Once again, sulfur is associated with pyrite (Fig. 4.29), and also occurs as globular grains and associated with chalcopyrite and covellite particles (Fig. 4.30).

Table 4.6 Spence modal mineralogy (mass,%)

Mineral	Head	Residue	Leach (%)
Chalcocite	0.00	0.00	-
Chalcopyrite	27.40	23.40	30.63
Covellite	7.50	1.80	80.50
Bornite	2.90	0.72	79.83
Native Copper	0.00	0.00	-
Enargite	4.10	1.50	70.28
Brochantite	0.01	0.00	-
Chrysocolla	0.01	0.00	-
Other copper minerals	0.12	0.01	93.13
Pyrite	50.80	58.70	6.13
Quartz	1.20	1.30	12.00
Galena	1.69	0.00	100.00
Sulfur	0.00	8.80	-
Other Gangue	2.57	2.75	-
Total	100	99	-

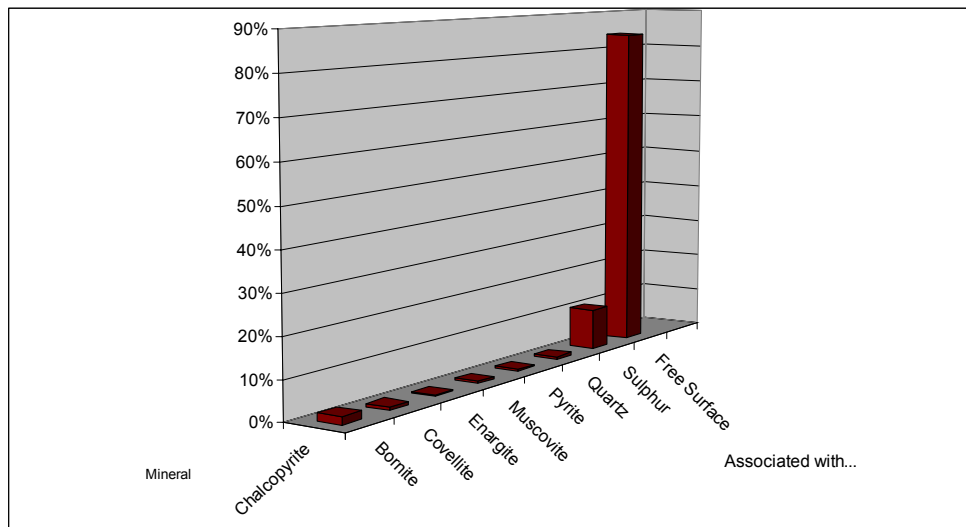


Figure 4.28 Association of chalcopyrite with other minerals in the Spence leach residue.

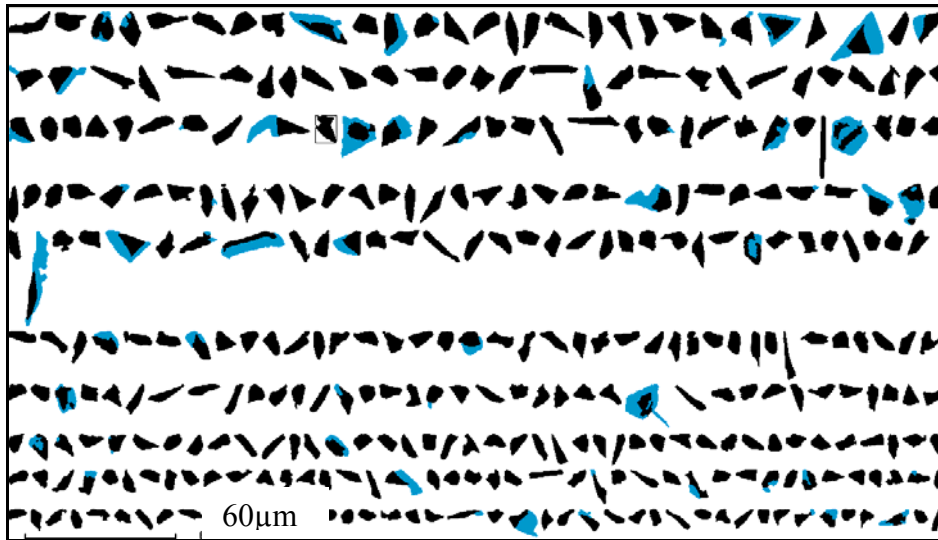


Figure 4.29 Mineral map of the residue from dissolution of the Spence concentrate showing sulfur (blue) associated with pyrite (black).

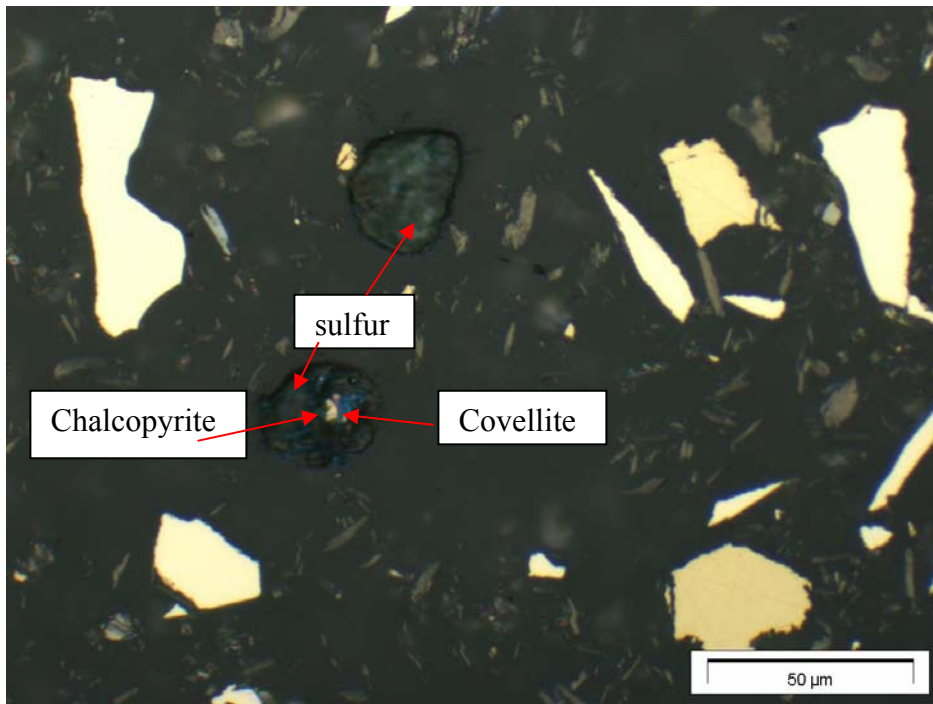


Figure 4.30 Optical micrograph showing globular sulfur and uncoated chalcopyrite particles in the Spence leach residue.

4.4.3.4 *Ok Tedi concentrate*

Table 4.7 shows that the Ok Tedi sample is predominately composed of chalcopyrite and pyrite and that almost all of the chalcopyrite is dissolved during leaching. 90% of the chalcopyrite in the residue is liberated with small amounts associated with sulfur and pyrite (Fig.4.31). Figure 4.32 shows small isolated sulfur globules with some association with chalcopyrite. As shown in Fig 4.33, the particle size of the sulfur appears to be bimodal with some large (greater than 50 μm) and smaller globules (less than 10 μm).

Table 4.7 Ok Tedi modal mineralogy (mass,%)

Mineral	Head	Residue	Leach (%) MLA
Chalcocite	0.00	0.00	-
Chalcopyrite	77.90	2.10	98.63
Covellite	0.00	0.00	-
Bornite	0.01	0.00	100.00
Native Copper	0.00	0.00	-
Enargite	0.00	0.00	-
Brochantite	0.00	0.00	-
Chrysocolla	0.00	0.00	-
Other copper minerals	0.00	0.00	-
Pyrite	17.90	86.40	-
Quartz	0.02	0.44	-
Galena	0.41	0.00	100.00
Sulfur	0.00	6.90	-
Other Gangue	4.02	4.39	44.56
Total	100	100	

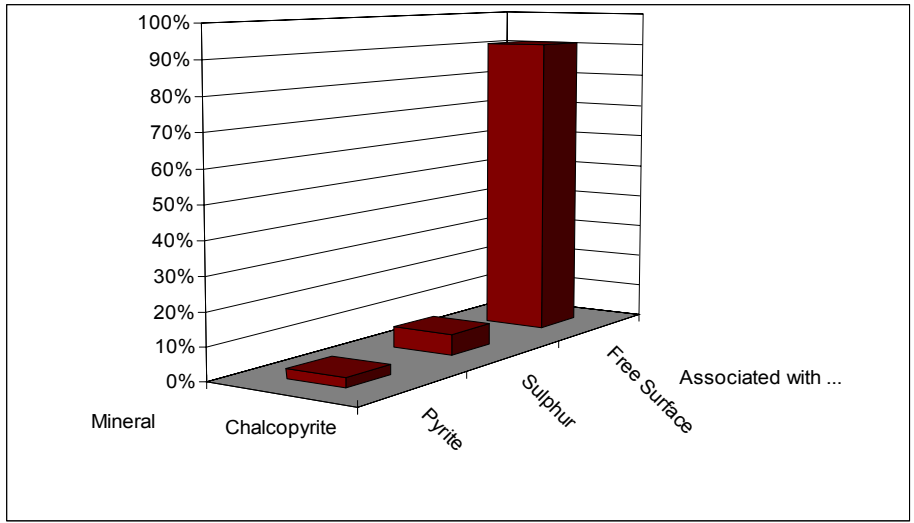


Figure 4.31 Association of chalcopyrite with other minerals in the Ok Tedi leach residue.

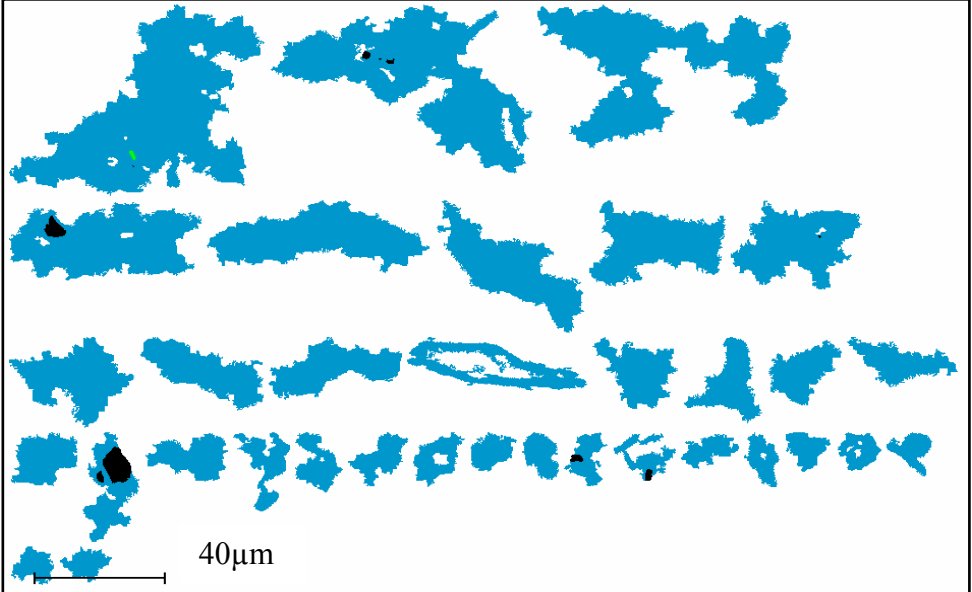


Figure 4.32 Partial mineral map showing sulfur associated with pyrite in the leach residue of the Ok Tedi concentrate.

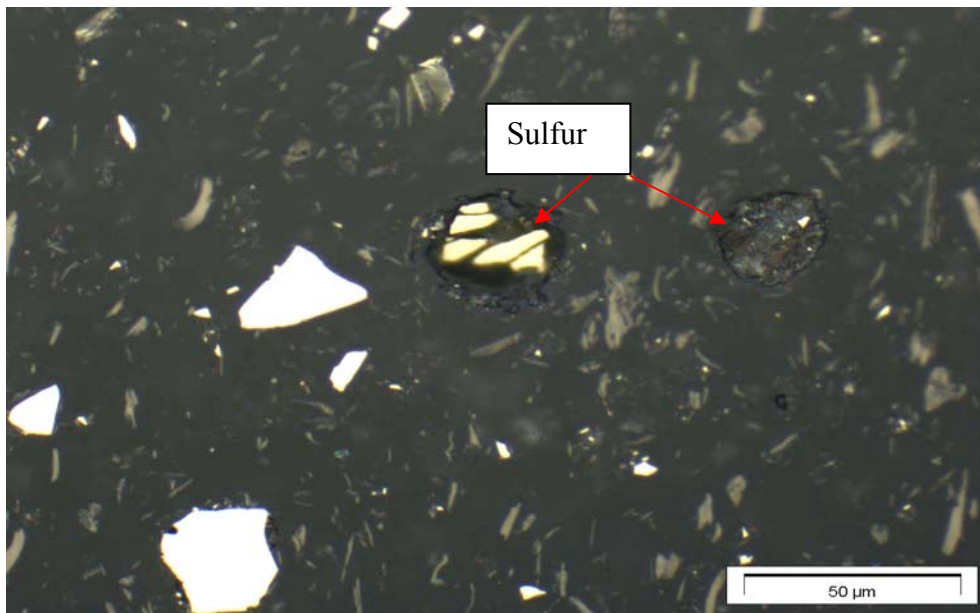


Figure 4.33 Optical micrograph globular sulfur in the Ok Tedi leach residue.

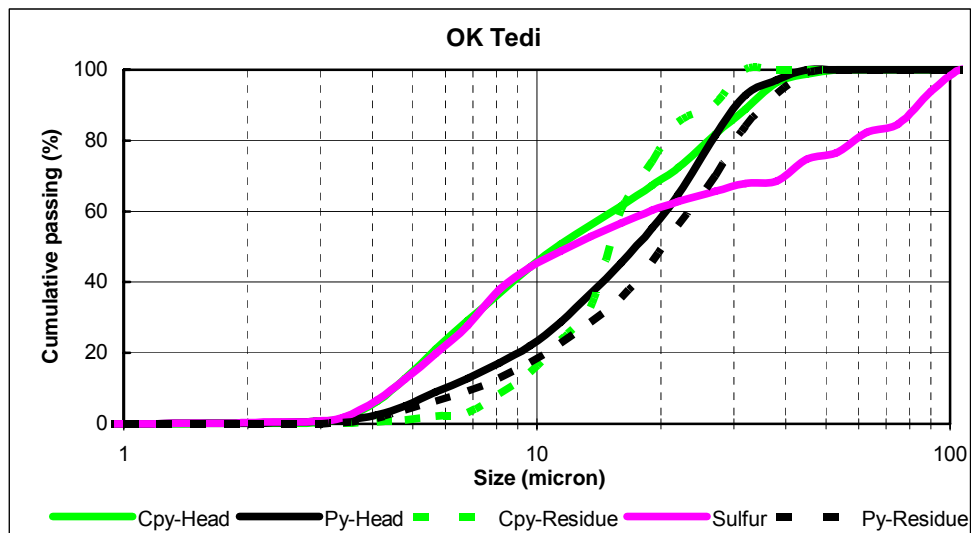


Figure 4.34 Size distribution for dry-screened Ok Tedi head samples (+25-38 μm) compared with the leach residue.

4.5 Summary and conclusions

A preliminary study of the leaching of chalcopyrite concentrates in chloride and mixed chloride/sulfate solutions has been carried out as the first phase of this project in order to establish the role of the important parameters that determine the rate. The following are the principal results obtained.

Shake flask leaching experiments showed that the presence of Fe(III) ions inhibits the rate of dissolution of chalcopyrite in that higher rates were obtained in the presence of dilute hydrochloric acid only. It was concluded that the presence of chloride ions is important in improving the kinetics of leaching, but it appears that an increase in the concentration of chloride ions above about 0.2 M does not improve the rate of dissolution at 35 °C. The results suggest that it is possible to work with a mixed chloride/sulfate system since similar rates to these obtained in chloride system were obtained and importantly sulphuric acid can be used in combination with a soluble salt as sodium chloride. An increase in the chloride ion concentration has a negligible effect on the solution and mixed potentials at 35 °C under these conditions.

Additional experiments in instrumented stirred reactors suggest that the rate is approximately constant under optimum conditions in the chloride system. The rate does not increase with increasing acidity, but the presence of copper ions increases the leaching rate. Under the rather limited set of conditions investigated, a maximum extraction of about 90% after 600 h was obtained with the Andina concentrate in 0.2 M HCl acid and 0.5 g L⁻¹

copper ions. Mixed and solution potentials were found to be similar in the chloride system. It appears that the rate of leaching is sensitive to the potential with lower rates at Eh values above about 600 mV at low chloride concentrations. It was further found that the rate is strongly dependent on particle size. The effect of the addition of Fe(II) to the leach solution has not been unequivocally established in that variations in the potential during the experiments may have masked any effect of Fe(II).

An attempt has been made to investigate the kinetics of the dissolution of copper from different chalcopyrite concentrates. However, mineralogical analyses have demonstrated that dry-screening of the concentrates resulted in poor classification with significant amounts of fine agglomerated material reporting to the desired size fraction. As a result, an attempt has been made to correlate the rates of leaching with surface areas obtained from the MLA analyses.

The apparent order of reactivity of the different concentrates of Ok Tedi>Andina>Spence>PQS1 appears to correspond to the relative particle size of the concentrates and there does not appear to be a significant variation in the reactivity of the different materials. However, variations in the potentials during the leach experiments, which were not carried out under potential control, may have influenced the results obtained. At 35 °C, the highest dissolution in dilute chloride media, (90% after 600 h) was obtained at the lowest potential (580 mV) with decreased rates at potentials above about 600 mV.

Leaching of mixtures of the concentrates showed that the greatest rate of dissolution was reached when the finer samples were mixed with coarser materials. The mineralogical analysis revealed that the secondary copper minerals were almost completely dissolved. It also revealed interesting aspects of the deportment of elemental sulfur, which does not appear to be associated with the chalcopyrite in the residues but occurs as discrete globules and in association with pyrite.

5. THE EFFECT OF THE SOLUTION POTENTIAL ON THE RATE OF LEACHING OF CHALCOPYRITE

5.1 Introduction

As it has been pointed out in Chapter 2, the dissolution of sulfide minerals, and, in particular, the passivation of chalcopyrite are potential-dependent reactions and many studies have been carried out in order to establish the relationship between the solution potential and the leaching rate. It is now well known that the leaching rate in sulfate solutions is dependent on the potential and that the rate is enhanced in a certain potential range (Nicol and Lazaro, 2002). Many studies have been devoted to the elucidation of the potentials at which dissolution is possible and at which apparent passivation occurs. Thus, Nicol and Lázaro (2002) used electrochemical and chemical experiments to establish the relevant leaching potential region as being 0.45 to 0.75 V under appropriate experimental conditions. However, few actual dissolution studies (Hiroyoshi et al., 2000; Rivera-Velasquez et al., 2006; Third et al., 2002) have been conducted under controlled potentials conditions, particularly in chloride media.

In addition, several studies have focused on enhanced dissolution at low redox potentials (Hackl et al., 1995; Hiroyoshi et al., 2000), and a reaction model to explain the phenomenon has been proposed by a Japanese research group (Hiroyoshi et al., 1997; 2001; 2000). Recently, preliminary experiments carried out at Murdoch University have been based on a simple experimental technique employed by the Japanese group. The results shown in Figures 5.1 and 5.2 confirmed the potential dependence of the rate of dissolution of chalcopyrite using a relatively pure chalcopyrite sample from Ok Tedi. According to these results, the rate of dissolution in both chloride and sulfate solutions is greater at potentials below the passivation region with an optimum potential that depends on the conditions.

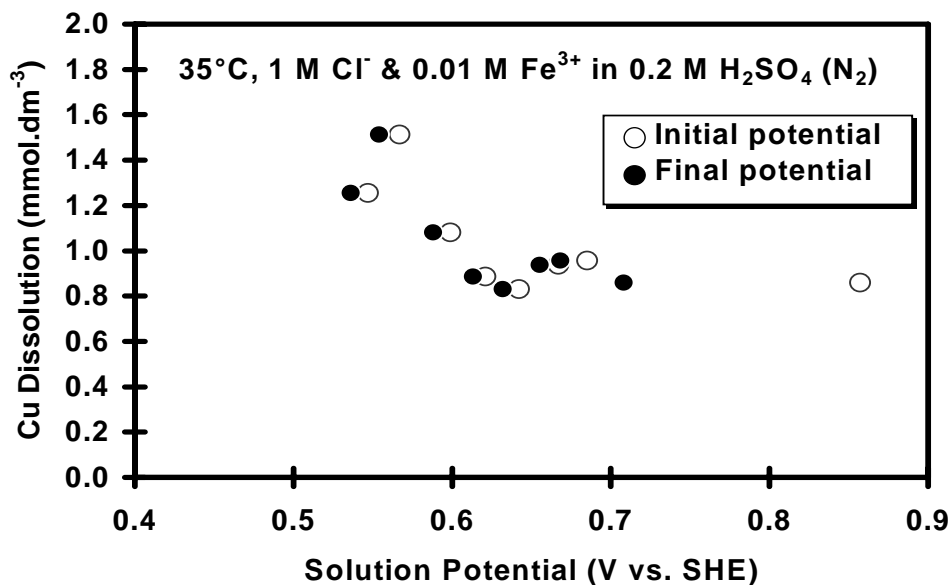


Figure 5.1 The effect of solution potential on the extent of copper dissolution from OKTedi after 24 h in the presence of chloride.

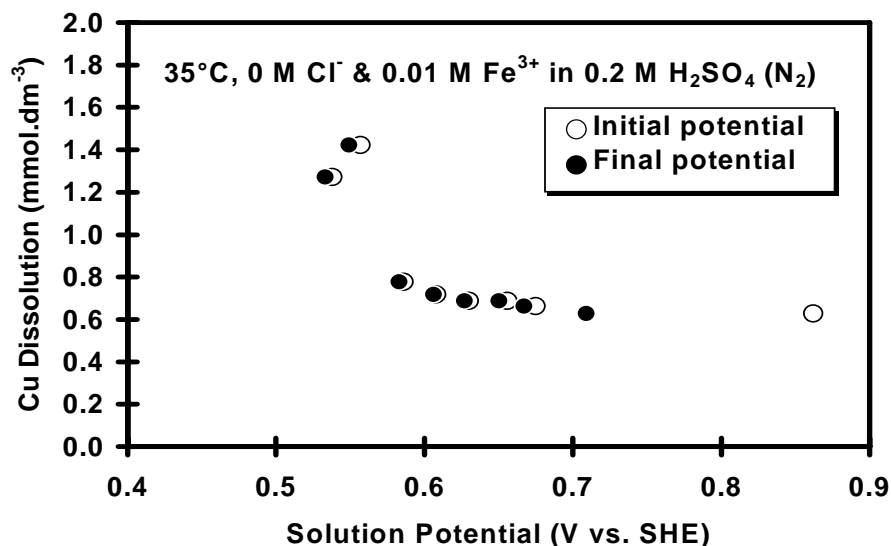


Figure 5.2 The effect of solution potential on the extent of copper dissolution from OKTedi after 24 h in the absence of chloride

In Chapter 4, it was shown that it is not possible to maintain constant potential conditions throughout the duration of a test due to the continuous changes in variables such as pH, chloride and iron and copper concentrations. In order to develop an ambient temperature process for successful leaching of chalcopyrite in a chloride or chloride–sulfate system it is not only appropriate to establish the boundaries of the potential range required for adequate leaching rates but also it is necessary to develop and implement potential control strategies.

The current study starts by defining the potential range for optimum chalcopyrite leaching using three different potential control systems i.e. electrochemical, nitrogen, and air/oxygen. In addition mineralogical data will be obtained which will focus on the minerals present in each concentrate, association of chalcopyrite with other minerals, surface impurities and the particle size distribution of the main sulfide minerals present in each chalcopyrite

concentrate and some leach residues. Leaching experiments to establish whether or not chalcopyrite concentrates from different localities leach at different rates under the same conditions will be shown. Because of the fact that dry screening of the concentrates produced significant amounts of agglomerated fine material that made comparisons of the relative leach rates difficult (Chapter 4), the procedure was modified to include wet screen of each concentrate to obtain a well-defined chalcopyrite size fraction. Table 5.1 shows the conditions of each experiment described in this chapter.

Table 5.1 Details of leaching conditions

Sample		Condition						
Figure	Test	Sample	Mass g	HCl M	NaCl g L ⁻¹	Cu g L ⁻¹	Set Pot. mV	E _h Control
5.3	(a)	Andina	9	0.2	0	0.5	560	electrochemical
	(b)						580	
	(c)						600	
	(d)						610	
5.4	(a)	Andina	9	0.2	0	0.5	580	N ₂
	(b)							O ₂
	(c)							Sealed
	(d)							air
5.6	(a)	Andina	9	0.2	0	0.5	540	air
	(b)						560	
	(c)						580	
	(d)						600	
	(e)						620	
5.11		Andina	9	0.2	0	0.5	580	N ₂ /air
		PQS	40					
		PV	20					
		CCHYP	18					
5.12	(a)	CCHYP	18	0.2	0	0.5	560	N ₂
	(b)						580	
	(c)						600	
	(d)						620	
	(e)						640	
	(f)						660	
5.13	(a)	CCHYP	18	0.2	50	0.5	660	O ₂
	(b)			0.2	0			
5.14	(a)	CCHYP	18	0.2	50	0.5	580	O ₂
	(b)						620	
	(c)						640	
	(d)						660	
5.15	(a)	Andina	18	0.2	0	0.5	450	N ₂
	(b)						450	
	(c)						580	

5.2 Electrochemical control of the potential

This system operates on the principle that anodic oxidation of iron(II) and copper(I) produced as products of reduction of iron(III) and copper(II) and also as products of the oxidation of sulfide minerals can be used to regenerate the oxidants and thereby control the potential. This requires that the cathode be separated from the leaching solution by in this case; a fritted glass disk sealed into the bottom of the cathode compartment which initially only contained acid. The system consists of an E_h electrode and two platinum electrodes (generating anode and cathode) as described in Chapter 3.

On the surface of platinum anode the following reactions occur



and the following at platinum cathode electrode



This electrochemical control system was used to investigate the effect of potential and dissolved oxygen concentration on the rate of dissolution of the Andina concentrate. Four experiments were carried out at potential set-points of 560, 580, 600 and 610 mV under otherwise standard conditions. The results are shown in Figure 5.3. It is apparent that the dissolution of chalcopyrite is lower than expected with a maximum of 17% in 1000 h. The potential under continuous nitrogen flow decreased to about 540 mV in each reactor suspected be the cause of this low dissolution. After 600 h, air was introduced into the reactor controlled at 580 mV and a slight increase of the rate was observed with an increase

of potential to 640 mV. It was suspected at this point that the presence of dissolved oxygen is important to achieve higher rates of dissolution of chalcopyrite.

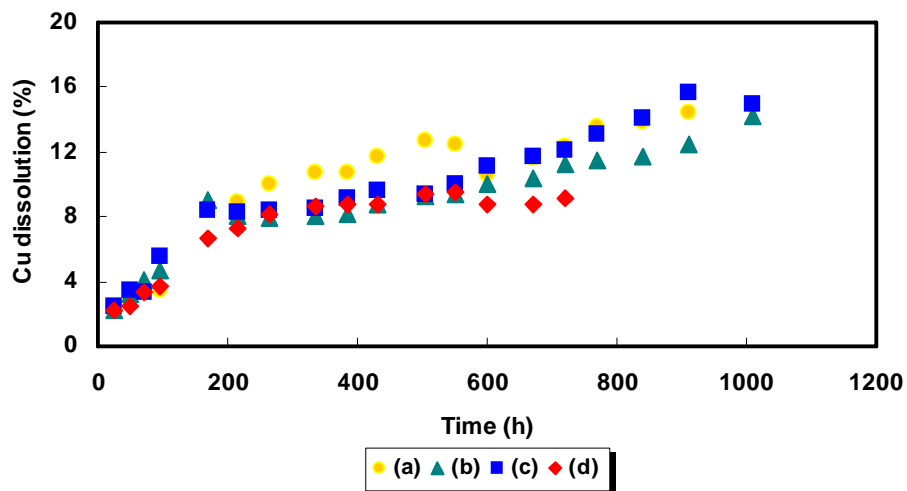


Figure 5.3 Copper dissolution from Andina concentrate under electrochemical control. (a) 560 mV, (b) 580 mV, (c) 600 mV and (d) 610 mV.

Three further experiments were conducted in which the potential was maintained at 580 mV by electrochemical reduction of iron(III) and copper (II). The dissolved oxygen concentrations were maintained approximately constant at different levels as shown on Figure 5.5. Clearly, the rate is higher in presence of dissolved oxygen but the effect does not appear to depend on the oxygen concentration with roughly the same rates being obtained with 5 and 15 ppm of dissolved oxygen.

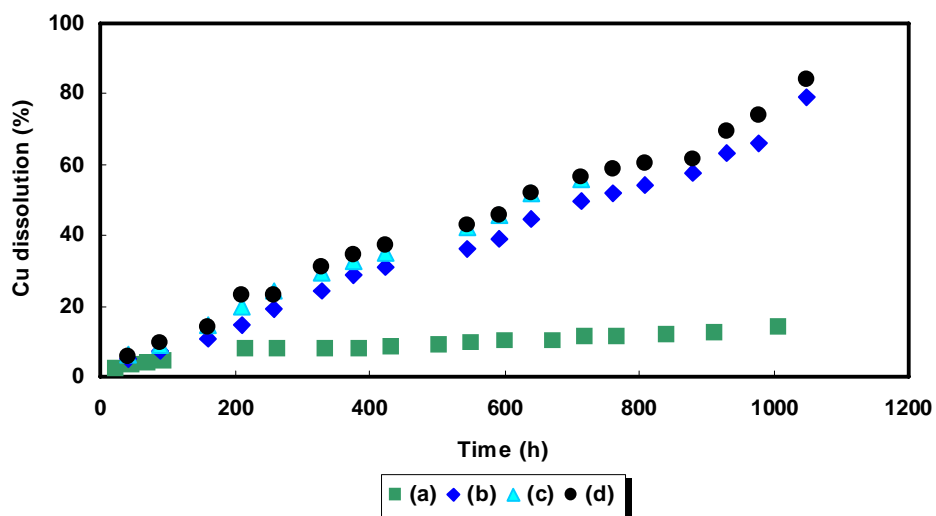


Figure 5.4 Copper dissolution from Andina concentrate under electrochemical control. (a) nitrogen, (b) oxygen, (c) reactor sealed and (d) air.

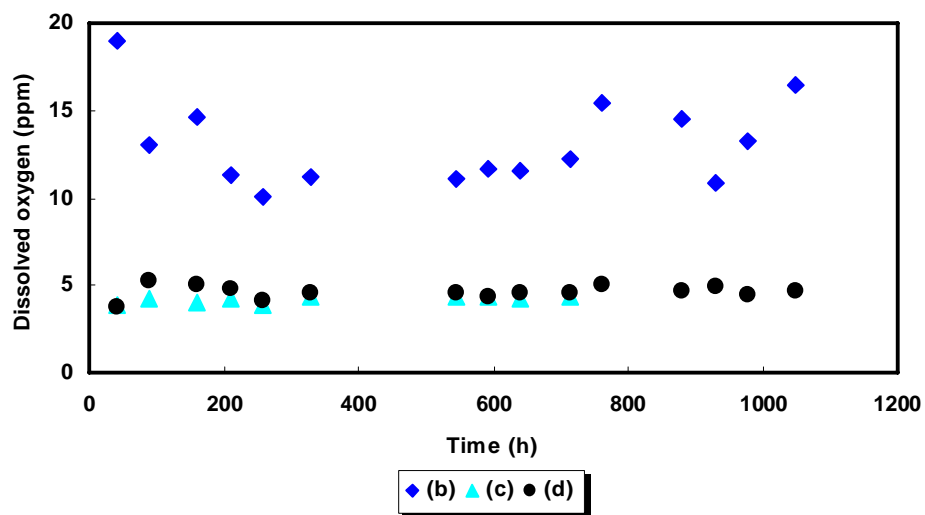


Figure 5.5 Concentration of dissolved oxygen. (b) oxygen, (c) reactor sealed and (d) air.

These rather unexpected observations that some dissolved oxygen are required for enhanced dissolution resulted in termination of this method for the control of the potential.

5.3 Control of the potential by oxygen addition

As a result of the need to have some dissolved oxygen present in the leach solution, it was decided to modify the control system to one which uses control of the amount of air injected into the leach pulp. In this system, the reactor is equipped with an Eh electrode, an air injection tube connected to a small air pump or a gas sparger and a gas control valve introduced into the reactor that can be activated by a solid-state switch driven by a digital output from the controlling computer. Five different experiments were carried out on wet screened Andina concentrate at 35 °C. The results presented in Figure 5.6 confirm the importance of dissolved oxygen in that, at the appropriate potentials, over 90% dissolution was achieved after 1200 h. The results also demonstrate that enhanced rates of leaching can be achieved in the potential window of about 560-600 mV with significantly lower rates at 540 and 620 mV. The reduction in rate at the low potential is due to the enhanced stability of covellite (CuS) at potentials below about 550 mV under these conditions while passivation of chalcopyrite occurs at potentials above about 620 mV. Of interest is the relatively constant rate of dissolution which is observed in most experiments even up to 80% dissolution. It should be noted that the initial relatively rapid dissolution of about 5-7% of the copper in these and subsequent experiments with the Andina concentrate is due to the greater reactivity of small amounts of bornite in the concentrate.

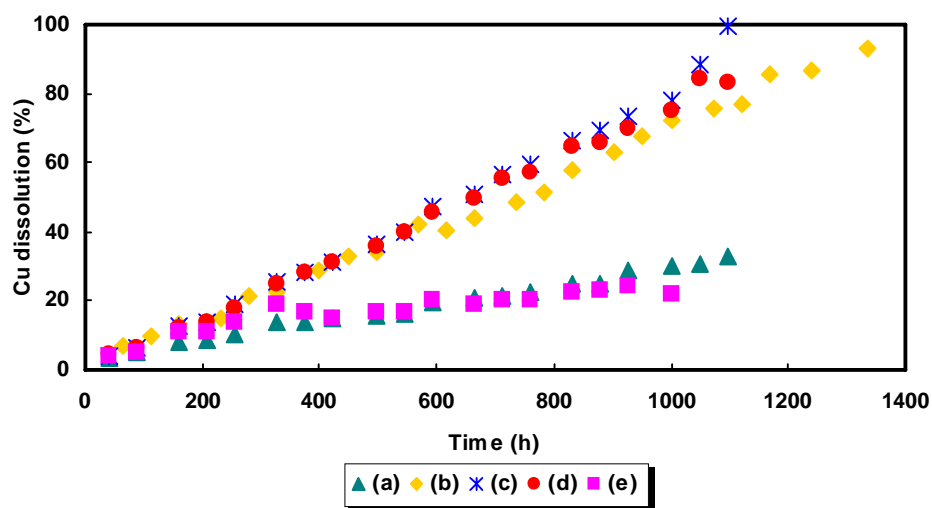


Figure 5.6 Copper dissolution from Andina chalcopyrite concentrate at 35 °C under air control. (a) 540 mV (b) 560 mV, (c) 580 mV, (d) 600 mV and (e) 620 mV.

5.4 Dissolution of chalcopyrite concentrates from different sources

A number of leach experiments were carried out using concentrates from Andina, PQS2 (Escondida), Pinto Valley (PV) and Cerro Colorado (CCHYP). It was decided to carry out the experiments with the +25-38 μm size fraction for Andina and with the -38 μm fraction with the other samples due to: (1) the limited amount of concentrate available from the last three sources; (2) the fact that the particle size distribution analysis of each concentrate, showed that the Andina material contained a significant proportion of fine chalcopyrite and; (3) the other materials contained less fine particles. Each sample was wet screened to the desired size, washed in acetone and air-dried. The various head samples were analyzed chemically and mineralogically. The chemical analyses of the screened samples are shown in Table 5.2. The Andina sample contains the highest proportion of copper followed by the

CCHYP, PV and PQS2 samples. The silver content of the various samples ranges from 50 to 10 ppm and this is of potential interest since soluble silver is known to accelerate the dissolution of chalcopyrite (Hiroyoshi et al., 2002; Hiroyoshi et al., 2007; Parker et al., 2003; Yuehua et al., 2002). Mineralogical studies were undertaken of both the sized head and residue samples for each concentrate at the Newcastle Technology Centre (NTC) using MLA (Mineral Liberation Analyser) and optical techniques. Mineralogical data obtained from the MLA analyses are presented in Table 5.3. It is apparent that the Andina concentrate is the highest grade with respect to chalcopyrite followed by the Pinto Valley and CCHYP samples. The Pinto Valley concentrate is predominately composed of chalcopyrite, pyrite and other gangue minerals, while the other samples comprise chalcopyrite and pyrite together with other copper sulfides such as bornite, enargite and covellite. The PQS2 sample contains relatively little chalcopyrite but significant amounts of pyrite. The pyrite content decreases in the sequence PQS2>CCHYP>PV>Andina. Due to the differences in the chalcopyrite content of each concentrate, it was decided to adjust the amounts of each concentrate used in each experiment to give roughly the same mass of chalcopyrite.

Table 5.2 Chemical data (elemental composition, %)

Sample	Size (µm)	Cu	Fe	S	Ag (ppm)
Andina	+25-38	30.8	28.3	32.4	50
PQS2	-38	8.1	30	35.3	20
PV	-38	13.2	21.8	23.3	30
CCHYP	-38	14.5	23.5	26.5	10

Table 5.3 Mineralogical composition of concentrates (Wt, %)

Mineral	Andina	PQS2	PV	CCHYP
	+25-38 μm	-38 μm	-38 μm	-38 μm
Chalcocite	0.00	0.0	0.0	2.49
Chalcopyrite	82.50	17.6	45.8	32.98
Covellite	0.16	5.0	0.0	5.65
Bornite	3.40	1.7	0.1	2.68
Native_Cu	0.00	0.0	0.0	0.00
Enargite	1.70	1.2	0.0	0.73
Brochantite	0.00	0.0	0.0	0.23
Chrysocolla	0.00	0.0	0.0	0.04
Other Cu Min.	0.00	0.0	0.1	0.05
Pyrite	2.70	62.2	20.9	34.33
Quartz	5.00	3.4	9.6	5.33
Galena	0.47	0.1	0.1	0.1
Sulfur	0.00	0.00	0.00	0.00
Other Gangue	4.03	8.8	23.4	15.39
total	100	100	100	100

Table 5.4 shows the copper source ratio (CSR) which represents the percentage of the copper content contained in each copper mineral present in a concentrate sample. It is clear that most of the copper in the Andina and PV concentrates is contained in chalcopyrite while the PQS2 and CCHYP concentrates contain significant amounts of copper as covellite with minor contributions from other copper sulfides. The MLA analyses show that chalcopyrite particles are mostly liberated in all samples with small amounts associated with others minerals also present in the concentrate as shown in Table 5.5.

Table 5.4 Pyrite content and CSR (copper source ratio) (mass %) of major copper minerals in concentrates

Sample	Andina	PQS2	PV	CCHYP
Mineral	+25-38 μm	-38 μm	-38 μm	-38 μm
Chalcopyrite	90.2	54.0	99	59.1
Covellite	0.2	31.0	0	19.6
Bornite	6.8	9.0	0.4	8.8
Enargite	2.6	5.0	0	1.8
Pyrite	2.7	62.2	20.9	34.3

Table 5.5 Percentage of chalcopyrite in head samples associated with other sulfide minerals

Minerals	Andina	PQS2	PV	CCHYP
Bornite	0.8	1.3	0.01	0.7
Covellite	0.2	0.6	0	0.5
Enargite	0.8	0	0	0
Pyrite	0.3	1.1	0.1	1.3
Free surface	95	95.5	99.2	95.1

In addition to the above analyses of the major elements and minerals, a number of samples were analysed for trace elements by ICP spectroscopy in order to understand differences in the trace element content that may enhance or negatively impact on leach performance. The results are shown in Table 5.6.

Table 5.6 Traces element analyses (ppm)

Sample	Size	Screened	Ag	Bi	Sb	Cd	Sn	Co	Ni	As
		μm								
Andina	head	wet	81	46.4	220.0	25.1	3.2	21.0	12.0	2650.0
PQS2	-38	wet	18.0	5.3	32.5	20.3	9.6	190.0	170.0	720.0
PV	-38	wet	24.0	1.4	2.3	10.4	13.4	110.0	105.0	40.0
CCHYP	-38	Wet	20.0	45.0	11.6	30.1	6.6	1120.0	245.0	80.0

5.4.1 Mineral particle size distribution

Figures 5.7 to 5.10 show the particle size distribution of the main sulfide minerals in each sample as obtained from the MLA analyses. It appears that the secondary copper minerals are generally finer than chalcopyrite except for the chalcocite particles in the CCHYP sample in which the chalcocite particle size is higher than that of chalcopyrite.

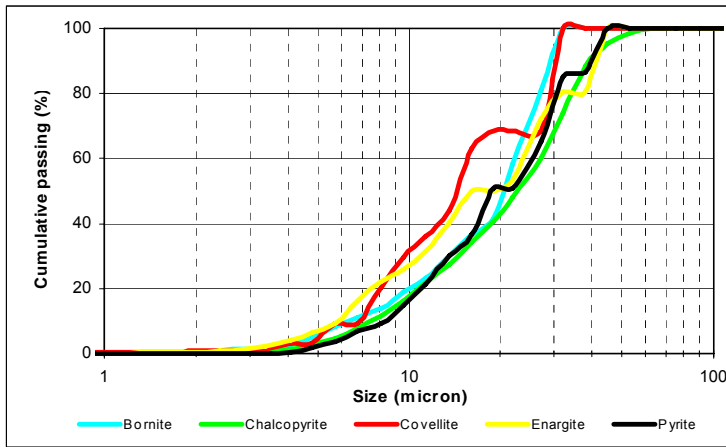


Figure 5.7 Andina +25-38 μm mineral size distribution

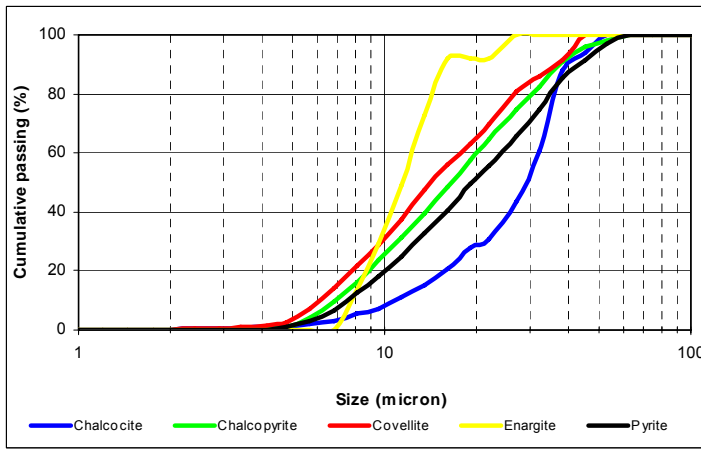


Figure 5.8 CCHYP -38 μm mineral size distribution

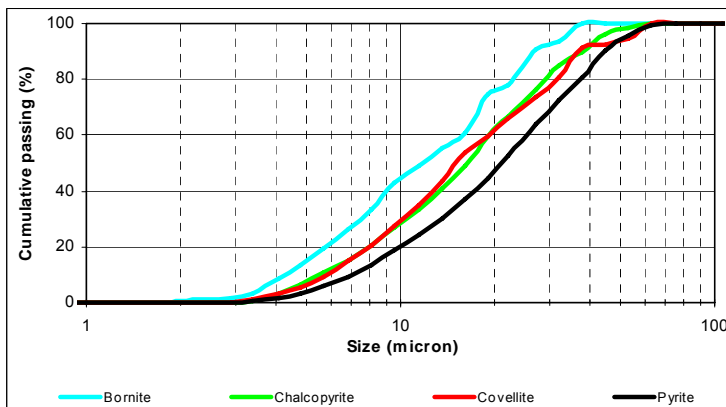


Figure 5.9 PQS2 -38 μm mineral size distribution

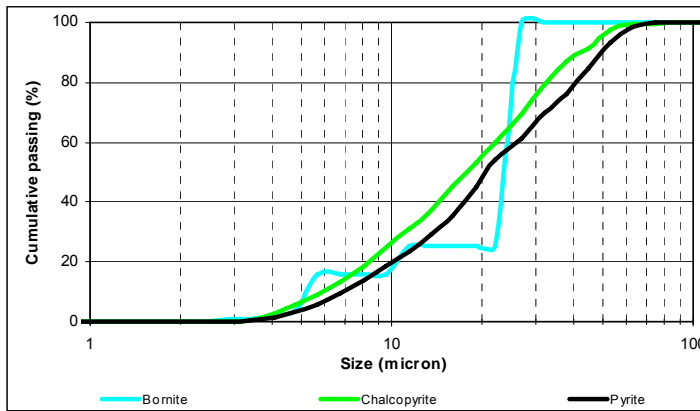


Figure 5.10 Pinto Valley (PV) -38 µm mineral size distribution

5.4.2 Leaching experiments within the optimal potential window

Each of the chalcopyrite samples were leached at a controlled potential of 580 mV using the nitrogen/air control system under standard conditions i.e., 0.2 M HCl and 0.5 g L⁻¹ Cu(II) at 35 °C. Either 9 g of Andina, 40 g of PQS2, 20 g PV or 18 g of CCHYP were leached in the instrumented reactors agitated at 800 rpm, and samples were extracted at fixed time intervals and analysed for copper and iron; the details of the method were presented in Chapter 3. Figure 5.11 summarizes the leaching curves, which are approximately linear with very similar rates for the Andina, PQS2, and CCHYP concentrates but considerably slower for the PV sample. The initial relatively rapid rate of dissolution in some cases is due to the greater reactivity of the secondary copper sulfide minerals.

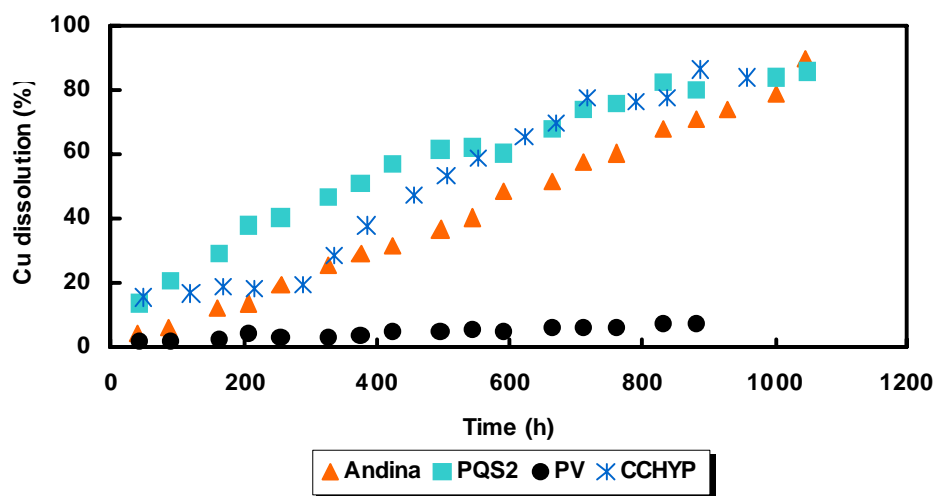


Figure 5.11 Dissolution of copper from chalcopyrite concentrates from different localities.

In order to examine whether the optimum potential window can be extended, a series of experiments were carried out at 35 °C with the CCHYP concentrate in a solution containing 0.2 M HCl-0.5 g L⁻¹ Cu(II) at different set potentials. The set potentials were obtained by bubbling nitrogen gas into the reactor to prevent an increase of the potential during the experiments. The results shown in Figure 5.12 indicate that the desired variations in the potential were not attained by this method and essentially all experiments were operated within the optimal potential window with similar rates in all runs except for the experiment at a lower potential of 560 mV for which the rate was somewhat lower.

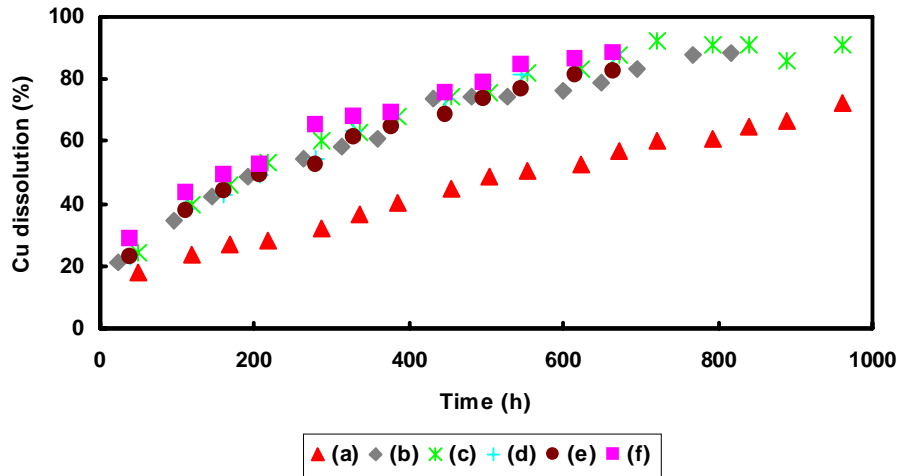


Figure 5.12 Dissolution of CCHYP concentrate under standard conditions at different nominal potential set-points as controlled by nitrogen addition. (a) 560 mV, (b) 580 mV, (c) 600 mV, (d) 620 mV, (e) 640 mV and (f) 660 mV.

Due to the inability to control the potential at values higher than 580 mV with the nitrogen/air control system, three experiments were carried out under the same conditions as above with the CCHYP concentrate. The chloride concentration was increased in two of these experiments and operation at a higher potential in the region of 650 mV was achieved by control of the potential with sparging of oxygen in the reactor when the potential is lower than the set point. The results are depicted in Figure 5.13. After 300 h, the chalcopyrite appeared to be passivated with an overall dissolution of only 60% of which about 50% is due to the non-chalcopyrite copper minerals in the concentrate. An attempt was made to reverse the slow rate as a result of passivation at the high potential by the introduction of nitrogen into the reactors after about 800 h and, although the potential was reduced, the rate of dissolution did not appear to recover.

Additional experiments were conducted to establish the effect of potential in the range of 580 to 660 mV on the rate of dissolution in solutions with higher chloride concentration of 50 g L⁻¹. The results summarized in Figure 5.14 show that, although dissolution started at potentials below the set points, the potential gradually increased and the rates were largely independent of potential. Note the increased rate on increasing the potential for the run shown by the blue points after about 700 h. It thus appears that the optimum potential window increases to 600-640 mV in the presence of higher chloride concentrations.

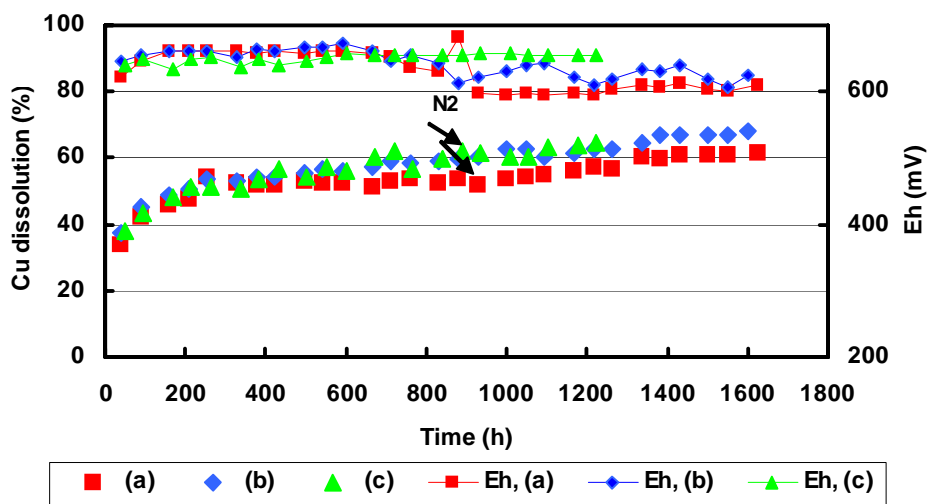


Figure 5.13 Dissolution of CCHYP concentrate under standard conditions and a higher chloride ions concentration at 660 mV with the oxygen control system. (a) 50 g L⁻¹ chloride ions, (b) standard conditions and (c) 50 g L⁻¹ chloride ions.

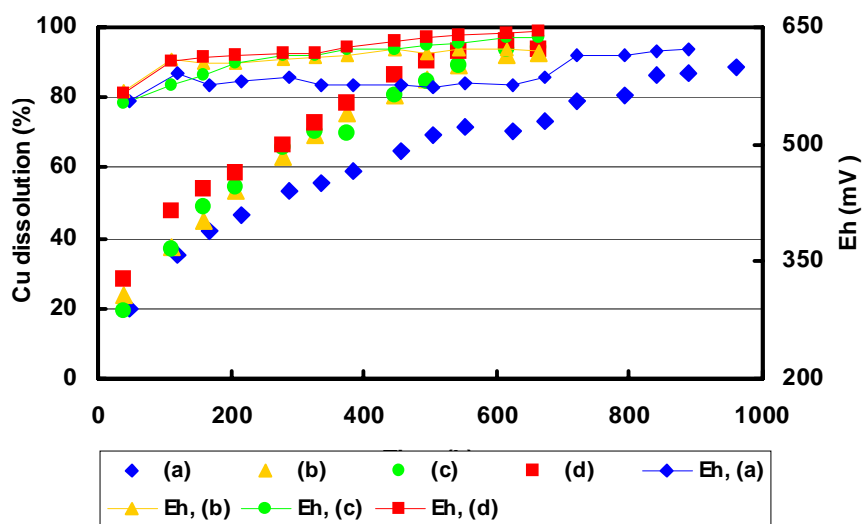


Figure 5.14 Dissolution of CCHYP concentrate in 0.2 M HCl, 0.5 g L⁻¹ Cu(II) and 50 g L⁻¹ chloride ions at various potentials

5.5 Effect of low potentials

Two tests were carried in order to establish the extent to which chalcopryrite dissolves at low potentials (450 mV) and whether a subsequent increase in potential results in similar or enhanced rates over those observed in the optimum potential window (550-600 mV) i.e. whether chalcopryrite is converted to a more reactive sulfide under mildly reducing conditions. The tests were carried out under otherwise standard conditions using nitrogen to maintain the low potentials. The results are shown in Figure 5.17 from which it is apparent that both tests at low potential showed negligible dissolution of copper until the potential was increased to 550 mV after 600 h in one and after 900 h in the second test. It is clear that the rate on increasing the potential is similar to that observed under standard conditions as shown by the orange points, i.e. there does not appear to be any net advantage in carrying out a 2-stage process with the first involving reducing conditions.

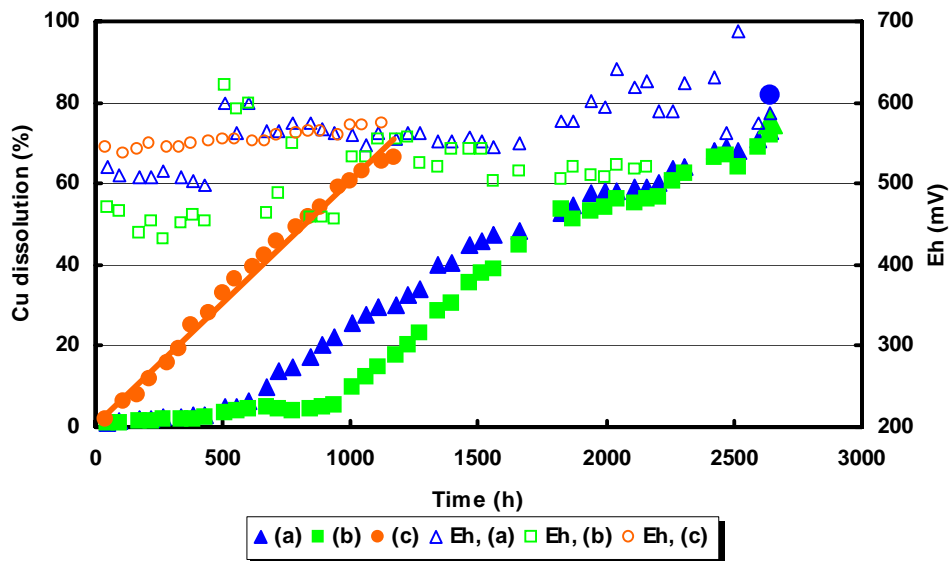


Figure 5.15 Dissolution of copper from Andina concentrate under standard conditions initially at low potential (450 mV) and subsequently at the optimum potential (550 mV). (a) potential increased after 600 h, (b) potential increased after 900 h, and (c) potential at 580 mV throughout.

Solid samples for mineralogical analysis were taken just before increasing the potential and on completion of the tests.

Figure 5.16 shows part of the surface of a chalcopyrite electrode that was placed for several days in a leach test of Andina concentrate conducted in standard conditions at a low potential of 450 mV. The microphotograph shows the formation of a thin blue/ pink layer on the surface which is characteristic of a covellite-like phase. This electrode was immersed in a magnetically stirred beaker open to the air containing a solution of 0.2 M HCl and 0.5 g L⁻¹ Cu(II) at a higher potential of 650 mV for two weeks. As is obvious from Figure 5.17 that the thin blue film dissolved under these conditions.

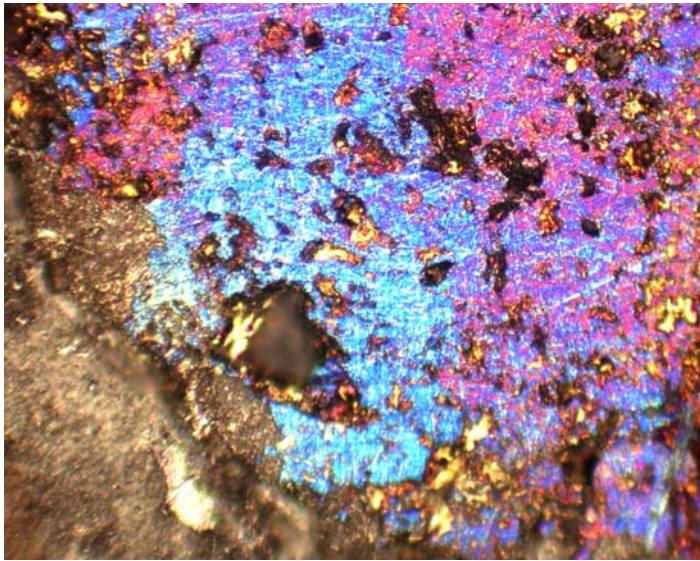


Figure 5.16 Chalcopyrite electrode after immersion in a solution containing 0.2 M HCl and 0.5 g L⁻¹ Cu(II) at a potential of 450 mV for several days.

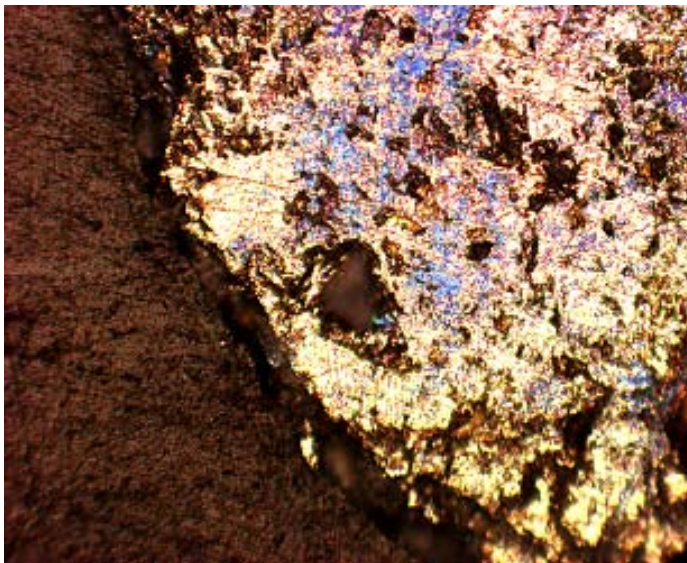


Figure 5.17 Same electrode as above immersed in the standard solution at 650 mV for one week.

The results of chemical analyses for the main elements in the head and residue samples from the test carried out at low potentials for 900 h as estimated from a QEMSCAN investigation are presented in Table 5.6. Similar data for the mineral distribution in these

samples is summarized in Table 5.7. After 936 h the copper, iron and sulfur content of the material is only slightly lower than in the head sample. As shown in Table 5.7, the chalcopyrite content is also only slightly reduced while there appears to be an increase in the content of covellite and bornite suggesting that chalcopyrite could have been reduced to these copper sulfides. Again as shown in Figure 5.18, the association of chalcopyrite with other minerals is almost unchanged after 900 h at low potential. The formation of covellite was confirmed as shown by the optical micrograph in Figure 5.19 and although the head sample contains undetectable amounts of chalcocite, it is clearly present after 936 h at 450 mV. On the other hand, mineral maps obtained from a parallel MLA study of the same samples (Figure 5.20) do not show the presence of chalcocite. Finally, these maps verify that most of chalcopyrite is liberated and that sulfur is not present.

Table 5.7 Chemical analysis of samples (mass %) as obtained by MLA of Andina concentrate (+25-38 μm) and residues after dissolution under the conditions of Test (b) in Figure 5.15

Chemical assay	Head	Residue 936, h	Residue 2640, h
Cu	32.0	30.5	22.3
Fe	30.5	27.4	23.9
S	32.4	34.5	35.6

Table 5.8 Modal mineralogical analysis (mass %) of Andina concentrate (+25-38 μm) and residues after dissolution under the conditions of Test (b) in Figure 5.15

Mineral	Head 0, h	Residue 936, h	Residue 2640, h
Chalcopyrite	82.5	80.2	57.1
Covellite	0.16	0.4	0.0
Bornite	3.4	4.0	1.9
Pyrite	2.7	5.5	12.0
Sulfur species	0.0	0.0	5.7
Total	100	100	100

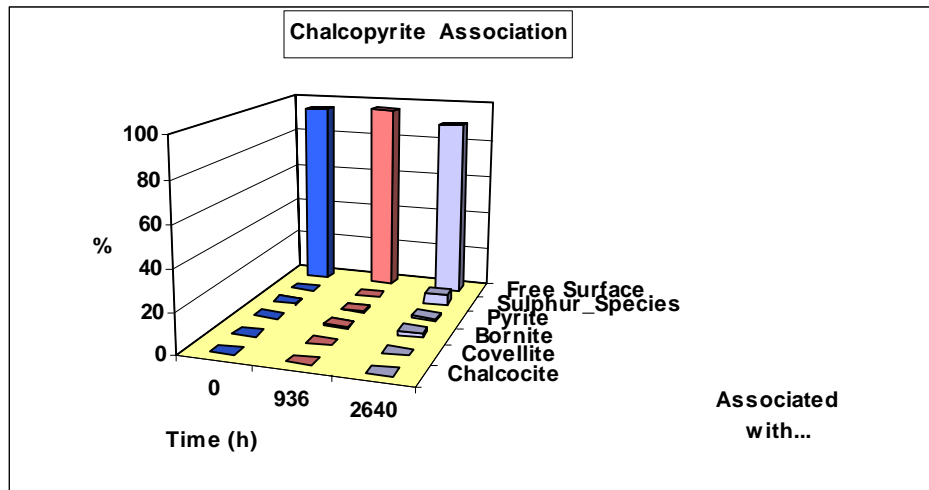


Figure 5.18 Association of chalcopyrite with other sulfides (the fraction of free surface of the mineral boundary that is in contact with other minerals in a polished section.)

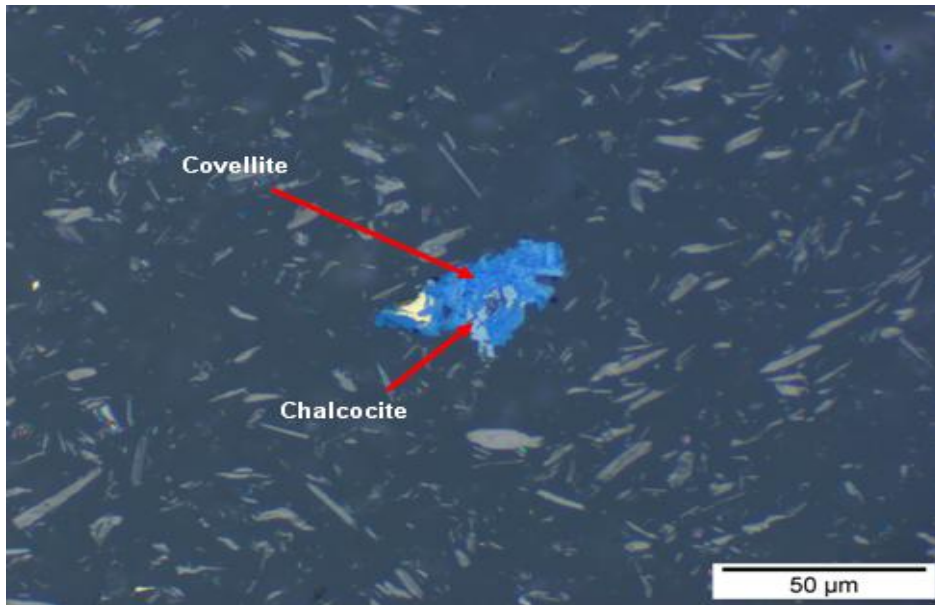


Figure 5.19 Optical micrograph showing the replacement of chalcopyrite by covellite and chalcocite after 936 h of dissolution of Andina concentrate under standard conditions at a low potential (450 mV).

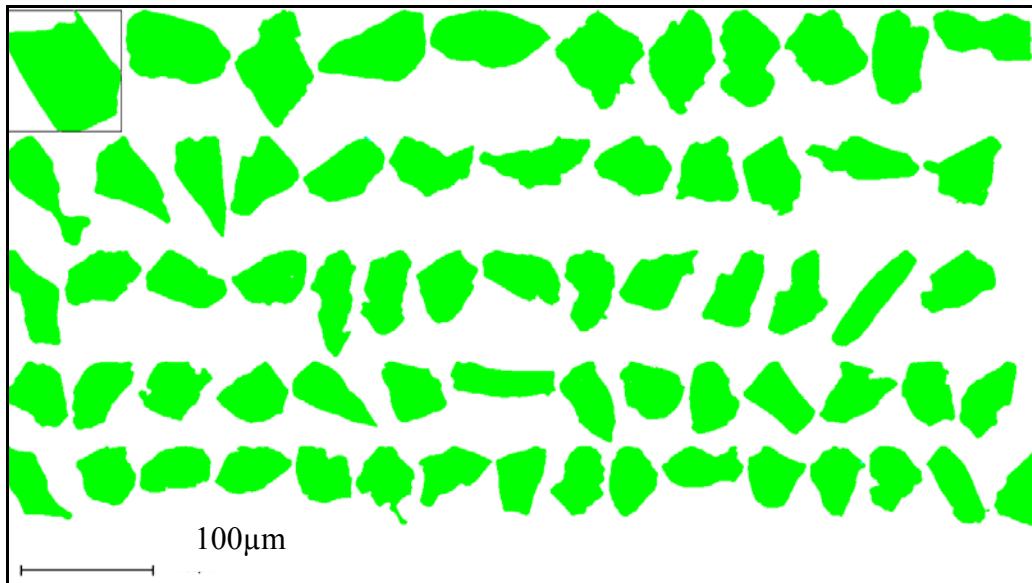


Figure 5.20 Partial mineral map of the residue after 936 h of dissolution at low potential (450 mV) showing free chalcopyrite particles.

After 2640 h, the copper and iron concentration in the residue decreased while the concentration of elemental sulfur increased. Mineralogical data (Table 5.7) shows that the amount of chalcopyrite and bornite has decreased while there is a no significant amount of covellite but increased amounts of sulfur in the residue. It should be pointed out that the method of preparation of the polished sections results in significant losses of elemental sulfur globules and that the amounts analyzed are therefore lower limits only. Association of chalcopyrite with sulfur, pyrite and bornite were observed as shown in Fig. 5.18. Optical micrograph (Figure 5.21) still shows instances of replacement of chalcopyrite by chalcocite and covellite. Figure 5.22 illustrates this replacement in terms of a particle of chalcopyrite with a covellite reaction rim occurring along the cracks and edges. According Elsherief (2002) this texture is expected as a result of the change in molar volume as chalcopyrite transforms to chalcocite and covellite. The mineral maps shown in Figure 5.23(a) and (b) show that most of the unreacted chalcopyrite is present as liberated particles with a few particles rimmed by elemental sulfur. In addition, is interesting to observe the occurrence of sulfur as isolated and relatively large globules suggesting that the formation of elemental sulfur occurs by precipitation from dissolved sulfur species such as H₂S (Dutrizac, 1990), Fig. 5.24.

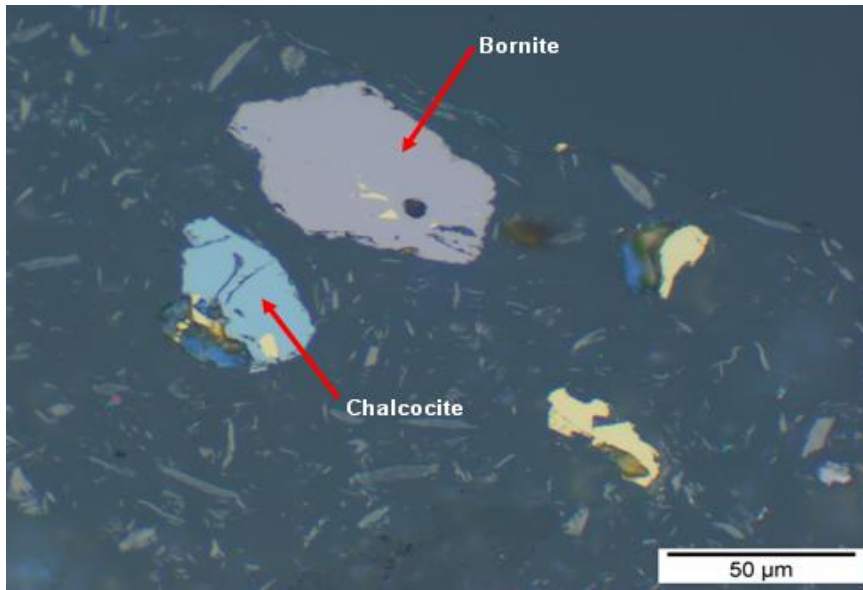


Figure 5.21 Optical micrograph of replacement of chalcopyrite by covellite and chalcocite after 2640 h of dissolution of Andina concentrate under standard conditions at 550 mV.

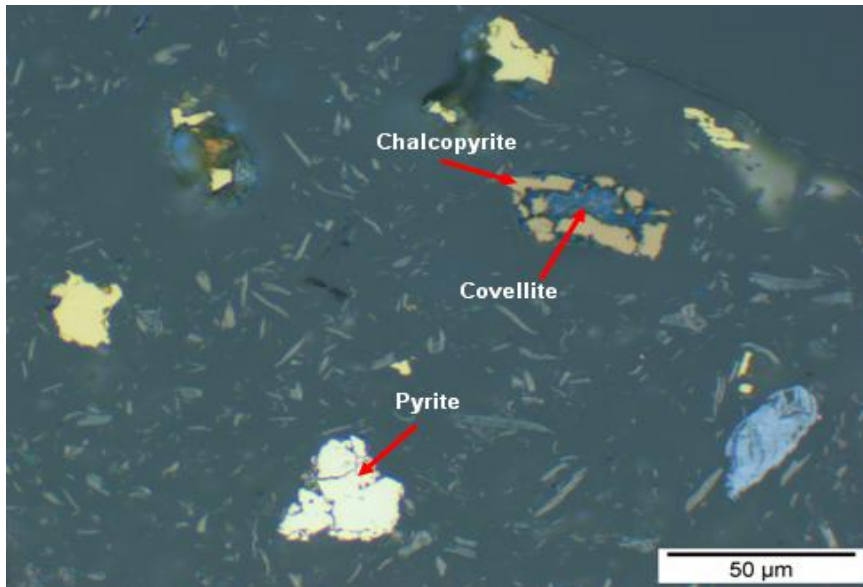


Figure 5.22 Optical micrograph showing covellite associated with partially reacted chalcopyrite and pyrite after 2640 h of dissolution of Andina concentrate under standard conditions at 550 mV.

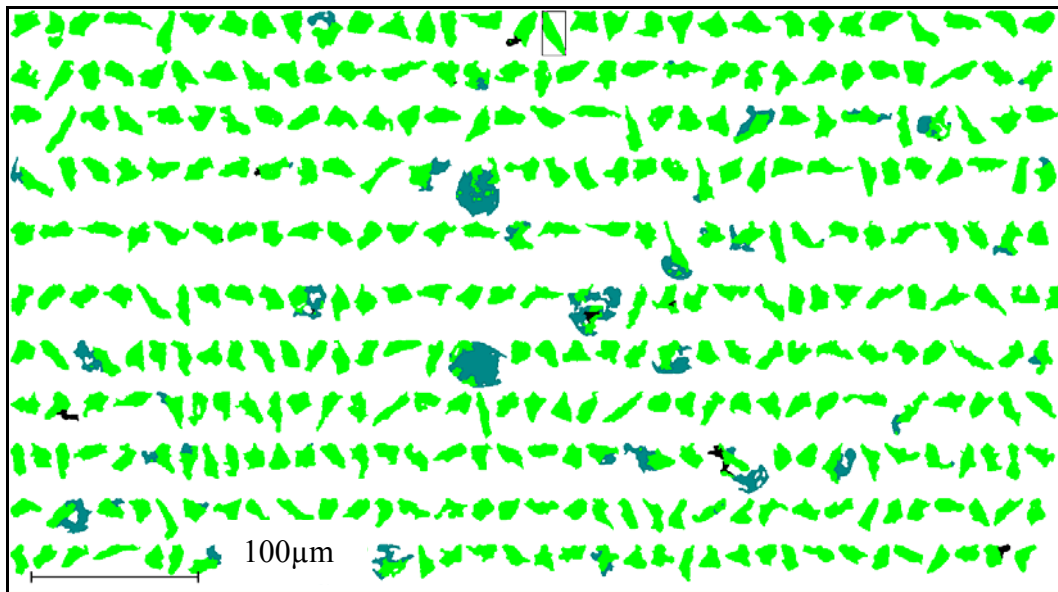


Figure 5.23 Mineral maps after 2640 h of leaching illustrating most of chalcopyrite particle are free and few of them rimmed by sulphur.



Figure 5.24 Mineral maps after 2640 h of leaching illustrating elemental sulfur.

5.6 Recovery

Chemical analyses of Cu, Fe and S of some of residues were completed at the Ultra Trace Laboratory, Perth. Table 5.9 lists the recovery calculated from residue analyses as well as the corresponding solution recovery. It is evident that similar values were obtained using both methods except for PV sample, which exhibited extremely low leach rates for some unknown reason (more recent studies with a fresh concentrate from Pinto Valley have shown normal rates of dissolution).

Table 5.9 Copper recovery based on solution and residue analysis

Figure	Test	Leached solution %	Residue %
5.4	(b)	77.3	77.6
	(c)	54.6	55.9
	(d)	82.0	74.8
5.11	Andina	68.9	78.2
	PQS	87.5	86.5
	PV	8.9	26.2
	CCHYP	83.6	87.3
5.12	(a)	72.2	74.2
	(b)	83.6	87.3
	(c)	90.8	96.3
	(d)	88.6	89.2
	(e)	82.5	86.0
	(f)	88.40	90.9
5.13	(a)	61.2	56.5
	(b)	68.0	60.7
5.15	(a)	75.4	81.7
	(b)	74.4	75.2

5.7 Summary and conclusions

Leaching experiments under controlled potential and standard conditions have demonstrated that the rate of dissolution of chalcopyrite is potential dependent and the presence of dissolved oxygen is essential for enhanced rates. However, it appears that increased concentrations of dissolved oxygen are not required above a minimum level of give magnitude of mg/L. The linear rate of dissolution of chalcopyrite concentrates in chloride solutions under standard conditions i.e., 0.2 M HCl-0.5 g L⁻¹ Cu(II) at 35 °C is enhanced within a range of potentials of 550 to 620 mV (potential window).

As a result of optical microscopy of a chalcopyrite electrode and a mineralogical investigation of intermediate and final residues after dissolution it is suggested that under standard conditions but at low potentials (450 mV), a covellite-like product is formed as intermediate during chalcopyrite leaching.

Even though dissolved oxygen is important in order to achieve acceptable rates of dissolution, an excess of oxygen can increase the potential into a region in which passivation is possible. Initial leaching at potentials above 630 mV for extended periods results in low rates that are not increased when the potential is subsequently reduced to 580 mV and it appears that the “passivation” is not reversible although it should be emphasized that this effect has only been tested with one concentrate under two sets of conditions.

On the other hand, leaching at low potential (<540 mV) results in reduced rates of copper dissolution which increase significantly when the potential is subsequently increased to above 580 mV. Mineralogical studies have shown that chalcopyrite remains unleached and

small amounts of covellite and chalcocite appear to be formed on the surface of the chalcopyrite under these conditions suggesting the possibility of a two stage process in which chalcopyrite is converted to a more reactive secondary copper sulfide. However, the overall rate in this two-stage process appears to be similar to that achieved by operation as a single stage within the potential window. In an attempt to extend the potential window, experiments at higher chloride ion concentration have shown that it is possible to obtain higher rates at higher potentials (up to 650 mV). Therefore, the upper limit of the potential window appears to increase at high chloride concentrations. However, the rates are similar to those obtained at lower chloride concentrations within the potential window. Again, it should be emphasized that this effect has only been tested with the CCHYP concentrate under one set of conditions.

With the exception of the Pinto Valley (PV) concentrate, all concentrates studied (Andina, PQS2 and CCHYP) appear to dissolve at roughly the same rate under the same conditions, despite differences in the composition and mineralogy of the concentrate samples.

6. KINETICS OF THE DISSOLUTION OF CHALCOPYRITE

6.1 *Introduction*

As reviewed in Chapter 2, a number of investigations have been conducted to elucidate the reaction kinetics and delineate the important variables for the leaching of chalcopyrite in both chloride and sulfate systems. Although many researchers have reported relevant work, some ambiguities still remain. Chapter 4 presented the kinetics of the dissolution of various chalcopyrite concentrates using mixed chloride/sulfate solutions using both a simple shake flask technique and instrumented reactors. Of major importance in the present chapter is the behaviour of the dissolution of chalcopyrite with various factors that could be expected to affect the rate of the dissolution process such as temperature, pulp density, chloride and cupric concentrations and particle size under controlled potential conditions that were established as being optimum, namely 560 – 620 mV. Table 6.1 shows the conditions of each leach experiment.

Table 6.1 Experimental conditions of leaching tests studied

Sample			Condition							
Figure	Test	Sample	Mass g	T °C	HCl M	NaCl g L ⁻¹	Fe(II) g L ⁻¹	Cu g L ⁻¹	Set Pot. mV	E _h Control
6.1	(a)	Andina	18	25	0.2	0	0	0.5	580	N ₂
	(b)			35						
	(c)			50						
	(d)			65						
	(e)			75						
6.2	(a)	CCHYP	18	25	0.2	43	0	0.5	580	N ₂
	(b)			35						
	(c)			50						
	(d)			75						
6.5, 6.7	(a)	Andina	9	35	0.2	0	0	0.5	580	N ₂
	(b)					13				
	(c)					63				
6.6	(a)	CCHYP	18	35	0.2	0	0	0.5	580	N ₂
	(b)					13				
	(c)					43				
6.8	(a)	Andina	18	35	0.2	0	0	0.1	580	N ₂
	(b)							0.5		
	(c)							1.0		
6.9	(a)	Andina	9	35	0.2	0	6	0.5	580	N ₂
	(b)						55			
	(c)						0			
	(d)						55			
6.10	(a)	And-25µm	9	35	0.2	0	0	0.5	580	N ₂
	(b)	Andina								
6.11	(a)	Andina	18	25	0.2	10	0	0.5	580	air
	(b)				H ₂ SO ₄					
6.12	(a)	Andina	9	35	0.2	0	0	0.5	580	O ₂
	(b)		18							O ₂
	(c)		27							O ₂
	(d)		9							N ₂
	(e)		18							N ₂
	(f)		27							N ₂
6.13,6.18-6.19	(a)	Andina	9	35	1	0	0	0.5	600	N ₂
	(b)				0.3	25				
	(c)				0.1	32				
	(d)				0.01	35				
6.16	(a)	CCHYP	18	35	0.2	0	0	0.5	600	N ₂
	(b)				0.03	17				
	(c)				0.01	18				
6.20-6.26		CCHYP	18	35	0.2	0	0	0.5	580	N ₂

6.2 The effect of temperature

Figure 6.1 and Figure 6.2 summarize the rate of copper dissolution obtained when Andina and CCHYP chalcopyrite concentrates are leached at various temperatures in 0.2 M HCl and 0.5 g L⁻¹ Cu(II) solutions under controlled potential within the potential window. The dissolution is approximately linear with time for the Andina concentrate in these chloride solutions although those for the CCHYP exhibit initial curvature due to the initial rapid leaching of secondary copper sulfides followed by slower chalcopyrite leaching.

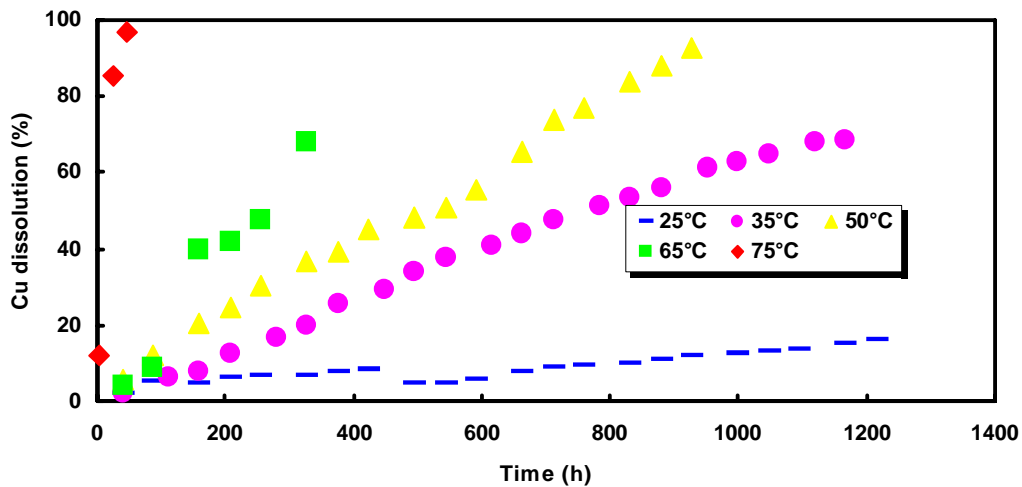


Figure 6.1 Effect of temperature on the rate of dissolution of copper from Andina chalcopyrite concentrate in 0.2 M HCl and 0.5 g L⁻¹ Cu(II) under controlled potential of 580 mV.

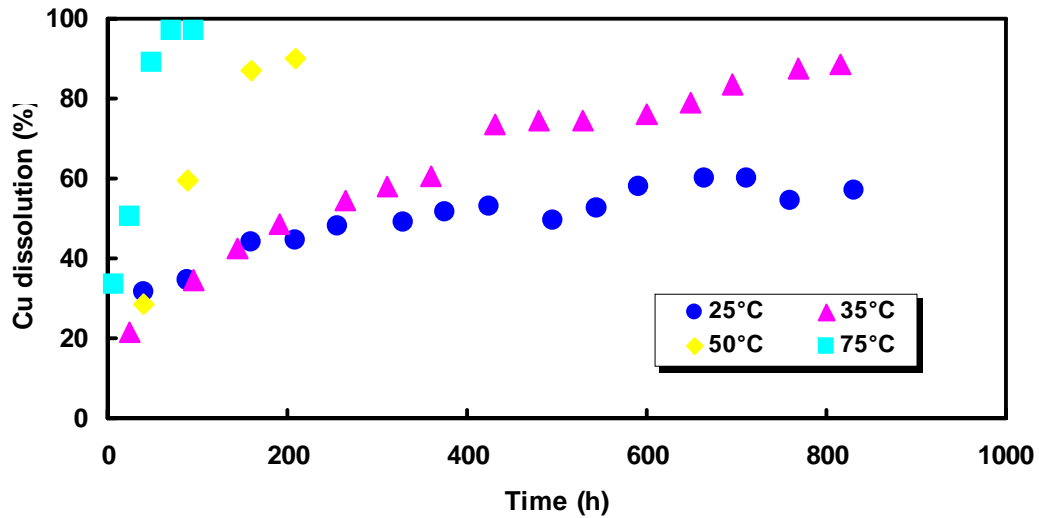


Figure 6.2 Effect of temperature on the rate of dissolution of copper from CCHYP concentrate in 0.2 M HCl, 0.5 g/L Cu(II) and 50 g L⁻¹ chloride ions at a controlled potential of 580 mV.

To obtain a value for the activation of energy for the dissolution of Andina and CCHYP chalcopyrite samples, leach rate constants were calculated from the slope of each linear section. The resulting rate constants are presented in Tables 6.2 and 6.3 for the Andina and CCHYP chalcopyrite samples respectively.

Table 6.2 Rate constants as a function of temperature for leaching of 25-38 μm Andina chalcopyrite concentrate

Temperature, $^{\circ}\text{C}$	10^{-4} Rate, %Cu s^{-1}
25	0.036
35	0.16
50	0.28
65	0.58
75	5.6

Table 6.3 Rate constants as a function of temperature for leaching of -38 μm of CCHYP chalcopyrite concentrate

Temperature, $^{\circ}\text{C}$	10^{-4} Rate, %Cu s^{-1}
25	0.079
35	0.12
50	1.2
75	3.7

Figures 6.3 and 6.4 show the Arrhenius plots obtained using the linear rate constants for the Andina and CCHYP chalcopyrite samples respectively. Both plots are essentially linear over the range of temperature employed with an apparent activation of energy of 73 kJ mole^{-1} for Andina and 71 kJ mole^{-1} for CCHYP. It should be point out these values of the activation energy correspond to the particular concentrate sample and not to pure chalcopyrite. The difference between these and published values may be due to the difference in the quantities of secondary copper mineralization which according Dutrizac (1981) can affect the rate of leaching, especially at low temperatures where the total dissolution is small. These high values of the activation energy confirm that the rate of the

reaction is controlled by the rate of the chemical/electrochemical reaction under the conditions of these experiments.

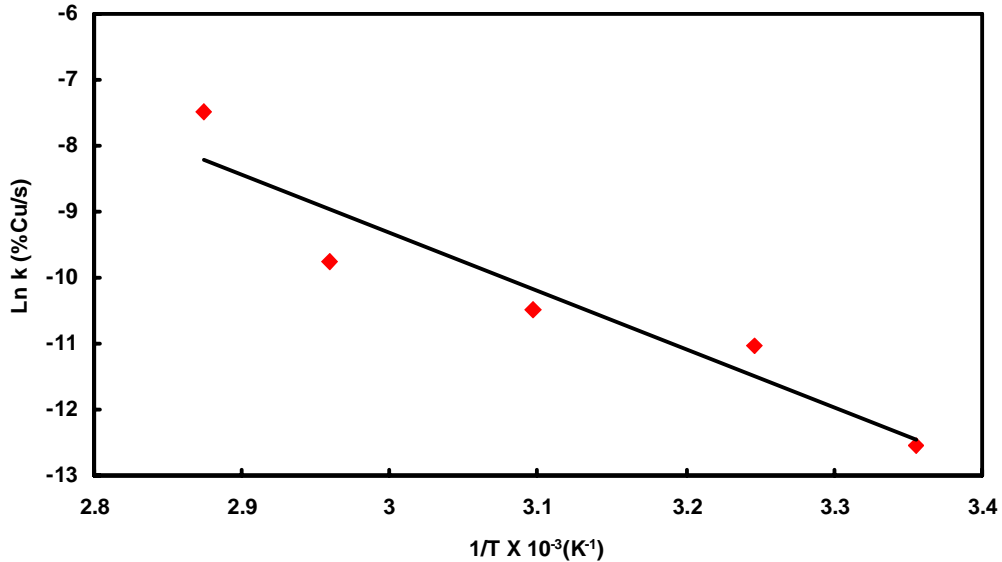


Figure 6.3 Arrhenius plot for the dissolution of chalcopyrite from Andina 25-38 μm concentrate between 25 and 65 $^{\circ}\text{C}$ under standard conditions

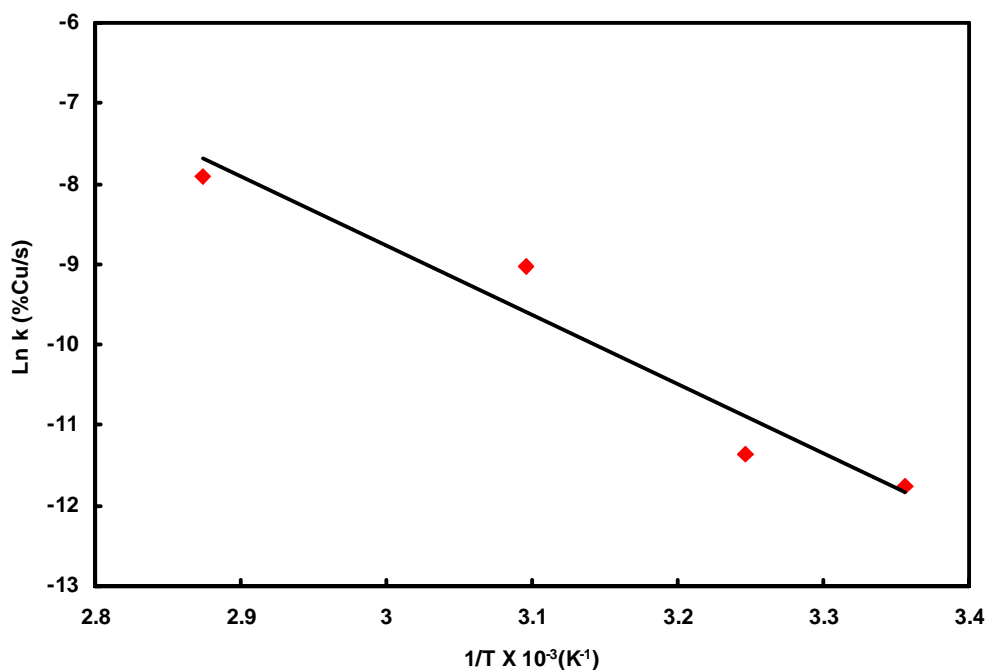


Figure 6.4 Arrhenius plot for the dissolution of chalcopyrite from CCHYP -38 μm concentrate between 25 and 65 $^{\circ}\text{C}$ under standard conditions

6.3 The effect of the concentration of chloride

The leaching rate of chalcopyrite was studied by using solutions containing 0.2 M HCl, 0.5 g L^{-1} Cu(II) and different sodium chloride concentrations at 35 $^{\circ}\text{C}$ for the Andina and CCHYP concentrates at controlled potentials within the potential window. Figures 6.5 and Figure 6.6 show the percentage of copper leached from Andina and CCHYP concentrates respectively. An increase in the concentration of chloride ions does not appear to affect the leaching rate of copper under the present leaching conditions. These results confirm preliminary results reported in Chapter 4 for which it was found that the presence of

chloride ions is necessary to improve the leaching kinetics but that high concentrations of chloride are not essential under the conditions studied.

It should be noted that data quoted in the literature review showing the effect of chloride on the rate of leaching of chalcopyrite were carried under different conditions of higher temperature and different acid media in the absence of controlled potential. Therefore, a comparison between these results and those of the present study is difficult. However, most studies agree that higher concentrations of chloride ions do not result in a higher copper extraction (Dutrizac, 1978; Hirato et al., 1987; Lu et al., 2000a; Wilson and Fisher, 1981).

Some authors have observed that the presence of sodium chloride during leaching resulted in the precipitation of iron as natrojarosite and thus, a lower iron recovery can be expected under these conditions. In the present study, the extent of iron dissolution is similar to that of copper except at higher pH values. Thus, the use of a low potential during the leach results in a low iron(III) concentration which would prevent jarosite formation in the present study.

Although a high chloride concentration does not increase the dissolution of chalcopyrite under the present conditions, chloride ions play a very important role in achieving a high leaching rate. Some of these factors are:

- In the presence of excess chloride ions the pH is maintained for longer at the desired value as shown in Figure 6.7.

- In the presence of chloride, copper(I) is more strongly complexed than copper(II) thus increasing the formal potential of the couple. In addition, the rate of oxidation of Cu(I) to Cu(II) by dissolved oxygen is reduced at high chloride concentrations thus facilitating control of the potential.
- Addition of chloride reduces the tendency for chalcopyrite passivation increasing the surface area and porosity of the product layer (Section 6.9).

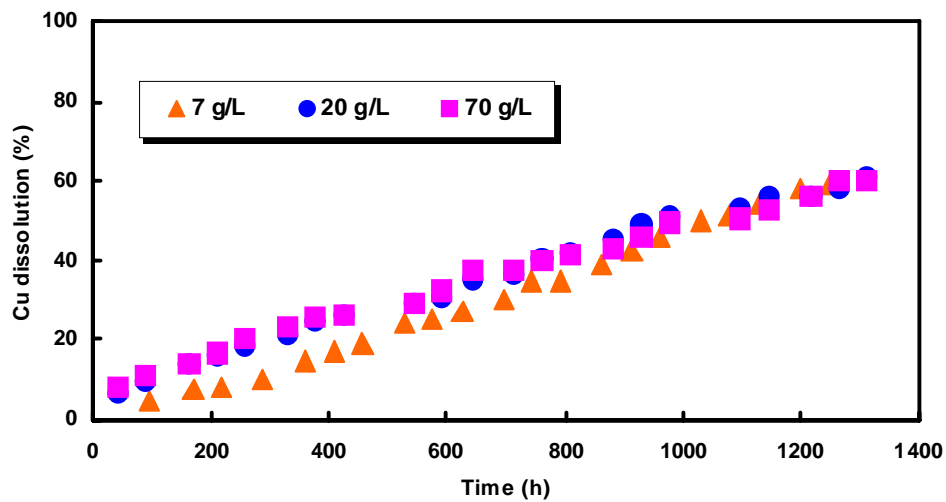


Figure 6.5 Effect of NaCl concentration on copper extraction from +25-38 μm Andina concentrate in 0.2 M HCl, $0.5 \text{ g L}^{-1} \text{ Cu}^{2+}$ at 35 °C.

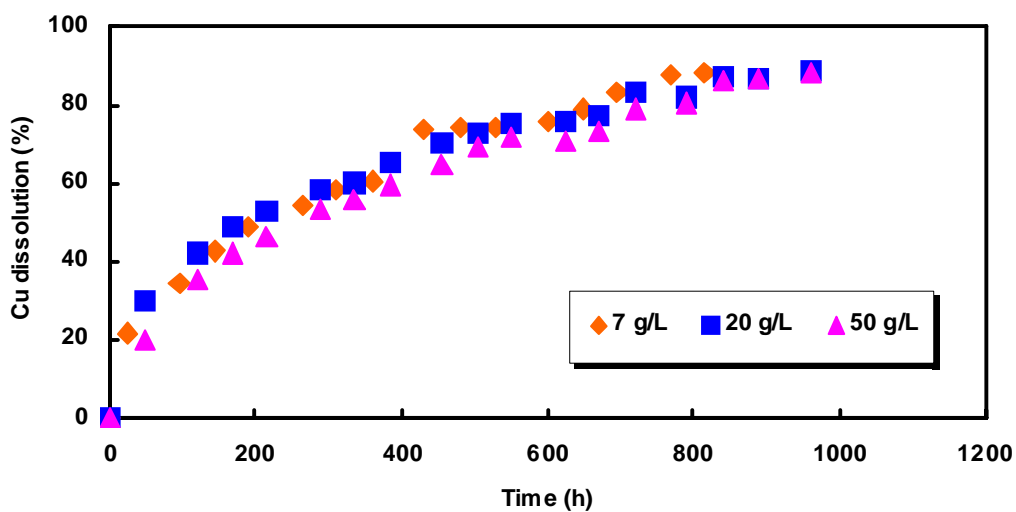


Figure 6.6 Effect of NaCl concentration on copper extraction from -38 μm CCHYP concentrate in 0.2 M HCl, 0.5 g L⁻¹ Cu²⁺ at 35 °C.

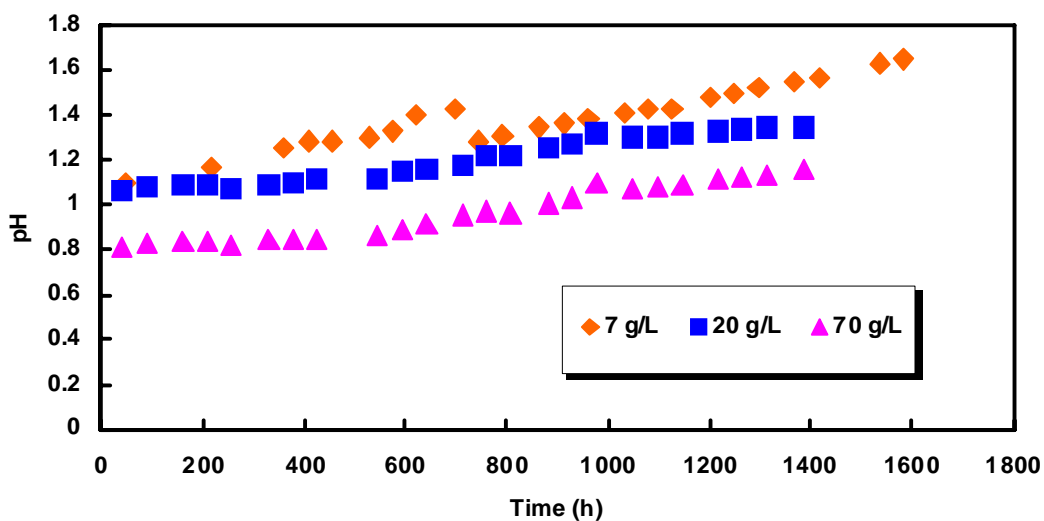


Figure 6.7 Variation of pH during dissolution of Andina concentrate in a solution containing 0.2 M HCl, 0.5 g L⁻¹ Cu²⁺ at 35 °C with various chloride concentrations.

6.4 *The effect of cupric ion concentration*

To examine the effect of the initial cupric ion concentration on the rate of leaching, three experiments were carried out using 0.2 M HCl solution with various initial concentrations of cupric ions with controlled potential between 560 and 620 mV. Figure 6.8 summarizes the leaching curves obtained at 35 °C. All the curves are essentially linear and the leaching rate does not increase with increasing cupric ion concentration. However, the presence of a small amount of cupric ion is important in order to achieve a high chalcopyrite leaching rate as was shown in Chapter 4 (Figure 4.12), but concentrations above about 0.1 g/L do not increase the rate of dissolution. These results are different from those found in literature, but once again, conditions are very different from those used in the current experiments. At higher temperatures, and chloride concentrations the rate could be affected by increasing cupric ions concentrations.

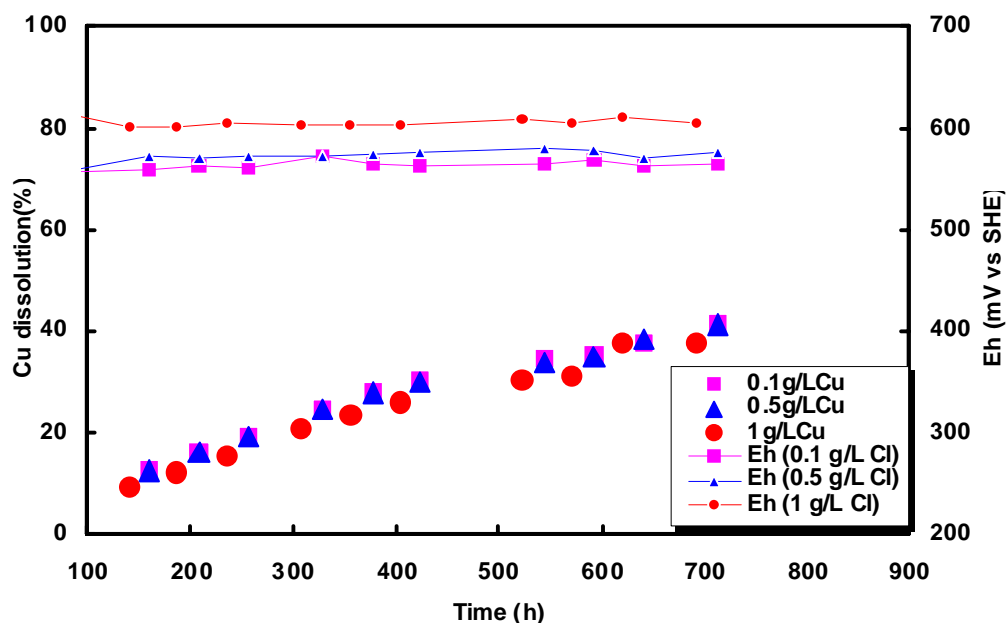


Figure 6.8 Effect of initial cupric ion concentration on copper dissolution from 25 - 38 μm Andina concentrate in 0.2 M HCl at 35 °C.

6.5 The effect of the iron(II) concentration

The effect of the iron(II) concentration on the leaching rate of chalcopyrite was examined in 0.2 M HCl solution containing 0.5 g L⁻¹ Cu(II) under controlled potential at 35 °C. The results obtained are shown in Figure 6.9. For reference, the result obtained under standard conditions without addition of ferrous ions is included. As it is obvious in this Figure, the addition of ferrous ions causes the rate to fall appreciably. The addition of 1 M ferrous ions together with ferric ions to achieve a potential in the relevant region, also results in a decrease in rate.

The present findings support the results of Dutrizac, and Jones and Peters (1976) in sulfate media but not the results obtained by the same authors in chloride media for which they reported that the rate of leaching of chalcopyrite was unaffected by increasing amounts of ferrous ions. In addition, the present results do not support the Japanese model (Hiroyoshi et al., 2000) in which an intermediate, suggested as Cu_2S , is formed in the low potential region by reduction of chalcopyrite by ferrous ions in the presence of copper ions.



In terms of this mechanism, the intermediate Cu_2S is more rapidly oxidized than chalcopyrite and this causes the enhanced copper extraction in the presence of cupric and ferrous ions.

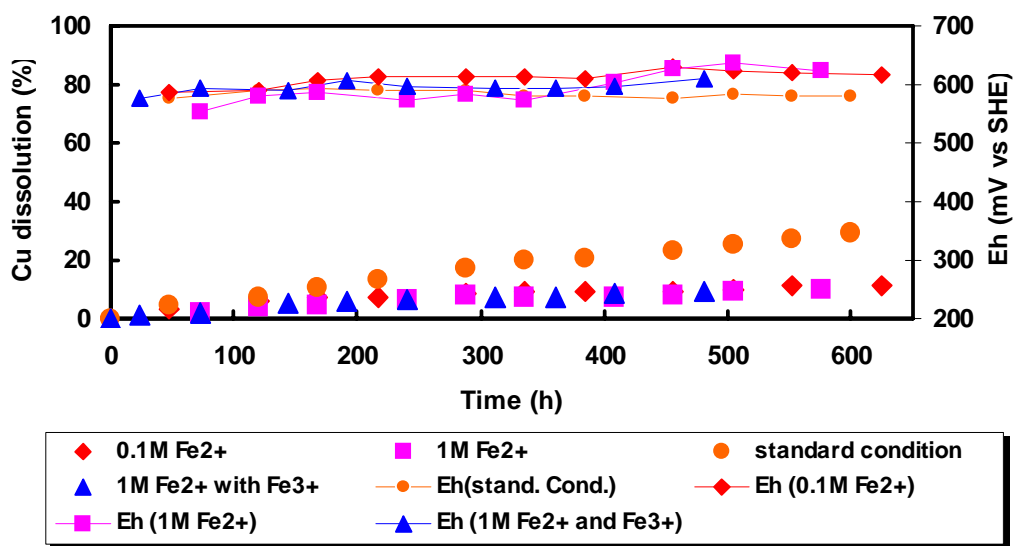


Figure 6.9 Effect of ferrous ion concentration on the dissolution of copper from 25-38 μm Andina concentrate in 0.2 M HCl at 35 °C.

6.6 The effect of particle size

It is generally accepted that fine grinding promotes more rapid dissolution of chalcopyrite and that the rate of chalcopyrite leaching increases in direct proportion to the initial surface area. However, as pointed out by (Dutrizac, 1981) problems with obtaining a well characterized surface area have resulted in erroneously reported results that the rate of dissolution is independent of surface area. In order to confirm this effect, two size fractions of the Andina chalcopyrite concentrate were leached at 35 °C in 0.2 M HCl and 0.5 g L⁻¹ Cu(II) under controlled potential conditions. Figure 6.10 shows clearly that the rate increases as the particle size decreases. Table 6.4 shows the surface areas of the chalcopyrite particles as obtained from the MLA analysis of the particular size fractions and the leaching rates of the different chalcopyrite concentrates samples studied.

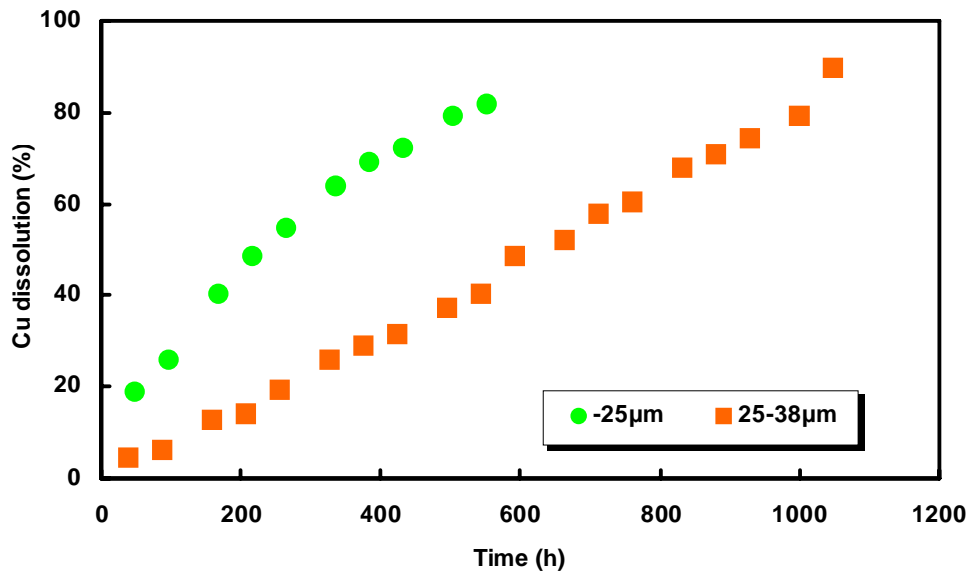


Figure 6.10 Leaching curves for the dissolution of two size fractions of Andina chalcopyrite sample in chloride media at 35 °C.

Table 6.4 Initial surface area of chalcopyrite present in each concentrate

Sample	Particle size	Surface area cm ²	Initial Mass, g	Rate mol cm ⁻² ·s ⁻¹
Andina	25-38 μm	6586	7.425	1.19E-12
PQS2	-38 μm	9239	7.04	1.19E-12
Spence	25-38 μm	2579	2.466	2.0E-10
CCHYP	-38 μm	10025	5.9364	6.27E-13
Pinto Valley (PV)	-38 μm	11178	9.16	4.43E-16

Clearly, it observed that, with the exception of the Pinto Valley concentrate which behaved anomalously, roughly similar rates were obtained.

6.7 The effect of the type of agitation

There is a common agreement (Burkin, 2001) that the rate of dissolution in either chloride or sulfate solutions is not promoted by increased agitation. This is the case because the rate of dissolution is not controlled by mass transfer across the liquid boundary layer (Dutrizac, 1981). Even though sufficient agitation must be provided to keep the particles in suspension and prevent agglomeration and inhomogeneities in solution, further agitation seems to be without effect. However, the type of agitation can affect the kinetics as shown in Figure 6.11, which summarizes the results obtained with two different types of agitation during the leaching of Andina chalcopyrite concentrate in H₂SO₄ at pH 0.5 with 10 g L⁻¹ of NaCl. It is obvious that under the same leaching conditions, the rate is much higher when the leach reactor is magnetically agitated than when is it mechanically agitated with a titanium impellor. These results confirm that abrasion or breakdown of the chalcopyrite

concentrate particles is occurring in the magnetically stirred reactor with an apparent greater rate of dissolution.

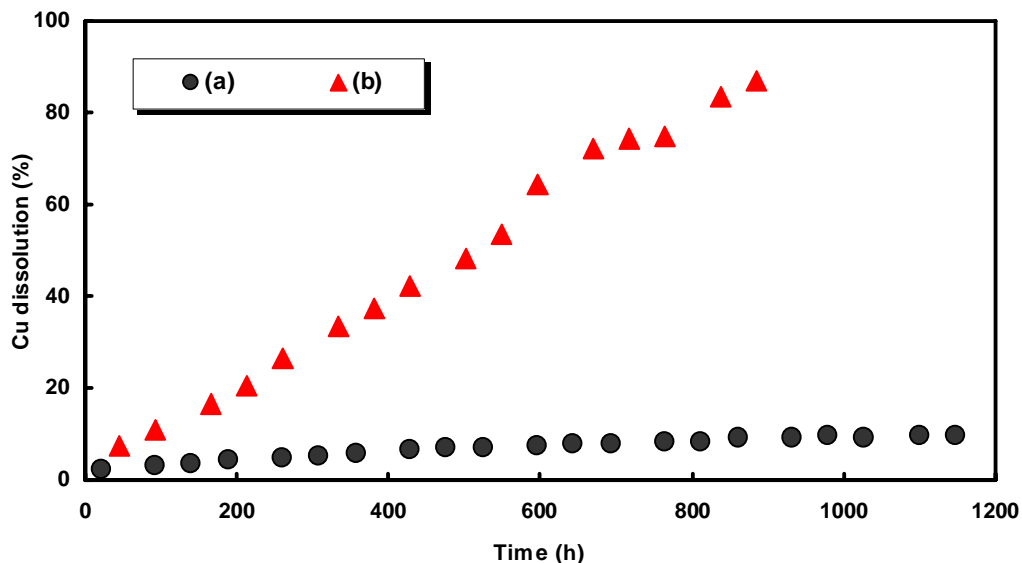


Figure 6.11 Effect of the type of agitation on the rate of dissolution of Andina concentrate . a) Instrumented reactor with Ti impellor, b) Magnetically stirred.

6.8 The effect of pulp density

The effect of pulp density was studied using three different amounts of 25-38 μm Andina chalcopryrite concentrate under standard conditions of 0.2 M HCl, 0.5 g L⁻¹ Cu(II) at 35 °C under controlled potential using either oxygen or nitrogen sparging for control. Figure 6.12 illustrates the leaching rate curves obtained at 35 °C in the solutions containing increasing pulp density. The leaching curves of all pulp densities studied are essentially linear and there is no clear trend with increasing pulp density. Control of the potential was found to be

considerably easier at the higher pulp densities due to the increased rate of consumption of dissolved oxygen.

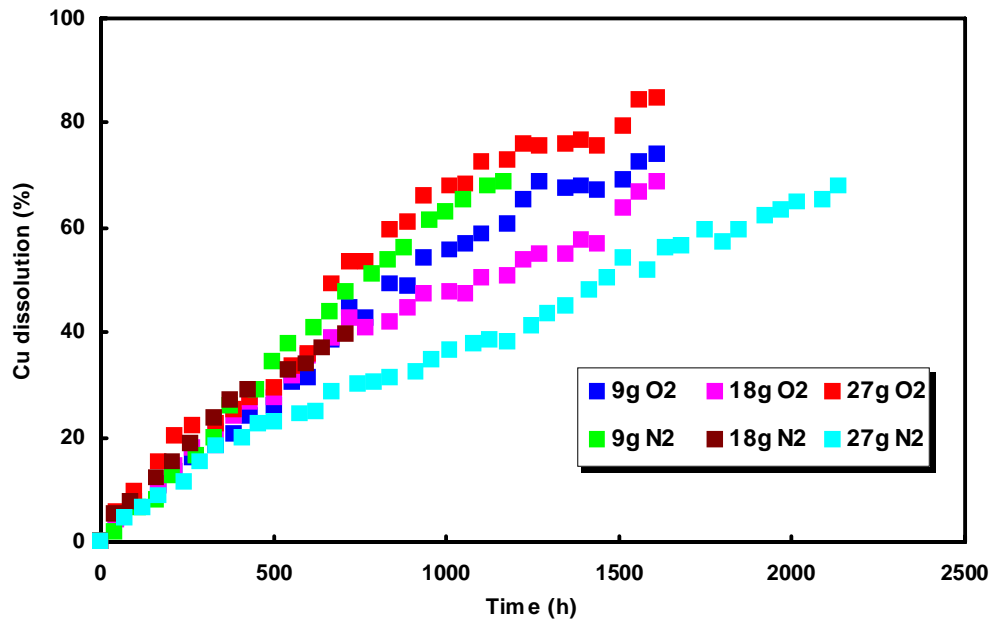


Figure 6.12 Effect of increasing pulp density on the rate of dissolution of Andina concentrate.

6.9 The effect of pH

To investigate the effect of pH on the rate of dissolution, leaching tests were carried out with the Andina and CCHYP concentrates at 35 °C under aerated conditions. The initial pH was adjusted with known amounts of hydrochloric acid and sodium chloride in the presence of 0.5 g L⁻¹ of copper ions. As is obvious in Figure 6.13 and 6.16, approximately linear rates were obtained which appear to increase with increasing pH for the Andina concentrate but are not affected by the pH for the CCHYP concentrate. It should be emphasized that

during dissolution of the Andina concentrate at low pH values (Figure 6.14) it was very difficult to control the potential in the desired window (560-620 mV) and it was necessary to introduce nitrogen gas into the reactors to decrease the potential. Small increases in the dissolved oxygen concentration resulted in significant increases in the potential to values above those desired as shown in Fig. 6.15. This sensitivity to small changes in dissolved oxygen makes control of the potential more difficult and is due to the enhanced rate of oxidation of copper(I) and iron(II) at lower pH values. The periodic slower rates of dissolution at the lower pH values shown in Fig. 6.13 can be correlated with periods of high potential and low dissolved oxygen concentration as shown in Fig. 6.15. On the other hand, according to Dutrizac (1981), low acidity (<0.1 M HCl) must be avoided to prevent iron hydrolysis and precipitation on the mineral surface. In the current experiments, visible precipitation products were observed at pH 2 as shown by the low dissolution of iron in Fig. 6.17. Despite this precipitation the dissolution of copper was not affected and almost 95% copper dissolution was obtained.

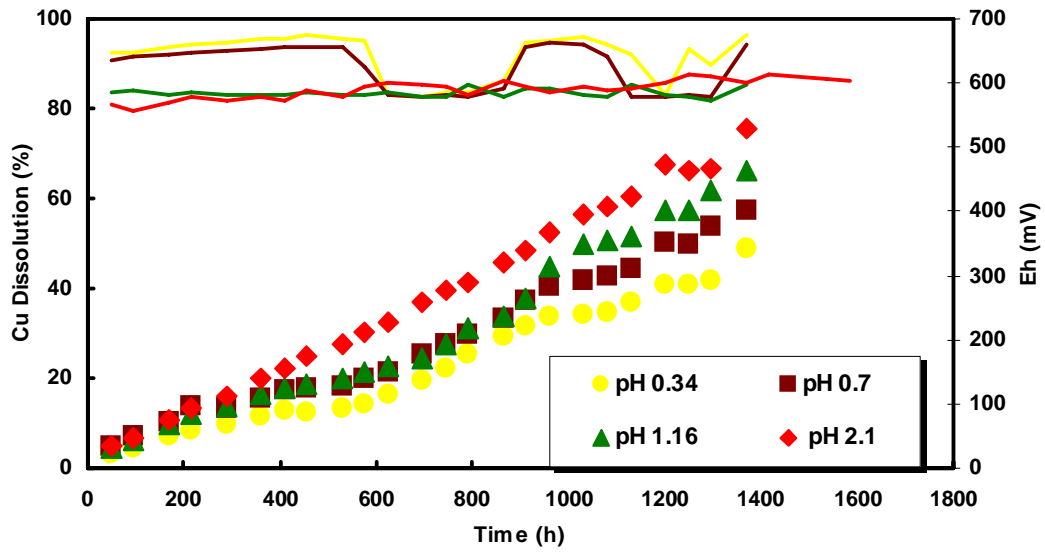


Figure 6.13 The effect of pH on the rate of dissolution of Andina chalcopyrite concentrate.

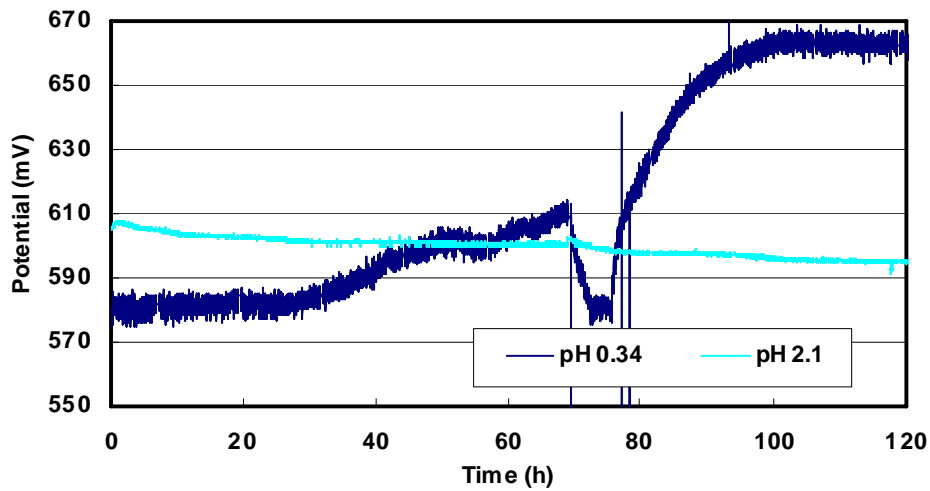


Figure 6.14 The effect of pH on the solution potential during the initial stage of dissolution of Andina concentrate at low and high pH

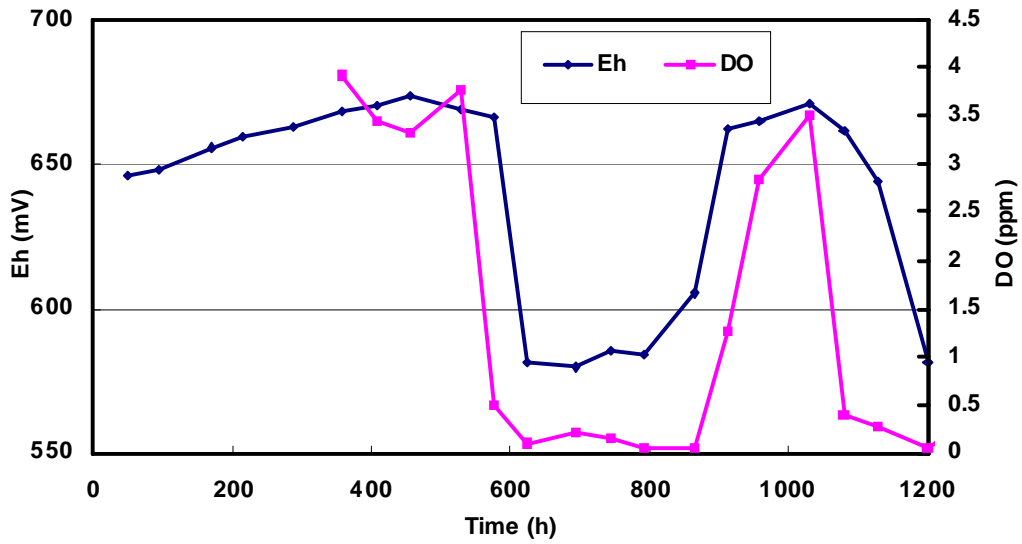


Figure 6.15 Sensitivity of potential to small change of dissolved oxygen during the leaching of Andina chalcopyrite concentrate at low pH (pH 0.34).

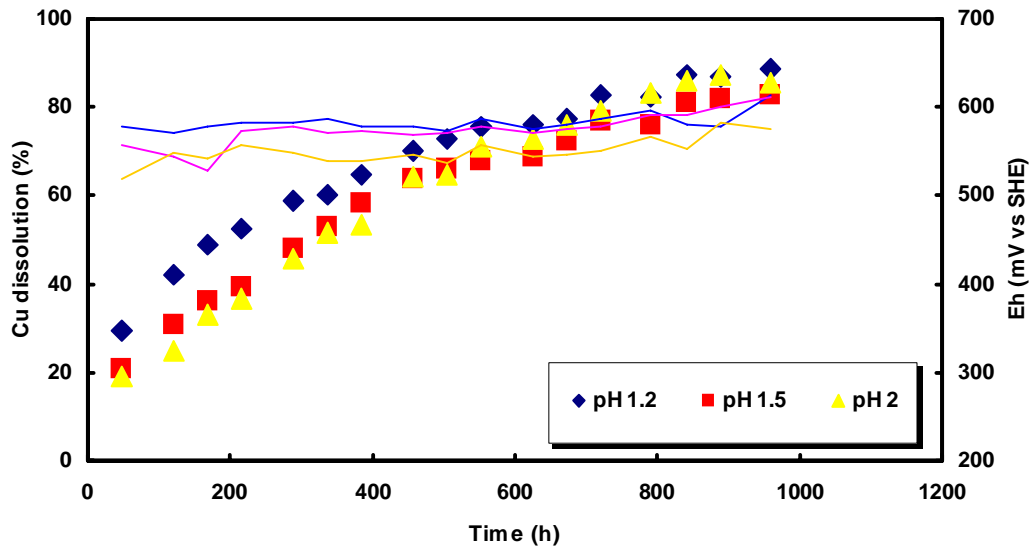


Figure 6.16 The effect of pH on the rate of dissolution of CCHYP chalcopyrite concentrate.

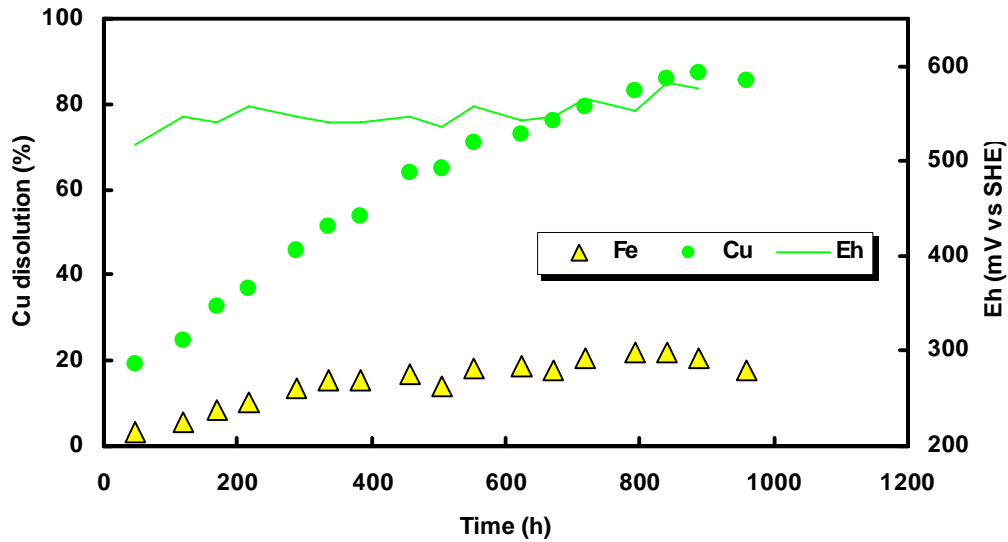


Figure 6.17 Comparison of the rates of dissolution of copper and iron from the CCHYP concentrate at pH 2. Conditions as in Fig. 6.16.

At the end of each leaching experiment, all residues were collected, washed, filtered, dried and sent to the Newcastle Technology Centre for mineralogical analysis. The results in Figure 6.18 show that the chalcopyrite concentration in the residue decreases as the pH of the solution increases while the amount of elemental sulfur increases with increasing pH. As shown in Fig. 6.19, most of the sulfur in the residues occurs as isolated globules with small amounts associated with both chalcopyrite and pyrite. At the higher pH values, the amount of elemental sulfur associated with pyrite and chalcopyrite increases somewhat.

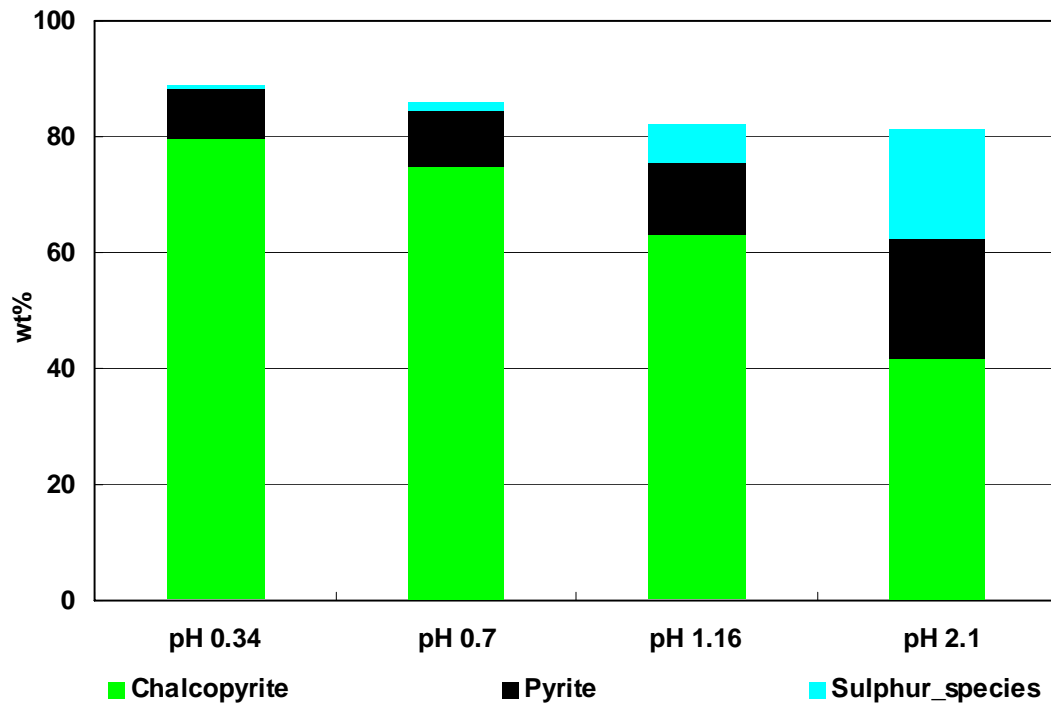


Figure 6.18 Effect of pH on the modal mineralogy of the residues from the dissolution of Andina concentrate at different pH values.

Figure 6.19 also shows the effect of increased pulp density at high pH on the mineralogy of the residue which shows increased association with chalcopyrite and pyrite. The residue contained significant amounts of an iron hydroxide, which was apparent from its red/orange color and the presence of 5% of iron oxides.

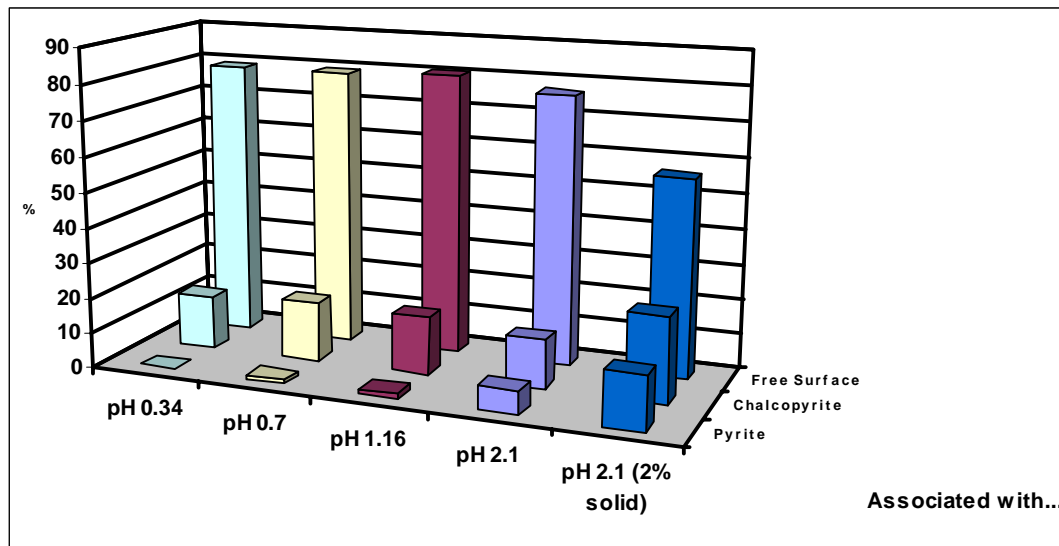


Figure 6.19 Department of sulfur in the residues from dissolution at various pH values.

6.10 Leaching profiles for the copper sulfide minerals

Most authors agree that the slow leaching kinetics of chalcopyrite is due to the formation of a film which builds up on the surface of the mineral preventing further dissolution. Although the dissolution of CuFeS_2 has been investigated for many years, the nature of the passivation film is still the subject of much debate. The major solid product formed during leaching is elemental sulfur that was often considered responsible for the slow transfer of electrons or/and ions across the solid-liquid during oxidative leaching (Dutrizac, 1981). However, this does not necessarily imply that sulfur causes passivation during the initial stages of mineral oxidation as many authors have found that it precipitates in chloride media as large crystals allowing the reactants to penetrate the sulfur layer and making the surface available for reaction (Dutrizac, 1990). Others postulate that the passivation

phenomenon is due, at least in part, to a copper species such as CuS or CuS₂. In the case of CuS, it has been suggested that it can dissolve and reform in the pores of the elemental sulfur and thus inhibit the reaction at the chalcopyrite surface (Jones and Peters, 1976 and Parker et al., 1981). Parker et al. (1981) postulated that the cause of the slow kinetics was the formation of a gradually thickening layer of a copper-rich species on the surface and suggested that the species might be a copper polysulfide, CuS_x. Recently Stott (2000) postulated that significant precipitation of jarosite on the minerals surface during leaching of chalcopyrite coincided with a decrease in the rate of dissolution.

In order to gain an insight into the dissolution profiles for each of the copper minerals present in a concentrate and whether or not copper dissolves preferentially from any minerals present in the material, the CCHYP concentrate was leached over an extended period under controlled potential conditions in hydrochloric acid. At intervals of approximately 100 h, solid sample were taken, filtered, washed and dried before mineralogical analysis.

According to data from the MLA analyses as shown in Table 6.4, the concentration of copper decreased, the iron concentration remained approximately constant while the amount of elemental sulfur increased. The corresponding modal mineralogy is provided in Table 6.5, with the head sample used as feed. Simplified modal results are presented in terms of weight percent for each mineral grouping by sample. The major copper mineral present in the CCHYP concentrate is chalcopyrite with approximately similar amounts of pyrite. According to the results in Table 6.5, pyrite clearly did not leach which was

expected given the low potential of the leach solution. Copper deportment in the various minerals was calculated using the quartz content as an indicator of mass loss during dissolution assuming that the silica did not dissolve under the mildly acidic conditions.

Table 6.5 Chemical assay data (%) obtained from MLA analyses for Cu, Fe S and Si in CCHYP concentrate samples taken during leaching with 0.2 M HCl-0.5 g L⁻¹ Cu(II) at 35 °C at a controlled potential of 580 mV.

	Head	144 h	264 h	432 h	528 h	696 h	816 h
Cu	14.7	12	10.3	6.4	5.8	5.5	3.5
Fe	23.8	24.7	24.6	22.3	24.1	24.4	28.9
S	26.8	29.2	29.2	26.3	28.2	27.7	32.7
Si	5.9	9.2	10.1	12.6	11.7	11.7	10.1

Table 6.6 Modal mineralogy analyses (weight %) for CCHYP concentrate samples during leaching in 0.2 M HCl-0.5 g L⁻¹ Cu(II) at 35 °C at a controlled potential of 580 mV.

Mineral	Head	144 h	264 h	432 h	528 h	696 h	816 h
Chalcopyrite	32.98	26.47	23.17	13.77	12.14	12.34	8.04
Chalcocite	2.49	0.034	0	0	0	0	0
Covellite	5.65	1.33	4.81	0.23	0.24	0.08	0.04
Bornite	2.68	1.08	3.45	0.13	0.13	0.04	0.03
Other copper	1.04	4.64	14.3	6.08	5.52	4.61	3.29
Pyrite	34.33	27.54	0	29.31	34.6	33.32	45.60
Quartz	5.33	5.59	0	7.24	6.99	7.15	7.18
Other gangue	15.49	33.02	0	42.51	39.5	41.31	34.98
Sulfur	0	0.29	0	0.72	0.87	1.16	0.84
Total	100	100	100	100	100	100	99.99

Table 6.6 shows that the major content of copper in the solid sample is present as chalcopyrite and as the leaching time increases, the copper content in covellite, chalcocite and bornite could be expected to decrease. The dissolution of copper sulfides minerals also results in formation of element sulfur in the solid samples as shown in Table 6.6.

Figure 6.20 shows the dissolution of copper and iron during leaching of the CCHYP concentrate in the experiment from which the above samples were taken.

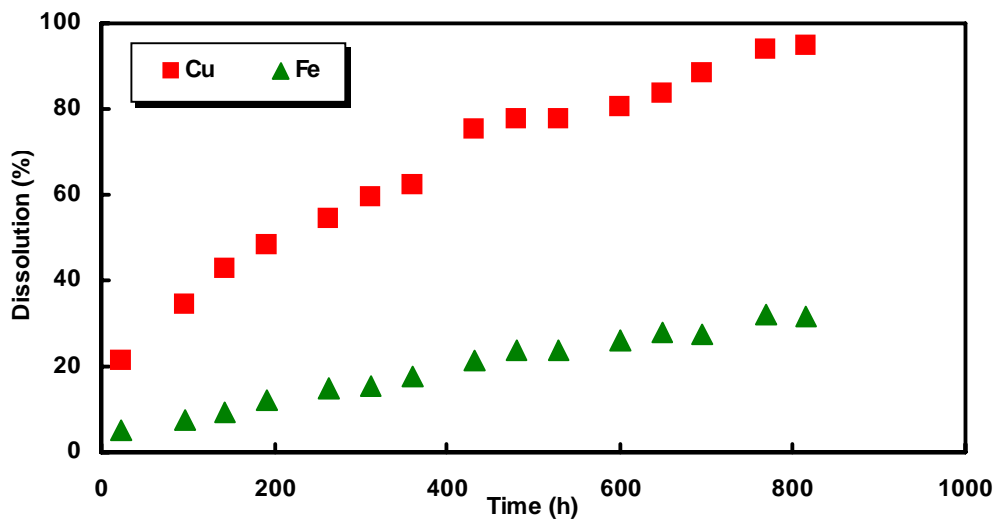


Figure 6.20 Dissolution of copper and iron from CCHYP concentrate leached under standard conditions at a controlled potential of 580 mV at 35 °C.

Mineralogical data from the feed and residues can also be used to estimate the extent of dissolution of each copper mineral using the quartz content as an indicator of mass loss during dissolution and the results are shown in Figure 6.21. It is apparent that the small amount of chalcocite leaches very rapidly, followed by covellite and bornite while, as expected, chalcopyrite leaching is slow. However, of considerable significance is the observation that chalcopyrite is leaching during the period of dissolution of the other

minerals with about 50% of the chalcopyrite dissolved in the time required to leach 90% of the other sulfides.

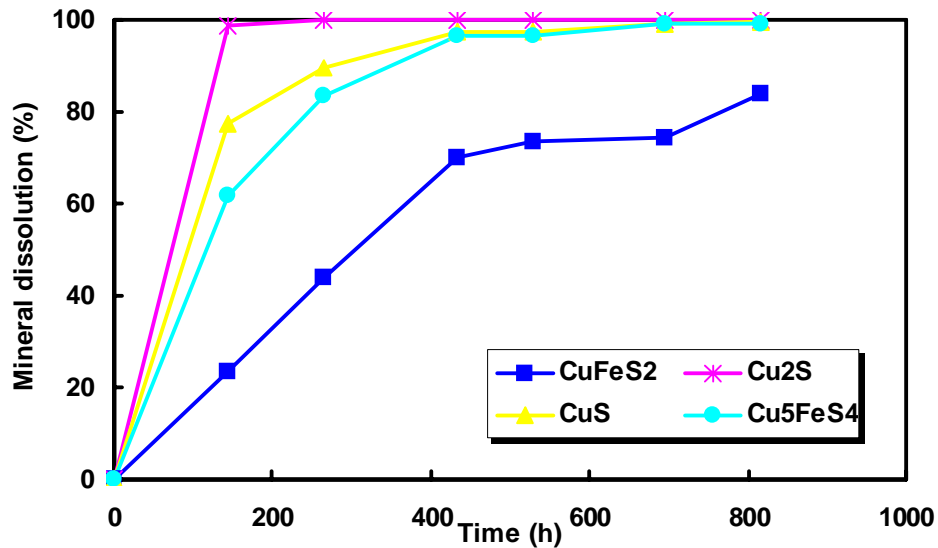


Figure 6.21 Mineral dissolution from CCHYP concentrate leached under standard conditions.

Results of dissolution of copper and iron obtained using chemical analysis of copper and iron in each solid sample from the MLA data were compared with results of dissolution using AAS analyses of solution samples. The comparative results presented in Figure 6.22 and Figure 6.23 show acceptable similarities in the results.

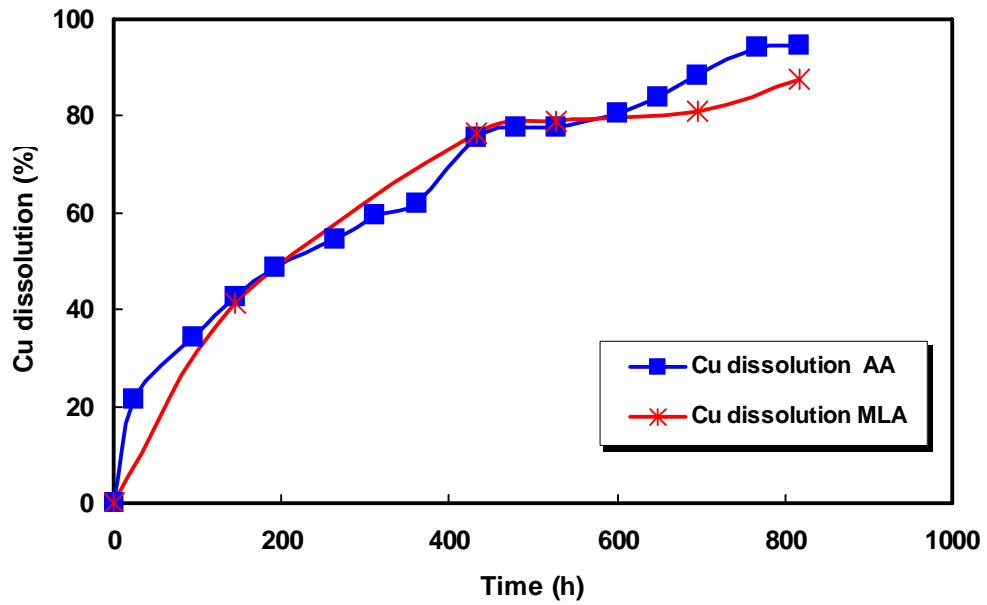


Figure 6.22 Dissolution of copper obtained from MLA and solution analyses.

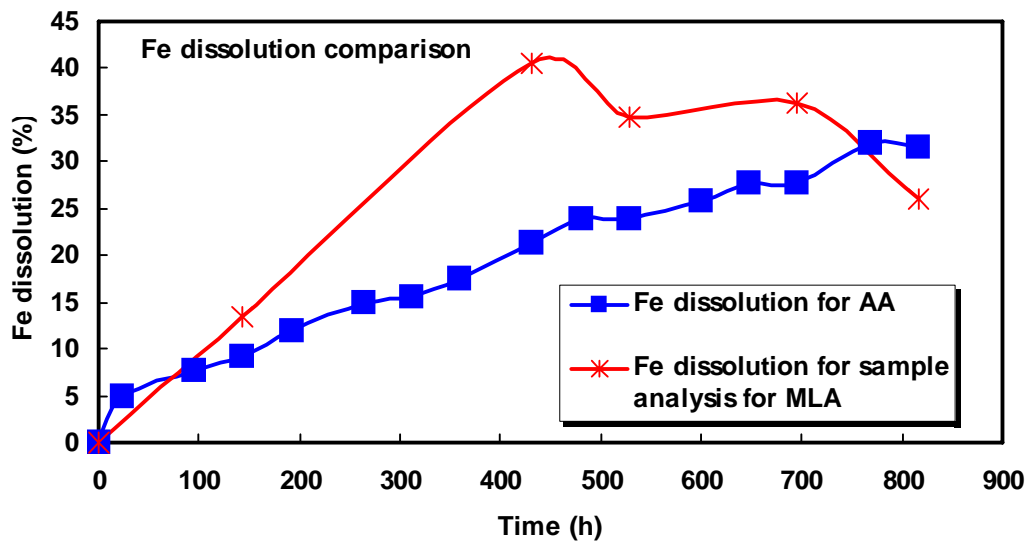


Figure 6.23 Dissolution of iron obtained from MLA and solution analyses

6.10.1 Mineralogical association of sulfur during leaching

Analysis of the MLA data shows (Figure 6.24) the sulfur association with the other sulfide minerals present in the concentrate. A free surface is described as the percentage of the sulfur boundary that is in touch with background and a high result denotes either extensive liberation or rimming. After 144 h of leaching most of the sulfur was liberated and as the leaching time increased small amounts of sulfur is associated with chalcopyrite and pyrite. However, at the end of the leaching period, most of the sulfur is free or associated with pyrite. Chalcopyrite is mainly liberated with a small extent of association with pyrite and bornite as shown in Figure 6.25.

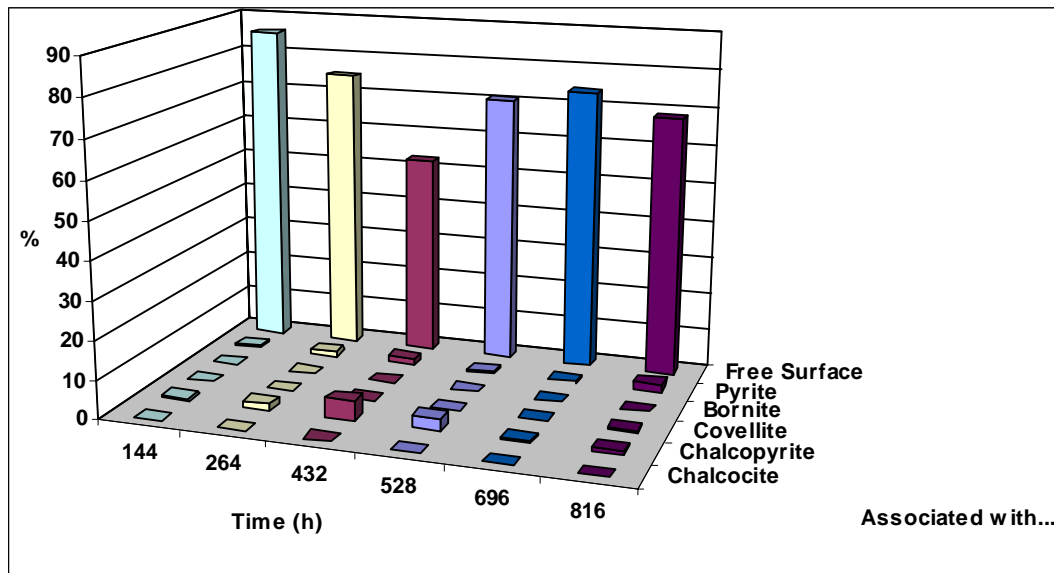


Figure 6.24 Sulfur association with other sulfides during leaching of CCHYP concentrate.

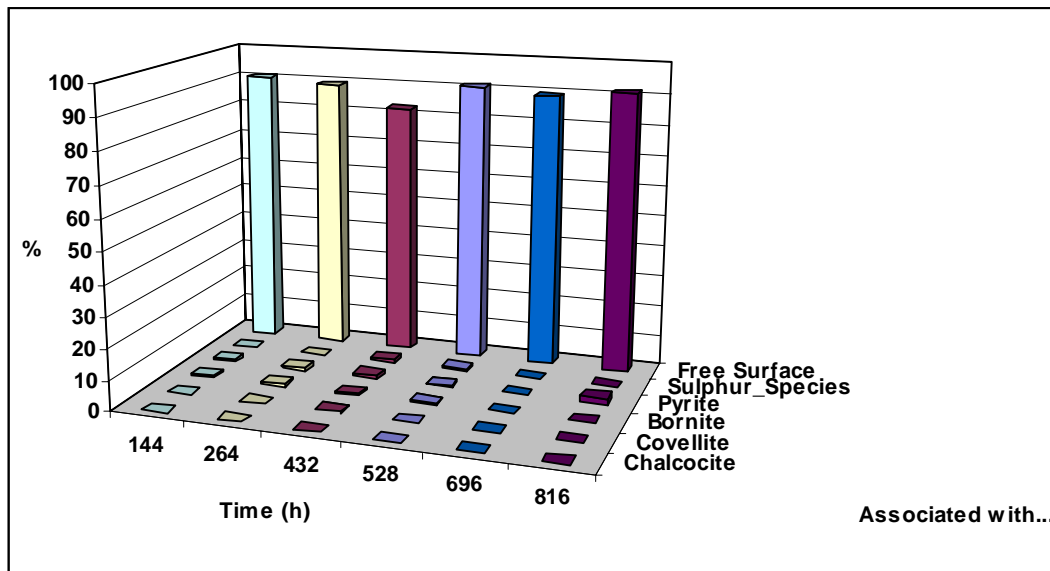


Figure 6.25 Chalcocite association with other sulfides during leaching of CCHYP concentrate.

The MLA results showed that most of the chalcocite in the head sample is liberated. After 144 h of leaching it is possible to optically detect unleached covellite and chalcocite as shown in Figure 6.26. It is clear from the partial mineral map of the sample after 144 h shown in Figure 6.27 that most of the chalcocite grains are liberated with a few associated with sulfur.

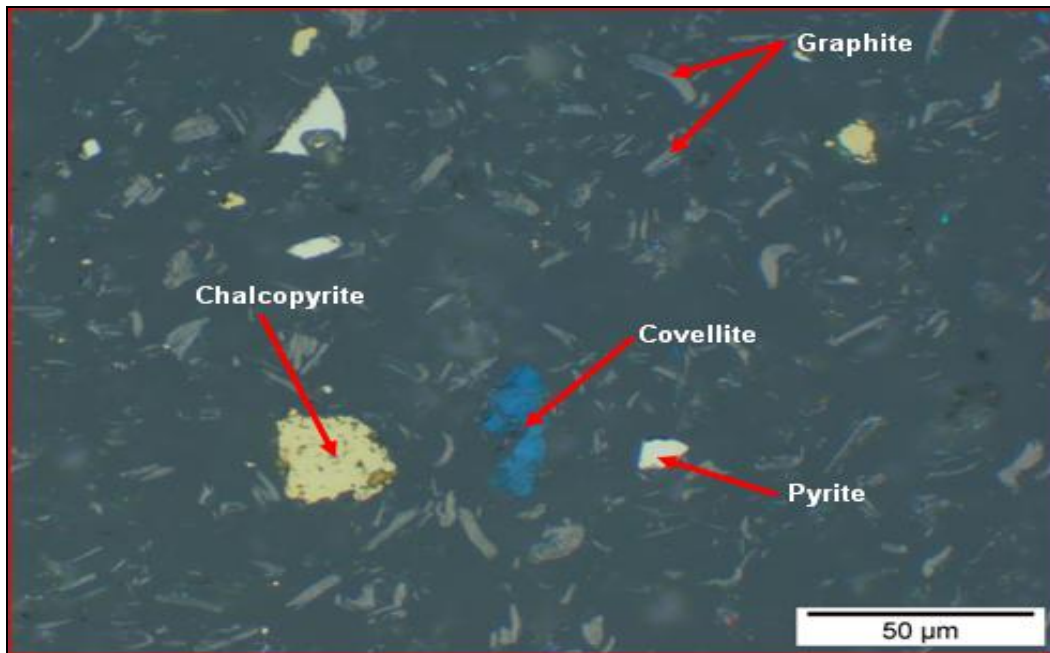


Figure 6.26 Optical micrograph of CCHYP concentrate sample after 144 h of leaching.

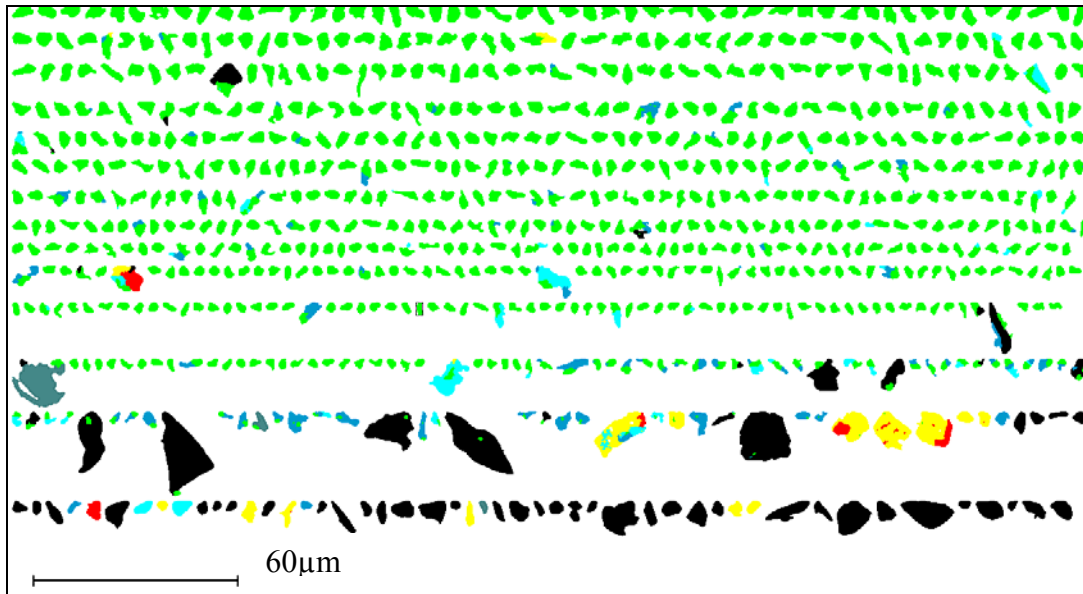


Figure 6.27 Partial mineral map of CCHYP concentrate after 144h of leaching under standard conditions chalcopyrite (bright green), pyrite (black), covellite (red), bornite (aqua), enargite (yellow).

After 264 h of leaching most of the chalcopyrite appears to be as shown in Figure 6.29 with no noticeable sulfur rims. Figure 6.28 shows clearly a grain of chalcopyrite completely surrounded by covellite and elemental sulfur. This observation is similar to those observed by Jones and Peter (1976) and Parker et al. (1981). According to these authors, blue CuS formed on the surface of chalcopyrite may be as a product of reaction of CuCl_2^- with sulfur (eq. (6.1)) or a product of non-oxidative processes (eq. (6.2) and eq.(6.3)).



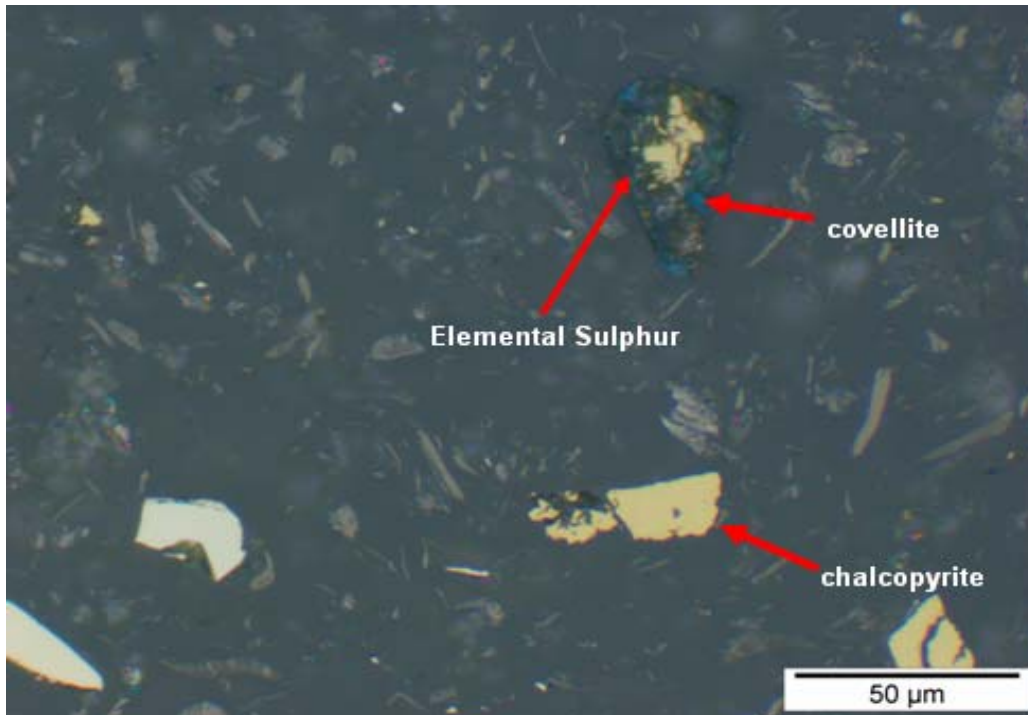


Figure 6.28 Optical micrograph of CCHYP concentrate sample after 264 h of leaching.

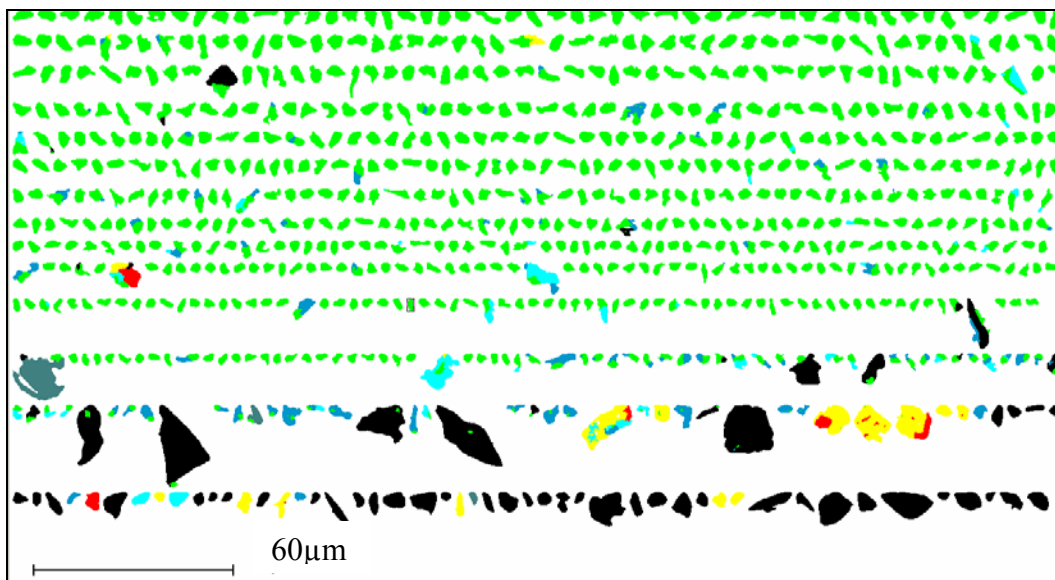


Figure 6.29 Partial mineral map showing liberated, uncoated chalcopyrite particles after 264 h of dissolution. Chalcopyrite (bright green), pyrite (black), covellite (red), bornite(aqua), enargite (yellow).

After 432 h of dissolution small well formed globular grains of sulfur and unleached pyrite can be observed, Fig. 6.30. Most of chalcopyrite grains are liberated and free of elemental sulfur coatings as shown in Figure 6.31.

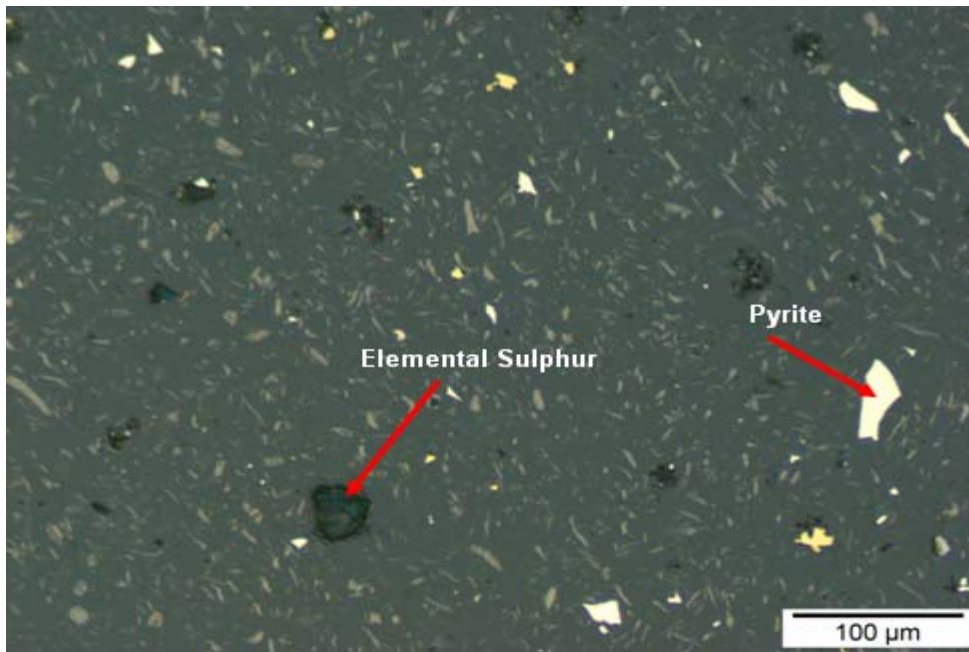


Figure 6.30 Optical micrograph of CCHYP concentrate sample after 432 h of leaching.

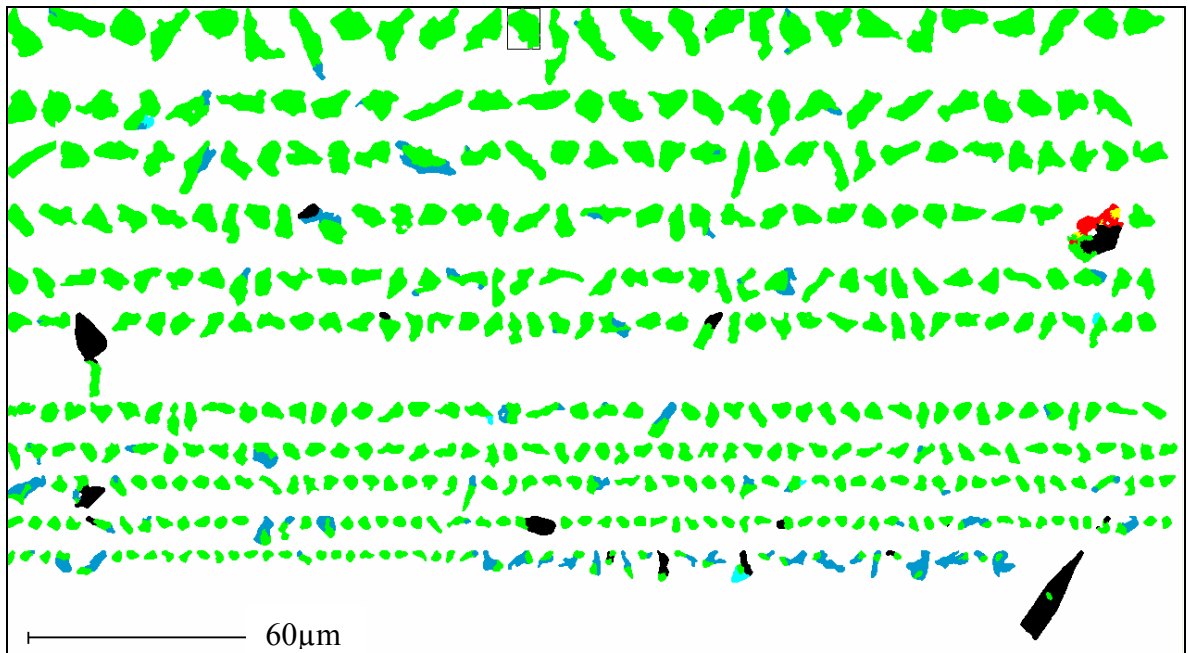


Figure 6.31 Partial mineral map showing liberated chalcopyrite (bright green) after 432 h of leaching.

After 528 h of leaching the mineralogy appears to be similar to that of samples taken at shorter times as shown in Figures 6.32 and 6.33. It has been suggested (Dutrizac 1981) that the globular sulfur may partly impede the transport of the leaching agents to the surface of the chalcopyrite. However, as shown in Figure 6.33 the grains of chalcopyrite do not appear to be associated with elemental sulfur.

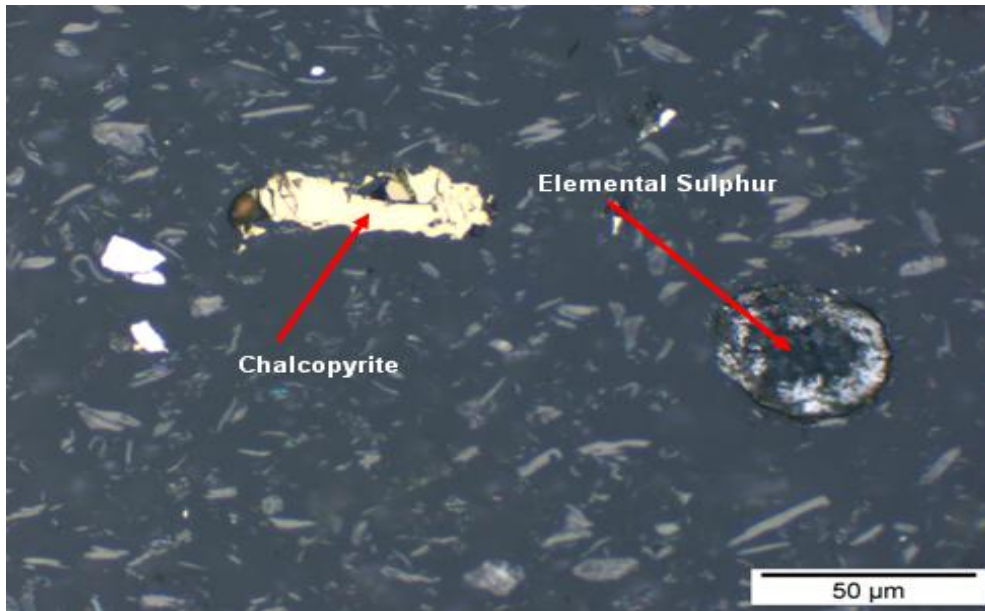


Figure 6.32 Optical micrograph of CCHYP chalcopyrite concentrate sample after 528 h of leaching.

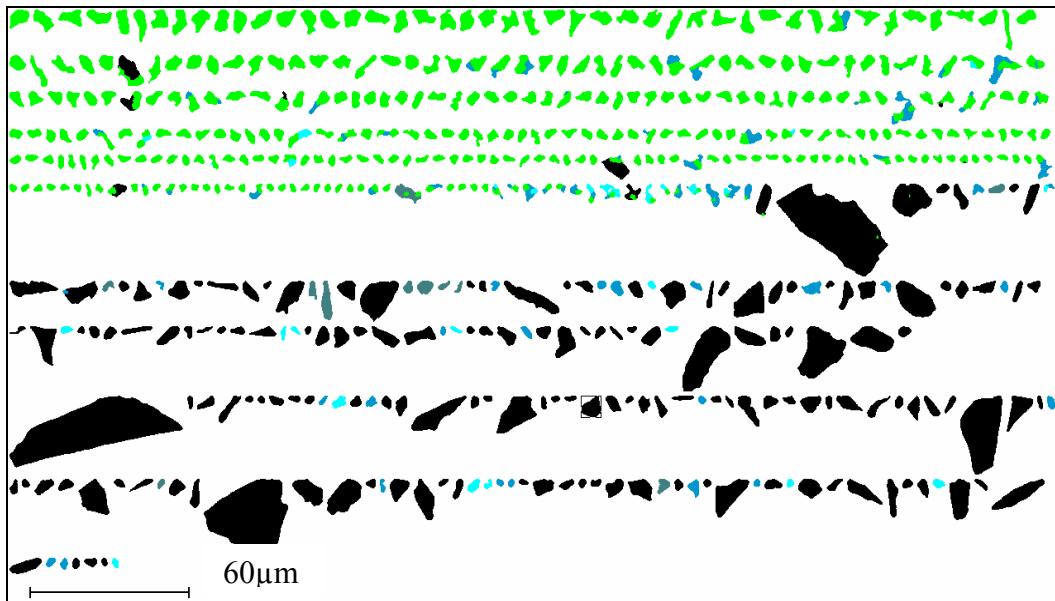


Figure 6.33 Partial mineral map showing largely liberated chalcopyrite particles after 528 h of leaching, chalcopyrite (bright green), pyrite (black), bornite (aqua) and sulphur (green).

Similar results were obtained in the analysis of a sample taken after 696 hours as shown in Figures 6.34 and 6.35.

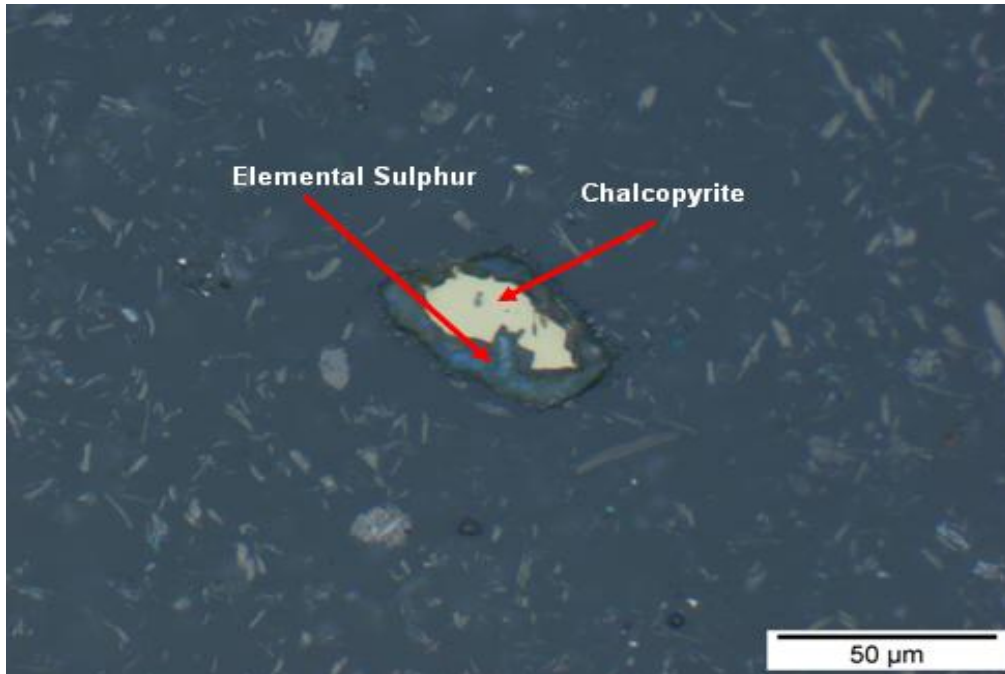


Figure 6.34 Optical micrograph of CCHYP concentrate sample after 696 h of leaching.

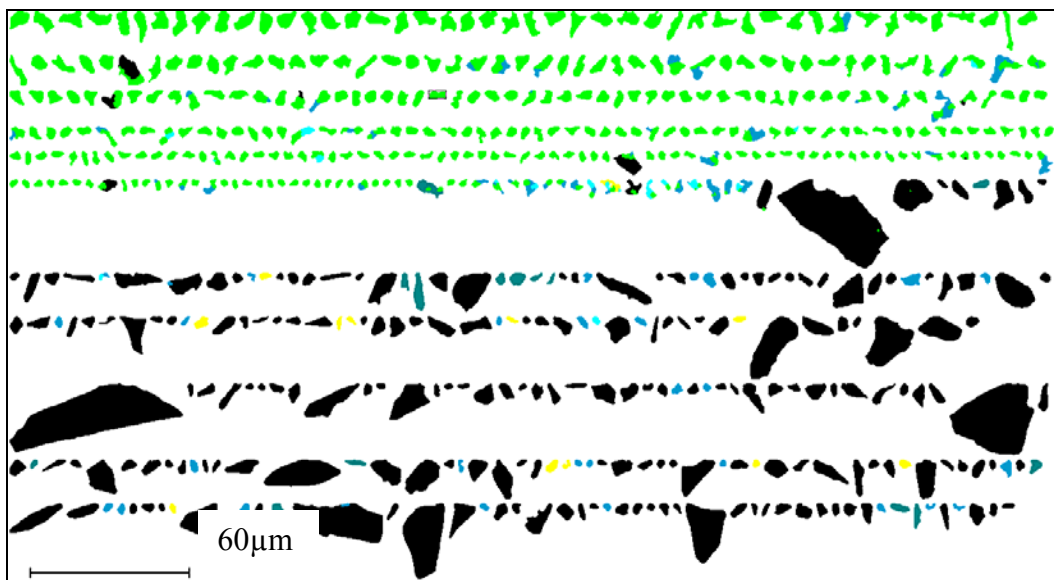


Figure 6.35 Partial mineral map showing liberated chalcopyrite after 696 h of leaching.

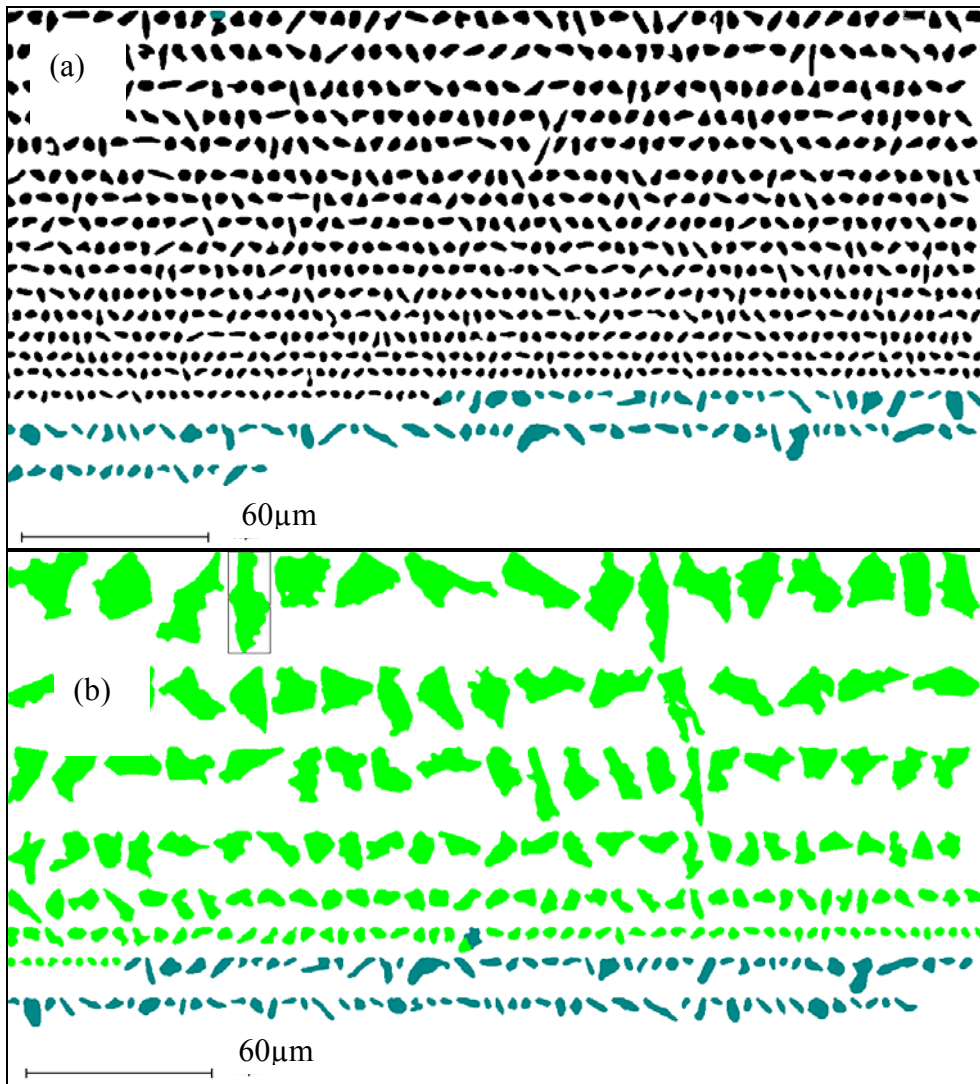


Figure 6.36 Partial mineral map after 696 h of leaching showing (a) liberated pyrite (black) and sulfur particles and (b) chalcopyrite (bright green) and sulfur grains (green).

After 816 h of dissolution (Figure 6.36) the analysis of the residue sample shows that most of chalcopyrite, pyrite and sulfur are liberated with very little association of sulfur with chalcopyrite.

6.11 Recovery

Chemical analyses of Cu, Fe and S in some of residues were completed at the Ultra Trace Laboratory, Perth. Table 6.7 lists the copper recovery calculated from the residue analyses as well as the corresponding recovery based on the solution analysis. It is evident that comparative data was attained between solution and residue balances.

Table 6.7 Copper recoveries based on solution and residue analyses

Figure	Test	Leached solution %	Residue %
6.1	(d)	68.1	73.6
	(a)	62.2	62.1
6.2	(b)	83.0	90.7
	(c)	89.8	84.5
	(a)	68.8	69.1
6.5	(b)	66.0	64.6
	(c)	60.7	59.4
	(a)	72.2	74.3
6.6	(b)	88.4	90.0
	(c)	83.0	90.7
	(a)	39.9	48.0
6.8	(b)	39.8	43.8
	(c)	36.6	38.0
	(a)	9.3	13.7
6.11	(b)	83.7	74.6

Figure	Test	Leached solution %	Residue %
6.13	(a)	49.7	52.8
	(b)	60.2	58.6
	(c)	69.6	65.2
	(d)	77.8	76.7
6.16	(a)	88.9	90.0
	(b)	85.6	90.7
	(c)	80.7	81.5
6.20		88.3	87.9

6.12 Summary and conclusions

A kinetic study of the dissolution of chalcopyrite concentrates in chloride solutions at controlled potentials in the optimal potential window of 560 and 620 mV has been completed to obtain fundamental data and to establish the role of the important parameters in the rate of dissolution of chalcopyrite. The following are the principal results obtained.

An increase in concentration of chloride ions in solution does not increase the leaching rate of chalcopyrite concentrates. This result confirms preliminary results outlined in Chapter 4, in which it was observed that the presence of chloride ions is fundamental for enhanced leaching kinetics, but high concentrations are not essential. It should be noted that although an increase in the concentration of chloride ions does not increase the leaching rate, the results of experiments in Chapter 5 have shown that high chloride concentrations can extend the potential window to higher values.

Arrhenius plots are approximately linear over the range of temperature employed with an apparent activation of energy of 73 kJ mole⁻¹ for Andina and 71 kJ mole⁻¹ for the CCHYP concentrate.

Although the presence of cupric ions is essential for enhanced dissolution rates increased concentrations do not improve the leaching rate in the optimum potential window. Addition of ferrous ions appears to decrease the rate of dissolution but this may be due to the presence of ferric ions and somewhat higher potentials. This observation is in contrast to that claimed in the Japanese model which requires the presence of both ferrous and cupric ions for enhanced leaching rates at low potentials.

It was confirmed that the rate of dissolution of chalcopyrite is proportional to the surface area under the conditions of the present experiments. Attention should be paid to the type of agitation used in leaching experiments in that it was found that magnetically agitated slurries leached at a higher rate due to abrasion/breakdown of the concentrate particles. Although an increase in the pulp density does not increase the leach rate appreciably, it assists in that control of the potential is facilitated in the presence of adequate dissolved oxygen in the system.

The rate is essentially independent of acid concentration in the range of pH values from 0.5 to 2, but a fairly low pH is necessary to keep iron in solution although there is no obvious evidence that precipitation of iron inhibits the rate of dissolution. Mineralogical analyses have shown the relatively small association of elemental sulfur with chalcopyrite remains

relatively constant while the amount of elemental sulfur associated with pyrite increases with increasing pH.

Mineralogical studies of samples taken at various times during an experiment have demonstrated that copper dissolve preferentially from chalcocite followed by covellite and bornite. Chalcopyrite appears to dissolve at a slower rate during dissolution of the other secondary sulfide minerals. MLA analyses revealed that sulfur is formed predominantly as isolated globular grains or is associated with fine pyrite grains with very little association with chalcopyrite.

7.THE EFFECT OF ADDITIVES

7.1 Introduction

In order to enhance the rate of leaching of chalcopyrite, several catalysts and or promoters have been proposed such as pyrite, activated carbon, and the ions of Ag(I), Sn(II), Co(II), Hg(II) and Mn(II). The effect of pyrite on the leaching of chalcopyrite has been investigated by some researchers (Abraitis et al., 2004; Al-Harabsheh et al., 2006a; Dixon et al., 2007; Dutrizac, 1982; Harmer et al., 2006; Mehta, 1983; Parker et al., 2003; You et al., 2007). Most of these investigations have focused principally on the role of galvanic interactions in the leaching of sulfides minerals. It has been postulated that when chalcopyrite and pyrite are in intimate electrical contact with each other, they form a galvanic couple, because of which chalcopyrite behaves as an anode and dissolves rapidly, while pyrite behaves as a cathode and is galvanically protected by the leaching process; thus, pyrite oxidation is minimal. However, none of these investigations has directly verified the formation of such galvanic couples by electrochemical experiments.

Of the catalytic ions which enhance chalcopyrite dissolution, silver ion is the most effective (Cruz et al., 2005; Gomez et al., 1999; 1997a; Hiroyoshi et al., 2002; 2007), but due to the costs involved and difficulty of recovering silver, this technique has limited industrial application. However, it is important to understand the basis for the catalysis from a mechanistic point of view.

The main aim in studying this aspect in this study is to improve the understanding of the mechanism of the catalytic effect exerted by pyrite on the dissolution of chalcopyrite in chloride media. The work comprised a study of the leaching of pure pyrite under standard conditions and the effect of pyrite on the leaching of chalcopyrite concentrates. In addition, the effect of the addition of silver ions on the dissolution of chalcopyrite concentrates under different conditions was investigated. Table 7.1 shows the conditions used in each leach experiments.

Table 7.1 Experimental conditions of leaching tests

Sample			Condition							
Figure	Test	Sample	Mass g	T °C	HCl M	NaCl g L ⁻¹	Cu g L ⁻¹	Py g	Ag ppm	E _h / mV
7.4	(a)	Pyrite	9	35	0.2	0	0.5	0	0	580 /N ₂
	(b)					35				
7.6	(a)	Andina	9	35	0.2	0	0.5	0	0	580 /N ₂
	(b)							7.4		
	(c)							14.8		
	(d)							37		
7.7	(a)	PQS2	40	35	0.2	0	0.5	0	0	580 /N ₂
	(b)							6.8		
7.8-7.9	(a)	Andina	9	35	0.2	0	0.5	0	0	580 /N ₂
	(b)							7.4		
	(c)							37(12µm)		
	(d)							37(5µm)		
7.10- 7.15	(a)	covellite	9	35	0.2	0	0.5	0	0	580 /N ₂
	(b)	covellite						37		
	(c)	covellite						37(12µm)		
		Andina						37(12µm)		
7.16	(a)	PV	20	35	0.2	0	0.5	0	1	580 /N ₂
	(b)	Andina	9							
	(c)	PQS2	40							
7.17	(a)	CCHYP	18	35	0.2	0	0.5	0	1	580 /N ₂
	(b)					43				580 /N ₂
	(c)					43				650 /N ₂
7.18*	(a)	PV	20	32	0.2	0	0.5	0	1	air
	(b)							37(12µm)	1	
	(c)							37(12µm)	1	
	(d)							37(12µm)	1	

* (b) addition of silver followed by addition of pyrite, (c) addition of pyrite followed by addition of silver and (d) addition of pyrite and silver at the beginning of leaching.

7.2 Effect of addition of pyrite

7.2.1 Pyrite in chalcopyrite concentrates

The chalcopyrite concentrates used were Andina, Pinto Valley, PQS2 and CCHYP together with a pure pyrite sample. Table 7.2 shows that all the concentrates contained pyrite with the largest amount contained in the PQS2 concentrate. Chalcopyrite is the main copper mineral in all the concentrates.

Table 7.2 Pyrite content (mass %) and CSR (copper source ratios) in the concentrates

Sample	Andina 25-38 μ m	PQS2 -38 μ m	PV -38 μ m	CCHYP -38 μ m	Pyrite 25-38 μ m
Chalcopyrite	90.2	54.0	99	59.1	
Covellite	0.2	31.0	0	19.6	
Bornite	6.8	9.0	0.4	8.8	
Enargite	2.6	5.0	0	1.8	
Pyrite	2.7	62.2	20.9	34.33	98.1

MLA analyses of the association of chalcopyrite with other minerals in each of the concentrates as shown in Table 7.3 reveal that greater than 95% of the chalcopyrite is completely liberated.

Table 7.3 Association (mass %) of chalcopyrite with others minerals

Minerals	Andina	PQS	Pinto Valley	CCHYP
Bornite	0.8	1.3	0.01	0.7
Covellite	0.2	0.6	0	0.5
Enargite	0.8	0	0	0
Pyrite	0.3	1.1	0.1	1.3
Free surface	95	95.5	99.2	95.1

According to the microchemical analysis (Figure 7.1) of the pyrite particles in the milled pyrite sample, it contained 45.8 wt% iron and 54.2 wt% sulfur. Figure 7.2 shows the size distribution of the pyrite in the -25 μm size fraction and Figure 7.3 that of the milled -25 μm fraction employed in the leaching experiments. The P_{80} of the -25 μm fraction is 12 μm and that for the milled sample is 5 μm . In the data shown below, these samples are referred to by their P_{80} values.

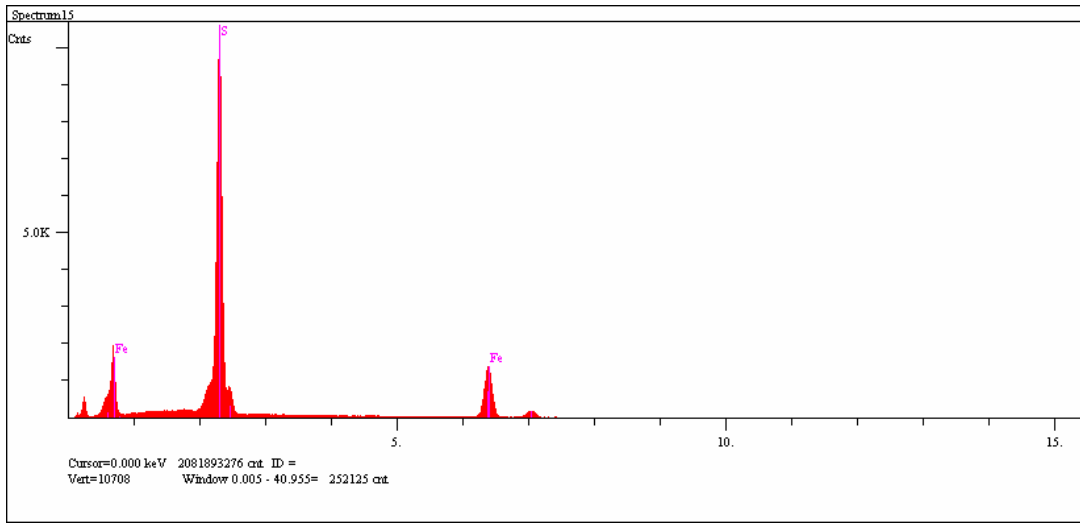


Figure 7.1 Typical EDS spectrum of pyrite particles.

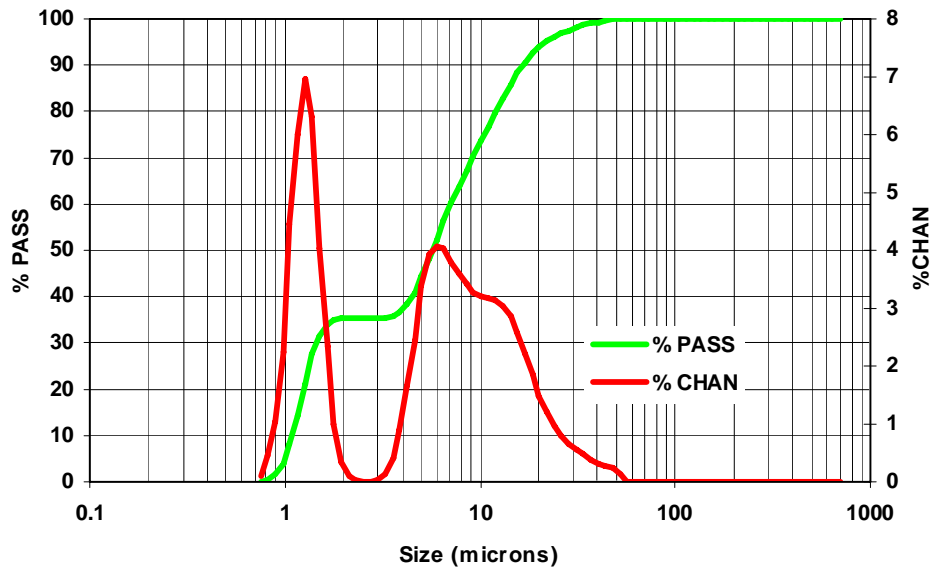


Figure 7.2 Particle size distribution of -25 μm pyrite sample.

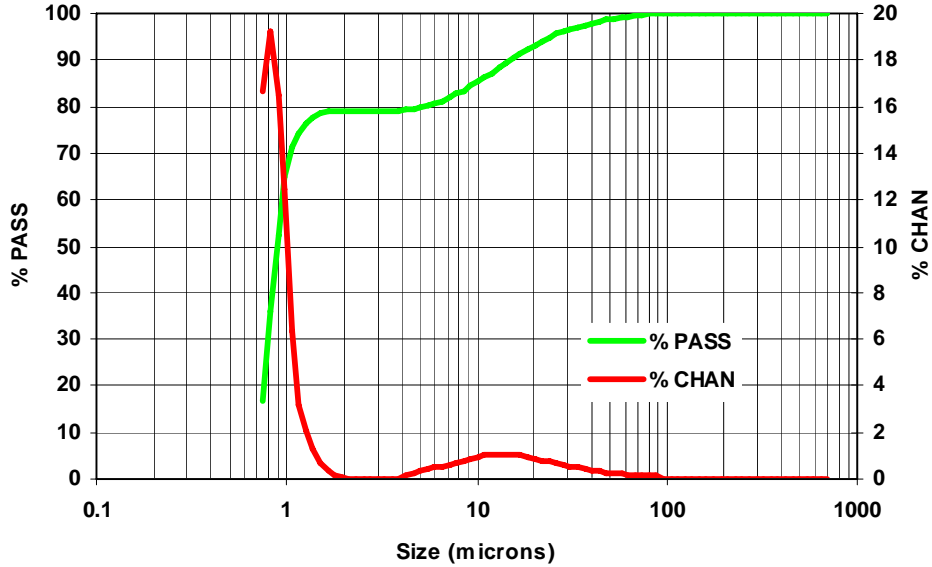


Figure 7.3 Particle size distribution of milled -25 µm pyrite sample.

7.2.2 Dissolution of pure pyrite

According to Cabral and Ignatiadis (2001)(2001) pyrite oxidation begins at potentials above +0.68 V at 25 °C in sulfuric acid solutions. To confirm that pyrite will not be oxidized at potentials below 0.60 V two leach experiments in instrumented reactors were conducted using 9 g of pure 12 µm pyrite. In both experiments, the potential was maintained at a value of 580 mV by control of the dissolved oxygen. Figure 7.4 confirms that less than 4% of pyrite is dissolved under these conditions. Optical analysis (Figure 7.5) revealed that the pyrite particles in the residues did not show evidence of rims of sulfur confirming that the mineral was not attacked under these conditions.

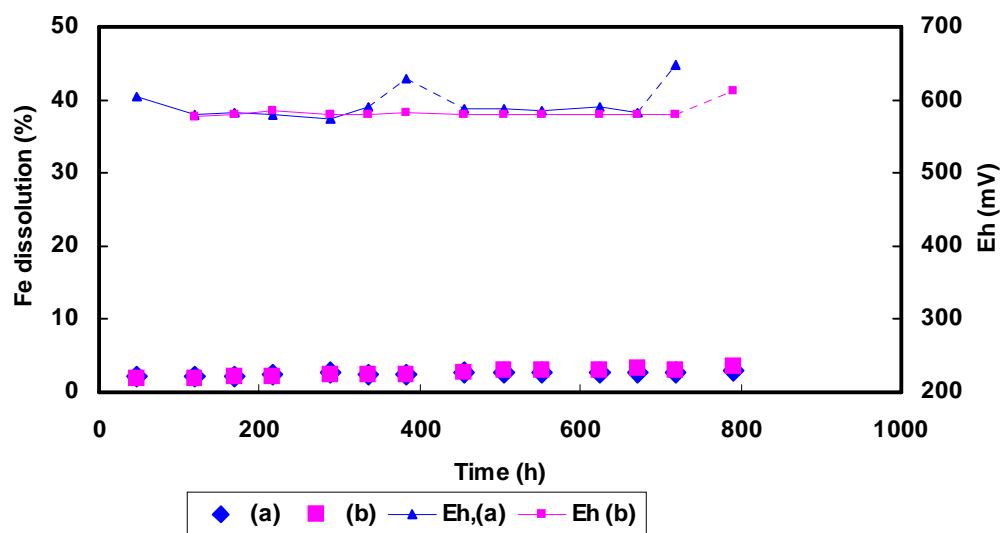


Figure 7.4 Dissolution of 12 μm pyrite. (a) Standard conditions 0.2 M HCl and 0.5 g L^{-1} Cu(II) at 35 °C, (b) as in (a) after adjustment of the pH to 2.0

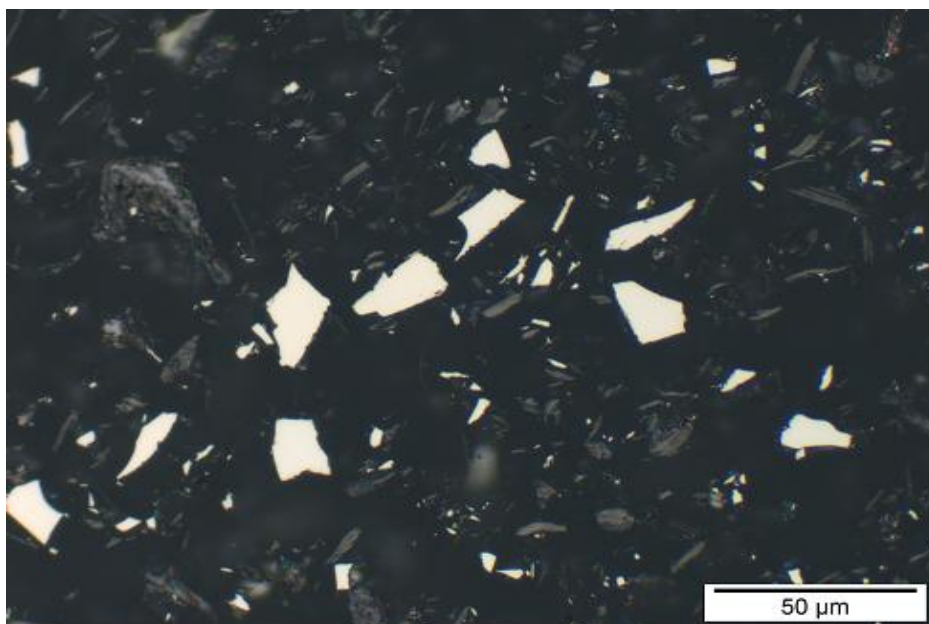


Figure 7.5 Optical micrograph showing pyrite particles in the residues after leaching for 800 h under standard conditions.

7.2.3 The effect of the ratio of chalcopyrite to pyrite

The effect of the addition of different amounts of pyrite on the dissolution of chalcopyrite was studied by using $\text{CuFeS}_2:\text{FeS}_2$ ratios of 1:0, 1:1, 1:2 and 1:5. In these experiments, the 25-38 μm size fractions of both chalcopyrite and pyrite were used. Leaching experiments were conducted in instrumented reactors at 35 °C under potential control using air and nitrogen.

Figure 7.6 shows a negligibly small effect of the addition of increasing amounts of pyrite to Andina concentrate under controlled potentials of 580 mV. Similar behavior was found when the PQS2 concentrate was leached at a 1:1 ratio with pyrite as shown in Figure 7.7. It should be noted that PQS2 concentrate contains 62.2% pyrite.

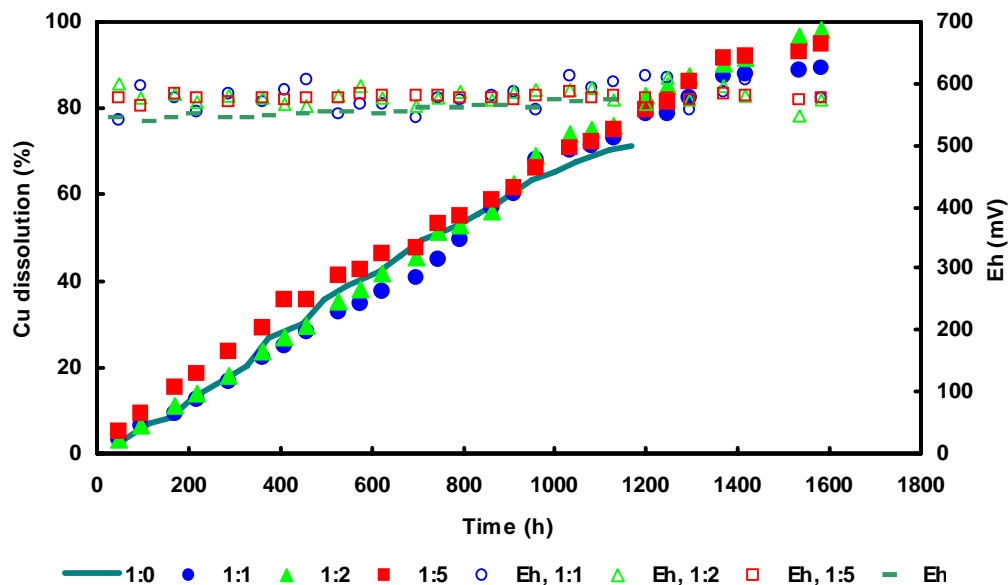


Figure 7.6 The effect of pyrite (25-38 μm) on the rate of copper extraction from Andina concentrate (25-38 μm) at 35 °C.

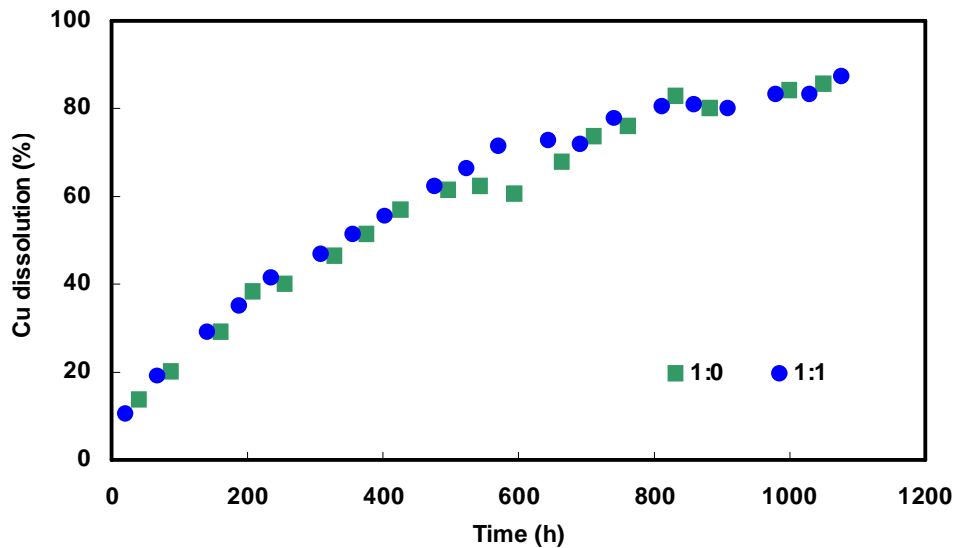


Figure 7.7 The effect of pyrite (25 μm) on the rate of copper extraction from PQS2 concentrate (-38 μm) at 35 $^{\circ}\text{C}$.

7.2.4 The effect of the particle size of pyrite

Although the above results show little influence of pyrite on the dissolution of chalcopyrite, it was noted that the use of fine pyrite (P_{80} of 12 μm) could have a measurably greater effect as shown by the result in Figure 7.8. However, when even finer (P_{80} of 5 μm) pyrite was used, the rate of copper extraction obtained was lower and it appears that there is an optimum pyrite particle size. These results are not in agreement with GALVANOX process in which a pulverized pyrite enhances chalcopyrite leaching. In all cases, the Eh could be controlled close to the set-point of 580 mV. However, it was observed that the pH in the reactor in which the rate was greatest increased more rapidly (due to consumption of protons in the reduction of dissolved oxygen) as shown in Figure 7.9. It is not therefore clear whether the higher rate in this case is due to the presence of the pyrite or/and to the increased pH.

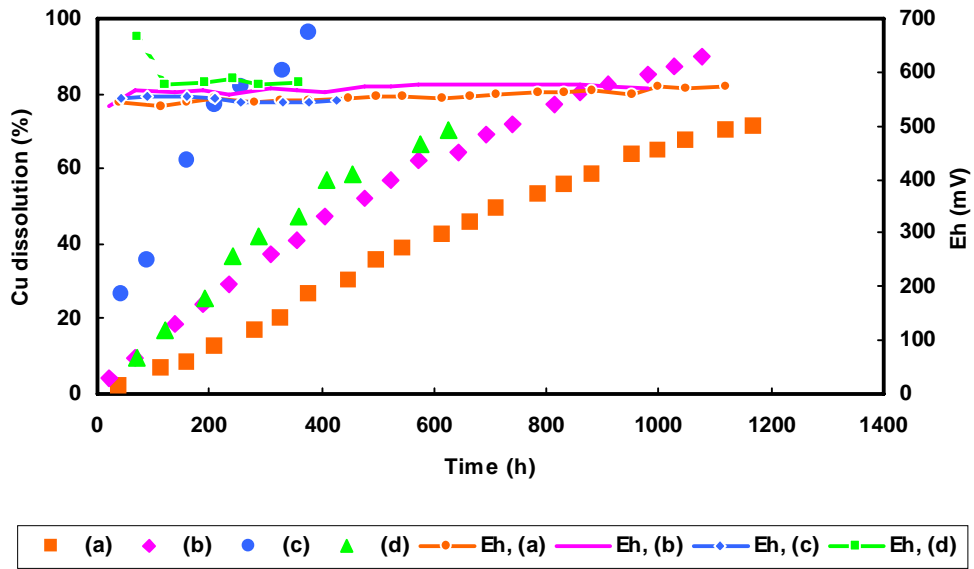


Figure 7.8 Effect of pyrite on the rate of copper extraction from Andina concentrate at various ratios of chalcopyrite to pyrite at 35 °C. Ratios (a) 1:0, (b) 1:1, (c) 1:5 with 12 μm pyrite particles (d) 1:5 with 5 μm pyrite particles.

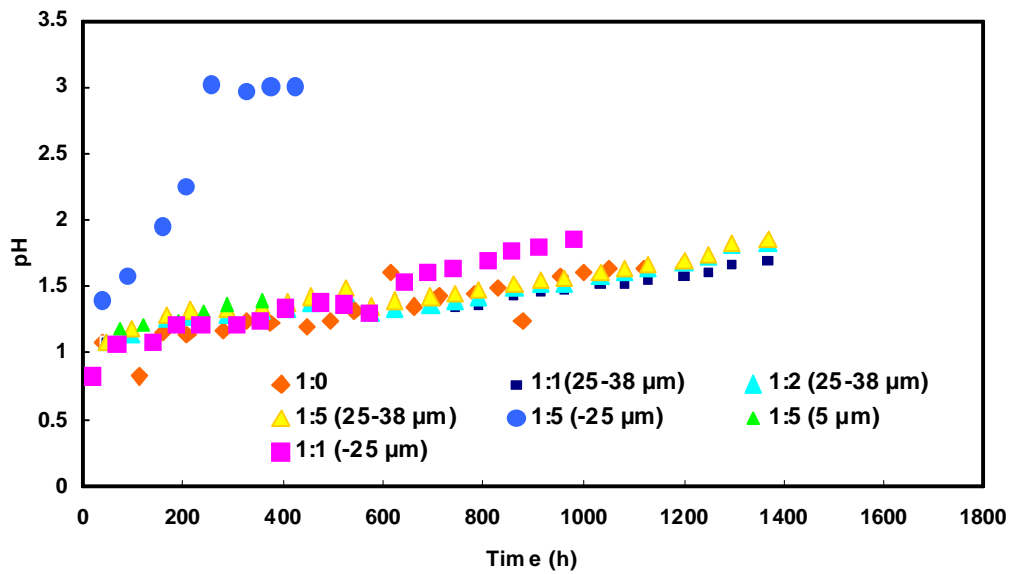


Figure 7.9 Effect of pyrite on the pH during dissolution of Andina concentrate at various ratios of CuFeS_2 to FeS_2 . Conditions as in Figure 7.8.

7.2.5 The effect of pyrite on the dissolution of covellite

In order to understand the influence of pyrite on the dissolution of secondary copper sulfides, experiments were carried out with synthetic covellite under the same conditions as used for the chalcopyrite concentrates. Previous experiments (not presented in this thesis) had shown that covellite dissolves at approximately the same rate as chalcopyrite and, as shown in Figure 7.10, the same behavior is observed when fine pyrite is added to the leach. However, the maximum increase in rate obtained with 1:5 ratio of chalcopyrite to pyrite and 12 μm of pyrite is lower than that measured for chalcopyrite under the same conditions.

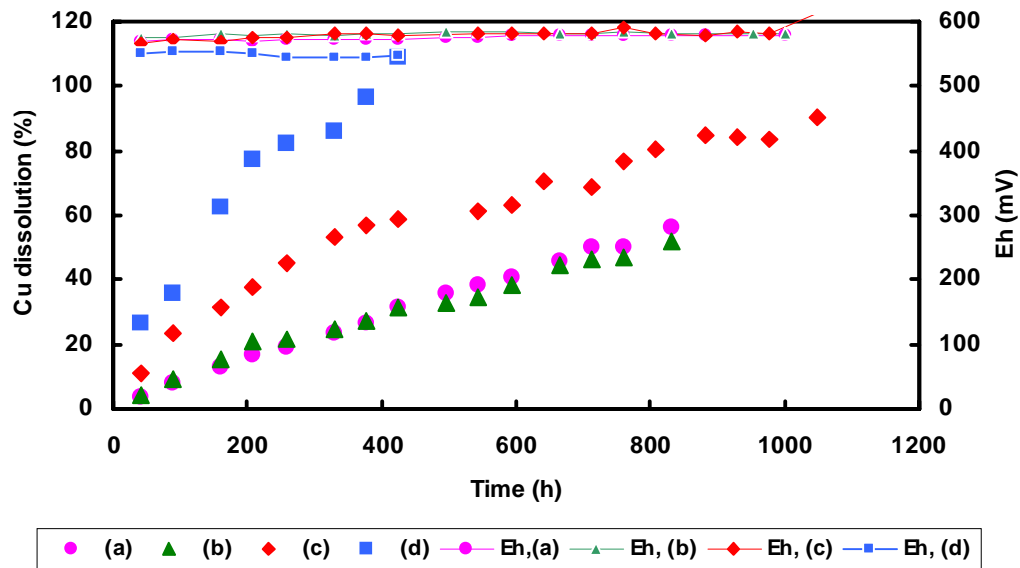


Figure 7.10 Comparison of the effect of pyrite on the dissolution of covellite and chalcopyrite (a) covellite, (b) covellite: pyrite ratio 1:5, 25-38 μm pyrite, (c) covellite: pyrite 1:5 ratio, 12 μm pyrite and (d) as in (c) but with chalcopyrite

7.2.6 Mineralogy of residues

In order to establish the mechanism of the action of fine pyrite on the leaching rate of copper, the leach residues were collected by filtration and subjected to mineralogical examination. Table 7.4 shows the main minerals present after each leaching experiment conducted with the addition of pyrite. It is clear that the chalcopyrite and sulfur content decreases with increasing addition of pyrite. In addition, as shown in Fig. 7.11, the fraction of sulfur particles associated with secondary copper minerals decreases, but the fraction associated with pyrite increases as the amount of pyrite increases and the particle size decreases. It should be emphasized again that there is very little sulfur associated with chalcopyrite. These results suggest that sulfur is formed from a soluble intermediate and that the pyrite surface can act a “catalyst” for the formation of elemental sulfur from this soluble intermediate.

Table 7.4 Modal analysis of residues (mass%)

Mineral	Head	Residue					
		1:0	1:1	1:2	1:5	1:5 (12 μ m)	1:5 (5 μ m)
Chalcopyrite	82.5	38.5	13.0	7.1	2.7	5.3	4.9
Covellite	0.16	0.0	0	0	0	0.7	0
Bornite	3.4	0.5	0.1	0	0	0.2	0
Enargite	1.7	6.1	1.6	0.7	0.4	0.7	0
Sulfur	0	3.8	0.7	0.5	0.2	0.8	1.7
Pyrite	2.7	28.2	77.7	87.5	94.6	79.6	91.7

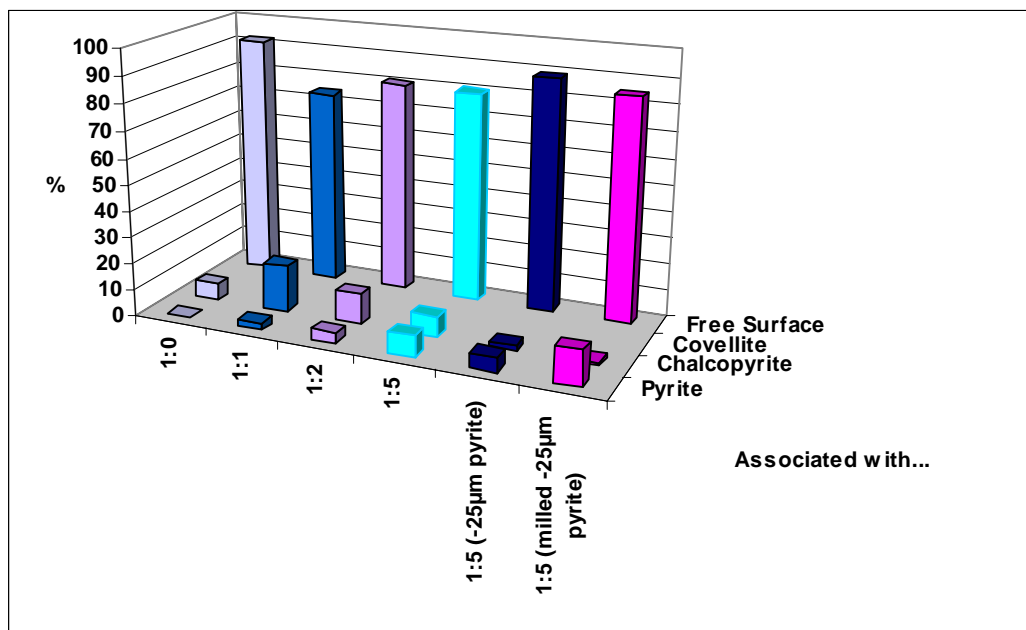


Figure 7.11 Department of sulfur in residues after dissolution of Andina concentrate in the presence of fine pyrite

Figure 7.12 illustrates the minerals present in the residue after leaching under standard solutions without addition of pyrite. Unexpectedly, there is little evidence of sulfur rims on the chalcopyrite particles and most of the sulfur is present as discrete grains.

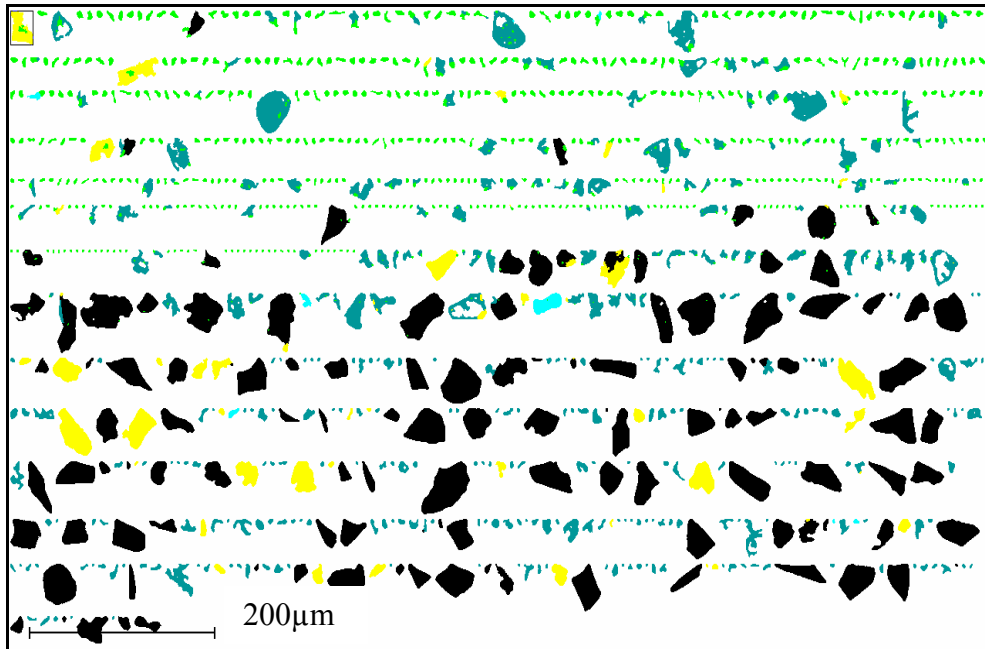


Figure 7.12 Mineral map of Andina concentrate residue after dissolution under standard conditions. Pyrite (black), chalcopyrite (bright green), sulfur (green) and enargite (yellow).

Figure 7.13 shows part of the mineral map of the residue from the leaching of Andina concentrate with addition of fine pyrite (12 μm) at a ratio of 1:5. As anticipated, there are more discrete spherical globules of sulfur than associated with chalcopyrite. Although most of the sulfur is liberated and not associated with the chalcopyrite, it is interesting to note that, as shown in Figure 7.14 sulfur is observed as layers around the smaller pyrite particles.

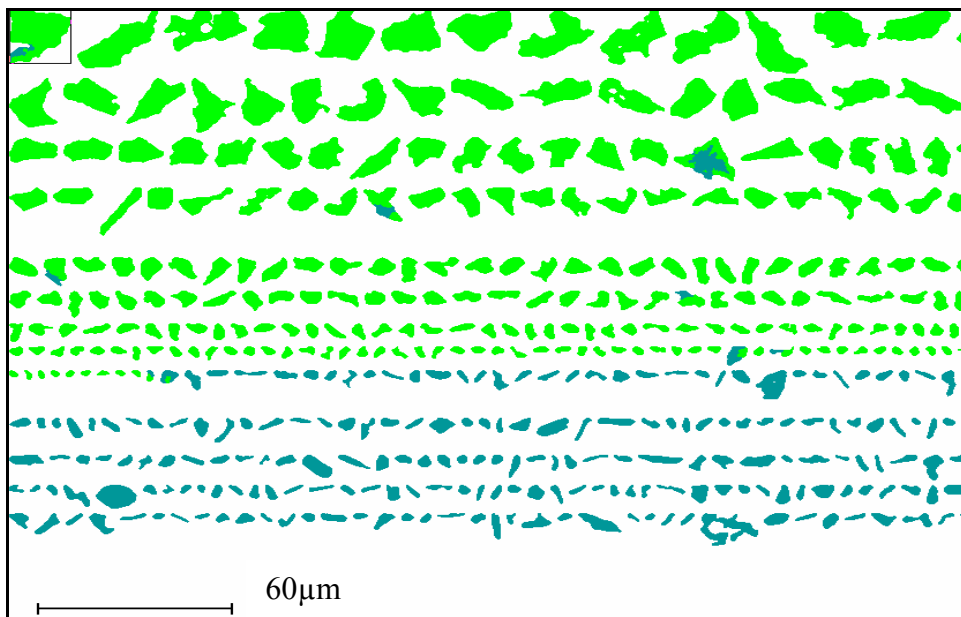


Figure 7.13 Partial mineral map of chalcopyrite and sulfur after dissolution in the presence of fine pyrite (12 μm) in a ratio of 1:5 under standard conditions. Chalcopyrite particles are bright green and sulphur green.

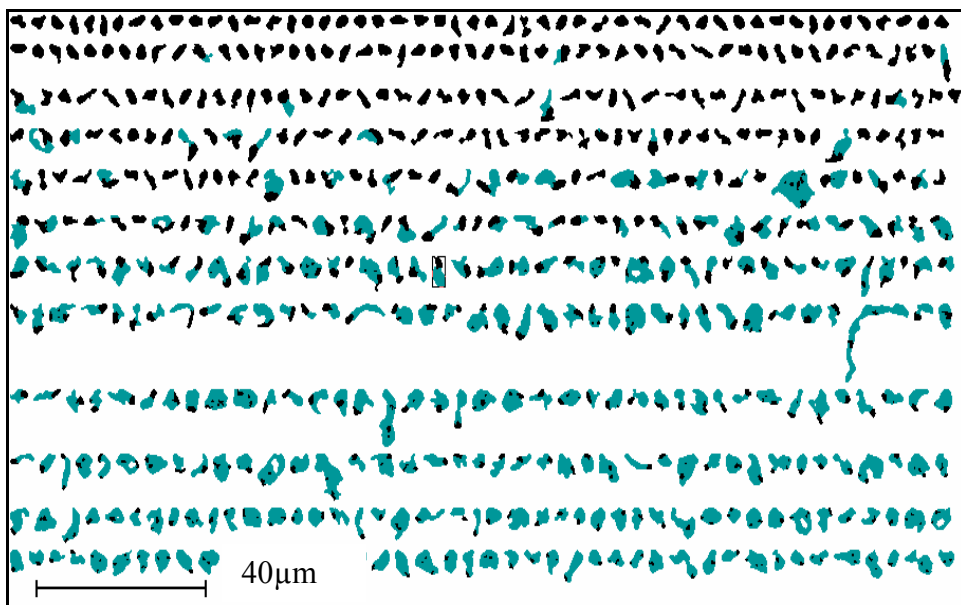
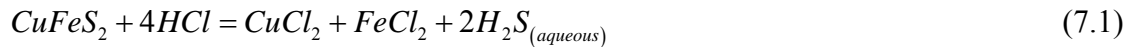


Figure 7.14 Partial mineral map showing layers of sulfur around fine pyrite particles. Pyrite particles are black and sulfur green. Conditions as in Figure 7.13.

According to Dutrizac (1990), the occurrence of sulfur as isolated and relatively large globules in the ferric chloride leaching of chalcopyrite suggests that the formation of elemental sulfur occurs by precipitation from an aqueous species. The reaction sequence according to his postulate involves dissolved H₂S



The H₂S formed is subsequently oxidized by ferric chloride.



and the addition of equations (1) and (2) produces the overall reaction



According to Dutrizac, it is not known whether dissolution occurs entirely by such an indirect mechanism or by a combination of direct oxidative and indirect mechanisms.

This model is consistent with the above mineralogical observations and will be expanded upon in a later section.

In a similar fashion, the residues from the dissolution of synthetic covellite were also examined mineralogically and the results shown as partial mineral maps in the absence of pyrite in Figure 7.15(a) and in the presence of fine pyrite in Figure 7.15(b). It is evident from Figure 7.15(a) that the residual covellite is strongly associated with elemental sulfur but, on the other hand, the covellite in the residue appears to be completely liberated i.e. not associated with sulfur when pyrite was added to the leaching reactor (Figure 7.15(b)).

7.3 Effect of addition of silver ions

Each of the concentrates was analyzed for the trace metal content and the results shown in Table 7.5. According to the literature some of these elements, such as silver and bismuth may affect the leaching rate of chalcopyrite. In order to study the effect of silver on the leaching rate of chalcopyrite, four different samples were leached with the addition of 1ppm of silver under standard conditions. Figure 7.16 shows the results of these experiments. It is apparent that silver appears to enhance the rate of dissolution of the PQS2 concentrate but to have a negligible effect on the dissolution of the Andina and PV concentrates under these conditions.

Table 7.5 Trace elements in concentrates (ppm)

Sample	Size μm	Ag	Bi	Sb	Cd	Sn	Co	Ni	As
Andina	25-38	81	46.4	220.0	25.1	3.2	21.0	12.0	2650.0
PQS	-38	18.0	5.3	32.5	20.3	9.6	190.0	170.0	720.0
PV	-38	24.0	1.4	2.3	10.4	13.4	110.0	105.0	40.0
CCHYP	-38	20.0	45.0	11.6	30.1	6.6	1120.0	245.0	80.0

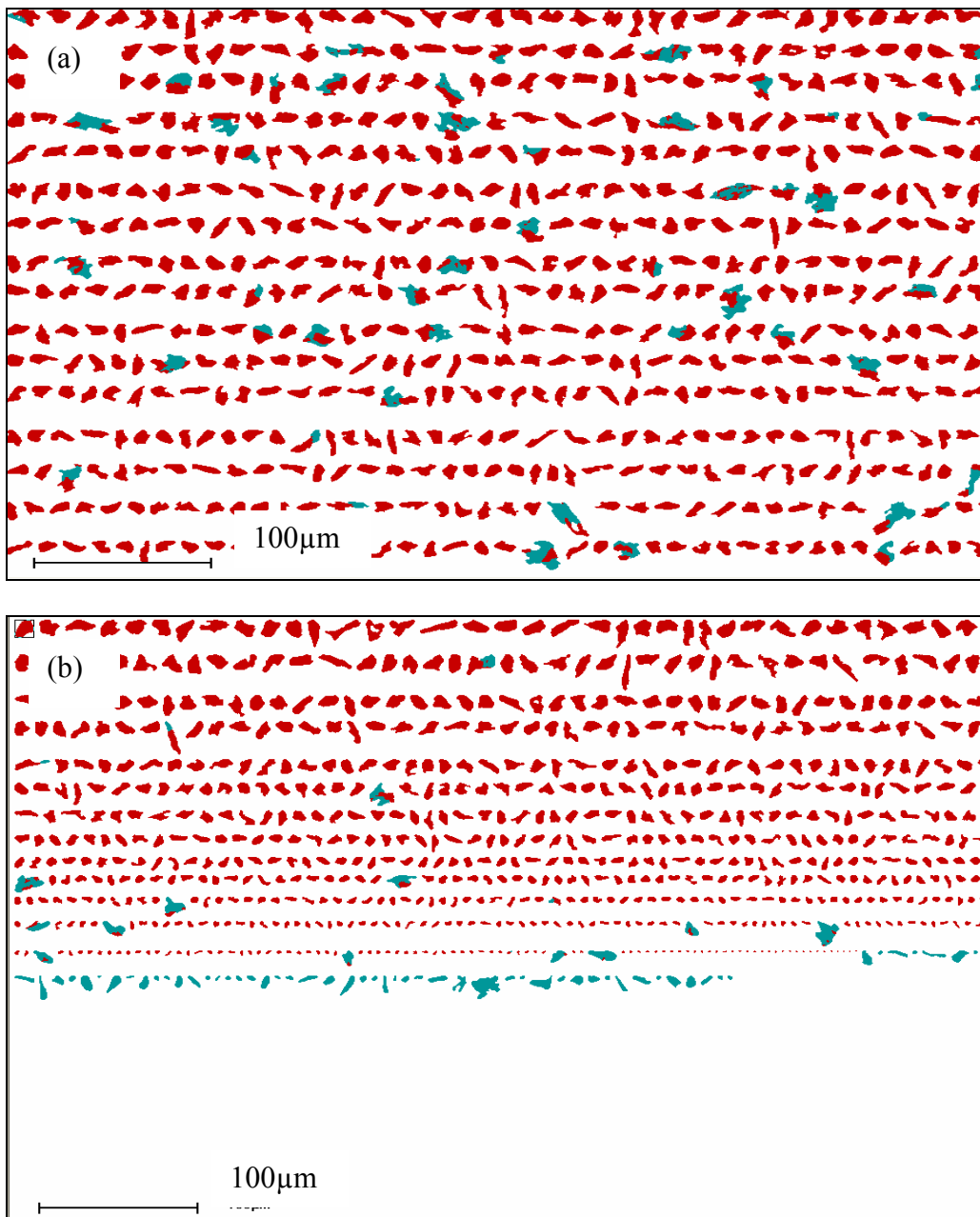


Figure 7.15 Partial mineral maps of residual covellite after dissolution using (a) standard conditions in the absence of pyrite, (b) standard conditions with addition of pyrite (12 μm) at a ratio of 1:5. Covellite particles are shown in red and sulfur blue/green.

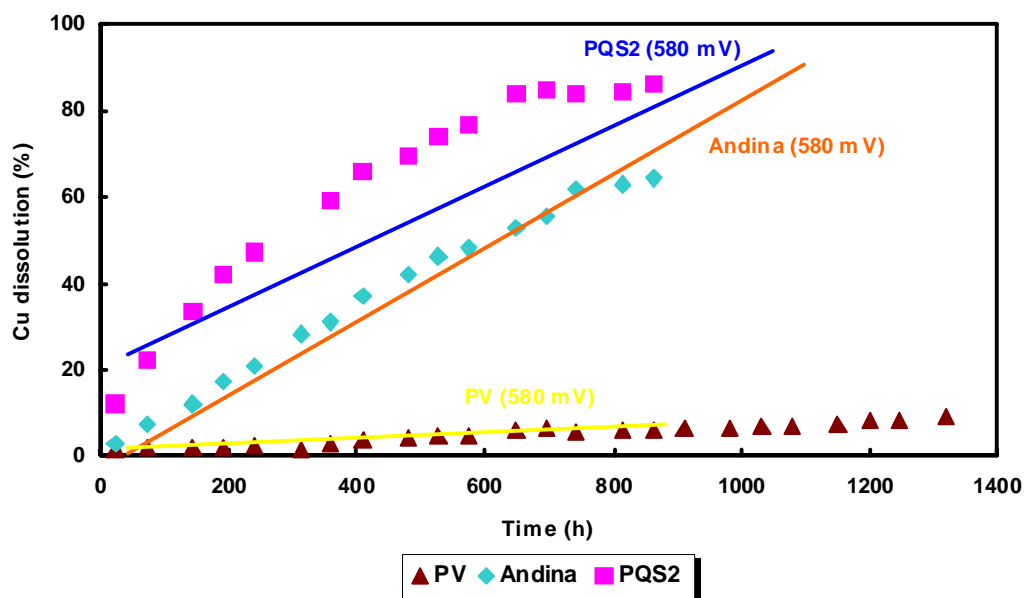


Figure 7.16 Effect of the addition of 1ppm of silver on the dissolution of several concentrates under standard conditions. The results obtained in the absence of silver ions are shown as the solid lines.

In order to elucidate whether or not addition of silver can enhance the leaching rate of chalcopyrite under different conditions, the CCHYP concentrate was leached under standard conditions with a higher chloride ion concentration at low and higher potentials. Figure 7.17 summarizes the leaching rates under these conditions compared to dissolution in the absence of silver ions. As it is obvious in this figure, the addition of 1ppm of silver enhances the leaching rate of CCHYP concentrate at 580 mV in a solution of 50 g L^{-1} of chloride ions with almost 100% dissolution in only 200 h. On the other hand, leaching experiments carried out under the same conditions but at 650 mV suggests that even though a small enhancement is observed, passivation of chalcopyrite has occurred even in the presence of silver ions (turquoise dots) and the rate is similar to that observed without addition of silver (bright turquoise line).

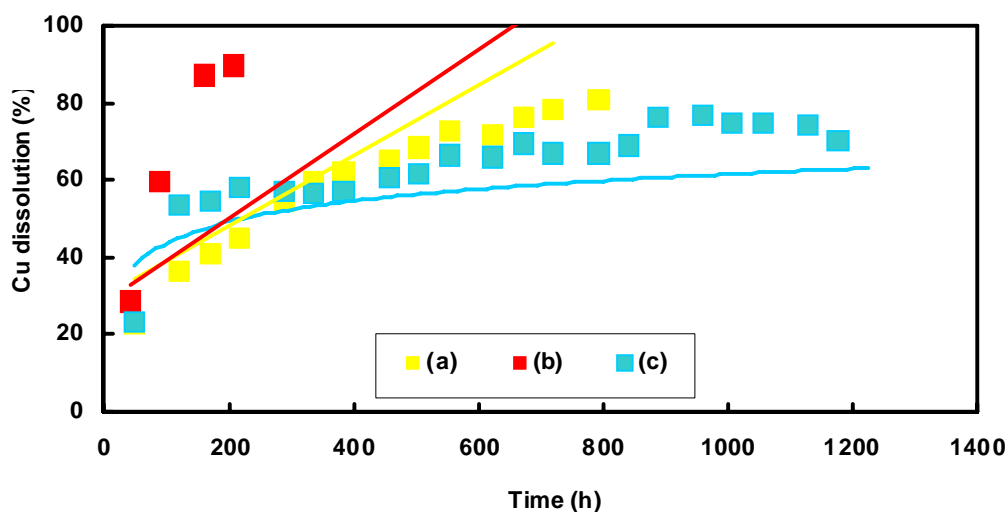


Figure 7.17 Effect of silver ions (1 ppm) on the dissolution of CCHYP concentrate (a) Standard conditions at 580mV, (b) 0.2 M HCl, 0.5 g L⁻¹ Cu(II) and 50 g L⁻¹ chloride ions at 580 mV and (c) 0.2 M HCl, 0.5 g L⁻¹ Cu(II) and 50 g L⁻¹ chloride ions at 650 mV. Results obtained in the absence of silver ions shown as solid lines.

As shown in a previous section, the dissolution of the PV concentrate was found to be very slow and it was thought that addition of pyrite and/or silver ions may enhance the rate of dissolution for this material. Figure 7.18 shows the results. When silver was added to the leach solution (brown circle markers), no effect was observed. Similar trends were observed when 12 µm of pyrite was added to the concentrate in the proportion 1:5 (pink diamond markers). However, the addition of silver ions after 1000 h resulted in an increased rate and 70% dissolution of copper was obtained. In order to establish whether pyrite or silver enhanced the dissolution rate in the above experiments, two experiments were carried out, the first involving the initial addition of pyrite, but no enhancement was observed and therefore 1 ppm of silver was added after 300 h. It appears that silver greatly increased the subsequent rate of dissolution. The next experiment was performed with addition of both pyrite and silver at the beginning of the leach experiment (turquoise square

markers) (Figure 7.18). It is obvious that a very small enhanced rate was obtained in this case. Therefore, it is clear from these apparently conflicting results that silver or pyrite alone or addition of both at the beginning of the leach does not have any noticeable effect on the rate of dissolution, but when pyrite is added followed of addition of silver, an enhanced rate is observed. The mechanism of this is not clear and more experiments are necessary to elucidate this phenomenon.

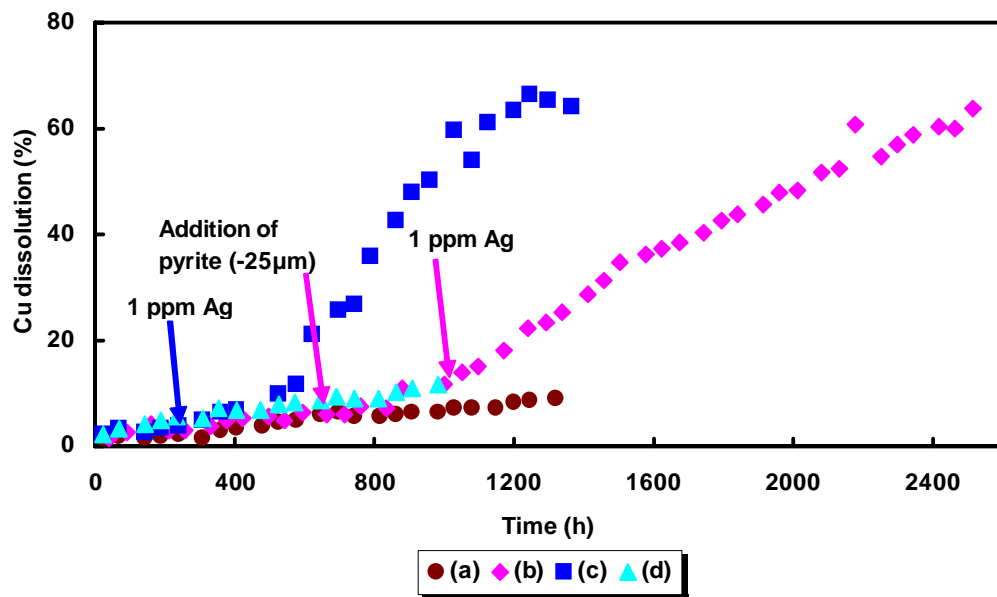
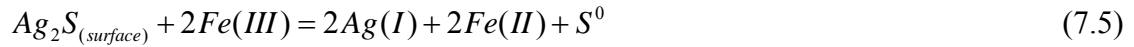
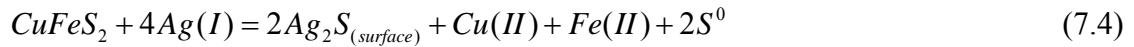


Figure 7.18 Effect of pyrite and silver ions on the rate of dissolution of PV concentrate under standard conditions (a) addition of 1 ppm Ag, (b) addition of Ag followed by addition of pyrite (12 μm), (c) addition of pyrite (12 μm) followed by addition of Ag and (d) addition of pyrite and Ag at the beginning.

Figure 7.19 shows the concentrations of silver present during the leaching experiments. It is interesting to observe that the amount of silver increases with the time. That can be partially explained by the model presented by Miller and Portillo (1979) in which silver undergoes an exchange reaction and subsequent oxidation/dissolution as follows



According to Miller et al. (1979) chalcopyrite reacts rapidly with silver ions to form a blue-black product on the chalcopyrite surface (Ag_2S) that is oxidized to release $\text{Ag}(I)$ back into solution.

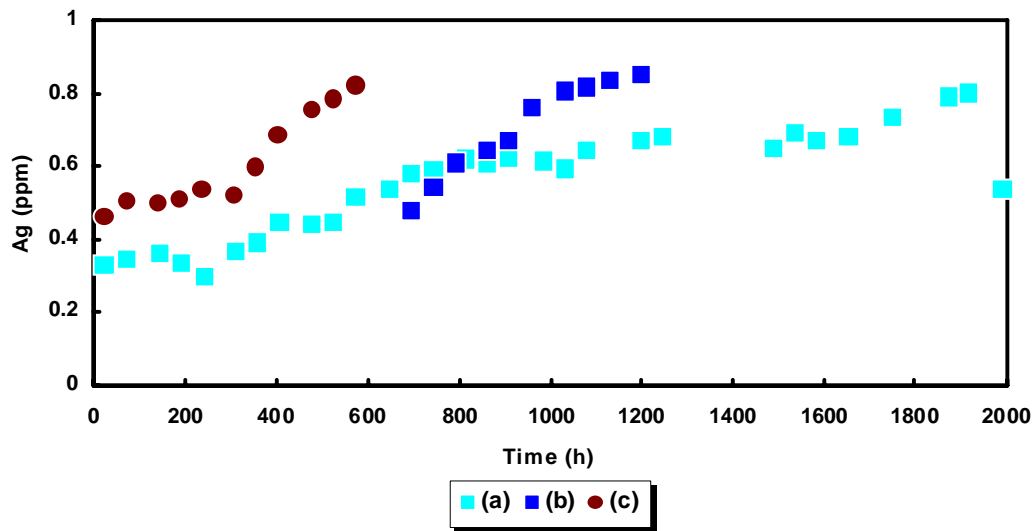


Figure 7.19 Concentration of silver ions during dissolution of PV concentrate under standard conditions. (a) Addition of 1 ppm Ag, (b) addition of pyrite (12 μm) followed by addition of 1 ppm Ag and (c) addition of pyrite and Ag at the beginning.

7.5. Recovery

Chemical analyses of Cu, Fe and S of some of residues were completed at the Ultra Trace Laboratory, Perth. Table 7.6 lists the copper recovery calculated from residue analyses as well as the corresponding values obtained from solution analyses. It is evident that comparative data was obtained between solution and residue balances.

Table 7.6 Copper recoveries based on solution and residue analysis

Figure	Test	Leached solution %	Residue %
7.6	(a)	86.9	83.0
	(b)	86.2	90.4
	(c)	94.5	90.9
	(d)	91.3	89.1
7.7	(a)	87.5	86.5
	(b)	89.1	89.3
7.8	(a)	86.9	83.0
	(c)	93.0	100.0
	(d)	67.7	75.1
7.16	(a)	17.3	30.2
	(b)	68.4	77.4
	(c)	80.5	97.9
7.18	(a)	17.3	30.2
	(b)	70.1	90.9
	(c)	70.3	91.5
	(d)	12.8	30.5

7.6. Summary and conclusions

The effect of the addition of pyrite and silver ions on the leaching of chalcopyrite concentrates has been investigated. These findings will assist to the construction of a mechanistic model that will need to integrate the observed effects. Some of the more important observations made during this study are reported in the next few paragraphs.

The presence of pyrite in the chalcopyrite concentrate samples apparently does not affect the dissolution of copper. Addition of pyrite with a particle size of 25-38 μm to chalcopyrite samples does not enhance the dissolution of chalcopyrite for the three chalcopyrite/pyrite ratios used. However, additions of finer 12 μm pyrite in a ratio of 1:5 increases the leaching rate of chalcopyrite although it is not clear whether this could also have been due to the higher pH during this experiment. The important mineralogical observation that under most conditions elemental sulfur is not formed at the chalcopyrite surface suggests that a soluble species is involved such as H_2S . Furthermore, the association of sulfur with fine pyrite suggests that this mineral catalyzes the oxidation of H_2S formed as an intermediate in the dissolution of chalcopyrite.

Under standard conditions of 0.2 M of HCl with 0.5 g L^{-1} Cu(II) at 35 °C at a controlled potential of 580 mV, small additions of silver ions do not appear to affect the dissolution of chalcopyrite. However, at higher chloride ions concentrations a rapid rate was observed in the presence of silver ions in the case of one concentrate.

In an attempt to understand the anomalous behavior of the Pinto Valley concentrate which dissolves very slowly relative to the other concentrates, leaching experiments were carried out with addition of pyrite and silver in different ways. The only effective method appears to involve the addition of small amounts of silver after the addition of pyrite into the leach solution.

At this stage, an overall reaction mechanism for the enhancement of the rate in the presence of pyrite and silver ions is not clear and for the case of pyrite will be discussed in more detail in the next chapter.

8. THE MECHANISM OF THE LEACHING OF CHALCOPYRITE IN CHLORIDE MEDIA

8.1. Introduction

In the present study involving an extensive set of leach experiments on various chalcopyrite-rich concentrates in chloride and chloride-sulfate media, a number of general observations have been made, the most important of which are the following:

1. Chalcopyrite leaching is enhanced in solutions having a “potential window” between 560-620 mV (SHE) in the presence of dissolved oxygen, copper ions and chloride ion. At higher potentials, the mineral undergoes typical passivation with substantially lower rates while lower potentials are not sufficient for oxidative dissolution.
2. The rate of dissolution under these conditions is generally constant compared to the parabolic rates observed under typical oxidative leach conditions.

3. Mineralogical studies have shown that very little of the elemental sulfur formed during dissolution in chloride solutions is associated with chalcopyrite particles but occurs largely as isolated spherical globules and as layers around smaller pyrite particles present in the concentrates.

4. When a chalcopyrite electrode is immersed for an extended period in the solution during leaching at low potentials the electrode surface takes on a purple tinge typical of covellite.

5. The addition of fine (-25 μm) pyrite enhances the rate of chalcopyrite leaching as does the addition of low concentrations of silver ions in the case of some concentrates.

These results have cast doubt on the validity of the conventional mixed potential model as applied to the oxidative dissolution of chalcopyrite at low potentials and have led to the development of an alternative mechanism based on a non-oxidative process coupled to oxidation of hydrogen sulfide by one of several oxidants as described by Nicol et al. (2003). A crucial step in this mechanism is the rate of oxidation of hydrogen sulfide and this chapter addresses this aspect as part of the overall mechanism in chloride solutions containing copper(II) ions as the main oxidant. The study involved measurements of the rate of consumption of dissolved oxygen by hydrogen sulfide in the presence of various ions and sulfide minerals.

In order to substantiate this model, the kinetics of the oxidation of H_2S by dissolved oxygen has been studied using a technique involving measurement of the rate of consumption of

dissolved oxygen. The effects of various solution conditions on the rate have been investigated and the catalytic effect of copper ions and fine pyrite has been confirmed.

8.2. Reaction Mechanism

8.2.1. High potential region. Oxidative Model

It is well known that chalcopyrite can be oxidatively dissolved according to the overall reaction (Dutrizac, 1981, 1990).



in which Ox and Red represent the oxidant and its reduced form respectively. In this case, the common oxidants are dissolved oxygen or ferric ions. Contrary to conventional expectation that the rate of dissolution should increase with increasing potential at the chalcopyrite surface, the rate does not follow such a trend at ambient conditions and the mineral generally requires elevated temperatures in order to dissolve at acceptable rates. During the dissolution of chalcopyrite, elemental sulfur is formed on the surface of chalcopyrite and it has been suggested that this elemental sulfur layer inhibits leaching (Dutrizac, 1990) although this is no longer accepted as the reason for “passivation” which is now thought to be due to the formation of a relatively thin copper-rich polysulfide layer . A schematic depiction of this reaction model is given in Figure 8.1.

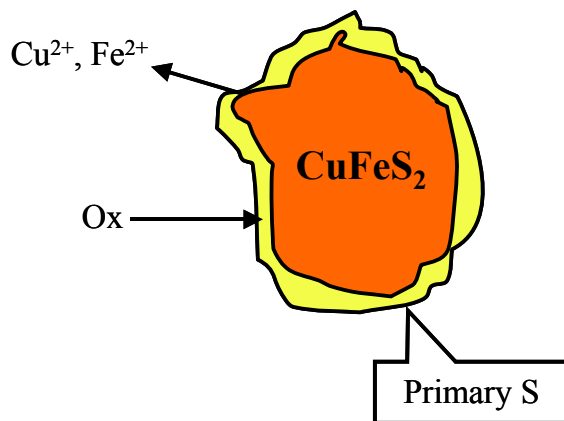


Figure 8.1 Oxidative leaching of chalcopyrite

8.2.2. Low potential region. Non-Oxidative model

At lower potentials, especially in the region between 560-620 mV (SHE), leaching experiments have confirmed that the rate of dissolution can be significantly greater than that observed at higher potentials. It has been found that this relatively high rate of dissolution can only be sustained in the presence of dissolved oxygen, copper ions and chloride ions.

In this potential region, direct oxidative dissolution of chalcopyrite by Eq.8.1 cannot occur and the passive layer also is not produced on the surface of chalcopyrite. It is proposed that dissolution occurs as a result of a non-oxidative process in two stages as shown in Figure 8.2. In the 1st stage, chalcopyrite is converted to CuS or dissolves to release copper ions and H_2S as shown in the following reactions.





In the 2nd stage, dissolved H₂S is oxidised by the reaction



Thus, in terms of this reaction model, elemental sulfur will only form on the surface of the chalcopyrite if the rate of reaction (8.4) is very rapid relative to mass transport of H₂S from the surface. Under most conditions, reaction (8.4) occurs away from the chalcopyrite surface and thus the sulfur can be considered as being formed in a secondary process.

The equilibrium constants of reactions (8.2) and (8.3) are very small and continued dissolution can only occur if H₂S is removed by precipitation and/or oxidation. In the chloride system, the copper(I) ion is stable and the following reaction is therefore possible



It is known that copper(I) can be oxidized by dissolved oxygen to copper(II)



with the overall reaction being



As will be shown, the direct reaction of dissolved H₂S with dissolved oxygen is very slow in the absence of a catalyst such as copper ions.

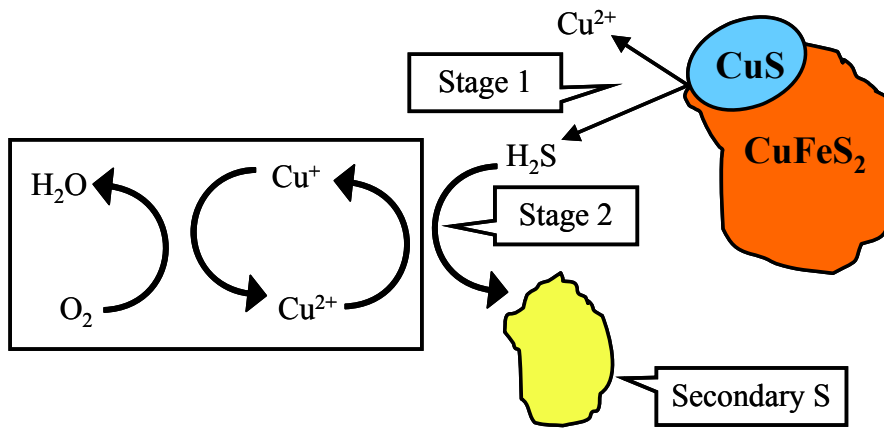


Figure 8.2 Non-oxidative leaching of chalcopyrite in chloride media

The results of the leaching experiments showed that fine pyrite can catalyse the dissolution of chalcopyrite at potentials within the potential window. It is suggested that the catalysis occurs as shown in Figure 8.3. This mechanism whereby H_2S is oxidised to form secondary sulfur explains why there is very little primary elemental sulfur associated with chalcopyrite particles but as isolated spherical globules and as layers around smaller pyrite particles.

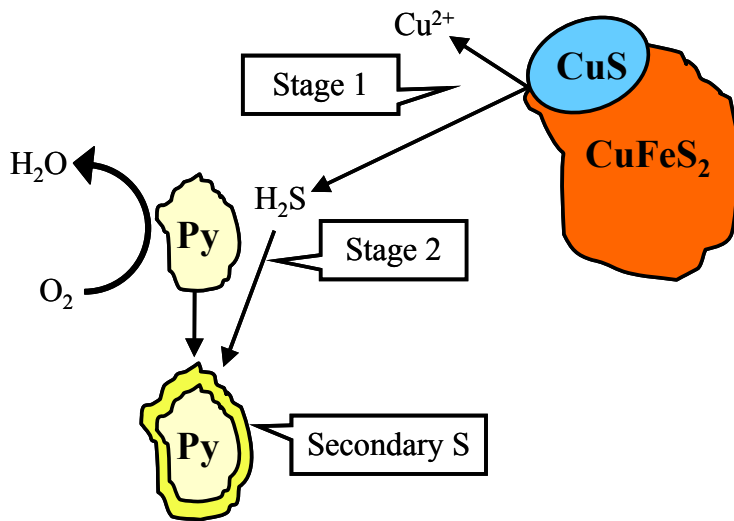


Figure 8.3 Catalytic effect of pyrite on chalcopyrite leaching

8.2.3. Relevant chemistry of the non-oxidative model

Although the above reaction models are consistent with the leach observations, a more direct confirmation of some aspects of the chemistry is desirable in that it could also be used for the purpose of creating appropriate quantitative kinetic models for the leaching reactions involving chalcopyrite and also possibly other sulfide minerals. In the above model a key component is the kinetics of the oxidation of H₂S by dissolved oxygen in the presence of homogeneous or heterogeneous catalysts.

It is well known that copper(II) ions are not stable in the presence of sulfide ions even in strongly acidic solutions due to precipitation by the reaction



The calculated equilibrium concentrations of the soluble species in a saturated solution of CuS in 0.2 M HCl containing increasing concentrations of chloride (added as NaCl) are shown in Figure 8.4 which shows that the equilibrium does not allow for measurable concentrations of copper(II) ions at equilibrium.

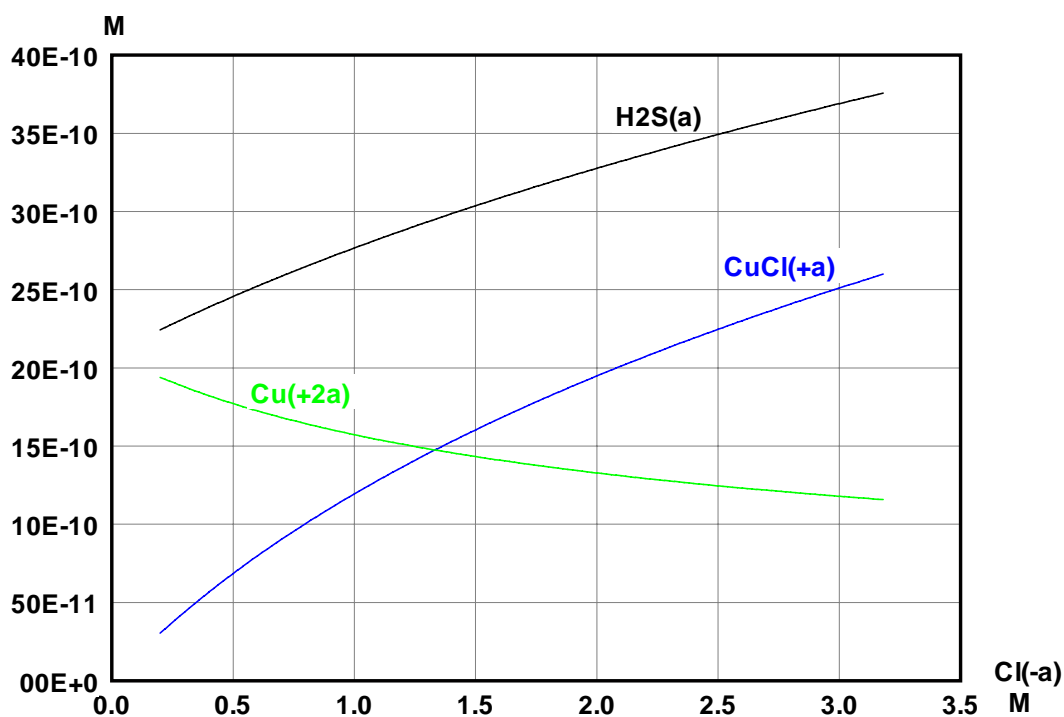


Figure 8.4 Species distribution in a saturated solution of CuS in 0.2 M HCl with increasing concentration of NaCl at 35 °C

However, as found in this study, addition of sulfide ions at low concentrations (less than 1mM) to acidic chloride solutions containing copper(II) ions does not result in the immediate precipitation of black CuS but a white turbidity appears after some minutes which is due to the precipitation of elemental sulfur. Thus, dilute solutions of copper(II) ions with dissolved H₂S are metastable and therefore it is not surprising that elemental

sulfur is often not observed on the surface of partially dissolved chalcopyrite grains. These observations are in accord with those made by Luther et al. (2002) who found that copper(II) reduction to copper(I) by sulfide occurs in solution prior to precipitation in sea water solutions.

In the chloride system, CuS is also not thermodynamically stable in the presence of copper(II) ions as shown by the data presented in Figure 8.5 which summarizes the thermodynamics of the various possible couples involved in this system. As a result of the increased stability of copper(I) in chloride solutions, copper(II) ions can oxidize both CuS and H₂S to elemental sulfur. As a comparison, it is also apparent that iron(III) can fulfill the same role. The important distinction between the Cu(II)/Cu(I) and Fe(III)/Fe(II) couples is that copper(I) ions are rapidly oxidized by dissolved oxygen whereas the corresponding oxidation of ferrous ions is very slow at ambient temperatures.

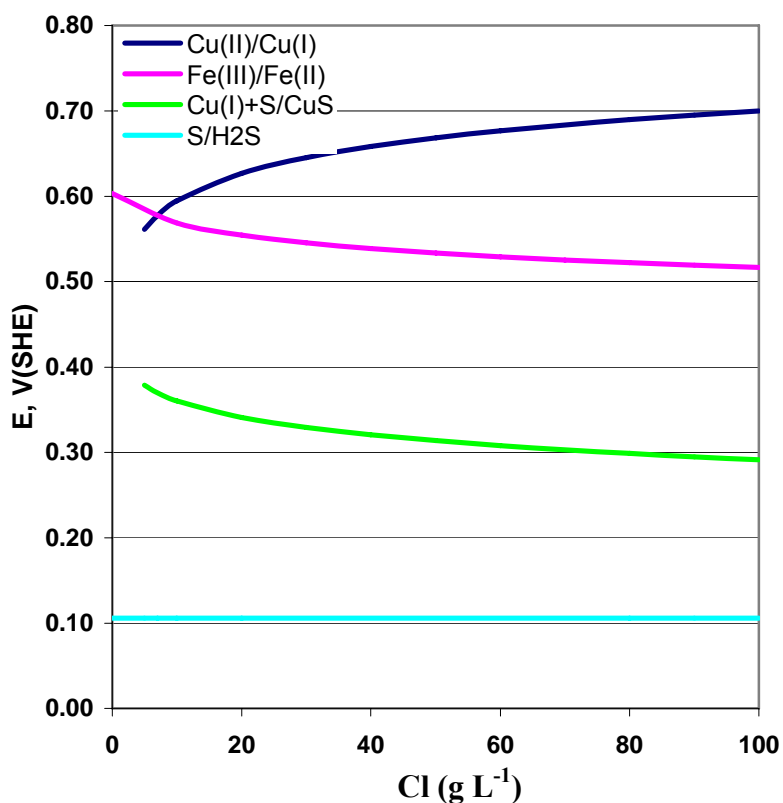


Figure 8.5 Formal potentials of the various couples in the system Cu(II)/Cu(I)/S/Cl at 25 °C at various chloride concentrations

The potentials in Fig. 8.5 confirm that CuS is not stable in solutions containing an excess of copper(II) ions even at low concentrations of chloride and that elemental sulfur should be the product of oxidation of H₂S. Thus, even if CuS is the first product of reaction with H₂S, it will be oxidized by copper(II) ions albeit at a slower rate than could be expected for the homogeneous oxidation of H₂S by copper(II) ions.

8.3. Consumption of dissolved oxygen with time

(The experimental results described below were obtained by Dr Hajime Miki in the same laboratory and are included as part of this thesis because of the relevance to the mechanism of the dissolution process).

It is not possible to conveniently directly measure the kinetics of the oxidation of H₂S by copper(II) ions under the conditions of the leach experiments. Therefore, an indirect method was adopted in which the rate of consumption of dissolved oxygen was measured using an oxygen probe with the apparatus shown in Figure 8.6. 4 mL of solution with known concentrations of HCl, Cu and chloride ions were placed into the cell which was stirred by a small magnetic bar. The dissolved oxygen probe holder was designed to act like a plunger which fitted the cylindrical glass cell. A small groove machined along the length of the probe holder the air to be expelled as the probe was lowered into the cell. The cell was immersed into a temperature controlled water bath maintained at 35 ° C. After temperature equilibration 40 µL of 0.01 M Na₂S solution was injected using a thin Teflon tube and micropipette inserted into the groove. The dissolved oxygen concentration was recorded as a function of time using data acquisition and Labview software.

In several comparative experiments, a copper(I) solution was injected into the reactor instead of a Na₂S solution. The copper(I) solution was prepared from reagent grade CuCl and HCl and was stored under a nitrogen atmosphere in the presence of a piece of copper wire to minimize oxidation to copper(II).

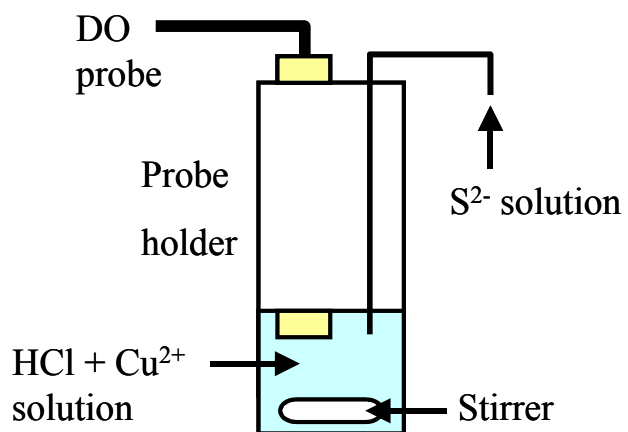


Figure 8.6 Apparatus for dissolved oxygen measurements

8.4. Analysis of experimental data

The rate of oxidation of H_2S by dissolved oxygen in the absence of copper(II) ions is shown in Figure 8.7 from which it is apparent that the rate is very slow with negligible reaction in 1000 s which is the maximum reaction period observed in the presence of the copper ions.

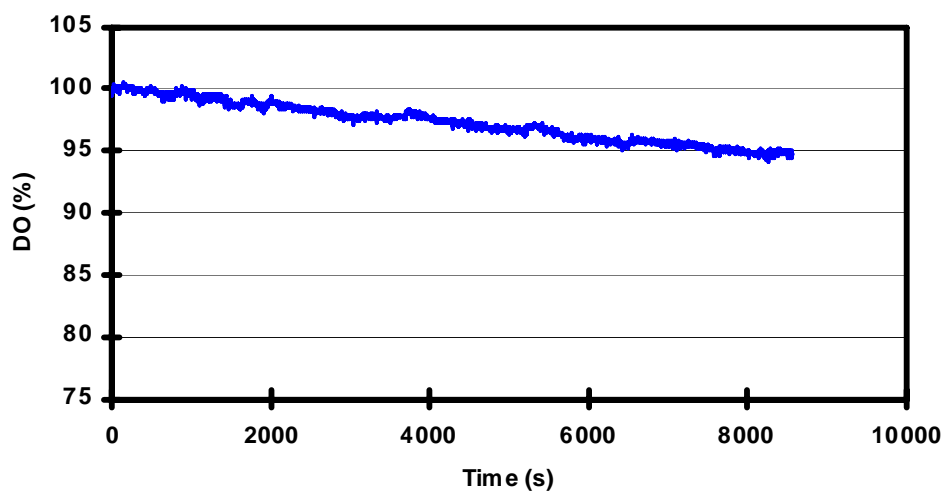


Figure 8.7 The consumption of dissolved oxygen at 35°C in 4 mL of 0.2 M HCl + 0.8 M NaCl solution after addition of 40 μL 0.01 M S²⁻ solution (Hajime Miki, personal communication).

The significant catalytic effect of copper ions is shown by the data in Fig. 8.8 which is a typical trace of the response of the oxygen probe with time at 35°C in 4 mL of solution (0.2 M HCl + 0.8M NaCl + 0.5g L⁻¹ Cu(II)) after the addition of 40μL of 0.01M Na₂S solution. Fig. 8.9 shows the result of a similar experiment in which the addition of sulfide was replaced by 40 μL of 0.0191 M copper(I) ions. The curve describing the rate of consumption of dissolved oxygen is almost identical to that in Figure 8.8 confirming that the oxidation of H₂S by copper(II) ions (Eq. 8.9) is rapid under these conditions and is followed by slower oxidation of the copper(I) formed by dissolved oxygen (Eq. 8.10).



and the overall reaction is

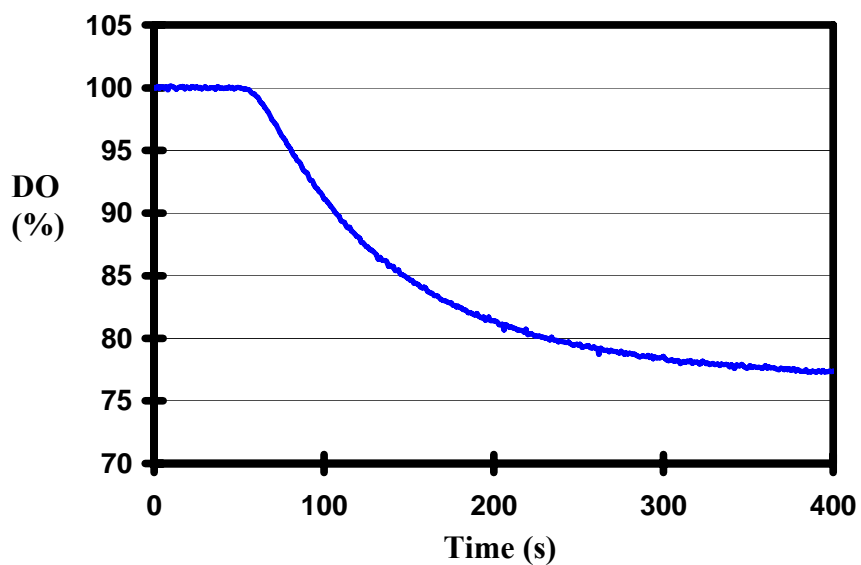


Figure 8.8 Experimental curve for the consumption of dissolved oxygen on addition of 40 μL 0.01 M S^{2-} solution to 4 mL of 0.2 M HCl + 0.8 M NaCl + 0.5 g L^{-1} Cu(II) at 35 $^{\circ}\text{C}$ (Hajime Miki, personal communication).

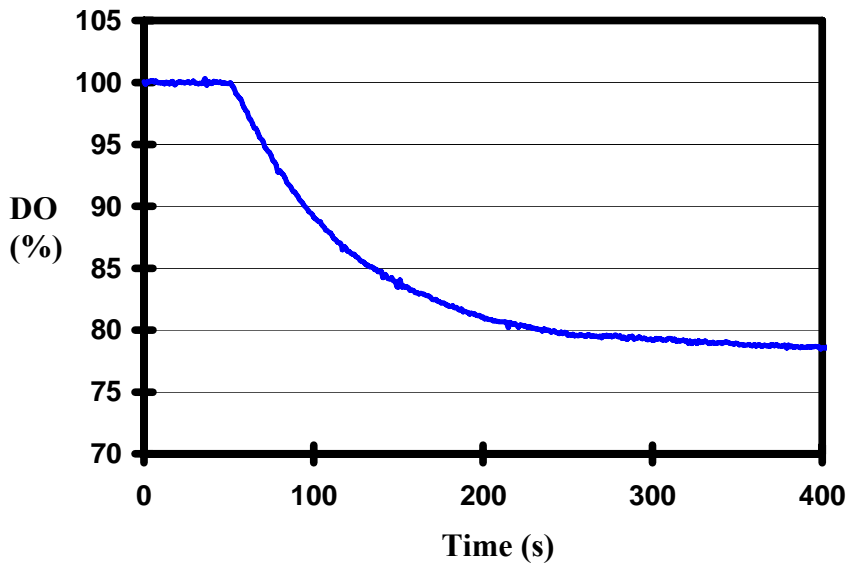


Figure 8.9 Experimental curve for the consumption of dissolved oxygen on addition of 40 μL 0.0191 M Cu(I) solution to 4 mL of 0.2 M HCl + 0.8 M NaCl + 0.5 g L^{-1} Cu(II) at 35 °C (Hajime Miki, personal communication) .

At low (less than about 0.2 g L^{-1} copper ions), the rate decreases significantly and, under these conditions is controlled at least partially by the rate of reaction (8.9). The kinetic analysis is different at high and low copper concentrations and each will be dealt with separately.

8.4.1. High (>0.2 g L^{-1}) copper concentration

Under these conditions the rate is controlled by reaction (8.10) and the kinetic data can be analyzed as follows by assuming that the decrease in the dissolved oxygen concentration is equivalent to the concentration of copper(I) oxidized i.e. the H_2S concentration is effectively zero soon after injection into the solution.

For an air-saturated solution at 35 °C, $[O_2]_0 = 0.20 \text{ mM}$ and $[O_2]_0 = \alpha D_0$ where D_0 is the % saturation as measured and α is a constant.

After the reaction has been completed

$$[O_2]_f = \alpha D_f \text{ while at any time, } t, [O_2]_t = \alpha D_t$$

Assuming the stoichiometric given in Eq. 8.10

one can write

$$\begin{aligned} [Cu(I)]_0 &= 4([O_2]_0 - [O_2]_f) \\ &= 4[O_2]_0 \left\{ (D_0 - D_f) / D_0 \right\} \end{aligned}$$

and, similarly,

$$[Cu(I)]_t = 4([O_2]_0 - \left\{ (D_t - D_f) / D_0 \right\})$$

$$[Cu(I)]_t = 4[O_2]_0 \left\{ (D_t - D_f / D_0) \right\}$$

Thus, for a reaction of first-order in copper(I)

$$-\frac{[Cu(I)]}{dt} = k_1 [Cu(I)]$$

or,

$$\ln \frac{[Cu(I)]_0}{[Cu(I)]_t} = k_1 t \tag{8.12}$$

while for a second-order reaction

$$-\frac{[Cu(I)]}{dt} = k_2 [Cu(I)]^2$$

or

$$\frac{1}{[Cu(I)]_t} - \frac{1}{[Cu(I)]_0} = k_2 t \quad (8.13)$$

The data shown in Figure 8.8 were analyzed in this way and the results are shown in Figure 8.10

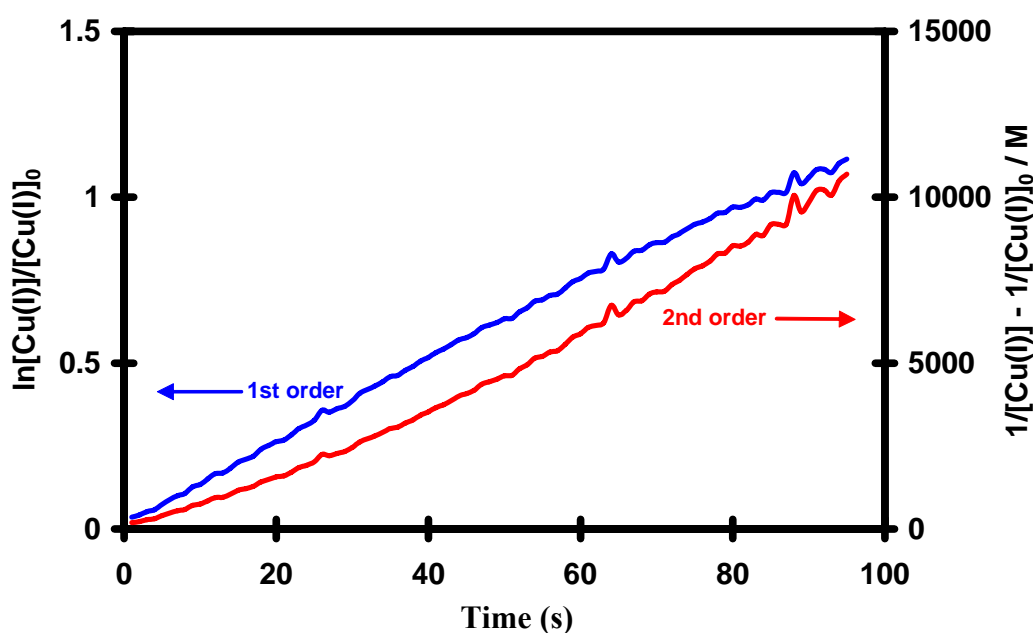


Figure 8.10 1st and 2nd order kinetic plots of the data from Figure 8.8.

It is apparent that, under these conditions, the reaction order is close to first-order in the initial stages of the reaction but approximates second order in the latter stages.

Previously published information on the kinetics of the oxidation of copper(I) by dissolved oxygen in chloride solutions (Nicol, 1983) has suggested a rate equation of the form

$$-\frac{d[\text{Cu(I)}]}{dt} = \frac{k_1' [\text{Cu(I)}]^2 [\text{O}_2]}{k_2' [\text{Cu(II)}] + [\text{Cu(I)}]} \quad (8.14)$$

in which both k_1' and k_2' are functions of the acid and chloride concentrations. Under conditions of constant $[\text{O}_2]$ and $[\text{Cu(II)}]$, this equation reduces to

$$-\frac{d[\text{Cu(I)}]}{dt} = \frac{k_1 [\text{Cu(I)}]^2}{k_2 + [\text{Cu(I)}]}$$

which can be integrated to give, for $[\text{Cu(I)}] = [\text{Cu(I)}]_0$ at $t=0$,

$$k_2 \left(\frac{1}{[\text{Cu(I)}]} - \frac{1}{[\text{Cu(I)}]_0} \right) + \ln \frac{[\text{Cu(I)}]_0}{[\text{Cu(I)}]} = k_1 t \quad (8.15)$$

Under conditions of high $[\text{Cu(II)}] \gg [\text{Cu(I)}]$, $k_2 \gg [\text{Cu(I)}]$ and the reaction becomes pseudo-2nd order in Cu(I), whereas at low $[\text{Cu(II)}]$, $k_2 \ll [\text{Cu(I)}]$ and the reaction is pseudo-1st order.

Figure 8.11 is a plot of the data in Fig. 8.7 using the full rate expression (8.15) with the value of k_2 adjusted to give the “best-fit” line. The value of k_1 can be obtained from the slope of this line.

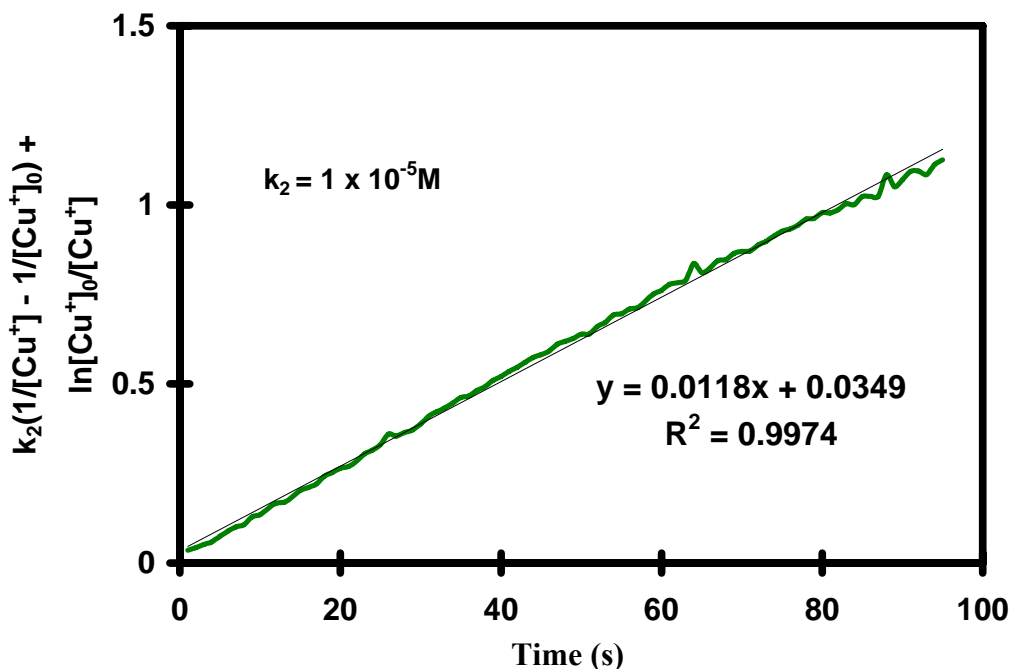


Figure 8.11 Plot of the data in Fig. 6 according to the overall rate equation (8.16) with $k_2 = 1 \times 10^{-5} \text{ M}$

It is apparent that this overall rate equation can be used to analyse the data under conditions for which the 1st- or 2nd-order approximations do not apply. Except for the runs at high initial concentrations of copper(II), the data was found to approximately fit a 1st-order reaction and the results have been given in terms of the pseudo-1st-order rate constant, k_1 . Because the deviation from first-order kinetics is relatively minor in most cases, it has not been possible to obtain values of k_2 of sufficient accuracy to establish the variations of k_2 with the experimental parameters.

8.4.2. Low (0.2 g L^{-1}) copper concentration

At low concentrations of copper(II), the rate decreased with decreasing concentration of copper(II) ions which is contrary to the trend at high concentrations and to that expected on the basis of rate equation (8.14). It is therefore suggested that under these conditions, the rate becomes controlled by the rate of the reduction of copper(II) by hydrogen sulfide i.e. reaction (8.9). Analysis of the kinetic data under these conditions shows that use of a second-order rate equation gives a good fit to the data while a first-order equation does not as is obvious from the plots in Fig 8.12. This trend is also contrary to that expected from rate in equation (8.15).

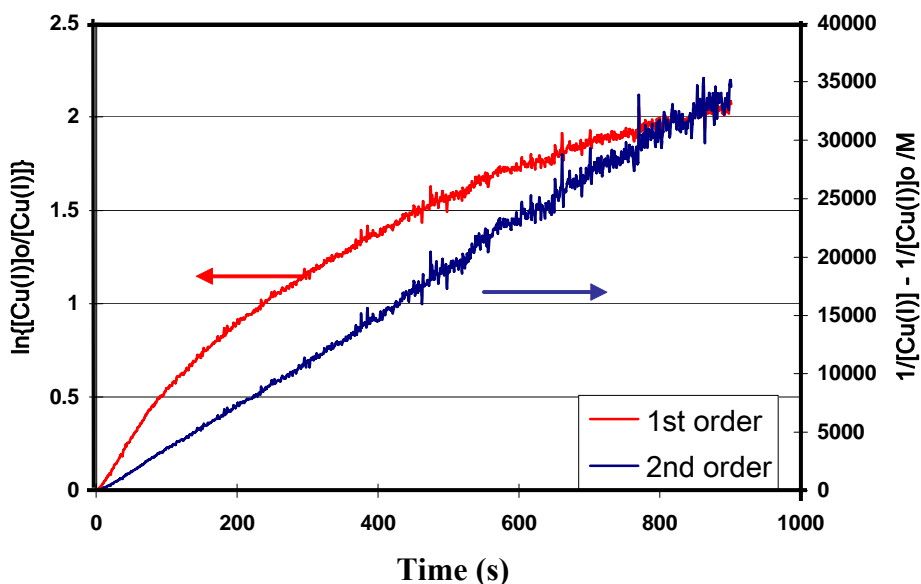


Figure 8.12 First- and second-order plots for the rate of consumption of dissolved oxygen on addition of 40 μL 0.01 M S^{2-} solution to 4mL of 0.2 M HCl + 0.8 M NaCl + 0.05 g L^{-1} Cu(II) at 35 $^\circ\text{C}$.

Note that the use of the same forms of the first- and second-order rate equations for this data assumes that the decrease in the oxygen concentration is equivalent to the amount of copper(I) ions oxidised and that therefore the integrated forms of the rate equations can be written in terms of copper(I) and not dissolved oxygen. While this is strictly only true if the formation of copper(I) by reduction with H₂S is rapid compared to the oxidation of copper(I) by oxygen, use of oxygen concentrations instead of copper(I) concentrations would result in the same integrated form.

8.4.3. Results at high copper concentration

The results of several experiments in which the rate of oxidation of copper(I) ions with dissolved oxygen in the absence of sulfide ions was measured are summarized in Table 8.1.

Table 8.1 Experimental conditions and results of oxidation of copper(I) at 35 °C.

Run	HCl M	Cu(II) g L ⁻¹	Cu(I) mM	Total Cl M	Rate constant k ₁ , /s	% Loss Oxygen
36	0.2	0.5	0.160	1.0	0.0113	20
37	0.2	0.5	0.192	1.0	0.0118	23.96
38	0.2	0.1	0.164	1.0	0.0186	20.49
39	0.2	0.5	0.104	1.0	0.0108	12.72
[O ₂] initial				0.2 MM		

The theoretical oxygen consumption based on Eq. 8.10 is 25% for an initial copper(I) concentration of 0.2 mM and the results in the last column are consistent with this expectation. The rate constants obtained are similar in magnitude to those obtained in a

previously published study (Nicol, 1983) at 25 °C with reduced rates at higher copper(II) concentrations as predicted by the rate law (Eq. 8.14). As could be expected from the close similarity of the curves in Fig. 8.8 and Fig. 8.9, the rate constants in Table 8.1 are very similar to those obtained with the addition of sulfide to a copper(II) solution as summarized in Tables 8.2 and 8.3(vide infra) under the same conditions.

The results of a number of experiments in which the rate of oxidation of copper(I) ions produced by reduction of 0.1 mM sulfide by copper(II) ions was measured under various conditions at 35 °C are summarized in Table 8.2. Similar data obtained from experiments using 0.05 mM sulfide are summarized in Table 8.3.

It should be noted that results for experiments at low copper(II) concentrations are also included in these tables although, as discussed above and demonstrated below, the data should not be expected to follow the same rate equation (8.15).

Table 8.2 Experimental conditions and results of experiments with $[\text{H}_2\text{S}]_0 = 0.1$ mM.

Run	HCl M	Cu(II) g L ⁻¹	pH	Total Cl M	Rate constant k ₁ , /s	% Loss Oxygen
1	0.2	0.5	1.1	0.2	0.0730	22.3
2	1	0.5	0.34	1.0	0.0291	19.7
3	0.3	0.5	0.7	1.0	0.0174	20.4
4	0.1	0.5	1.6	1.0	0.0062	20.9
5	0.01	0.5	2.1	1.0	0.0008	24.2
6	0.2	0.1	1.1	1.0	0.0162	23.7
7	0.2	0.2	1.1	1.0	0.0150	20.3
8	0.2	1.0	1.1	1.0	0.0065	18.7
9	0.2	0.5	1.1	1.0	0.0095	23.1
10	0.2	0.5	1.1	0.3	0.0449	18.5
11	0.2	0.5	1.1	0.5	0.0298	18.7
12	0.2	0.5	1.1	0.7	0.0210	18.5
13	0.2	0.01	1.1	1.0	0.0012	30.2
14	0.2	0.02	1.1	1.0	0.0068	30.9
15	0.2	0.05	1.1	1.0	0.0128	24.1
16	0.2	0	1.1	1.0	v. slow	N/A
17	0.2	0	1.1	0.2	v. slow	N/A
34	0.2	0.5	1.1	1.0	0.0111	24.7
40	0.2	0.01	1.1	0.2	2 nd order	16.8
41	0.2	0.02	1.1	0.2	0.0312	19.3
42	0.2	0.05	1.1	0.2	0.0345	19.3
43	0.2	0.1	1.1	0.2	0.0375	20.2
44	0.2	0.2	1.1	0.2	0.0422	20.6
45	0.2	0.5	1.1	0.2	0.0359	21.5
46	0.2	1.0	1.1	0.2	0.0328	21.6
Mean						21.3
[H ₂ S] initial	0.1 mM		[O ₂] initial	0.2 mM		Theoretical
						25

Table 8.3 Experimental conditions and results of experiments with $[\text{H}_2\text{S}]_0 = 0.05$ mM

Run	HCl M	Cu(II) g L ⁻¹	pH	Total Cl M	Rate constant k ₁ , /s	% Loss Oxygen
18	0.2	0.5	1.1	0.2	0.0720	15.2
19	1	0.5	0.34	1.0	0.0296	10.9
20	0.3	0.5	0.7	1.0	0.0159	13.3
21	0.1	0.5	1.6	1.0	0.0061	11
22	0.01	0.5	2.1	1.0	0.0007	12.9
23	0.2	0.1	1.1	1.0	0.0177	10.3
24	0.2	0.2	1.1	1.0	0.0155	9.3
25	0.2	1.0	1.1	1.0	0.0045	11.5
26	0.2	0.5	1.1	1.0	0.0091	9.9
27	0.2	0.5	1.1	0.3	0.0491	9.3
28	0.2	0.5	1.1	0.5	0.0282	11.4
29	0.2	0.5	1.1	0.7	0.0200	11.7
30	0.2	0.01	1.1	1.0	0.0011	19.8
31	0.2	0.02	1.1	1.0	0.0074	14.4
32	0.2	0.05	1.1	1.0	0.0124	13.8
33	0.2	0	1.1	1.0	0.0002	14.9
35	0.2	0.5	1.1	1.0	0.0102	13.8
Mean						12.5
[H ₂ S] initial	0.05 mM		[O ₂] initial	0.2 mM	Theoretical	12.5

As shown in the final column of each Table, the mean extent of oxygen consumption is 21.3% for an initial concentration of H₂S of 0.1 mM and 12.5% for an initial concentration of 0.05 mM. These values are consistent with the stoichiometric of Eq. 8.11 in terms of which the corresponding oxygen consumption values should be 25% and 12.5% respectively. Some variability can be expected in the extent of oxygen utilization given that partial reduction of oxygen to peroxide has been observed in similar systems.

The kinetic data will be discussed in more detail in terms of the effects of the various solution conditions on the overall pseudo first-order rate constants observed.

8.4.4. The effect of copper (II) concentration

In the absence of copper ions in the solution, the consumption of oxygen is negligible over a period of several hours confirming the very slow oxidation of sulfide by dissolved oxygen. Figure 8.13 and Figure 8.14 combine the experimental curves of all runs at various copper concentrations for high (Fig. 8.13) and low (Fig. 8.14) chloride concentrations. Note that the initial sulfide concentration was not the same in all of these runs. It is apparent from an examination of these curves that a) the rates are significantly lower at the higher chloride concentration and b) the variation in the rate with increasing initial copper concentration is more significant at the higher chloride concentration.

The rate constants obtained as described above are plotted as a function of the copper concentration for the data at 1M total chloride in Figure 8.15.

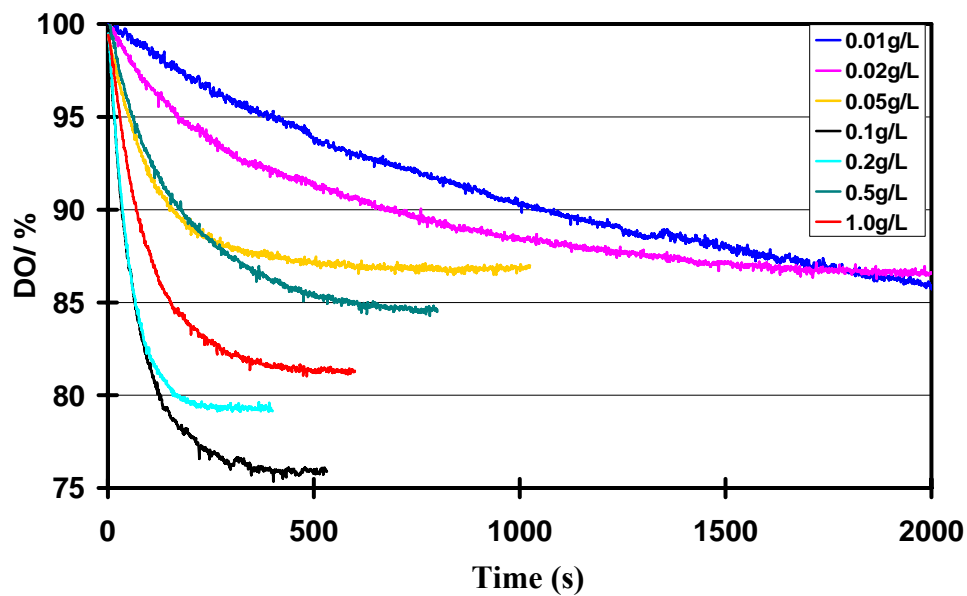


Figure 8.13 The effect of initial copper(II) concentration on the rate of consumption of oxygen at 35 °C in 4 mL of 0.2 M HCl + 0.8 M NaCl with addition of either 40 μL or 20 μL 0.01 M S^{2-} solution.

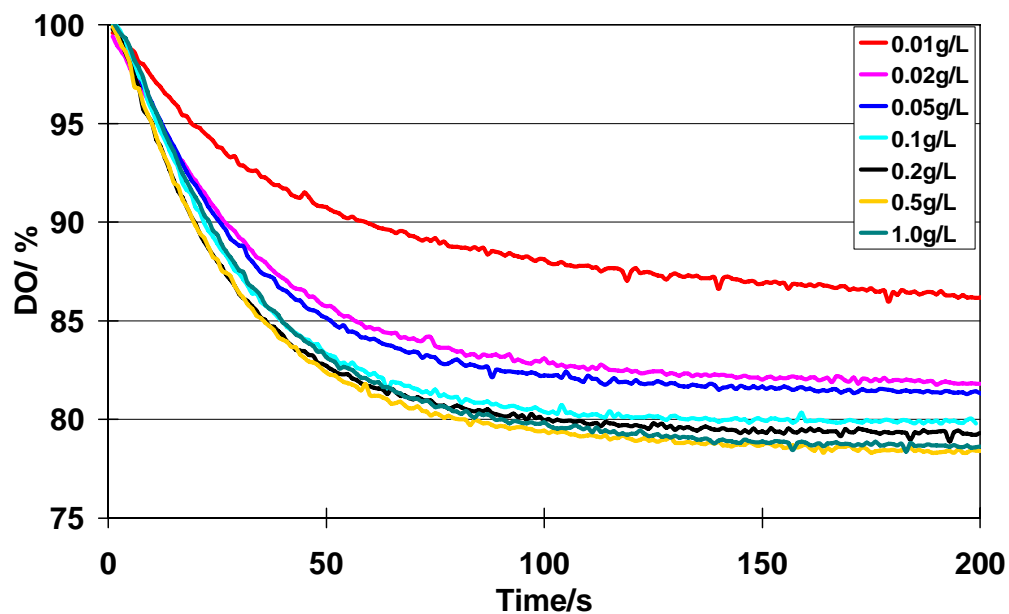


Figure 8.14 The effect of initial copper(II) concentration on the rate of consumption of oxygen at 35 °C in 4 mL of 0.2 M HCl with addition of 40 μL 0.01M S^{2-} solution.

At concentrations above about 0.1 g L^{-1} of copper, the rate decreases with increasing concentration with a maximum rate under these conditions for a copper concentration of about $0.1\text{-}0.2 \text{ g L}^{-1}$. The inverse dependence at concentrations above 0.1 g L^{-1} is expected from Eqn. 8.14 if the rate-determining step for the consumption of oxygen is the rate of oxidation of copper(I) produced by the reduction of copper(II) by H_2S .

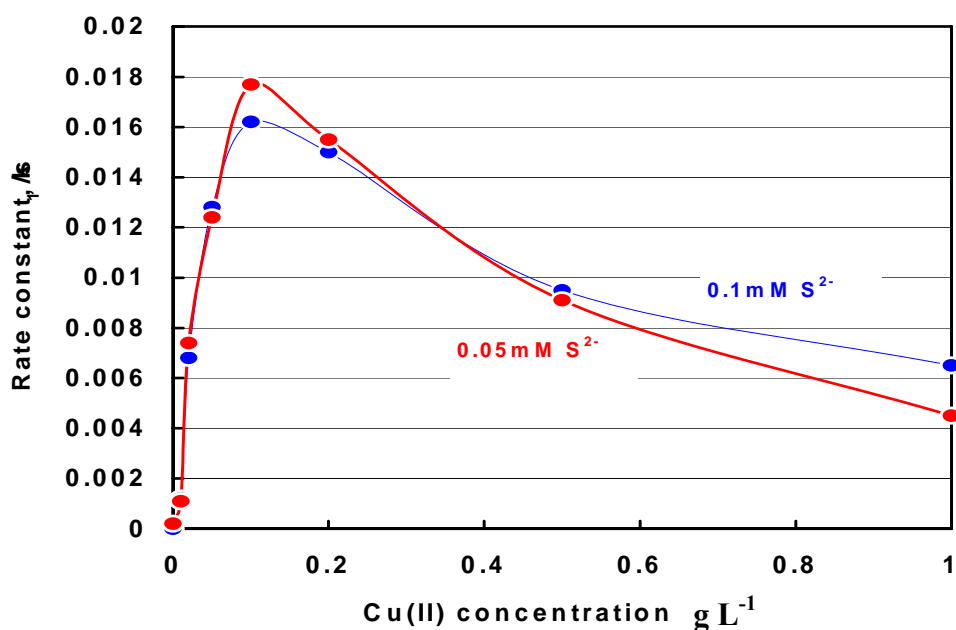


Figure 8.15 The effect of copper(II) concentration on the first-order rate constant at $35 \text{ }^\circ\text{C}$ in $4 \text{ mL } 0.2 \text{ M HCl} + 0.8 \text{ M NaCl}$ with addition of $40 \text{ }\mu\text{L } 0.01 \text{ M}$ or 0.005 M S^{2-} solution.

It is apparent that the rate increases with increasing concentration at concentrations below about 0.2 g L^{-1} and it appears that the rate of formation of copper(I) by reaction (8.9) becomes comparable in rate with the oxidation of copper(I). At the lowest copper

concentration, the reaction appears to better fit a second-order rate equation which becomes first-order as the concentration of copper increases.

More experimental work would be required in order to establish more fully the rate equation and the mechanism for the reduction of copper(II) ions by H₂S in acidic chloride solutions. As the copper(II) concentrations in heap leach solutions are likely to be in the range of 0.5 – 5 g L⁻¹, the importance of resolving the mechanistic issues at concentrations much lower than this range will be of limited practical value.

8.4.5. The effect of chloride ion concentration

Figure 8.16 shows the effect of the addition of increasing concentrations of NaCl on the rate constant at a high initial concentrations of copper(II). Under these conditions, the rate of oxidation of copper(I) is rate-determining in terms of the consumption of oxygen and the inverse dependence on chloride concentration is expected based on a similar observation in the previously published data (Nicol, 1983) for this reaction as shown in Eq. 8.8.

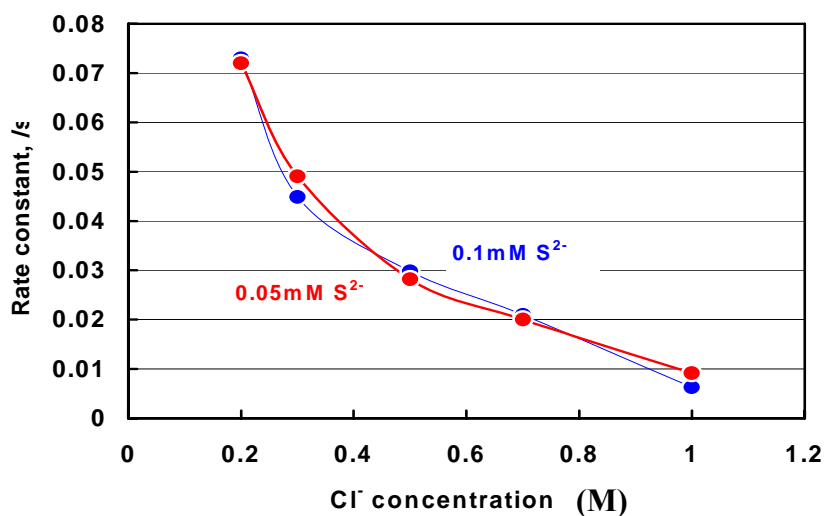


Figure 8.16 The effect of the concentration of chloride on the rate constant at 35 °C in 4 mL of 0.2 M HCl + 0.5 g L⁻¹ Cu(II) + x M NaCl

8.4.6. The effect of acidity

Figure 8.17 shows the effect of pH on the first-order rate constant under conditions of high copper(II) concentration. As expected from Eq. 8.8, the rate increases with increasing acidity for the oxidation of copper(I) by oxygen.

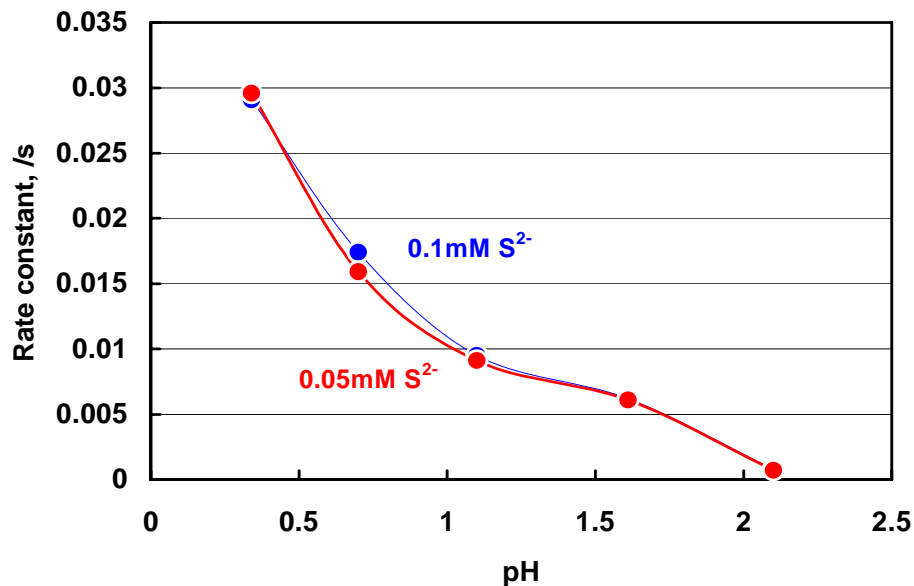


Figure 8.17 The effect of pH on the rate constant at 35 °C in 4 mL of x M HCl + (1-x) M NaCl + 0.5 g L⁻¹ Cu(II)

8.4.7. The effect of the addition of fine pyrite

The effect of fine pyrite (0.04 g) on the consumption of oxygen in the absence and presence of H₂S (1 mM) in 4 mL of a solution of 0.2 M HCl is shown in Figure 8.18. In the absence of pyrite, the consumption of oxygen is very slow and similarly, in the absence of added sulfide ions, the oxidation of pyrite is also slow. However, in the presence of pyrite, the oxidation of sulfide is rapid as shown with complete removal of dissolved oxygen in less than 400 s.

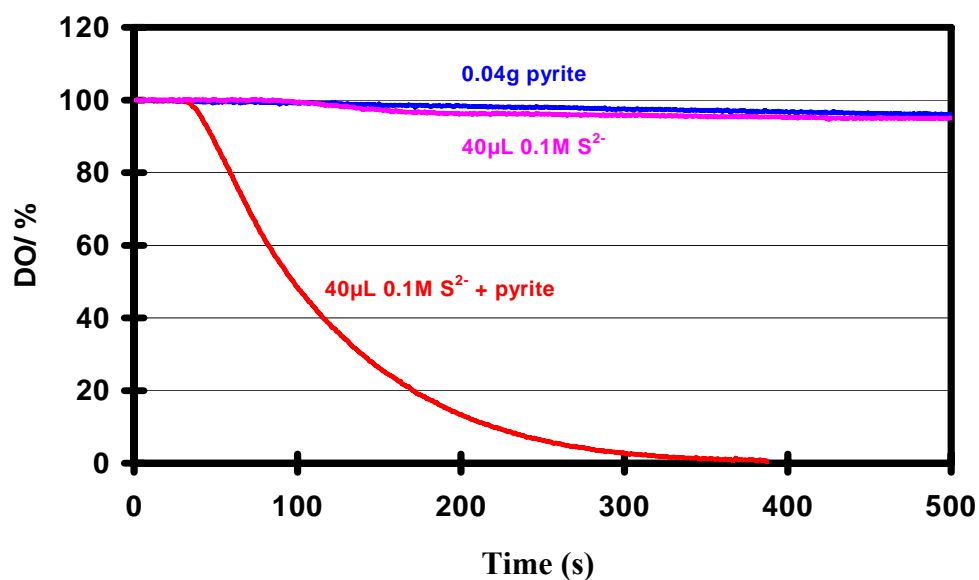


Figure 8.18 Consumption of dissolved oxygen at 35 °C in 4 mL of 0.2 M HCl + 0.04 g pyrite suspension with and without addition of 40 µL 0.1 M S²⁻ solution.

It is obvious that the oxidation of H₂S by dissolved oxygen is catalyzed in the presence of fine pyrite particles. This observation is consistent with the results of leaching experiments that showed enhanced dissolution rates of chalcopyrite in the presence of fine (<25 µm) pyrite and the mineralogical observation of sulfur coatings around fine pyrite particles in the residues from the leaching experiments. The model shown schematically in Figure 8.3 is therefore consistent with these observations.

The enhanced dissolution rate of chalcopyrite in the presence of fine pyrite can be explained by the model proposed, but can not be explained by the galvanic model proposed by Dixon et al. (2007) in relation to the GALVANOX process. According to this model, galvanic contact between chalcopyrite and pyrite is required, which enhances the overall rate due to enhanced reduction of ferric ions on the surface of the galvanically coupled

pyrite particles. However, this seems unlikely in that it is very clear from the schematic diagram provided by Dixon et al. (2007) that the chalcopyrite surface is covered with a layer of elemental sulfur which could be expected to minimize electron transfer between the two minerals. Furthermore, enhancement of the cathodic reaction on a pyrite surface would serve to increase the mixed potential for chalcopyrite dissolution, which is contrary to the requirement for reduced potentials in the GALVANOX process.

8.5. Summary

A new mechanism for the enhanced dissolution has been developed in terms of which the well-known passivation of chalcopyrite under ambient, oxidative conditions is avoided by controlling the potential at values below that at which passivation occurs. Under these conditions, it is proposed that the reaction involves non-oxidative dissolution or conversion of chalcopyrite to covellite-like phases that can be oxidized by dissolved oxygen. The H₂S formed in these reactions is oxidized by dissolved oxygen which reaction is catalyzed by copper ions and other sulfide mineral surfaces such as pyrite.

It has been found that the oxidation of dissolved H₂S by copper(II) ions is rapid and that the rate of oxidation of the copper(I) ions formed by dissolved oxygen is the slow step in the process at concentrations of copper(II) ions above about 0.1 g L⁻¹. At low concentrations of copper(II), the rate-determining step becomes the reduction of copper(II) to copper(I) by H₂S.

The main conclusions arising out of this study of the kinetics of the oxidation of sulfide and its implications for the mechanism of the dissolution of chalcopyrite are

1. The oxidation of hydrogen sulfide in acidic chloride solutions by dissolved oxygen is very slow in the absence of catalysts.
2. Copper ions are very effective in catalyzing the reaction by a mechanism that involves oxidation of sulfide by copper(II) and reoxidation of copper(I) by dissolved oxygen.
3. The rate-determining step is re-oxidation of copper(I) by oxygen at copper concentrations above about 0.2 g L^{-1} while at lower concentrations, reduction of copper(II) by hydrogen sulfide becomes rate-limiting.
4. At high copper concentrations, the rate of the reaction follows the published rate law for the kinetics of the oxidation of copper(I) by oxygen in chloride solutions.
5. Under typical heap leaching conditions, the rate of re-oxidation of copper(I) decreases with increasing concentration of copper and chloride ions and with increasing pH. This implies that control of Eh in a heap leach operation can be expected to be easier with increasing concentrations of copper and chloride and increasing pH.

6. Catalysis of the oxidation of hydrogen sulfide by fine pyrite particles has also been demonstrated. This confirms observations of the effect of fine pyrite on the leaching of chalcopyrite concentrates.

7. The non-oxidative model for the dissolution of chalcopyrite at potentials below 600-650 mV can be extended on the basis of the results of this investigation.

9. CONCLUSIONS

This thesis has described the results of a fundamental study of the rate of dissolution of chalcopyrite concentrates in chloride solutions under controlled potentials. A range of samples were studied, including chalcopyrite concentrates from different locations with different compositions. Covellite was also briefly examined as a potential intermediate in the dissolution process.

It has been demonstrated that enhanced rates of dissolution of copper from chalcopyrite concentrates in chloride media can be achieved at ambient temperatures by the application of controlled potentials in a “potential window” between 560 and 620 mV (SHE). The presence of dissolved oxygen is also essential for satisfactory rates of leaching under these conditions.

A relatively high activation energy of 70-80 kJ mole⁻¹ for dissolution under these conditions was established from experiments carried out in the temperature range from 25

to 75 °C. This has confirmed that the rate of dissolution is controlled by the rate of slow chemical or electrochemical processes.

Although the presence of chloride and cupric ions are essential for adequate rates of dissolution under these conditions, high concentrations do not improve the leaching rate in the potential window. On the other hand, an increase in the concentration of chloride ions can extend the potential window to higher values. The rate is essentially independent of acid concentration in the pH range from 0.5 to 2 with slightly lower rates at the lower pH values. Precipitation of iron as a poorly crystalline akaganeite does not appear to inhibit the rate of dissolution. Chalcopyrite from different sources appears to dissolve at roughly the same rate under the same conditions.

The effect of the addition of pyrite and silver ions on the leaching of chalcopyrite concentrates has been investigated. The results show that addition of excess fine pyrite with a particle size of less than 25 μm to the leach system can significantly enhance the rate of dissolution of copper from a particular concentrate. The effect is reduced in the presence of coarser or finer pyrite. Addition of silver ions does appear to increase the rate at higher chloride ions concentrations.

These results have culminated in the establishment of a mechanism that is consistent with the data obtained in an extensive study of the kinetics of dissolution. Mineralogical investigations of chalcopyrite surfaces and the residues from dissolution experiments have

shown that the surface of the mineral is converted to a covellite-like phase during leaching at potentials just below the potential window. The product of elemental sulfur forms largely as isolated spherical globules and as layers around smaller pyrite particles but seldom on the surface of chalcopyrite confirming that initial dissolution involves a soluble sulfur intermediate.

These phenomena can be explained by an extended non-oxidative reaction model in which chalcopyrite dissolves non-oxidatively to form a covellite-like surface species within the potential window. The H_2S that is in equilibrium with the mineral is oxidized by oxygen in a reaction catalysed by copper ions and other minerals such as pyrite. Confirmation of this reaction model has been enhanced by a detailed study of the kinetics of the copper-catalysed oxidation of H_2S . The oxidation of hydrogen sulfide in acid chloride solution by dissolved oxygen was found to be very slow, but is catalysed by the presence of copper ions or fine pyrite. In the case of copper the reaction is catalysed by a mechanism that involves oxidation of sulfide by copper(II) and re-oxidation of copper(I) by dissolved oxygen. These results have further confirmed observations of the effect of fine pyrite on the leaching of chalcopyrite concentrates and the accumulation of sulfur around fine pyrite particles during dissolution of chalcopyrite

10. RECOMMENDATIONS FOR FUTURE STUDY

It would be appropriate to conduct kinetic studies at higher temperatures to investigate whether or not the passivation process is reversible. This could be assessed by a study of the leaching rate of chalcopyrite at potentials above the potential window for extended periods with a subsequent reduction in the potential to values within the optimum range at different chloride concentrations.

Correlation of the chloride leaching data with electrochemical studies aimed at establishing the role of passivation and its reversibility coupled with a study of the reduction of iron(II) and copper(II) on chalcopyrite surfaces could provide further valuable mechanistic information..

In order to enhance the rate of leaching of chalcopyrite in chloride media it would be appropriate to conduct more experiments with silver ions, pyrite and other possible catalysts and promoters such as activated carbon, nanosized silica and other metal ions such as Sn(II), Co(II), Hg(II) and Mn(II) ions under low potential conditions. Pyrite would be of the particular interest since, in the present study, its addition enhanced the dissolution of chalcopyrite, but a possible galvanic effect was not established and this would be best conducted using electrochemical techniques.

Finally, any industrial application of this ambient temperature process will require a strategy for the control of the potential during the leaching of chalcopyrite in either agitated tanks or heaps.

REFERENCES

- Abraitis, P.K., Patrick, R.A.D., Kelsall, G.H. and Vaughan, D.J., 2004. Acid leaching and dissolution of major sulphide ore minerals: processes and galvanic effects in complex systems. *Mineralogical Magazine*, 68(2): 343-351.
- Ahonen, L. and Tuovinen, O.H., 1990. Catalytic effects of silver in the microbiological leaching of finely ground chalcopyrite -containing ore materials in shake flasks. *Hydrometallurgy*, 24(2): 219-236.
- Al-Harashseh, M., Kingman, S., Rutten, F. and Briggs, D., 2006a. ToF and SEM study on the preferential oxidation of chalcopyrite. *Int. J. Miner.*, 80: 205-214.
- Al-Harashseh, M., Rutten, F., Briggs, D. and Kingman, S., 2006b. Preferential oxidation of chalcopyrite surface facets characterized by ToF-Sims and SEM. *Applied Surface Science*, 252: 7155-7158.
- Ammou-Chokroum, M., Sen, P.K. and Fouques, F., 1981. Electrooxidation of chalcopyrite in acid chloride medium: kinetics, stoichiometry and reaction mechanism. *Development in mineral processing*, 2: 759-809.
- Antonijevic, M.M. and Bogdanovic, G.D., 2004. Investigation of the leaching of chalcopyrite ore in acidic solutions. *Hydrometallurgy*, 73: 245-256.
- Arce, E. and Gonzalez, I., 2002. A comparative study of electrochemical behavior of chalcopyrite, chalcocite and bornite in sulfuric acid solution. *International Journal of Mineral Processing*, 67: 17-28.
- Ballester, A., Gonzalez, F., Blazquez, M.L., Gomez, C. and Mier, J.L., 1992. The use of catalytic ions in bioleaching *Hydrometallurgy*, 29(1-3): 145-160.
- Ballester, A., Gonzalez, F., Blazquez, M.L. and Mier, J.L., 1990. The influence of various ions in the bioleaching of metal sulphides. *Hydrometallurgy*, 23(2-3): 221-235.
- Barr, G., Defreyne, J. and Mayhew, K., 2005. CESL copper process — an economic alternative to smelting., *CESL Engineering*.

Barriga Mateos, F., Palencia Perez, I. and Carranza Mora, F., 1987. The passivation of chalcopyrite subjected to ferric sulfate leaching and its reactivation with metal sulfides. *Hydrometallurgy*, 19: 159-167.

Berger, J.M. and Winand, R., 1984. Solubilities, densities and electrical conductivities of aqueous copper (I) and Copper(II) chloride in solutions containing other chlorides such as iron, zinc, sodium and hydrogen chlorides. *Hydrometallurgy*, 12(1): 61-81.

Berry, V.K., Murr, L.E. and Hiskey, J.B., 1978. Galvanic interaction between chalcopyrite and pyrite during bacterial leaching of low grade waste *Hydrometallurgy*, 3(4): 309-326.

Bonan, M., Demarthe, J.M., Renon, H. and Baratin, F., 1981. Chalcopyrite leaching by CuCl_2 . *Metallurgical Transactions B*, 12B: 269-273.

Burkin, A.R., 2001. *Chemical Hydrometallurgy: Theory and principles*. Imperial College Press, London, 414 pp.

Cabral, T. and Ignatiadis, I., 2001. Mechanistic study of the pyrite-solution interface during the oxidative bacterial dissolution of pyrite (FeS_2) by using electrochemical techniques. *International Journal of Mineral Processing*, 62: 41-64.

Carneiro, M.F.C. and Leão, V.A., 2007. The role of sodium chloride on surface properties of chalcopyrite leached with ferric sulphate. *Hydrometallurgy*, 87(3-4): 73-82.

CESL, CESL Web Site: www.CESL.com.

Cheng, C.Y. and Lawson, F., 1991. The kinetics of leaching covellite in acidic oxygenated sulphate-chloride solutions. *Hydrometallurgy*, 27: 269-284.

Crundwell, F.K., 1988. The influence of the electronic structure of solids on the anodic dissolution and leaching of semiconducting sulphide minerals. *Hydrometallurgy*, 21: 155-190.

Crundwell, F.K., 2003. How do bacteria interact with minerals? *Hydrometallurgy*, 71: 75-81.

Cruz, R., Luna-Sanchez, R.M., Lapidus, G.T., Gonzalez, I. and Monroy, M., 2005. An experimental strategy to determine galvanic interactions affecting the reactivity of sulfide minerals concentrates. *Hydrometallurgy*, 78: 198-208.

Cuprochlor, P., 2001. Chilean Patent # 40891, Chile.

Dalton, R.F., Price, R., Hermana, E. and Hoffman, B., 1988. Cuprex - new chloride-based hydrometallurgy to recover copper from sulfide ores. *Mining Engineering*, 40: 24-28.

Devi, N.B., Madhuchhanda, M., Srinivasa Rao, K., Rath, P.C. and Paramguru, R.K., 2000. Oxidation of chalcopyrite in the presence of manganese dioxide in hydrochloric acid medium. *Hydrometallurgy*, 57: 57-76.

Dixon, D.G., Mayne, D.D. and Baxter, K.G., 2007. GalvanoxTM - A Novel Galvanically - Assisted Atmospheric Leaching Technology for Copper Concentrates. In: D.D. P.A. Riveros, D.B. Dreisinger, J. Menacho (Editor), *Cu2007*. The Canadian Institute of Mining, Metallurgy and Petroleum, Toronto, Canada, pp. 491.

Dreisinger, D., 2006. Copper leaching from primary sulfides: Options for biological and chemical extraction of copper. *Hydrometallurgy*, 83(1-4): 10-20.

Dutrizac, J.E., 1978. The kinetics of dissolution of chalcopyrite in ferric ion media. *Metallurgical Transactions B*, 9B: 431-439.

Dutrizac, J.E., 1981. The dissolution of chalcopyrite in ferric sulfate and ferric chloride media. *Metallurgical Transactions B*, 12B: 371-378.

Dutrizac, J.E., 1982. Ferric ion leaching of chalcopyrite from different localities. *Metallurgical Transactions B*, 13B: 303-309.

Dutrizac, J.E., 1989. Sulphate control in chloride leaching processes. *Hydrometallurgy*, 23: 1-22.

Dutrizac, J.E., 1990. Elemental Sulphur Formation During the Ferric Chloride Leaching of Chalcopyrite. *Hydrometallurgy*, 23: 153-176.

Dutrizac, J.E., 1992. The leaching of sulphide minerals in chloride media. *Hydrometallurgy*, 29: 1-45.

Dutrizac, J.E. and MacDonald, R.J.C., 1971. The effect of sodium chloride on the dissolution of chalcopyrite under simulated dump leaching conditions. *Metall. Trans. B*, 2: 2310-2312.

Dutrizac, J.E., MacDonald, R.J.C. and Ingraham, T.R., 1969. The kinetics of dissolution of synthetic chalcopyrite in aqueous acid ferric sulfate solution. *Transactions of the Metallurgical Society of AIME (Amer. Inst. Mining, Met., Petrol. Eng.)*, 245: 955-959.

Edelbro, R., Sandström, Å. and Paul, J., 2003. Full potential calculations on the electron bandstructures of Sphalerite, Pyrite and Chalcopyrite. *Applied Surface Science*, 206(1-4): 300-313.

Elsherief, A.E., 2002. The influence of cathodic reduction, Fe^{2+} and Cu^{2+} ions on the electrochemical dissolution of chalcopyrite in acidic solution. *Minerals Engineering*, 15: 215-223.

Escudero, M.E., Gonzalez, F., Blazquez, M.L., Ballester, A. and Gomez, C., 1993. The catalytic effect of some cations on the biological leaching of a Spanish complex sulphide. *Hydrometallurgy*, 34(2): 151-169.

First Quantum Minerals, L., 2009. Web Site: <http://www.first-quantum.com>.

Flett, D.S., 2002. Chloride hydrometallurgy for complex sulphides: a review. In: P.a.G.V.W. E (Editor), *Chloride Metallurgy 2002: Practice and theory of Chloride*. 32nd Annual Hydrometallurgy Meeting. Met Soc, Montreal, pp. 255-275.

Godocíková, E., Baláz, P. and Boldizárová, E., 2002. Structural and temperature sensitivity of the chloride leaching of copper, lead and zinc from a mechanically activated complex sulphide. *Hydrometallurgy*, 65: 83-93.

Gomez, E., Ballester, A., Blazquez, M.L. and Gonzalez, F., 1999. Silver-catalysed bioleaching of chalcopyrite concentrate with mixed cultures of moderately thermophilic microorganisms. *Hydrometallurgy*, 51: 37-46.

Gomez, E., Figueroa, M., Munoz, J., Ballester, A. and Blazquez, M.L., 1997a. Technical Note: A study of bioleached chalcopyrite surfaces in the presence of Ag (I) by voltammetric methods. *Minerals Engineering*, 10(1): 111-116.

Gomez, E., Roman, E., Blazquez, M.L. and Ballester, A., 1997b. SEM and AES studies of chalcopyrite bioleaching in the presence of catalytic ions. *Minerals Engineering*, 10(8): 825-835.

Guy, S., Broadbent, C.P. and Lawson, G.J., 1983. Cupric chloride leaching of a complex copper/zinc/lead ore. *Hydrometallurgy*, 10: 243-255.

Haavanlammi, L., Hyvärinen, O. and Yllö, E., 2005. Hydrocopper® - A versatile copper process for different kinds of concentrates., *Hydrocopper 2005*, Santiago, Chile.

Habashi, F., 1978. Chalcopyrite its chemistry and metallurgy. McGraw-Hill International Book Company. McGraw-Hill, New York, 165 pp.

Hackl, R.P., Dreisinger, D.B., Peters, E. and King, J.A., 1995. Passivation of chalcopyrite during oxidative leaching in sulfate media. *Hydrometallurgy*, 39: 25-48.

Harmer, S.L., Thomas, J.E., Fornasiero, D. and Gerson, A.R., 2006. The evolution of surfaces layers formed during chalcopyrite leaching. *Geochimica et Cosmochimica*, 70: 4392-4402.

Havlik, T. and Kammel, R., 1995. Leaching of chalcopyrite with acidified ferric chloride and carbon tetrachloride addition. *Minerals Engineering*, 8(10): 1125-1134.

Hirato, T., Kinoshita, M., Awakura, Y. and Majima, H., 1986. The leaching of chalcopyrite with ferric chloride. *Metallurgical Transactions B*, 17B: 19-28.

Hirato, T., Majima, H. and Awakura, Y., 1987. The leaching of chalcopyrite with cupric chloride. *Metall. Trans. B*, 18B: 31-39.

Hiroiyoshi, N., Arai, M., Miki, H., Tsunekawa, M. and Hirajima, T., 2002. A new reaction model for the catalytic effect of silver ions on chalcopyrite leaching in sulfuric acid solutions. *Hydrometallurgy*, 63: 257-267.

Hiroiyoshi, N., Hirota, M., Hirajima, T. and Tsunekawa, M., 1997. A case of ferrous sulfate addition enhancing chalcopyrite leaching. *Hydrometallurgy*, 47(1): 37-45.

Hiroiyoshi, N., Kuroiwa, S., Miki, H., Tsunekawa, M. and Hirajima, T., 2004. Synergistic effect of cupric and ferrous ions on active-passive behaviour in anodic dissolution of chalcopyrite in sulfuric acid solutions. *Hydrometallurgy*, 74: 103-116.

Hiroiyoshi, N., Kuroiwa, S., Miki, H., Tsunekawa, M. and Hirajima, T., 2007. Effects of coexisting Metal ions on the redox potential dependence of chalcopyrite leaching in sulfuric acid solutions. *Hydrometallurgy*, 87(1-2): 1-10.

Hiroiyoshi, N., Maeda, H., Miki, H., Hirajima, T. and Tsunekawa, M., 2001. Enhancement of chalcopyrite leaching by ferrous ions in acidic ferric sulfate solutions. *Hydrometallurgy*, 60: 185-197.

Hiroiyoshi, N., Miki, H., Hirajima, T. and Tsunekawa, M., 2000. A model for ferrous-promoted chalcopyrite leaching. *Hydrometallurgy*, 57: 31-38.

Hurlbut Cornelius S., J.W.E.S., 1998. Dana's Minerals and How to Study Them. John Wiley & Sons, Inc., New York 328 pp.

Jones, D.L. and Peters, E., 1976. The leaching of chalcopyrite with ferric sulphate and ferric chloride. In: e. J.C. Yannopoulos and J.C. Agarwa (Editor), Extractive Metallurgy of Copper. AIME, New York, Mississauga, Canada, pp. 633-653.

Kinnunen, P.H.-M. and Puhakka, J.A., 2004. Chloride-promoted leaching of chalcopyrite concentrate by biologically-produced ferric sulfate. Journal of Chemical Technology and Biotechnology, 79: 830-834.

Klauber, G., Parker, A., Van Bronswijk, W. and Watling, H., 2001. Sulphur speciation of leached chalcopyrite surfaces as determined by X-ray photoelectron spectroscopy. Int. J. Miner. Process, 62: 65-94.

Lázaro-Báez, M.I., 2001. Electrochemistry of the leaching of chalcopyrite, Murdoch University, 313 pp.

Lazaro, I. and Nicol, M.J., 2003. The mechanism of the dissolution and passivation of chalcopyrite: and electrochemical study. In: A.M.A. C.A. Young, C.G. Anderson, D.B. Dreisinger, B. Harris and A. James (Editor), Hydrometallurgy 2003- Fifth International Conference in Honor of professor Ian Ritchie-. TMS Canada, pp. 405-416.

Lopez-Juarez, A., Gutierrez-Arenas, N. and Rivera-Santillan, R.E., 2006. Electrochemical behavior of massive chalcopyrite bioleached electrodes in presence of silver at 35°C. Hydrometallurgy, 83: 63-68.

Lu, Z.Y., Jeffrey, M.I. and Lawson, F., 2000a. The effect of chloride ions on the dissolution of chalcopyrite in acidic solutions. Hydrometallurgy, 56: 189-202.

Lu, Z.Y., Jeffrey, M.I. and Lawson, F., 2000b. An electrochemical study of the effect of chloride ions on the dissolution of chalcopyrite in acidic solutions. Hydrometallurgy, 56: 145-155.

Lundstrom, M., Alomaa, J., Forsen, O., Hyvarinen, O. and Barker, M.H., 2007. Cathodic reactions of Cu^{2+} in cupric chloride solution. Hydrometallurgy, 85(1): 9-16.

Lundstrom, M., Aromaa, J., Forsen, O., Hyvarinen, O. and Barker, M., 2005. Leaching of chalcopyrite in cupric chloride solution. Hydrometallurgy, 77: 89-95.

- Majima, H. and Awakura, Y., 1981. Measurement of the activity of electrolytes and the application of activity to hydrometallurgical studies. *Metall. Trans. B*, 12B: 141-147.
- Majima, H., Awakura, Y., Hirato, T. and Tanaka, T., 1985. The leaching of chalcopyrite in ferric chloride and ferric sulfate solutions. *Canadian Metallurgical Quarterly*, 24: 283-291.
- Maurice, D. and Hawk, J.A., 1998. Ferric chloride leaching of mechanically activated chalcopyrite. *Hydrometallurgy*, 49: 103-123.
- McMillan, R.S., MackKinnon, D.J. and Dutrizac, J.E., 1982. Anodic dissolution of n-type and p-type chalcopyrite. *Journal of applied electrochemistry*, 12: 743-757.
- Mehta, A.P., 1983. Fundamental studies of the contribution of galvanic interaction to acid-bacterial leaching of mixed metal sulfides. *Hydrometallurgy*, 9: 235-256.
- Miki, H., Hiroyoshi, N., Kuroiwa, S., Tsunekawa, M. and Hirajima, T., 2003. Mechanism of catalytic leaching of chalcopyrite. In: D.D. P.A. Riveros, D.B. Dreisinger, J. Menacho (Editor), *Copper 2003-Cobre 2003*, Santiago, Chile, pp. 383-394.
- Miller, J.D., McDonough, P.J. and Portillo, H.Q., 1981. Electrochemical in silver catalysed ferric sulfate leaching of chalcopyrite. In: J. Laskowski (Editor), *13th International Mineral Processing Congress*. Elsevier, Amsterdam, pp. 851-894.
- Moyes, J. and Houllis, F., 2002. Intec base metal processes realising the potential of chloride hydrometallurgy. In: P.a.G.V.W. E (Editor), *Chloride Metallurgy 2002*, 32nd Annual Hydrometallurgy Meeting. MET SOC, Montreal, Canada, pp. 577-593.
- Muir, D.M., 2002. Basic principles of chloride Hydrometallurgy. In: E.P.a.G.V. Weert (Editor), *Chloride Metallurgy 2002*, 32nd Annual Hydrometallurgy Meeting. MET SOC, Montreal, Canada, pp. 759-791.
- Munoz, P.B., Miller, J.D. and Wadsworth, M.E., 1979. Reaction mechanism for the acid Ferric Sulfate Leaching of Chalcopyrite. *Metallurgical Transactions* 10B: 149-158.
- Nicol, M.J., 1975. Mechanism of aqueous reduction of chalcopyrite by copper, iron and lead. *Inst. Min. Metall., Trans., Sect. C*, 84: C206-C209.
- Nicol, M.J., 1983. Kinetics of the oxidation of copper(I) by oxygen in acid chloride solutions. *S.-Afr. Tydskr. Chem.*, 37: 77-80.

Nicol, M.J. and Lazaro, I., 2002. The role of Eh measurements in the interpretation of the kinetics and mechanism of the oxidation and leaching of sulphide minerals. *Hydrometallurgy*, 63: 15-22.

Nicol, M.J. and Lazaro, I., 2003. The role of non-oxidative processes in the leaching of chalcopyrite. In: D.D. P.A. Riveros, D.B. Dreisinger, J. Menacho (Editor), *Copper 2003-Cobre 2003*, Santiago, Chile, pp. 367-381.

O'Malley, M.L. and Liddell, K.C., 1987. Leaching of CuFeS_2 by aqueous FeCl_3 , HCl and NaCl : effects of solution composition and limited oxidant. *Metallurgical Transactions B*, 18B: 505-509.

Olli Hyvarinen, M.H., 2005. HydroCopperTM-a new technology producing copper directly from concentrate. *Hydrometallurgy*, 77: 61-65.

Olubambi, P.A., Ndlovu, S., Potgieter, J.H. and Borode, J.O., 2006. Influence of applied mineralogy in developing and optimal hydrometallurgical processing route for complex sulphide ores. *Mineral Processing and Extractive Metallurgy Review*, 2(27): 143-158.

Olubambi, P.A., Ndlovu, S., Potgieter, J.H. and Borode, J.O., 2007. Effects of ore mineralogy on the microbial of low grade complex sulphide ores. *Hydrometallurgy*, 86(1-2): 96-104.

Parker, A., Klauber, C., Kougiannos, A., Watling, H.R. and van Bronswijk, W., 2003. An X-ray photoelectron spectroscopy study of the mechanism of oxidative dissolution of chalcopyrite. *Hydrometallurgy*, 71: 265-276.

Parker, A.J., Paul, R.L. and Power, G.P., 1981. Electrochemical aspect of leaching copper from chalcopyrite in ferric and cupric salt solutions. *Aust. J. Chem*, 34: 13-34.

Parker, G.K., 2005. Spectroelectrochemical investigation of chalcopyrite leaching. PhD Thesis, University of Griffith, Brisbane, 269 pp.

Peacey J., X.J.G., Eduardo Robles, 2005. Copper hydrometallurgy-current status, preliminary economics, future direction and positioning versus smelting. In: H.a. Ltd. (Editor), *Copper Hydrometallurgy*, Mississauga, Ontario, pp. 1-18.

Peters, E., 1976. Direct leaching of sulfides: Chemistry and applications. *Metallurgical Transactions B*, 7B: 505-517.

Prasad, S. and Pandey, B.D., 1998. Alternative processes for treatment of chalcopyrite- A review. *Minerals Engineering*, 11(8): 763-781.

Rivera-Velasquez , B., Viramontes-Gamboa, G. and Dixon, D.G., 2006. Leaching of chalcopyrite concentrates in acid ferric sulfate media at controlled redox potential. In: E.M. Domic and J.M. Casas de Prada (Editors), *HydroProcess 2006, International Workshop on Process Hydrometallurgy*. GEGAMIN, Santiago, Chile, pp. 287-299.

Romero, R., Mazuelos, A., Palencia, I. and Carranza, F., 2003. Copper recovery from chalcopyrite concentrates by the BRISA process. *Hydrometallurgy*, 70: 205-215.

Sato, H., Nakazawa, H. and Kudo, Y., 2000. Effect of silver chloride on the bioleaching of chalcopyrite concentrate. *International Journal of Mineral Processing*, 59: 17-24.

Scholz, F.E., 2005. *Electroanalytical Methods: Guide to Experiments and Applications*, 2nd printing. Springer, Berlin, 331 pp.

Senanayake, G., 2007a. Chloride assisted leaching of chalcocite by oxygenated sulphuric acid via Cu(II)-OH-Cl. *Minerals Engineering*, 20(11): 1075-1088.

Senanayake, G., 2007b. Review of theory and practice of measuring proton activity and pH in concentrated chloride solutions and application to oxide leaching. *Minerals Engineering*, 20(7): 634-645.

Skrobjan, M., Havlik, T. and Ukasik, M., 2004. Effect of NaCl concentration and particle size on chalcopyrite leaching in cupric chloride solution. *Hydrometallurgy*, 77: 109-114.

Stott, M.B., Watling, H.R., Franzmann, P.D. and Sutton, D., 2000. The role of iron-hydroxy precipitates in the passivation of chalcopyrite during bioleaching. *Minerals Engineering*, 13(10-11): 1117-1127.

Third, K.A., Cord-Ruwisch, R. and Watling, H.R., 2002. Control of the redox potential by oxygen limitation improves bacterial leaching of chalcopyrite. *Biotechnology and Bioengineering*, 78: 433-441.

Wang, M., Y., Z., Deng, T. and Wang, K., 2004. Kinetic modeling for bacterial leaching of chalcopyrite catalyzed by silver ions. *Minerals engineering*, 17: 943-947.

Wang, M., Zhang, Y. and Muhammed, M., 1997. Critical evaluation of thermodynamics of complex formation of metal ions in aqueous solutions III. The system Cu (I,II)-Cl⁻ -e at 298.15 K. *Hydrometallurgy*, 45: 53-72.

Wang, S., 2005. Copper leaching from chalcopyrite concentrates. *JOM*, 57(7): 48-51.

Watling, H.R., 2006. The bioleaching of sulphide minerals with emphasis on copper sulphides - a review. *Hydrometallurgy*, 84: 81-108.

Wilson, J.P. and Fisher, W.W., 1981. Cupric chloride leaching of chalcopyrite. *Journal of Metals*, 33(2): 52-57.

Winand, R., 1991. Chloride Hydrometallurgy. *Hydrometallurgy*, 27: 285-316.

Wood, P., 2001. Intec's dendritic copper process poised for commercialization. *Metal Powder Report*, 56(3): 26-30.

You, L.Q., Heping, L. and Zhou, L., 2007. Study of galvanic interactions between pyrite and chalcopyrite in a flowing system: implications for the environment. *Environ Geol*, 52: 11-18.

Yuehua, H., Guanzhou, Q., Jun, W. and Dianzuo, W., 2002. The effect of silver-bearing catalysts on bioleaching of chalcopyrite. *Hydrometallurgy*, 64: 81-88.

APPENDIX

Raw data from leaching experiments described in Chapters 4 to 7 provided on a CD